

The Pennsylvania State University

The Graduate School

**CARBON FIBER PRECURSORS BASED ON POLYETHYLENE GRAFT PITCH
COPOLYMER**

A Dissertation in
Materials Science and Engineering

by

Houxiang Li

© 2021 Houxiang Li

Submitted in Partial Fulfillment
of the Requirements
for the Degree of

Doctor of Philosophy

May 2021

The dissertation of Houxiang Li was reviewed and approved by the following:

T.C. Mike Chung
Professor of Materials Science and Engineering
Dissertation Advisor
Chair of Committee

Ralph Colby
Professor of Materials Science and Engineering

Michael A. Hickner
Professor of Materials Science and Engineering

Semih Eser
Professor of Energy and Geo-Environmental Engineering

John Mauro
Professor of Materials Science and Engineering
Chair, Intercollege Graduate Degree Program in Materials Science and
Engineering
Head of the Department or Chair of the Graduate Program

ABSTRACT

Today, both of the mainstream precursors of carbon fibers (CFs)—PAN and pitch—have many downsides, which are limiting the cost reduction and improvement on production efficiency of CFs. With a rapidly increasing global demand for this type of high-performance material, there is growing interest in finding a better precursor. However, despite numerous studies, researchers have yet to develop a new polymeric precursor that is less expensive, melt-spinnable, and offers a high carbon yield. In this thesis, I discuss our research approach and the experimental results that may address this important technological issue. We have developed a new class of hydrocarbon polymer precursors, called "PE-g-Pitch," based on polyethylene (PE) polymer chain with grafted pitch-like side groups with the structure of polycyclic aromatic hydrocarbon (PAH). Some ungrafted pitch is also present in the precursor to reduce the overall melt viscosity during the melt-spinning process. In addition to its low-cost raw materials (PE-copolymer and petroleum pitch), the resulting PE-g-Pitch precursors with some suitable compositions also show good melt processability and high carbon yield under a simple one-step thermal conversion process in N₂ atmosphere. Additionally, PE-g-Pitch can also be solution-spun as an alternative option.

In Chapter 1, I present the background information on CFs and the mainstream CF precursors applied in the industry today. Some recent research studies about CF precursors are also discussed, along with their scientific considerations and the challenges hindering them from further development. This chapter also includes the studies that inspired us in designing the new CF precursor PE-g-Pitch. Chapter 2 is about the research at the early stage of our study before the invention of PE-g-Pitch. I explain our research approach for designing new synthetic hydrocarbon polymers, as well as the experimental results showing the desirable hydrocarbon structures that can be thermally transformed into a carbon crystal structure with high carbon yield. Specifically, I focus on a new hydrocarbon polymer system based on poly(phenylacetylene) derivatives that

have a π -electrons conjugated molecular structure and the active side groups for Diels-Alder-type cycloaddition reaction. One with a para-substituted acetylene group shows an exceptionally high carbon yield of more than 90%. The other one with a para-substituted phenylacetylenyl group also offers a high carbon yield of 75%, as well as good solubility in common organic solvents. This polymer is suitable for electro-spinning processes to form the corresponding precursor fibers. In Chapter 3, I expand the structure-designing strategy to the PE copolymer and discuss the preparation of the melt-spinnable PE-g-Pitch precursor. To prepare the precursor, a semi-crystalline PE copolymer containing diphenylacetylenyl side groups was applied to undergo a Diels-Alders cycloaddition reaction with petroleum pitch to allow the PAH molecules to be grafted onto the PE backbones. A systematic study was conducted on the blend samples of PE-g-Pitch and unreacted petroleum pitch that serve as a plasticizer to reduce melt viscosity for the melt-spinning process. Furthermore, the investigation shows the detailed condition of precursor preparation and the thermal conversion process forming the corresponding CFs with a high carbon yield of 73% and the desirable polymorphous CF morphology. In Chapter 4, to understand the stabilization mechanism of PE-g-Pitch, this material was obtained by using the toluene-soluble portion of petroleum pitch as the reactant that can be completely removed by Soxhlet extractor after the cycloaddition reaction. I discuss the crucial role that PAH side groups play in forming cross-linkages via polycondensation reactions during the stabilization at low temperature, and subsequently in promoting the dehydrogenation of PE chains to form a more extensively conjugated structure that facilitates the carbon conversion. In Chapter 5, I focus on the PE-g-Pitch precursor prepared by the Diels-Alder cycloaddition reaction between petroleum pitch and a lower-cost and more easily-prepared PE copolymer with 4-bromophenyl side groups (PE-co-4-bromostyrene), which was synthesized by the copolymerization of ethylene and 4-bromostyrene. A systematic study is discussed to provide important information about the effect of the size of pitch-like side groups on the solution-spinnability and carbon yield of PE-g-Pitch.

The enlarged side groups generate strong π -interaction and form physical cross-linking between polymer chains in the solution. They also facilitate a higher carbon conversion by creating a more conjugated structure. Additionally, the preparation of precursor fibers by both solution- and melt-spinning methods, as well as the procedures for CF conversion, are discussed. Some resulting CFs show mechanical properties suitable for general applications even without optimizing on the stabilization and carbonization conditions. In Chapter 6, I discuss an alternative method for preparing the poly(ethylene-4-bromostyrene) copolymer via the bromination of a poly(ethylene-styrene) copolymer that has been widely commercialized at a very low cost. The brominated poly(ethylene-styrene) copolymer has a more random microstructure than the previous PE-co-4-bromostyrene synthesized by direct copolymerization of ethylene and 4-bromostyrene. PE-g-Pitch prepared from this PE copolymer with a more random structure has good solution-spinnability and can achieve a carbon yield of about 60%.

Overall, this thesis provides details on several strategies for preparing a PE-g-Pitch precursor for the economic and efficient production of high-performance CFs. The new precursor exhibits a combination of advantages, including

- (i) Low raw materials cost
- (ii) Less energy consumption
- (iii) Melt-spinnable or solution-spinnable in a common solvent
- (iv) High carbon yield of >50%
- (v) More thorough structural stabilization
- (vi) Easily scaled-up production

TABLE OF CONTENTS

LIST OF FIGURES.....	ix
LIST OF TABLES.....	xvi
ACKNOWLEDGEMENTS.....	xvii
Chapter 1 Introduction to Carbon Fibers	1
1.1 Background of Carbon Fibers	1
1.2 Structure of Carbon Fiber.....	3
1.3 Economics Justifications	5
1.4 Carbon Fiber Precursors in Industry	6
1.4.1 Polyacrylonitrile (PAN)	7
1.4.2 Pitch.....	16
1.4.3 Cellulose.....	23
1.5 Recent Studies on Carbon Fiber Precursors.....	26
1.5.1 Melt Spinnable Polyacrylonitrile.....	26
1.5.2 Polymer-Lignin Blend.....	28
1.5.3 Carbon-Based Additives	32
1.5.4 Others	33
1.6 Inspirational Studies Relating to Our Works	34
1.6.1 PE-based CFs Precursors	34
1.6.2 Polymer-Pitch Blend	38
1.6.3 Conclusion.....	40
Chapter 2 A New Precursor System Based on Poly(phenylacetylene) Derivatives	42
2.1 Introduction.....	42
2.2 Experimental Section	44
2.2.1 Materials & Instrumentation	44
2.2.2 Synthesis of Monomers and Polymers	45
2.3 Results & discussion	48
2.4 Conclusion	64
Chapter 3 Preparation and Evaluation of Polyethylene-graft-Pitch Precursors by Cycloaddition Reaction between Diphenylacetylenyl Side Groups-Contained PE copolymer and Pitch.....	66
3.1 Introduction.....	66
3.2 Cycloaddition Reaction Between PAH Molecules and Acetylene Derivatives	68
3.3 Experimental Section	71
3.3.1 Materials.....	71
3.3.2 Characterization	72
3.3.3 Synthesis of Poly (4-bromostyrene).....	73
3.3.4 Synthesis of Poly (4-phenylacetylenyl styrene)	73
3.3.5 Copolymerization of Ethylene and 4-Bromostyrene	74

3.3.6 Synthesis of Poly(ethylene-co-4-phenylacetylenyl Styrene).....	75
3.3.7 Preparation of Melt-Spinnable PE-g-Pitch/Pitch Blend Precursors	75
3.3.8 Gel Content Measurement.....	76
3.4 Results and Discussion.....	77
3.4.1 Preparation of Diphenylacetylenyl Side Group-Contained Polymers and Reactivity of Diphenylacetylenyl Side Group.....	78
3.4.2 Preparation and Thermal Conversion of PE-g-Pitch/Pitch Blend Precursors	85
3.4.3 Melt Rheology of PE-g-Pitch//Pitch Blend Precursors	92
3.4.4 Melt-spinning of PE-g-Pitch//Pitch Blend Precursor Fibers	96
3.4.5 Carbon Structures Resulted from PE-g-Pitch//Pitch Precursors	98
3.5 Conclusion	101
 Chapter 4 Mechanistic Study of Thermal Transformation from Polyethylene-graft-Pitch to Carbon Materials.....	 103
4.1 Introduction.....	103
4.2 Experimental Section	104
4.2.1 Characterization	104
4.2.2 Materials.....	104
4.2.3 Copolymerization of Ethylene and 4-Bromostyrene	105
4.2.4 Synthesis Poly(ethylene-co-4-phenylacetylenyl Styrene).....	105
4.2.5 Preparation of Toluene-soluble Pitch	106
4.2.6 Preparation of PE-g-Pitch//Pitch Blend.....	106
4.2.7 Free Pitch Removal from PE-g-Pitch/Pitch Blend	107
4.2.8 Heat Treatment of Pure PE-g-Pitch Graft Copolymer	107
4.3 Results and Discussion.....	108
4.3.1 Proposed Stabilization Mechanism	108
4.3.2 Synthesis of Pure PE-g-Pitch Graft Copolymer	111
4.3.3 Thermal Conversion of PE-g-Pitch Graft Copolymer.....	112
4.3.4 Stabilization Reaction of PE-g-Pitch Graft Copolymer	115
4.4 Conclusion	120
 Chapter 5 Synthesis and Evaluation of Polyethylene-graft-Pitch Precursors Prepared by Cycloaddition between Pitch and Poly(ethylene-co-4-bromostyrene) by Direct Polymerization Method.....	 123
5.1 Introduction.....	123
5.2 Experimental Section	125
5.2.1 Characterization	125
5.2.2 Materials.....	126
5.2.3 Copolymerization of Ethylene and 4-Bromostyrene	127
5.2.4 Toluene-soluble Pitch 250M(S) Extraction.....	127
5.2.5 Preparation of PE-g-Pitch/Pitch Blend.....	128
5.2.6 Free Pitch Removal	128
5.2.7 Fiber Spinning.....	129
5.2.8 Stabilization and Carbonization of PE-g-Pitch Fibers.....	129
5.2.8 Gel Content Measurement.....	130
5.3 Results and Discussion on PE-g-Pitch Precursors	130

5.3.1 Preparation of PE-g-Pitch Graft Polymer by Cycloaddition between Poly(ethylene-4-bromostyrene) Copolymer and Pitch	131
5.3.2 Thermal Conversion and Solution-Spinnability of Pure PE-g-Pitch Graft Copolymers	135
5.3.3 Carbon Fibers Prepared from PE-g-Pitch Stabilized Precursor Fibers.....	145
5.3.4 Melt Spinnable Carbon Fiber Precursor by PE-g-Pitch Graft Copolymer with Unreacted Pitch	147
5.4 Conclusion	154
Chapter 6 Synthesis and Evaluation of PE-g-Pitch Precursors Prepared from Poly(ethylene-co-4-bromostyrene) by Post Polymerization Process: Bromination of Poly(ethylene-co-styrene)	155
6.1 Introduction.....	155
6.2 Experimental Section	157
6.2.1 Characterization	157
6.2.2 Materials.....	157
6.2.3 Preparation of Poly(ethylene-4-bromostyrene) Copolymer via Direct Copolymerization	158
6.2.4 Copolymerization of Poly(ethylene-styrene) copolymer	158
6.2.5 Synthesis of Brominated Poly(ethylene-styrene) Copolymer	159
6.2.6 Toluene-soluble Pitch 250M(S) Extraction.....	159
6.2.7 Preparation of PE-g-Pitch/Pitch Blend.....	160
6.2.8 Free Pitch Removal	160
6.2.9 Fiber Spinning.....	161
6.2.10 Stabilization and Carbonization of PE-g-Pitch Fibers.....	161
6.3 Results and Discussion.....	162
6.3.1 Synthesis of PE-BrSt Copolymers by Post Polymerization Process	162
6.3.2 Comparison of PE-BrSt Copolymers Prepared by Direct and Post Polymerization Processes	164
6.3.3 Preparation of PE-g-Pitch Precursor from the PE-BrSt Copolymers Prepared by Post Polymerization Process	167
6.3.4 Solution Spinning of PE-g-Pitch Precursor Fibers	171
6.3.5 Carbon Fibers Prepared from PE-g-Pitch Precursors.....	173
6.4 Conclusion	174
Chapter 7 Summary and Future Research Directions	175
7.1 Summary and Conclusions.....	175
7.2 A New Precursor System Based on Poly(phenylacetylene) Derivatives	176
7.3 PE-g-Pitch Precursors Prepared by Cycloaddition between Petroleum Pitch and Diphenylacetylenyl Side Group-Contained PE Copolymer	177
7.4 PE-g-Pitch Precursors Prepared by Cycloaddition Reaction between Petroleum Pitch and 4-bromophenyl Side Groups-Contained PE Copolymer	178
7.5 Future Work	180
Reference	182

LIST OF FIGURES

Figure 1.1 The main applications of CFs today. ¹	2
Figure 1.2 Microstructures of the carbon crystal.	4
Figure 1.3 Mechanical properties of CFs comparing to mainstream structural materials. ²⁴	5
Figure 1.4 The pie chart of cost contributors to PAN-based CFs. ²⁵	6
Figure 1.5 A Schematic of carbon fibers manufacturing process. ²⁷	7
Figure 1.6 Polymerization route of PAN with itaconic acid and methyl methacrylate as comonomers.	8
Figure 1.7 Simplified process flow of industrial PAN precursor fiber manufacturing using DMSO solvent.....	9
Figure 1.8 SEM micrographs of cross-section for the as-spun PAN precursor fibers fabricated by (a) wet spinning and (b) gel spinning. ⁴⁴	11
Figure 1.9 (a) Cyclization in PAN initiated through free radical mechanism (b) Cyclization in P(AN-IA) initiated through ionic mechanism.	12
Figure 1.10 Model reaction paths from PAN to a carbon phase. ³⁵	15
Figure 1.11 Chemical structure (left) and appearance (right) of petroleum pitch.....	16
Figure 1.12 The dependence of viscosity on temperature for various pitches and a melt-spun polymer. ⁷¹	18
Figure 1.13 Simplified process flow of pitch precursor fiber manufacturing by melt-spinning.....	19
Figure 1.14 Observed microstructures of mesophase pitch-based carbon fibers. ⁷⁷	20
Figure 1.15 Processing steps of CFs starting from pitch as precursor material. ³⁵	21
Figure 1.16 Model reaction paths from mesophase pitch to a carbon phase. ⁷⁹	22
Figure 1.17 Chemical structure of cellulose.	23
Figure 1.18 Model reaction paths from cellulose to a carbon phase. ⁸⁵	25
Figure 1.19 Chemical structure of PAN-MA-ABP (left) and PAN-VIM (right).....	28
Figure 1.20 Synthesis of (a) esterified LS and (b) LS-AN copolymer. ¹⁰⁰	31

Figure 1.21 Scheme showing E1cB elimination reaction (top) and the radical chain reaction (bottom). ¹³²	36
Figure 1.22 A simplified mechanistic transformation of sulfonated PE to carbon. ¹³³	37
Figure 1.23 Scheme of the condensation reaction of pitch initiated by the formation of free radicals. ⁷⁹	40
Figure 1.24 The proposed preparation route of PE-g-Pitch.	41
Figure 2.1 Schematic structures of poly(PA) and two derivatives poly(PA-A) and poly(PA-PA) polymers.	43
Figure 2.2 The reaction route to prepare poly(PA-ASi) and poly(PA-A) homopolymers from 4-triisopropylsilylethynyl-phenylacetylene (PA-ASi) monomer.	49
Figure 2.3 ¹ H NMR spectra of (a) 4-triisopropylsilylethynyl-phenylacetylene (PA-ASi) monomer and (b) the corresponding poly(PA-ASi) polymer.....	50
Figure 2.4 FTIR spectra of (a) poly(PA-ASi) and (b) poly(PA-A) polymers.....	51
Figure 2.5 Reaction route to prepare 4-phenylethynyl-phenylacetylene monomer (III) and the corresponding poly(PA-PA) polymer.	52
Figure 2.6 ¹ H NMR spectra of (a) 1-trimethylsilylethynyl-4-phenylethynyl benzene intermediate (II) and (b) the corresponding 4-phenylethynyl-phenylacetylene monomer (III).....	53
Figure 2.7 (a) ¹ H NMR and (b) ¹³ C NMR spectra of poly(PA-PA) polymer.....	55
Figure 2.8 TGA-MS spectrum of poly(phenylacetylene) polymer, with a heating rate of 10°C/min under N ₂ atmosphere.....	56
Figure 2.9 TGA-MS spectrum of (a) poly(PA-A) and (b) poly(PA-PA) polymers, with a heating rate of 10°C/min under N ₂ atmosphere.....	57
Figure 2.10 DSC curves of (a) poly(PA-A) and (b) poly(PA-PA) hydrocarbon polymer precursors.	60
Figure 2.11 SEM image of the electro-spun poly(PA-PA) fibers from a 30 wt.% polymer/THF solution, with voltage of 15 kV, flow rate of 7.5 mL/hr., and distance of 20 cm.	61
Figure 2.12 (a) Raman spectra of carbon fibers after carbonization at various heating temperatures and (b) the peak intensity ratio between D and G bands vs. carbonization temperature.	63

Figure 2.13 (a) XRD patterns of several carbon fibers and their (b) interlayer d-spacing and (c) stacking height (Lc). They are prepared by sequential heat treatment of the same poly(PA-PA) fiber at various temperatures (with 1 hour at each temperature) under an N ₂ atmosphere.	63
Figure 3.1 Molecular structures of poly(PA-PA) with DPA side groups, PE-DPA copolymer, and the corresponding PE-g-Pitch precursor.....	67
Figure 3.2 Diels-Alder cycloadditions of diethyl acetylenedicarboxylate to (a) 4,11-dimesitylbisanthene and (b) perylene. ¹⁵⁰	69
Figure 3.3 Activation energies calculated for Diels-Alder cycloadditions of acetylene to aromatic hydrocarbon bay regions. ¹⁵⁰	70
Figure 3.4 Schematic diagram of high-pressure reactor with (1) gas cylinder, (2) heating mantle, (3) reaction vessel and (4) temperature/pressure monitor.	75
Figure 3.5 Illustration of structural transformation from PE-DPA copolymer to PE-g-Pitch precursor, to precursor fiber, and to stabilized fiber. (*one of the many PAH structures in petroleum pitch).....	77
Figure 3.6 Synthesis equations of (top) poly(4-phenylacetylenyl styrene) and (bottom) PE-DPA copolymer.....	78
Figure 3.7 (top) ¹ H NMR and (bottom) ¹³ C NMR spectra of poly(4-phenylacetylenyl styrene).....	80
Figure 3.8 ¹ H NMR spectra of (a) PE-BrSt copolymer and (b) the corresponding PE-DPA copolymer with 7.2% functional group content and (c) ¹³ C NMR spectrum of PE-DPA copolymer with 7.2% functional group content.	81
Figure 3.9 (a) DSC curve of poly(4-phenylacetylenyl styrene) in N ₂ with two heating/cooling cycles and (b) images illustrating solubility of poly(4-phenylacetylenyl styrene) without (left) and with (right) heat treatment at 220°C in N ₂ for 1 hour.	83
Figure 3.10 H ₂ gas evolution in EGA-MS Spectra of PE-DPA (7.2%) copolymer, pitch (250M), and their mixture with 1 to 3 weight ratio.....	84
Figure 3.11 TGA curve comparisons of (a) PE-DPA (7.2 mol% DPA content)/pitch (250M) blend with 1/5 weight ratio, (b) pitch (250M), (c) PE/pitch blend with 1/5 weight ratio, and (d) PE-DPA copolymer (7.2 mol% DPA content).	87
Figure 3.12 TGA curve comparisons (top) between three PE-DPA (7.2 mol% DPA content)/pitch (250M) blends with (a) 1/10, (b) 1/5, and (c) 1/3 weight ratios and (d) pitch (250M), (bottom) PE-DPA (7.2 mol% DPA content)/pitch (250M) with 1/10 weight ratio blend prepared at different temperature (a) 310°C, (b) 280°C, and (c) 250°C for 1 hour before the TGA measurement.	89

Figure 3.13 TGA comparisons of three PE-DPA/pitch (250M) blends with (a) 7.2 mol%, (b) 3.2 mol%, and (c) 2.1 mol% of DPA content in the copolymer and (d) PE/pitch (1/5) blend as the reference.....	91
Figure 3.14 (a) oscillatory rheology by temperature-sweep measurement of three PE-g-Pitch/pitch blends prepared from PE-DPA(7.2mol%)/pitch (250M) blends with 1/10, 1/5, and 1/3 weight ratios, (b) time-sweep rheology measurement of the precursor from the PE-DPA/pitch (1/10) sample at different temperatures of 320, 340 and 350°C.....	93
Figure 3.15 (a) optical picture and (b) SEM micrograph of as-spun precursor fibers by melt-spinning of PE-DPA (7.2%)-1/10 blend.....	97
Figure 3.16 SEM micrograph of carbon fiber by melt-spinning of PE-DPA (7.2%)-1/10 blend.....	98
Figure 3.17 (top) XRD and (bottom) Raman spectra of carbon products prepared from PE-DPA (7.2%)/pitch (250M) 1/10 blend at carbonization temperature of 800°C, 1100°C, 1400°C, 1700°C, and 1900°C, respectively.....	99
Figure 3.18 Plots of (a) d-spacing (002), (b) lateral size (Lc), (c) stacking height (La) of the crystallite, and (d) the peak intensity ratio between D and G bands in Raman spectra vs carbonization temperature.....	100
Figure 4.1 General equation of elimination reaction.....	109
Figure 4.2 Nonoxidative dehydrogenation of (left) isobutane and (right) cyclohexane. ¹⁶³	110
Figure 4.3 Proposed stabilization mechanism of PE-g-Pitch backbone via dehydrogenation.....	110
Figure 4.5 TGA curve comparisons of (a) PE-DPA copolymer (6.2 mol% DPA content) (b) pitch 250M(S), and (c) PE-g-Pitch-1 prepared from 250M(S) and PE-DPA copolymer (6.2 mol% DPA content).....	113
Figure 4.6 TGA curve comparisons of PE-g-Pitch samples prepared from 250M(S) and PE-DPA copolymer with comonomer percentage of (a) 1.4 (b) 3.2 (c) 6.2 mol%.....	114
Figure 4.7 DSC curves of PE-g-Pitch-1 heated to (a) 300°C and (b) 400°C with the heating/cooling rate of 10°C/min in N ₂ atmosphere.....	116
Figure 4.8 XRD comparisons of PE-g-Pitch-1 heat-treated at different temperature of (a) 310°C (b) 380°C (c) 400°C (d) 420°C and (e) 440°C for 1 hour.....	117
Figure 4.9 Solid State CP-MAS ¹³ C NMR spectrums of PE-g-Pitch-1 heat-treated at different temperatures of (a) 310°C (b) 380°C (c) 400 °C (d) 420°C and (e) 440°C for 1 hour.....	118

Figure 4.10 EGA-MS spectra on H ₂ evolution of PE-g-Pitch-1, PE-DPA copolymer with 6.2mol% comonomer percentage, and Pitch 250M(S) heated from 320-420°C, and stayed at 420°C for 1hour.....	120
Figure 4.11 Proposed chemical structural transformation of functionalized PE copolymer and petroleum pitch to stabilized PE-g-Pitch.....	121
Figure 5.1 The electron density distribution affected by the inductive effect and resonance effect on bromostyrene. (o: ortho, m: meta, p: para).....	123
Figure 5.2 Scheme of proposed reaction route of preparation of PE-g-Pitch by PE-BrSt copolymer and pitch via Diels-Alder cycloaddition.	124
Figure 5.3 A schematic diagram of the solution-spinning setup.....	129
Figure 5.4 EGA-MS of PE-BrSt (8.4%) copolymer, 250M(S), and their mixture (1:3 in weight) targeting on H ₂ (left) and Br (right) fragments.	131
Figure 5.5 ¹ H NMR of (a) PE-BrSt (8.4%) copolymer and PE-g-Pitch(8.4%) samples prepared with different reaction time of (b) 1, (c) 2, and (d) 3 hours at 310°C.....	133
Figure 5.6 EGA-MS targeting on H ₂ of the mixture of poly(4-bromostyrene) and 250M(S) (1:3 in weight).	134
Figure 5.7 Calibration curve of PE composition vs. intensity ratio of the aliphatic and aromatic region from ¹ H NMR spectra of the PE-BrSt(8.4%) copolymer/250M(S) mixture.	135
Figure 5.8 The structural transformation of PE-g-Pitch during the blending process. (The black circle represents the PAH side group)	137
Figure 5.9 Pictures of PE-g-Pitch(8.4%)/TCB solutions showing (a) no spinnability and (b) good spinnability in the coagulation bath.....	138
Figure 5.10 Oscillatory rheology (frequency-sweep) comparison of PE-g-Pitch(8.4%)-1, 2 and 3 with blending time of 1, 2 and 3 hours, respectively, in 10wt.% TCB solution at 90°C.....	139
Figure 5.11 The SEM images of PE-g-Pitch(8.4%)-1 (top) fibers surface and (bottom) cross-section.....	142
Figure 5.12 TMA of PE-g-Pitch (8.4%)-1 in N ₂ with a heating rate of 10°C/min.....	142
Figure 5.13 (a) DSC measurement of PE-g-Pitch (8.4%)-1 in air with two heating cycles. (b) images illustrating solubility of PE-g-Pitch (8.4%) fibers with heat-treatment in air at 230°C for (left) one and (right) two hours.	143

Figure 5.14 Comparisons of (a) XRD spectra and calculated (b) d002, (c) Lc, and (d) La of carbonized PE-g-Pitch (8.4%)-1 at temperatures of 900, 1100, 1300 and 1500°C.....	145
Figure 5.15 Comparisons of (left) Raman spectra and (right) calculated I(D)/I(G) of carbonized PE-g-Pitch (8.4%)-1 fibers at temperatures of 900, 1100, 1300, and 1500°C.....	145
Figure 5.16 SEM image of (top) fiber surface and (bottom) cross-section CF converted from PE-g-Pitch (8.4%)-1 at 900°C.	146
Figure 5.17 Temperature sweep oscillatory melt-rheology results of PE-g-Pitch/pitch blends with 66.00%, 43.66%, 25.60% of free pitch removed.	148
Figure 5.18 DSC results of PE-BrSt(8%)-56% with two heating-cooling cycles in an air atmosphere (10°C/min).	150
Figure 5.19 Time-sweep oscillatory rheology results of PE-BrSt(8.4%)-56% in the air atmosphere at 210°C.	151
Figure 5.20 TGA comparison of PE-BrSt(8.4%)-56% samples with and without heat treatment in air at 210°C.	152
Figure 5.21 Optical microscopy images of (left) surface and (right) cross-section of PE-BrSt(8.4%)-56% melt-spun precursor fiber.	153
Figure 6.1 A schematic diagram of the solution-spinning setup.....	161
Figure 6.2 Synthetic equation of PE-BrSt copolymer via bromination of PE-St copolymer.....	162
Figure 6.3 ¹ H NMR spectrums of (bottom) PE-St copolymer and (top) brominated PE-St with 8.5% comonomer content.	163
Figure 6.4 Aliphatic region of ¹³ C NMR spectra of PE-BrSt copolymers with (top) 8.4mol% comonomer by direct copolymerization and (bottom) 8.5% comonomer by post-polymerization bromination.	165
Figure 6.5 Chemical shift assignments of the poly(ethylene-4-bromostyrene) copolymers with different microstructure arrangements.	165
Figure 6.6 DSC comparison of (a) PE-BrSt (8.4%) copolymer by direct-copolymerization and (b) PE-BrSt (8.5%) copolymer by post-polymerization bromination in N ₂ atmosphere with heating rate of 10°C/min.	167
Figure 6.7 ¹ H NMR of PE-g-Pitch samples prepared with different reaction temperatures and time of (a) 310°C, 1hr and (b) 250°C, 30min.	169

Figure 6.8 Oscillatory rheology (frequency-sweep) of PE-g-Pitch (8.5%)-3 with blending time of 30min at 250°C, in 10wt.% TCB solution at 90°C.	171
Figure 6.9 SEM images of as-spun fiber of PE-g-Pitch (8.5%)-3 on (top) cross-section and (bottom) fiber surface.....	172
Figure 6.10 Comparisons of (a) XRD spectra and calculated (b) d002, (c) Lc, and (d) La of carbonized PE-g-Pitch (8.5%)-3 at temperatures of 900°C, 1100°C, 1300°C and 1500°C.....	173

LIST OF TABLES

Table 1.1 Prediction of production capacity and demand in 2020 of CFs. ¹¹	3
Table 3.1 Summary of PE-BrSt copolymers synthesized by CGC metallocene catalyst.	79
Table 3.2 A summary of cycloaddition reaction between PE-DPA copolymers and Pitch(250M) under various experimental conditions.	86
Table 4.1 Blending conditions in the preparation of PE-g-Pitch graft copolymers.	111
Table 5.1 Preparation conditions of PE-g-Pitch samples.....	132
Table 5.2 Comparisons of solution fiber-spinnability and carbon yield of PE-g-Pitch samples.....	135
Table 5.3 The preparation conditions for PE-g-Pitch/pitch blends with different amount of free pitch removed.	148
Table 6.1 Preparation conditions of PE-g-Pitch samples.....	167
Table 6.2 The comparisons of experimental results of PE-g-Pitch samples preparation with different reaction temperatures and times.	170

ACKNOWLEDGEMENTS

I would first like to thank my principal advisor, Dr. T.C. Mike Chung, for providing me with the opportunity, guidance, and support to pursue my Ph.D. degree. Dr. Chung not only has taught me how to become a scientist with independent and critical thinking, but also serves as a good example of how a man becomes successful in his life and career. I will always remember the day in 2013 when I asked him if I could join his group to do research for my undergraduate thesis. I am very lucky to have him as my mentor in the most challenging stage of my life. I also want to express my gratitude to my committee members, Dr. Ralph Colby, Dr. Michael Hickner, and Dr. Semih Eser, for serving on my committee and for their insightful feedback that furthered the completion of the dissertation.

I would also like to give thanks to current and previous members of Dr. Chung's research group—Dr. Gang Zhang, Dr. Changwoo Nam, Dr. Wei Zhu, Joseph Vandy Sengeh, and Matt Agboola—for their guidance and support. I also appreciate Dr. Jiho Seo (Dr. Colby's group), Dr. Logan Kearney, and Dr. Amit Naskar at the Oak Ridge National Laboratory for their collaboration on rheology measurements and fiber spinning, and the US Department of Energy for the financial support through grant DE-EE0008096. The findings and conclusions in this dissertation do not necessarily reflect the view of the funding agency.

Last, I would like to express my greatest gratitude toward my mom, Qing Gu, and my girlfriend, Sixiu Liu, who will also be my wife in the future, for their encouragement, caring, sacrifice, and continuing support during my Ph.D. study. I also want to deeply express how much I miss my dad—Guanghui Li. His strength constantly provided me power and confidence to overcome the challenges in the past years, and will inspire me for the rest of my life.

Chapter 1

Introduction to Carbon Fibers

1.1 Background of Carbon Fibers

Since the first carbon fibers (CFs) were synthesized by Thomas Edison from cotton threads and bamboo slivers in 1879, this type of carbon-based material has been well-developed. It is playing a very important role as a high-performance material in the modern world today. CFs are defined as a type of micro-sized fiber with at least 92 wt.% of sp^2 hybridized carbon atoms that are covalently bonding in order arrangements of one dimension. They are most well-known for their exceptional mechanical properties due to their highly ordered crystalline structure.² The first high-performance CFs were successfully prepared by Royal Aircraft Establishment in 1963 with a tensile strength of 1.7GPa and Young's modulus of 400GPa.³ After decades of extensive study, the CFs produced by modern technology can have a tensile strength of up to 7GPa and modulus up to 900GPa.⁴ Additionally, they have a relatively low density ($1.75\text{-}2\text{ gcm}^{-3}$) and good corrosion resistance to most chemicals except oxidizing agents, such as hot air and flames.⁵ Though the improvement in CFs' mechanical properties has been continually discussed and investigated, the maximum practical tensile strength and modulus of CFs today are still less than 10% and 30%, respectively, compared to the theoretical values of carbon-carbon interaction.⁶ The applications of CFs can be divided into two main sectors: the high technology sector, which has extremely high requirements for material performance, and a general technology sector, which is dominated more by cost constraints and the need for production efficiency and which has lower performance needs. As shown in Figure 1.1, the applications of CFs in the high technology sector include aerospace (aircraft and outer

space), military, high-pressure vessels, and nuclear engineering, while the general technology sector includes automobiles, sporting goods, music instruments, etc.

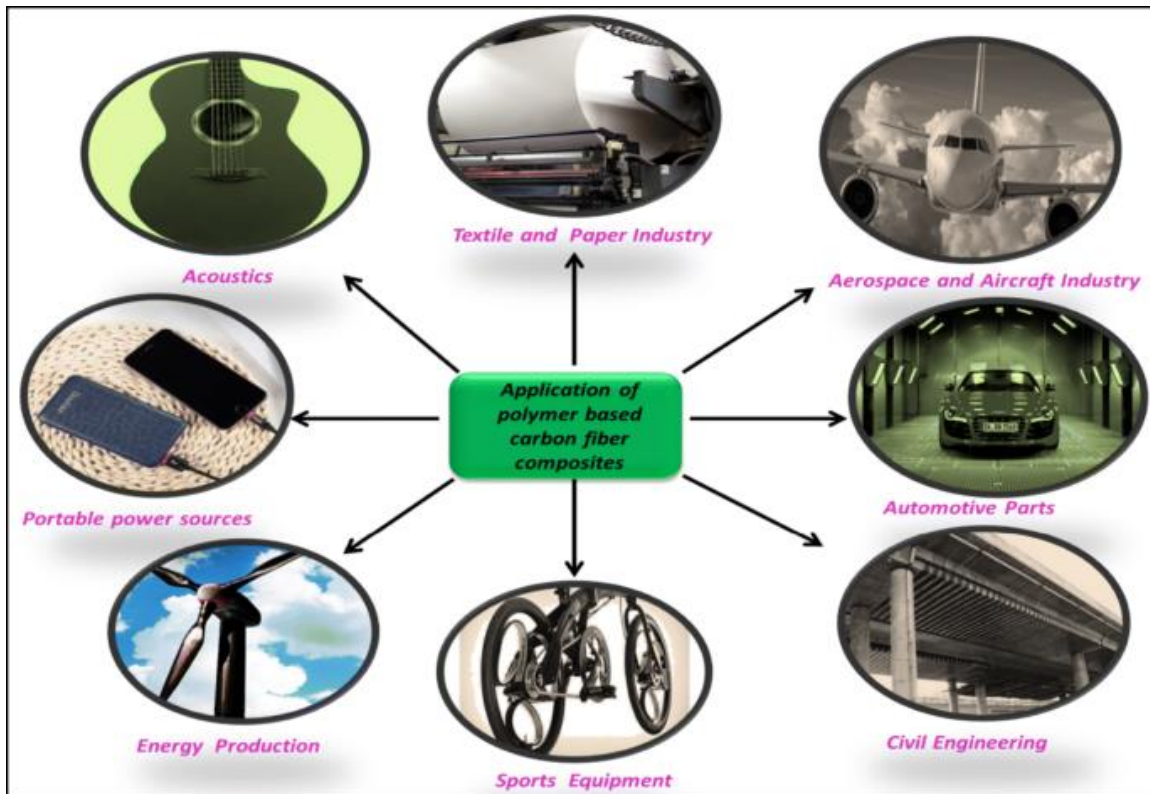


Figure 1.1 The main applications of CFs today.¹

Over the past 20 years, the market for CFs has steadily increased, growing at an average rate of 12% per year; by 2011, the global annual demand reached approximately 45,800 metric tons.⁷ Though CFs are becoming a more significant part in both general and high technology sectors, as mentioned, the scale-up applications of this material in some areas have not yet been well developed, although they show considerable potential. The automobile industry, for example, is currently experiencing a transformation from producing vehicles with conventional internal combustion engines to electric-motor-driven vehicles. To accommodate this change, car bodies need to be built with lightweight material, to increase the mileage per charge for practical use, yet with exceptional mechanical properties, for safety reasons. CFs have been recognized as among the best alternatives to traditional steel for building car body parts such as frames and

doors.⁸ However, this replacement is very challenging and hindered by current production technology because of CFs' high cost and low productivity. We can mostly find CFs on some luxury sports cars in the form of composite with polymer resins such as epoxy. Additionally, due to high resource-intensity, the major global manufacturers of CFs production nowadays include only AKSA (AKSACA), Cytec (Thornel®), Formosa Plastics (Tairyfil), Toho Tenax (Tenax®), Hexcel (HexTow®, HexForce®), Mitsubishi Rayon (PYROFILTM), SGL (SIGRAFIL® C), Teijin (TENAX®), Toray (TORAYCA®), and Zoltek (PANEX®).⁹ It was predicted that in 2020, the CF manufacturing capacity will be 27,132 tons less than global demand (Table 1.1).¹⁰

Table 1.1 Prediction of production capacity and demand in 2020 of CFs.¹⁰

Region	2020 CF Manufacturing Capacity (Red and Zimm 2012) ^a		2020 CF Demand (Industry Experts 2013)		2020 Excess Manufacturing Capacity (Tonnes)
	Tonnes	% of Total	Tonnes	% of Total	
North America	31,487	27.5	33,140	23.4	-1,653
Europe	28,995	25.3	60,550	42.7	-31,555
Asia (Japan and China)	48,149	42.0	43,330	30.6	+4,819
Rest of the world	5,957	5.2	4,700	3.3	+1,257
Total	114,588	100.0	141,720	100.0	-27,132

^a Capacity figures account for projected plant efficiency of 72%.

1.2 Structure of Carbon Fiber

CFs have a polycrystalline structure consisting of parallel stacking of graphene layers made up of hexagonal carbons.¹¹ Their structure is similar to graphite. A single graphite crystal has a graphitic structure with graphene layers regularly parallel to each other with weak Van der Waals force as the interaction. The d-spacing between two graphene layers, in pristine graphite crystal, is 0.335nm.^{12,13} For CFs, the structure can be either turbostratic or graphitic depending on the type of precursor the CF is made from (Figure 1.2).¹¹ CFs precursors are defined as the materials that can be processed and fabricated to fibers and stabilized at a lower temperature before conducting

carbonization. Polyacrylonitrile (PAN) and pitch are two mainstream precursors for CFs production today. CFs derived from PAN have a turbostratic structure. This structure has sp^3 carbon linkages between graphene layers that cause these layers to be packed in a crumbled fashion.^{14,15} Due to the sp^3 linkages and irregular packing, the minimum d-spacing of perfect turbostratic graphite is approximately 0.344nm, which is larger than the d-spacing of pristine graphite crystal.^{16,17} It has been reported that the turbostratic structure plays a significant role in enhancing the tensile strength of CFs due to the stronger covalent bonding as interconnection.¹⁸ By contrast, CFs derived from the pitch show a more graphitic structure after being treated at the same graphitization temperature. Their interlayer d-spacing is less than PAN-based CFs, usually ranging from 0.338-0.340 nm.^{19,20} The more graphite-like characteristic offers the pitch-based CFs relatively higher modulus and lower tensile strength.²¹ The reason why the structure and properties of CFs by pitch vary from PAN is because of their different nature of the carbonization process.²² Pitch has a polycyclic aromatic structure that contains clusters of 6-membered rings. The growth of these rings to a larger graphite network is driven naturally by thermodynamic driving force via dehydrogenation polycondensation at high temperatures. PAN, on the other hand, has a linear polymeric structure with heteroatoms that is very different from pitch. It requires bond breakages and rearrangements to turn from a linear structure to a more stable carbon structure. Therefore, the choice of precursor is extremely essential to CFs' structure and properties as illustrated in Figure 1.3.

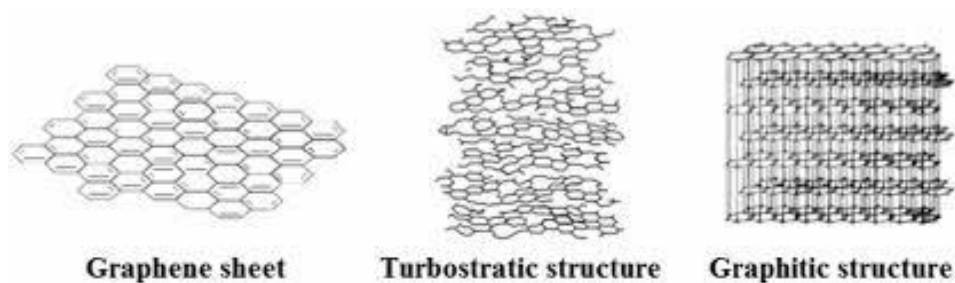


Figure 1.2 Microstructures of the carbon crystal.

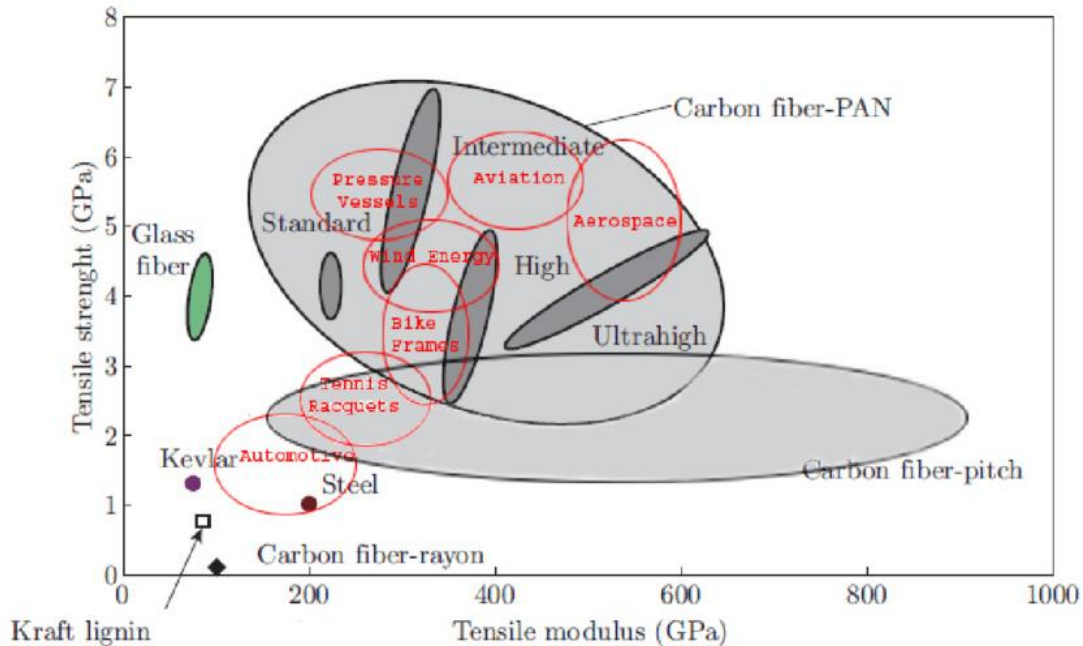


Figure 1.3 Mechanical properties of CFs comparing to mainstream structural materials²³.

1.3 Economics Justifications

Besides its mechanical properties and versatility, cost is another crucial factor for considering whether a structural material can be competitive in the market. Although the price of CFs has dropped to 30 times less than the very beginning, it plateaued at about \$10/lb in the 1980s and has decreased very little in recent years. Steel, in contrast, has a unit price of about \$0.4/lb, which is much cheaper than CFs. The cost of CFs depends on several factors, including raw materials, operating cost, capital cost, etc. To understand the effect of these contributing factors during manufacturing, Nunna et al.²⁴ created a cost model by simulating CF production from PAN in a common facility of 24K tow size, with reasonable considerations of the entire process chain and the costs involved at each stage. Based on their model, the cost of precursor contributes to 53.4% of the total manufactured cost of CFs, which is about three times more than the second biggest contributor (Figure 1.4). Ellringmann et al.²⁵ used a similar method to build a cost model for a facility of 12K tow size and found energy to be the highest cost component at

34%, followed by the precursor cost at 19%. Based on these studies, the influence of cost factors varies depending on the tow size, but the cost of the precursor is always a major contributor to the cost.

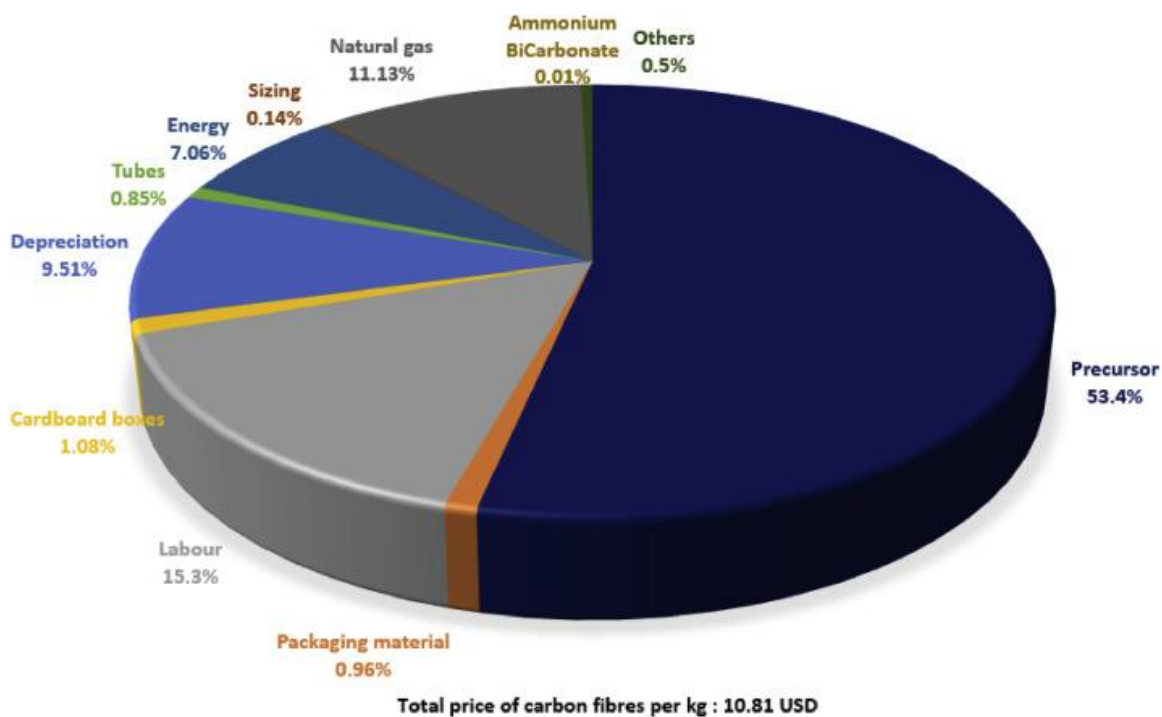


Figure 1.4 The pie chart of cost contributors to PAN-based CFs.²⁴

1.4 Carbon Fiber Precursors in Industry

Today, almost all commercial CFs on market are prepared from PAN and pitch. Additionally, biopolymers that exist abundantly in nature such as cellulose are also being considered in numerous recent studies as low-cost alternatives for CFs production. In general, as shown in Figure 1.5, CFs from all of these precursors are produced by similar steps that first spin the carbonaceous precursor into fiber form. Then, the as-spun precursor fibers are stabilized by the dehydrogenation and cross-linking reaction, usually with the involvement of oxygen, to generate a highly π -conjugated network structure within the fibers and render the fibers infusible. In the end, the stabilized precursor fibers are heated at a high temperature (1200-3000°C) in an

inert atmosphere to remove all of the non-carbon elements and promote the graphite structure, converting the precursor fibers into CFs as a result. Although the conversion of most precursors to CFs follows this route, the processing and treatment conditions vary highly, because the materials involved differ in their physical and chemical properties, such as softening point, decomposition temperature, and solubility.

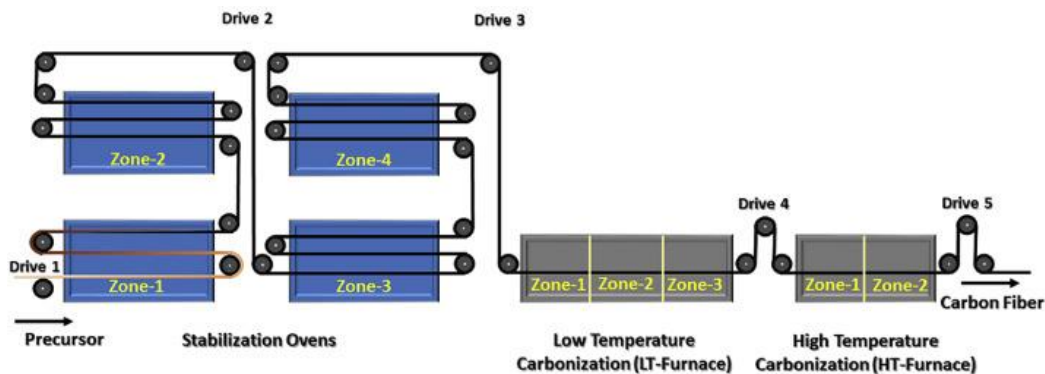


Figure 1.5 A Schematic of carbon fibers manufacturing process.²⁶

1.4.1 Polyacrylonitrile (PAN)

PAN-based fibers occupy more than 80% of the CF production market today. PAN has a synthetic polymer linear structure in chemical formula $(C_3H_3N)_n$ that contains ~68% of carbon content. It is commonly synthesized by free radical polymerization from acrylonitrile either in solution or in water-solvent suspension during mass production. In addition to being a precursor for CFs, PAN is also a versatile polymer used in many other applications, including the precursors of conductive polymer, hollow fibers for reverse osmosis, and fibers for textiles.²⁷

Polymerization

As the monomer of PAN, acrylonitrile cannot be directly obtained from nature. Instead, it is mainly synthesized by propylene ammoxidation on an industrial scale. This reaction requires heterogeneous catalysts such as Bismuth(III) molybdate to increase reactivity and reduce side reactions.^{28,29} The synthetic-only process causes acrylonitrile to become a more expensive

monomer compared to most of the olefins, which can be derived from steam cracking of petroleum and natural gas.

The polymerization of acrylonitrile can be achieved by anionic reaction and free radical reactions in bulk, suspension, emulsion, and solution, while free radical solution and suspension polymerizations are the two most common production methods in industry. Solution polymerization of acrylonitrile is usually carried out in an organic polar solvent such as dimethylformamide (DMF) or dimethyl sulfoxide (DMSO). This adds convenience by allowing the product solution to directly transit into the step of fiber spinning. However, this polymerization method can only produce PAN with a relatively low yield of 50%-70% and low molecular weight, due to greater impurities and chain transfer reactions resulting from the use of solvent. It also requires extra expense and steps to remove and recover the unreacted monomers.^{30,31} Therefore, compared to solution polymerization, suspension polymerization is preferred for production of PAN fibers, although it requires an extra step of dissolution before conducting the spinning process. This method can produce PAN almost without any byproducts and with an easily adjustable molecular weight, as well as a high conversion of >90%.³² All of the commercially produced PAN now on the market has a molecular weight ranging from 70000 to 260000 g/mol, with a polydispersity index (PDI) between 1.5 and 3.5.³³

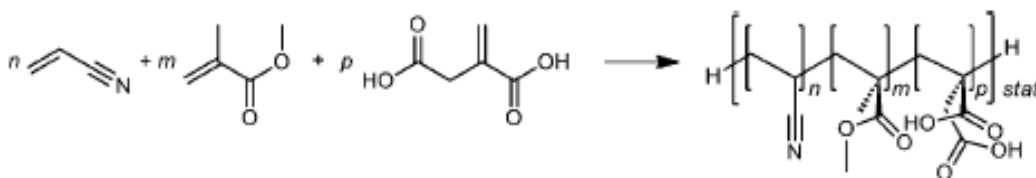


Figure 1.6 Polymerization route of PAN with itaconic acid and methyl methacrylate as comonomers.

Processing

PAN has a high melting temperature of 320°C due to the existence of polar nitrile side groups that offer strong intermolecular forces between the polymer chains. When it is heated in

an inert atmosphere, cyclization happens between these nitrile groups before reaching the melting temperature. Therefore, PAN cannot be processed in a molten state by using the traditional melt-spin technique in industrial manufacturing. Instead, a preferred method in the industry for spinning PAN into fibers is called “wet spinning,” which first dissolves PAN in a solvent and makes a highly concentrated solution before the fiber injection and drawing processes take place. The strong dipole interaction between the nitrile groups means that PAN can only be dissolved in a highly polar organic solvent such as DMF or DMSO, and also in ionic liquids. In a typical wet-spinning process for PAN, the solution is prepared with a concentration value ranging from 15-30wt.%, with a corresponding zero shear-rate viscosity in a range between 10 and 200 Pa.s.³⁴ As shown in Figure 1.6, PAN is usually copolymerized with monomers such as itaconic acid and methyl methacrylate. These comonomer units can effectively enhance the processability of PAN in a solution by improving its solubility, drawability, and spinnability when their content is about 5 mol%.^{35,36}

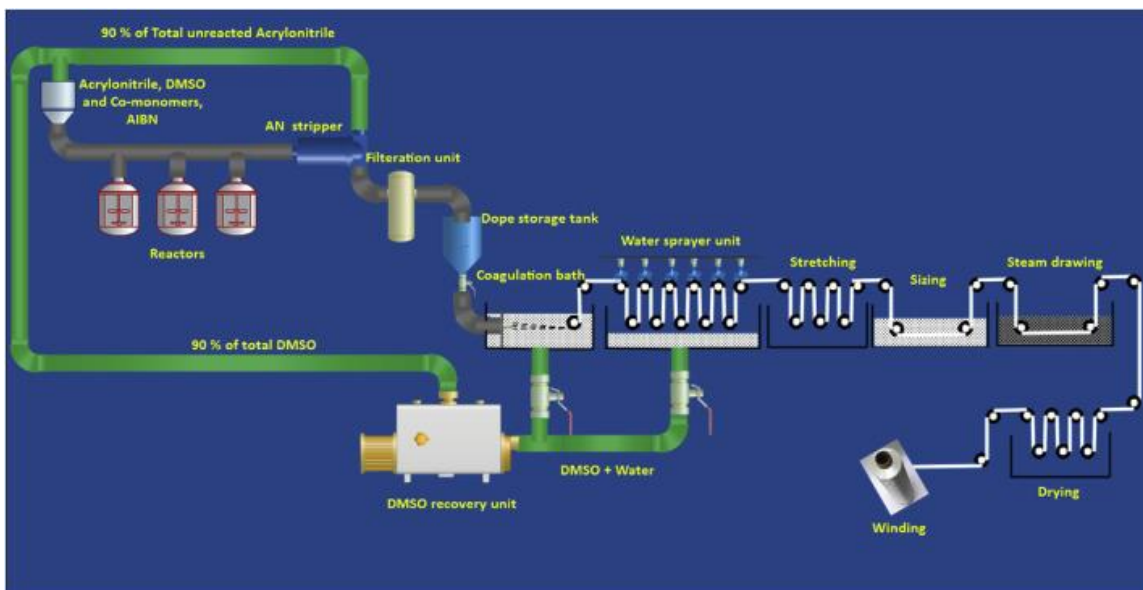


Figure 1.7 Simplified process flow of industrial PAN precursor fiber manufacturing using DMSO solvent.

Figure 1.7 illustrates an industrial production scheme for wet spinning of PAN precursor fibers. After PAN is completely dissolved in a polar solvent, this prepared solution is then spun

through a spinneret with multiple holes and injected into a precipitation media such as a water bath, where both the solidification and coagulation of the polymer happen by extracting organic solvent out of the as-spun fibers. Meanwhile, one end of the fibers is stationary on a take-up godet that provides constant rolling and stretching with water as plasticizer, and hence generates a highly oriented polymeric structure in the fibers. Before moving forward to the heat treatment, the as-spun PAN fibers undergo extra steps of relaxation and drying to remove water and reduce the stress in the supramolecular structure. The wet spinning of PAN not only determines the initial state of precursor fibers before carbonization but has significant effects on the mechanical properties of produced CFs. The effects of spinning conditions have been investigated by researchers to obtain CFs with a better mechanical performance. Masahiri et al.³⁷ at Mitsubishi Rayon Co. discovered that, by applying an ultrasonic wave in the coagulation bath, they were able to improve the strength of PAN precursor fibers due to an assist on the coagulation process. Knudsen et al.³⁸ reported that the shape of the cross-section in PAN fibers can be changed by using a coagulation bath with different temperatures. Moreton and Watt found that, by conducting the entire PAN fiber spinning process in a clean room, they could improve the tensile strength of the final CFs by 80% compared to conventionally spun fibers.³⁹ They postulated that this strength enhancement is due to the removal of small impurities that can initiate crack within the material structure.

Some recent studies on PAN focus on improving the precursor fibers by applying a new fiber spinning technique called gel spinning. Different from the conventional wet spinning, gel spinning starts from preparing a semi-dilute solution with high molecular weight PAN, then turns this solution from a fluid state to a three-dimensional gel network by thermal phase transition at a temperature lower than the gel point before applying stretching on the produced precursor fibers.⁴⁰ Because this improves the polymer orientation and reduction on the defects in the precursor fibers during the coagulation process (Figure 1.8), it has been verified that the CFs

produced from gel spinning have better tensile strength and modulus, as well as larger crystal size and smaller interplanar d spacing than those produced from solution spinning.^{41–43}

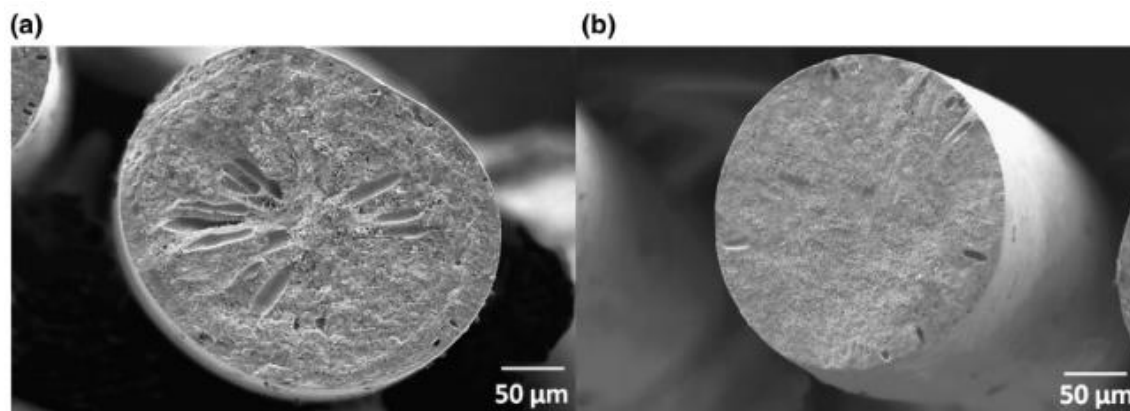


Figure 1.8 SEM micrographs of cross-section for the as-spun PAN precursor fibers fabricated by (a) wet spinning and (b) gel spinning.⁴³

Gel-spinning techniques on PAN can effectively improve the mechanical properties of both the precursor fibers and produced CFs and provide extra potential strategies such as adding cellulose nanocrystal to optimize the spinning and stabilization processes,⁴⁴ However, they do not eliminate the remaining problems of PAN-based CFs, such as costly solvent recovery, expensive polymer, and low carbon yield.

Heat Treatment

To make PAN fibers infusible, as well as increase their carbon yield, a stabilization process with stretching applied must be conducted on them before carbonization. Based on a study by Watt and Johnson, who performed comparative experiments on PAN fibers heating in vacuum and air, there are two steps in PAN stabilization: a prefatory step involving the formation of the cyclic structure without oxygen participation, and a sequent step associated with the oxidation of the cyclic structure in air.⁴⁵

As shown in the scheme shown below in Figure 1.9a, the prefatory step of stabilization is the cyclization reaction by the polymerization of nitrile groups that transforms the polymer into a cyclic ladder structure at a temperature between 200 and 300°C with no oxygen involved. The

mechanism of this cyclization can be explained by “inter/intramolecular jumping of free radicals”—a thermally activated free radical on nitrile group interacts with a pendant nitrile group from a nearby chain segment and creates a new free radical as a return^{46,47} Every agitated free radical can impact 2 to 5 units of segments on average.⁴⁸ Besides generating free radicals, the cyclization reaction can also be conducted under an ionic mechanism with a lower temperature requirement if there are itaconic acid groups present as comonomers in PAN. The heat released from cyclization is reduced, thus preventing damage to the fiber surface and enhancing the quality of the fiber.⁴⁸ Besides itaconic acid, function groups including acrylic acid, methacrylic acid, can effectively improve the stabilization process based on many studies (Figure 1.9b).^{49–51} The formed cyclic ladder structure enhances the thermal resistance and increases the carbon yield of the PAN precursor. This stabilization process also transforms PAN fibers from a linear polymeric structure to a polymer network, and thus results in infusibility of the fibers at a higher temperature.

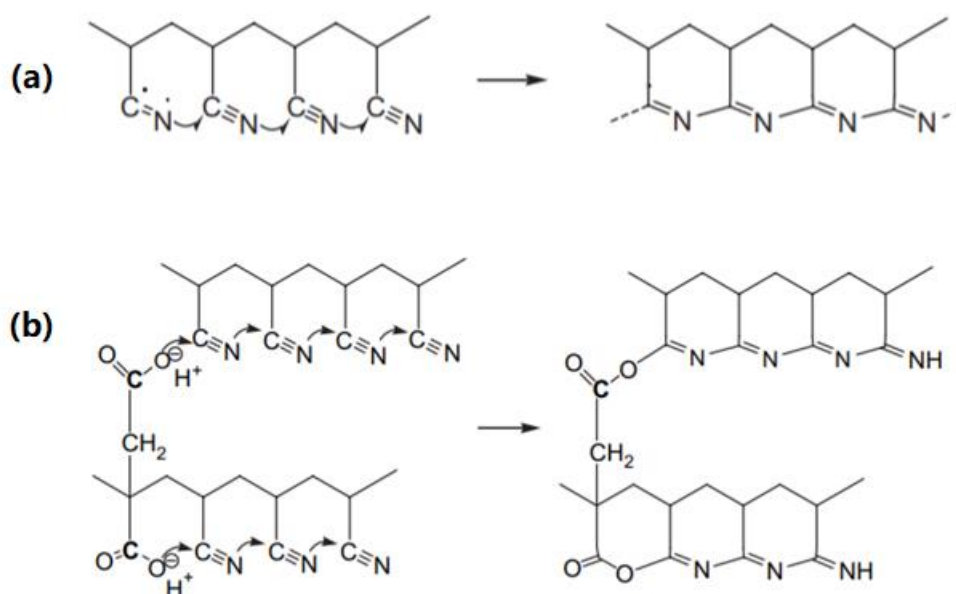


Figure 1.9 (a) Cyclization in PAN initiated through free radical mechanism (b) Cyclization in P(AN-IA) initiated through ionic mechanism.

Though cyclization reactions can happen in an inert atmosphere, to achieve high-performance CFs, the PAN fibers must be stabilized in a sequent step.⁵² In this step, the formed cyclic ladder structure is heat-treated in an oxidizing atmosphere at the same temperature range as the prefatory step. The oxidation reaction promotes the dehydrogenation reactions that generate a more conjugated cyclic structure along the polymer chain. It also introduces oxygen-containing groups such as hydroxyl groups into fibers that assist the coalescence of cyclic structures during the following carbonization process, hence resulting in a final product with a more graphite-like structure. This oxidation process of PAN fibers is highly exothermic. The rapid evolution of heat may cause local overheating, which creates defects within the fibers that diminish the strength of both precursor fibers and produced CFs. Therefore, the oxidation of PAN requires extremely precise control. It is usually accomplished by passing the fibers through an oven that has different heating zones with gradually increased temperatures. Additionally, factors such as line speed, temperature distribution, airflow, oxygen content, and applied tension must be strictly controlled to produce high-quality precursor fibers. After the oxidation process, the density of the precursor would increase from 1.18 to 1.38 g/cm³ with an oxygen uptake of 5-10 wt.%.^{34,53}

Both the prefatory step and sequent step are significant for stabilizing the precursor fibers and increasing their carbon yield. However, due to the slow diffusion of oxygen within the precursor fiber, the surface section always has more oxygen content than the inner core section. This difference causes the surface section to become highly stabilized and densified at the early stage of stabilization, thus preventing the oxygen from diffusing into the inner section. In the core section of fibers, only prefatory reactions happen and cannot be fully stabilized. After carbonization, because the core has more weight loss and less graphitic arrangement than the skin, a heterogeneous structure, or so-called “sheath-core” structure with internal porosities, would be formed that reduces the mechanical properties of CFs.^{46,54}

Besides the reactions involved, the stretching applied on PAN fibers during stabilization also plays an important role in improving the mechanical properties of the CF product. In the

manufacturing process, this stretching is usually applied by controlling the speed differences between rollers. Gupta et al.⁵⁵ found that the stabilization reaction on PAN fibers occurs earlier in the amorphous phase than it does in the crystalline phase. The difference in stabilization rate can result in inhomogeneity along with the whole fiber. Wu et al.⁵⁶ studied the effect of stretching on PAN fibers' microstructure during stabilization at different temperatures and found that the stretching in the range of 160-190°C can effectively orient the disorder regions in the amorphous phase and pack them into an ordered structure. Several reports have shown that stretching can also prevent the relaxation of polymer chains during stabilization, reduce the diameter of the fibers for more thorough oxygen diffusion, and eliminate surface defects.^{57,58}

The stabilized precursor fiber would be continually heated and carbonized in an inert atmosphere with an increasing temperature, as illustrated in Figure 1.10. At 400-500°C, cross-linkages are formed by the condensation reactions between oxygen-containing groups. As a result of the cross-linking reaction, reorganization and coalescence of the previous ladder structure arise and convert the stabilized polymer matrix into a more graphite-like heteroaromatic structure. Meanwhile, nitrogen atoms start to be released in the form of N₂ via a denitrogenation reaction.⁵⁹ As the heating temperature continues to increase and approaches 1000°C, most heteroatoms evolve in the form of volatile compounds such as CH₄, NH₃, HCN, H₂O, and O₂.⁶⁰ At 1000-1600°C, due to the elimination of heteroatoms within the material matrix and the formation of plain graphite layers, a turbostratic structure forms gradually that contains graphite layers oriented in the fiber direction, along with a tetrahedral sp³ carbon linkage between these layers.⁶¹

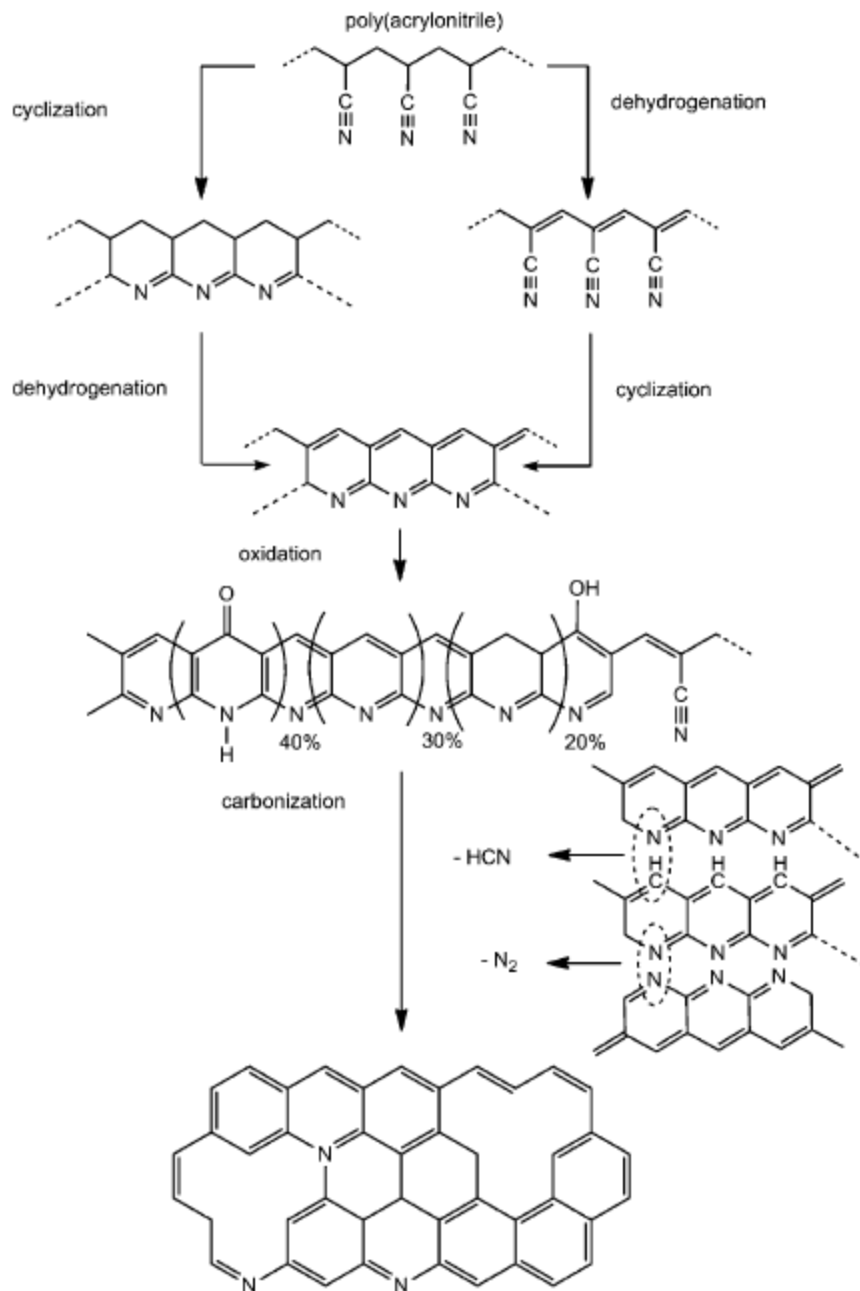


Figure 1.10 Model reaction paths from PAN to a carbon phase.³⁴

Pros and Cons

PAN can produce CFs with high tensile strength because of the turbostratic structure, as well as the improvement in fibers' morphological order that comes from the mechanical stretching applied during stabilization. Additionally, stretching that is processed under good control can heal the defects formed by the released volatiles and thermal relaxation under high

temperatures. However, one disadvantage of using PAN as a CF precursor is that when being heated, PAN begins to undergo thermal decomposition before reaching its melting temperature, making solution spinning the preferred method for drawing PAN into fiber form. The use of an expensive solvent (e.g., DMF) and solvent recovery methods increase the cost and complexity of the processing procedures compared to melt spinning. PAN can only be prepared from synthetic only acrylonitrile; therefore, the cost of PAN fibers contributes 30-50% of the cost of CFs.⁶² PAN also generates toxic gases (e.g., hydrogen cyanide) during heat treatment due to the nitrile groups and may cause severe environmental issues if not handled carefully. Moreover, the carbon yield of common stabilized PAN fibers is below 50%, which may not be sufficient to meet demand in a rapidly growing market.

1.4.2 Pitch

Preparation

Pitch is also used for CF production as an inexpensive precursor, but with a smaller market share than PAN due to its lower mechanical strength. It is usually in the form of complex mixtures of polycyclic aromatic hydrocarbons (PAHs) having some aliphatic side groups (Figure 1.11); their molecular weights range from 200 g/mol to more than 2500 g/mol.⁶³

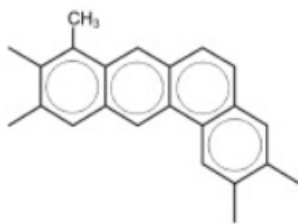


Figure 1.11 Chemical structure (left) and appearance (right) of petroleum pitch.

In general, there are two different types of pitch, based on preparation methods. The first is natural pitch, produced by destructive distillation of petroleum and coal tar. Pitch derived from coal tar contains a high content of carbon particles, which increase the probability of filament breakage during fiber extrusion and heat treatment.⁶⁴ It is also a highly carcinogenic substance, potentially causing lung, skin, and kidney cancers.⁶⁵ The second type, petroleum pitch, is derived from the heavy gas oil fraction of crude oil; compared to coal tar pitch, it is less carcinogenic and contains only trace amounts of carbon particles. Hence, it is preferred as a CF precursor.¹¹ Besides pitches collected from petroleum and coal tar, pitch can also be synthesized by pyrolysis from polyaromatic compounds and polymers; however, the preparation of synthetic pitch requires harsh conditions such as high pressure and temperatures, limiting the scale-up production of this substance.⁶⁶ Both natural and synthetic pitch are classified as isotropic pitch (IP) with isotropic nature and can be converted to general-purpose CFs as long as the precursor has homogeneity and appropriate fluidity. Although isotropic pitch-based carbon fibers (IPCFs) have a relatively low price due to their lower energy cost, they have limited mechanical properties, i.e., 0.5-1.0 GPa of tensile strength, 30-40 GPa of modulus, and 1.2-2.4% elongation.⁶⁷

To obtain high-performance CFs with a tensile strength greater than 2.4 GPa and Young's modulus higher than 380 GPa, the better pitch precursor would be anisotropic pitch, also called mesophase pitch (MP).²² MP is a disk-like liquid-crystalline state of polycyclic aromatic hydrocarbon (PAH) molecules subject to the polycondensation of IP with much smaller molecular weight.⁶⁸ The formation of MP requires heat treatment of IP at a temperature of 350-500°C to conduct dehydrogenation polycondensation and with a long soaking time (from hours to days) to obtain the desired degree of anisotropy. MP also can be prepared from aromatic hydrocarbons such as naphthalene and anthracene by using HF/BF₃ as the catalyst. Using this method, MP with 100% anisotropy can be produced at a much lower temperature of approximately 260°C and a shorter duration of heat treatment (approximately four hours), compared to the preparation method using thermal condensation of IP. The catalytic reaction also

creates extra methyl groups from the fission of aromatic rings; this reduces the softening point of MP to as low as 215°C and increases its oxidative reactivity.⁶⁹ This method was utilized by Mitsubishi Gas Chemical Company in the commercial production of CFs. However, the catalyst HF-BF₃ can potentially cause severe corrosion and health problems. Hence, the commercial production of synthetic MP has been discontinued.

Processing

Although MP is melt-spinnable at a temperature beyond its softening temperature, the processing of this material is very difficult. One of the reasons is that the melt viscosity is highly sensitive to temperature change.⁷⁰ Figure 1.12 shows a comparison of melt viscosity between MP, nylon-6, and IP at different temperatures. It is obvious that MP is more temperature-dependent than nylon-6, and even slightly more sensitive than IP.

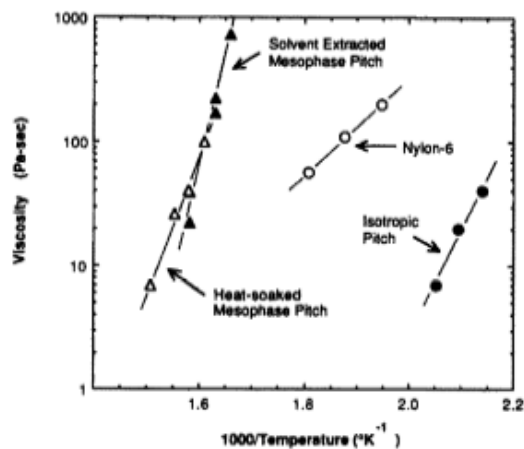


Figure 1.12 The dependence of viscosity on temperature for various pitches and a melt-spun polymer.⁷⁰

A simplified design of the setup for a pitch melt-spinning process is shown in Figure 1.13, with a setup similar to the device for the polymer extrusion. It starts with loading raw material into the melting zone, where it is turned into liquid in a molten state, then densifies along the rotating screw with continued heating beyond the softening temperature of MP. As pressure accumulates, the melt is extruded out of the nozzle holes located at the other end, then turned into fiber form. After cooling by air, the as-spun fibers are wound onto a take-up godet.

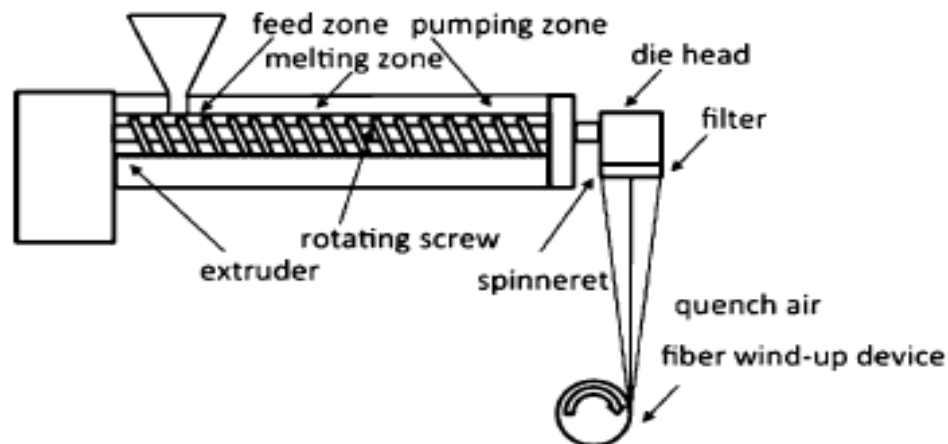


Figure 1.13 Simplified process flow of pitch precursor fiber manufacturing by melt-spinning.

However, compared with the typical polymer extrusion process, the production of pitch fibers has far harsher requirements. Besides the need to carefully control temperature in the melting zone, as mentioned previously, both the spinning temperature at the die head and the nozzle structure have a significant effect on the mechanical properties of CF products, which are both closely related to the CFs' microstructure. MP-based CFs can yield different transverse microstructures depending on the spinning temperature. At a lower temperature, a radial-type structure will be more likely to form due to higher viscosity, while spinning under a higher temperature is more likely to generate the onion-skin-type of structure.⁷¹ Besides the viscosity, the microstructure can also be changed with the orientation of liquid crystals; the orientation is highly dependent on the spinneret geometry. If the MP liquid crystals have a laminar flow when passing through the spinneret, the radial-type texture will form, while the switch to turbulent flow will cause the formation of random texture. Turbulent flow can be achieved by using either a narrower spinneret hole and wider flow path, or the hole with a layer of stainless-steel particles as a filter. It can also be achieved by adding stirring near the nozzle.^{71,72} Mochida et.al⁷³ studied the differences in properties of MP-based CFs with four typical textures: radial, radial-skin/random-core, random, and quasi-onion (Figure 1.14). Although the CFs with these four textures have similar values of L_c , L_a , and degree of preferred orientation, the one with radial texture has the

lowest tensile strength and modulus, while the one with random texture shows the best mechanical properties among all these samples. Nevertheless, the as-spun precursor fibers are both very brittle and have a limited tensile strength of $<0.04\text{GPa}$ that further increases the difficulty of handling in the winding-up process and the following heat treatment steps.⁷⁴ As a result, usually no stretching is applied on precursor fibers during the melt-spinning of either MP or IP.

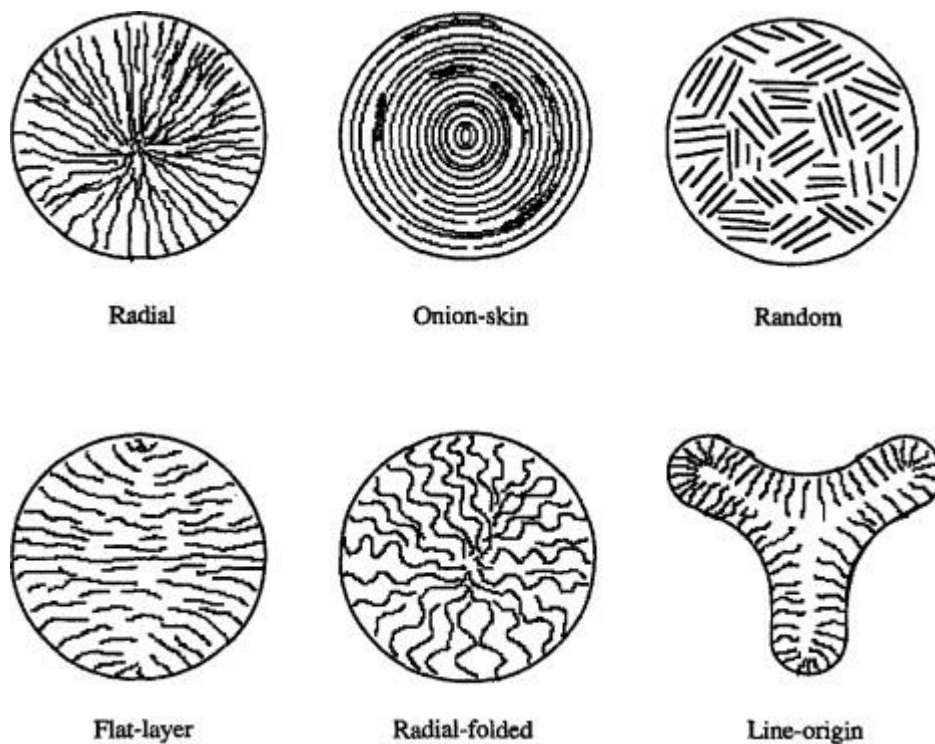


Figure 1.14 Observed microstructures of mesophase pitch-based carbon fibers.¹¹

Stabilization and Carbonization

Figure 1.15 illustrates the thermal conversion processes of the pitch-based precursor fibers, which are stabilized and infusibilized via an oxidation process by exposing these fibers to an air environment at a temperature of 200-400°C for several hours. The role of oxygen is to introduce functional groups such as carbonyl and carboxyl groups that create linkages in the form of covalent bonding between pitch molecules.⁷⁵ After the fibers become infusible, they can be heated to a much higher temperature in the noble gas environment. At approximately 350°C, a

dehydrogenation reaction begins that condenses the adjacent pitch molecules to a more graphene-like structure by creating additional covalent bonds (Figure 1.16).⁷⁶ When the temperature reaches $\sim 1500^{\circ}\text{C}$, heteroatoms such as oxygen and nitrogen are released from fibers in the form of gas molecules, accompanied by some loss of small hydrocarbon fragments. The molecules experience further condensation and reorganization at temperatures greater than 1500°C , resulting in the graphite structure at the end.³⁴

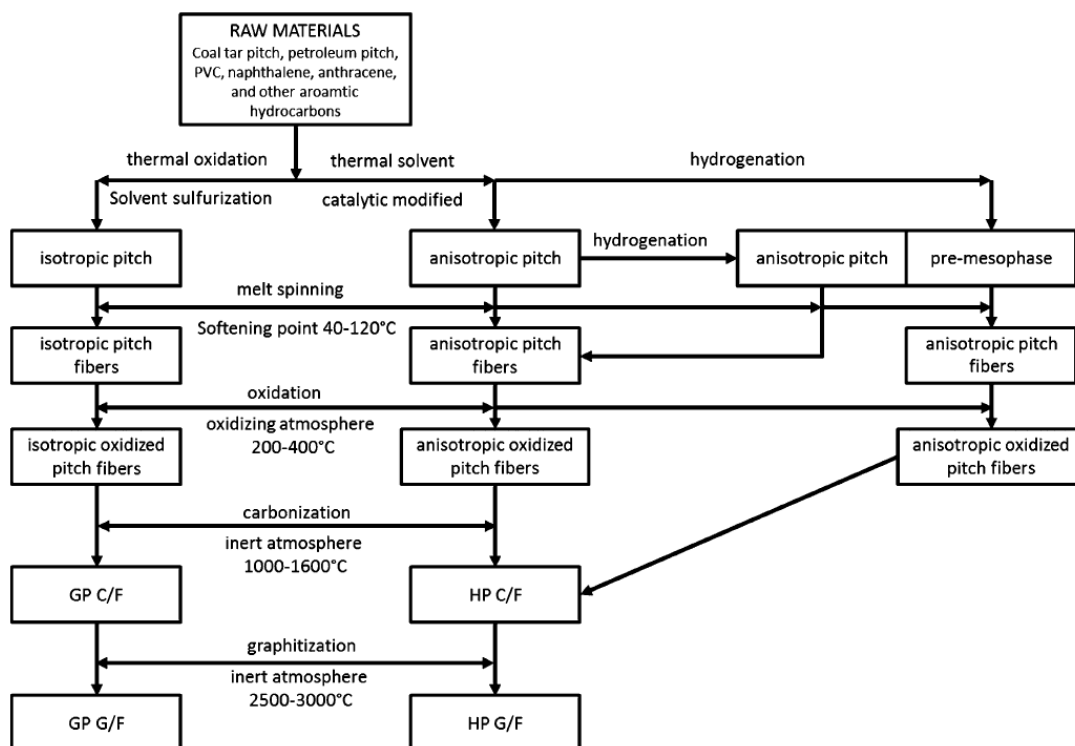


Figure 1.15 Processing steps of CFs starting from pitch as precursor material.³⁴

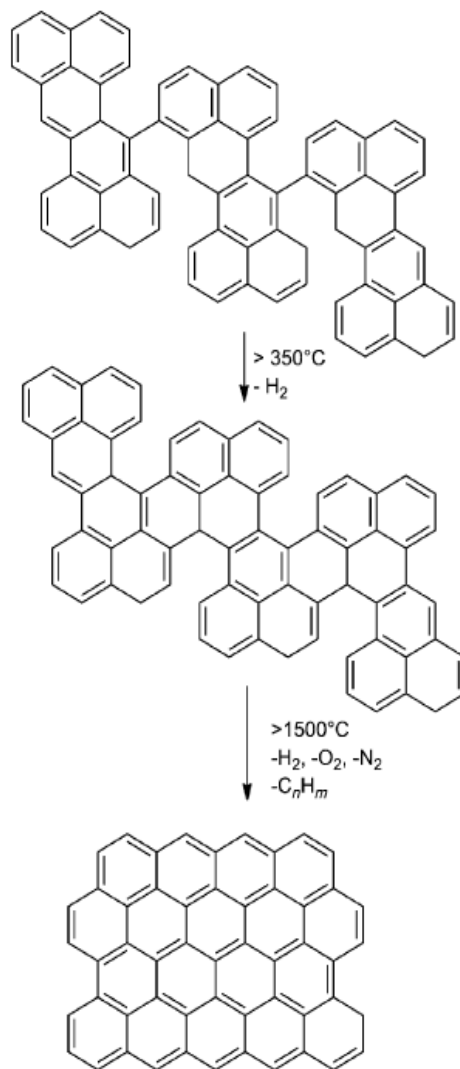


Figure 1.16 Model reaction paths from mesophase pitch to a carbon phase.⁷⁶

Pros and Cons

The major advantages of using pitch as a CF precursor are its low cost and high carbon yield, especially in the case of MP, where carbon yield can reach $>80\%$ due to its extremely high carbon content, as well its large and thermally stable polycyclic aromatic structure.⁷⁷ The cost saving is also from its melt-spinnability, which requires no organic solvent and solvent recovery, compared to PAN.

However, although all of the raw materials for pitch-based CF production are inexpensive due to their abundant existence in nature, the cost of the final products is still high, which limits

them from reaching a large market share like PAN-based CFs. The main reason is that the processing, as mentioned, requires very precise control and complex design to produce high-quality CFs. Additionally, the formation of mesophase requires a long soaking process that inevitably consumes a large amount of energy. Both of these restrictions increase the cost of mass production of pitch-based CFs. In addition, the brittleness and weakness cause the as-spun precursor fiber to become un-stretchable during stabilization and carbonization, while stretching is a key procedure for PAN fibers for elimination of defects.³⁴ Pitch molecules can also form large crystallinities that result in high-stress concentration on grain boundaries.¹¹ Therefore, even with a higher elastic modulus, pitch-based CFs have a relatively lower tensile strength than those made from PAN fibers.

1.4.3 Cellulose

Cellulose is the most abundant organic compound in the world, and has a linear polysaccharide structure consisting of β -1,4-glycosidic linked d-glucose units (Figure 1.17).⁷⁸ It is found in many living creatures such as trees, plants, tunicates, algae, and bacteria. The first use of cellulose to prepare carbon fiber was in 1880, by Thomas Edison, who used the carbon filament to conduct electricity for the light bulb. Decades later, in 1959, Curry Ford and Charles Mitchell at Union Carbide designed an improved method that carbonized cellulose material under a controlled heating process in an inert atmosphere.⁷⁹ In 1965, this type of CF was first commercially produced by Union Carbide by using a hot stretching process.

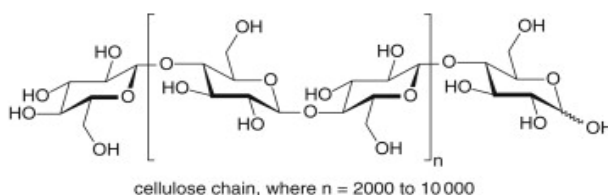


Figure 1.17 Chemical structure of cellulose.

For cellulose-based CFs to have the appropriate mechanical properties for industrial use, they cannot be directly prepared from natural cellulose fibers due to their structural disorderliness, high porosity, and impurities such as hemicelluloses and lignin. Instead, treated materials called regenerated cellulose fibers are used as a precursor; these fibers have a finer structure, higher degree of orientation, and higher purity. They are classified into four major types, based on the production method: 1) viscose rayon fiber, which is prepared by reacting alkali cellulose with carbon disulfide; 2) lyocell rayon fibers, produced from the solution of cellulose with N-methyl morpholine-N-oxide (NMMO) as the solvent; 3) cupro rayon fibers, which are formed by dissolving cellulose into cuprammonium solution followed by a wet-spinning process; and 4) acetate fibers, synthesized by acetylating cellulose using acetic anhydride liquid as a reagent and sulfuric acid as catalyst.⁸⁰ Viscose rayon fiber is the dominant type of regenerated cellulose fiber, occupying more than 93% of the market of cellulose-based CFs today.

The solution-spinning process used in making cellulose fibers involves the injection of cellulose solution into a coagulation bath, followed by stretching and winding processes. The conversion of cellulose fibers to final products also includes heat treatment steps: oxidative stabilization and carbonization. As illustrated in Figure 1.18, the first step of heat treatment is stabilization, which is carried out in the air atmosphere at a temperature greater than 120°C to form a network structure, resulting from inter/intramolecular dehydration between the hydroxyl groups. When the temperature goes beyond 240°C, thermal scission reactions happen along the polymer chains and cause the molecular weight of cellulose to drop dramatically. Meanwhile, small molecules such as CO and CO₂ are eliminated due to the thermal scission, increasing the overall carbon content. The carbon aromatization and formation of carbon crystal structure begin when the temperature reaches 700°C.

The main disadvantage of using cellulose as a CF precursor in the industry is its low carbon yield, which ranges from only 10% to 30%, even with an optimized stabilization

process.⁸¹ Another problem is that the stabilization of cellulose takes hours to finish because of its high sensitivity to heating rate.

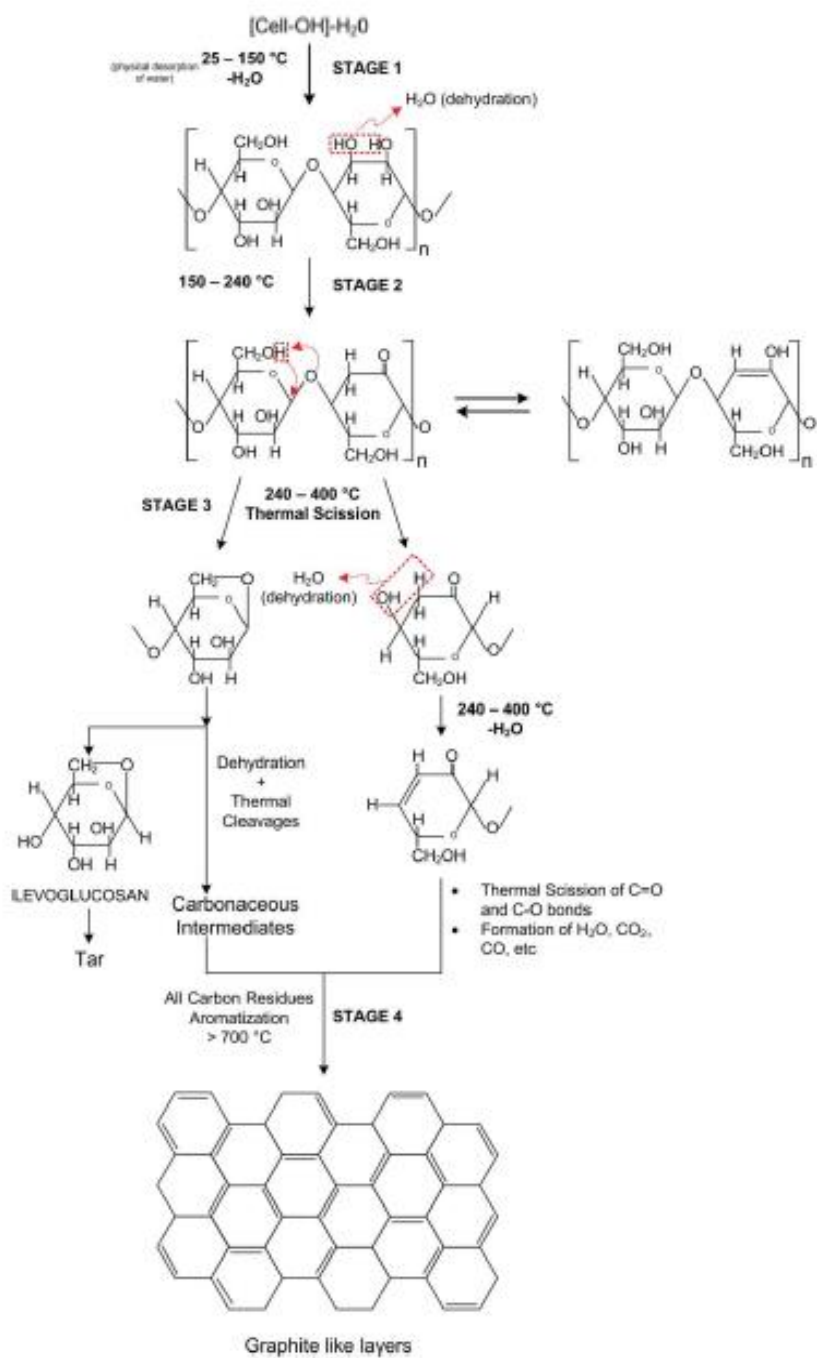


Figure 1.18 Model reaction paths from cellulose to a carbon phase.⁸²

1.5 Recent Studies on Carbon Fiber Precursors

As previously discussed, although the CF industry has progressed considerably since the first appearance of high-performance CFs in 1963, current CF precursor technologies still have significant drawbacks. As the global demand for CFs will continue to grow for the foreseeable future, many recent studies are focusing on improving CF precursors, by either modifying the precursor's chemical structure or blending with additives to make it a binary system.

1.5.1 Melt Spinnable Polyacrylonitrile

As mentioned, the cyclization reaction of PAN happens before reaching its melting point at around 300°C. In industry, PAN fibers can only be spun by solution spinning, which is more costly and hazardous than melt spinning because it requires large amounts of toxic and organic polar solvents such as DMSO and DMF. Hence, much work so far has focused on designing melt-spinnable PAN. An interesting approach is to design PAN with high comonomer content. It is believed that the excessive presence of comonomers can interrupt the ordered structure of PAN, therefore eliminating the crystallinity as well reducing the softening point to make the copolymer melt-spinnable.

Rangarajan et al.⁸³ discovered that when PAN is polymerized with 10% methyl acrylate (MA), it can be melt-spun at 220°C with complex viscosity (a four-order drop of magnitude) compared to PAN that is polymerized with 2 to 7% of MA content. However, the study implies two trade-offs. The first is that the theoretical carbon yield of copolymer would decrease as a result of increasing MA content. The second is that a lower softening temperature can cause the conventional stabilization method to be unsuitable for the spun fibers, although the authors suggest that the viscosity could increase four times with the heat treatment with a long residence time of 30 min at 220°C, which is considered the lower temperature limit for the stabilization

reaction of PAN. As mentioned, the cyclization of PAN is usually conducted at a higher temperature. Without a rapid formation of the cross-linked network structure before reaching that temperature, the precursor fibers may not maintain their form. Therefore, the incorporation of reactive side groups as cross-linking agents is favorable to make melt-spinnable PAN. Naskar et al.⁸⁴ developed a new stabilization method involving UV by incorporating acryloyl benzophenone comonomer as a UV cross-linker into the polymer chains of acrylonitrile and methyl acrylate. The resulting copolymer (PAN-MA-ABP) shown in Figure 1.19 (left) was found to be melt-processable with good thermal stability at 220°C. It can also be rapidly cross-linked when exposed to a high energy UV beam for about one minute. Hence, the premature melting before oxidative stabilization can be eliminated by the addition of UV-cross-linkable ABP comonomers. However, in a later report, Naskar et al.⁸⁵ showed that the tensile strength of the produced CFs is only 400-700MPa, which is much lower than the conventional PAN-based CFs on the market. They concluded that the major problem limiting the tensile strength of produced CFs is that the UV treatment cannot fully cross-link the whole material matrix. The maximum gel fraction that can be achieved is only 65%, based on their results. The advantages of the incorporation of cross-linkable comonomers as a strategy to prepare melt-spinnable PAN has attracted more researchers to follow this route. Deng et al.⁸⁶ reported studying a new type of PAN copolymer (Figure 1.19, right) with 1-vinyl imidazole (VIM) as a comonomer. In addition to reducing the crystallinity of PAN, the presence of VIM comonomers disrupts the strong dipole force within PAN by charge transfer from imidazole groups to nitrile groups. The unsaturated pendant imidazole groups can also stabilize the fiber form via thermal cross-linking reaction. Due to the combination of the disruption on polymeric order and reduction of polar interaction between polymer chains, this copolymer could be successfully melt-spun to fibers at 192°C. Additionally, the rheology and gel-fraction results show that the cross-linking can be finished in two hours with a gel fraction of 90% at 210°C, which is slightly higher than the processing temperature. Later, Mahmood et al.⁸⁷ reported continued work on (PAN-VIM) for a melt-spinnable CF precursor. They studied the

thermal stabilization behavior, carbonization behavior, and mechanical properties of precursor fibers and CFs, and found that the mechanical properties of CFs made from PAN-VIM were improved with higher molecular weight. Among the samples they prepared, the one with 47kDa shows the highest tensile strength of 975MPa and modulus of 158GPa after stabilization, with a carbon yield of about 40%.

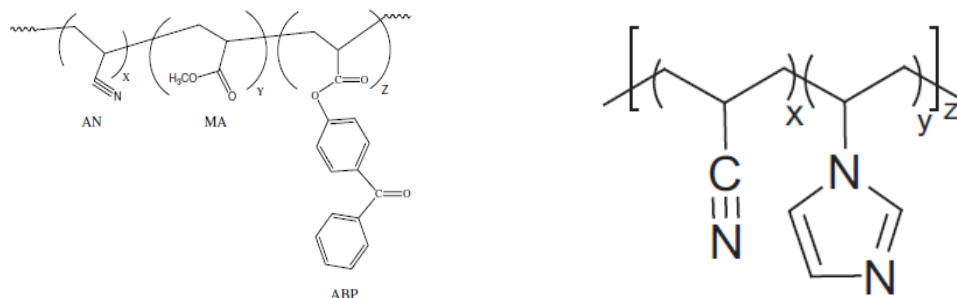


Figure 1.19 Chemical structure of PAN-MA-ABP (left) and PAN-VIM (right).

In general, most of the studies on melt-spinnable PAN have focused on copolymerize acrylonitrile with a high content of comonomer to reduce the softening point. Because the lower softening point may cause the conventional stabilization method to be unsuitable for the PAN copolymers, the most promising way is to incorporate cross-linkable comonomers into PAN to promote the rapid formation of network structure at a temperature slightly higher than the processing temperature, but lower than the temperature of oxidative stabilization. Although these studies provide insightful inspirations for strategies for controlling the melt rheology behavior of the polymer and avoiding premature melting, the carbon yield of the resulting copolymer is lower compare to conventional PAN precursors, because the incorporated comonomers cannot be involved in the cyclization reaction.

1.5.2 Polymer-Lignin Blend

Lignin is the second most abundant natural biomaterial after cellulose. It has a high molecular weight polyaromatic structure, making it a green alternative precursor for CFs. Lignin

can be found in the cell walls of pith, roots, fruit, and bark. It also can be synthesized by dehydrogenative polymerization of monolignol, which is a type of source material for biosynthesis also known as hydroxyl cinnamyl alcohol monomer. As a byproduct of the “wood-free” papermaking process, lignin is commonly burned as a heat source to fuel the chemical recovery process during paper production. As an increasing number of paper mills have stopped this recovery process due to the energy inefficiency and environmental hazard, lignin is losing its role as a fuel in the paper making industry. The abundance and low price of wasted lignin draw the attention of researchers to study its potential use as a precursor for CF production.

The main problem with using lignin as a carbon precursor is that its brittleness and lack of melting property create processing limitations. Blending lignin with a polymer can effectively improve the processability of the material in terms of mechanical properties and melting behavior. Lignin has a highly branched structure with abundant benzene rings that affect its miscibility. Therefore, the compatibility with lignin becomes the most important factor in whether a polymer is a good candidate to blend with. An incompatible blend of polymer and lignin will create porosity after carbonization and therefore produce CFs with a poor mechanical performance for structural applications. In previous studies, researchers found that blending polymers such as polylactic acid (PLA) and polypropylene with lignin caused phase separation due to their incompatibility.⁸⁸⁻⁹⁰ Polymers such as poly (ethylene oxide), polyethylene terephthalate (PET), and PAN are all compatible with the blend.⁹¹⁻⁹⁴ Since PAN has been known as the most mainstream CF precursor with acceptable carbon yield and good properties, most studies focus on investigating the potential of PAN/lignin blends as an alternative to the conventional PAN precursor. Liu et.al⁹⁵ investigated the stabilization kinetics of composite fibers made from PAN and softwood lignin (SWL) and found that the SWL can facilitate PAN cyclization and cross-linking reactions. The fast kinetics is due to the fewer activation energies required for cyclization reaction based on their DSC analysis. Additionally, the incorporation of

SWL allows higher tension to apply on fibers during stabilization, which is also favorable for the PAN cross-linking network formation.

To develop a highly compatible polymer/lignin blend as a CF precursor, Culebras et al.⁹⁶ designed a melt-spinnable polymer/lignin blend based on thermoplastic elastomer polyurethane (TPU) and hardwood lignin. They found the blend not only has a homogeneous morphology that prevents the formation of pores, it also shows good melt-spinning processability because of the good compatibility. The viscosity of this precursor material decreases with higher lignin content and can reach below 100Pa.S at 230°C. The carbon yield of the sample with 30% TPU content can reach a maximum of 40% at 1400°C, slightly less than stabilized PAN. The size of the precursor fibers is in the range of 70-150um and can be further reduced to 50um by applying stretching along the drawing direction. The X-ray diffraction patterns show that after carbonization at 1400°C, the lignin/TPU-based CFs have a carbon crystal structure similar to PAN-based CFs, with d_{002} around 0.37nm, L_a in the range 3.4-3.65 nm, and L_c in the range 0.98-1.08 nm. The produced CFs have a maximum tensile strength of 1100 MPa and maximum modulus of 80 GPa, which was obtained from the lignin and PAN blended precursor with a 50:50 ratio. However, this sample only less than 30% carbon yield at 1400°C.

Synthetic lignin has also been designed and investigated by researchers for use in CF precursors. Xia et al.⁹⁷ synthesized lignosulfonate (LS) -acrylonitrile (AN) copolymer-based precursors, first esterifying LS by reacting with acryloyl chloride to remove the highly reactive hydroxyl groups, then copolymerizing the esterified LS with AN via free radical polymerization; see Figure 1.20. The resulting copolymer overcomes the processing difficulties in fiber spinning due to the highly interconnected structure of lignin, as well as the strong hydrogen bonding caused by the presence of a large amount of hydroxyl groups. The researchers found that the LS-AN copolymer is soluble in DMSO and dimethylacetamide (DMAc) to prepare a solution for wet-spinning. The precursor fibers made from the LS-AN copolymer have significantly fewer micro-voids beneath the fiber surface compared to LS/AN blend-based precursor fibers based on

the SEM images these researchers provided, indicating that phase separation was prevented by copolymerization of LS and AN, while phase separation was still found in a blend due to their limited compatibility. The LS/AN copolymer-based precursor was successfully converted to CFs with a minimum diameter of 12 μ m and maximum tensile strength of ~1100MPa, which is two times higher than the LS-AN blend-based CFs.

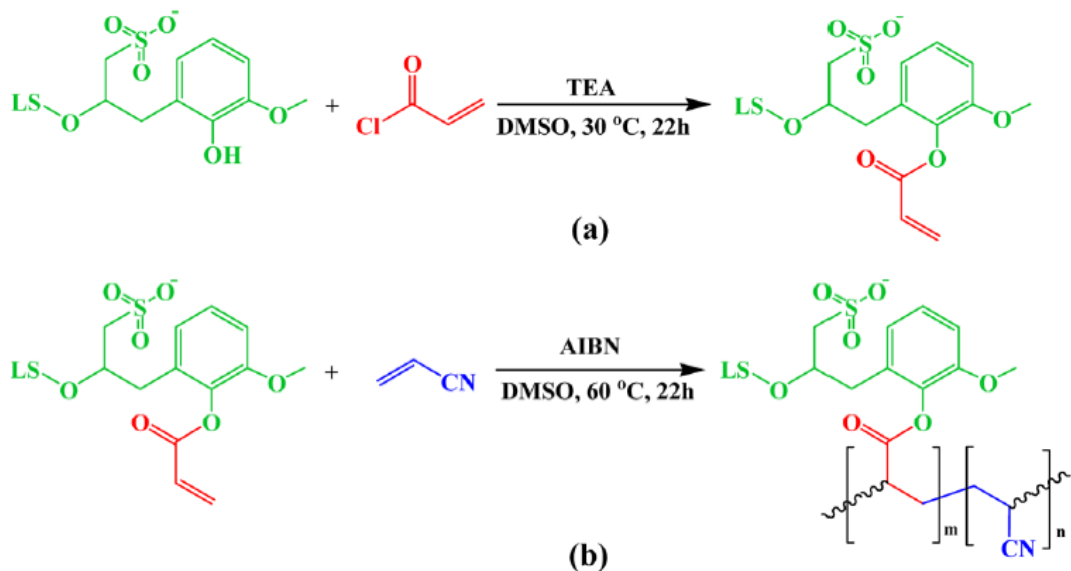


Figure 1.20 Synthesis of (a) esterified LS and (b) LS-AN copolymer⁹⁷

In general, the relative studies on lignin demonstrate an interesting point: that miscibility is the most crucial factor for preparing a CF precursor with binary components. The phase separation formed by two immiscible components can cause the formation of destructive pores in the produced CFs with a greatly negative impact on mechanical performance. Despite the advantages of being eco-friendly and inexpensive, the lignin/polymer blending and copolymerization methods face several inherent limitations. First, lignin does not involve the stabilization mechanism of the polymer; as a result, the carbon yields of resultants prepared by both the blending and synthetic methods are less than those of origin PAN fibers. Additionally, lignin has poor miscibility with many of the polymers. Although PAN/lignin blends do not show obvious phase separation, in the relative studies, the blends were spun to fibers via

electrospinning and gel-spinning instead of the solution spinning that is widely applied in industry, indicating that the processability of the blend is not superior to the PAN precursor.

1.5.3 Carbon-Based Additives

Many recent studies have focused on blending carbon-based additives such as carbon nanotubes (CNTs) to CF precursors. CNTs are large cylindrical molecules in the form of single or multiple sheets of graphene that consists of sp^2 hybridized carbon atoms arranged hexagonally in two dimensions.⁹⁸ They are widely used in applications such as nano-sensors and atomic transportation, because of their exceptional electrical, thermal, and mechanical properties.^{99,100} Additionally, with ultra-high tensile strength ranging from 11-63 GPa and Young's modulus around 1TPa,¹⁰¹ this type of material has also been extensively investigated for its great potential as an additive to enhance the mechanical properties of many types of polymers, including polyethylene, polypropylene, poly(ethylene terephthalate), nylon, poly(vinyl alcohol) and PAN.¹⁰²⁻¹⁰⁶ An advantage of using CNTs as an additive is that their surface can be modified to improve their chemical compatibility in the material matrix and their dissolution properties in the solvent.¹⁰⁷ The reinforcement effect results from their ability to not only increase the rate of crystallization of the polymer but also act as templating agents for polymer chains orientation.¹⁰⁸⁻¹¹⁰ Much attention has also been focusing on using CNTs to reinforce CFs. Results from Chae et.al¹¹¹ found that the tensile strength and modulus of PAN-based CFs can be increased by 64% and 49%, respectively, by adding 1wt.% of CNTs in the precursor. The researchers also investigated the effect of CNTs on the oxidative stabilization of PAN and found that the composite fiber generates much less heat during this process. Additionally, the composite fibers exhibit better-oriented morphology, smaller d-spacing, and larger crystal after carbonization, compared to PAN-based CFs.

These studies explore the potential to further develop the mechanical performance of CFs based on the existing precursors. The addition of CNTs, graphene, and graphene oxide (GO) can also be potentially applied to the new precursors we will discuss later in this thesis. The most common method to synthesize CNTs is chemical vapor deposition (CVD) combined with the usage of catalysts (Co, Ni, Fe, and combination powder). This method starts with the preparation of the substrate with the catalyst particles, which are usually mixed with catalyst supports to increase the surface area. Then the decomposition of a hydrocarbon, such as methane, in the gas phase acts as feedstock and produces carbon atoms that are transported toward the edge of the catalyst particles to form CNTs. Although CNTs can be produced in kilograms via CVD, their price of about \$1000/g on the market would dramatically increase the cost of CFs if CNTs were used as additives. Besides the CNTs, the effect of additives such as graphene and graphene oxide in PAN-based CFs have also been extensively investigated and have proven to be similar to the CNTs in their ability to improve the mechanical properties of the CFs.¹¹²⁻¹¹⁴

1.5.4 Others

Numerous polymers with linear or cyclic structures have also been investigated as possible precursors in commercial production; examples include phenolic polymers, polyvinyl chloride (PVC), polyvinyl alcohol (PVOH), polyamide, polyphenylene, and polybenzoxazole.¹¹⁵⁻¹²² Among all of these polymers, the ones with linear structures can be stretched to fibers in a molten or solution state but also have lower carbon yields than PAN (<50%). The ones with cyclic structure show potential in terms of high carbon yield but pose difficulties in the way they must be processed. The lack of competitiveness in cost and production efficiency compared to the precursors currently on the market limits their further development on an industrial scale.

1.6 Inspirational Studies Relating to Our Works

Most of the studies on CF precursors today still focus on PAN, pitch, and biomaterials such as lignin and cellulose. Although some improvements on the mechanical properties of produced CFs have been achieved in recent studies, such improvements are becoming increasingly limited since most of these materials have been studied for decades, some for more than a century. PAN, the precursor that owns the largest market share, can make CFs with high tensile strength as a result of its polymeric linear structure, but it has limited melt-processability, high cost, and low carbon yield. Pitch as a precursor yields poor mechanical strength and presents difficulties in processing and handling; thus it occupies only a small part of the market. The shortcomings of these precursors are highly related to their inherent chemical structure, thermal properties, and mechanical properties on which only limited modification can be applied. As the global demand for CFs is rapidly growing, the need is urgent for a new type of precursor that meets the following requirements:

- 1) High carbon yield, i.e., more than 50% after stabilization
- 2) Good melt/solution spinnability (viscosity can reach <100 Pa.S at a processing temperature)
- 3) Easy stabilization
- 4) Low cost and energy-efficient on raw material, synthesis, processing, and carbonization
- 5) Comparable or better mechanical strength of the produced CFs, relative to current PAN-based and pitch-based CFs

1.6.1 PE-based CFs Precursors

To achieve these goals, we proposed the design of a new type of functionalized polyethylene (PE) copolymer as a strong starting point. As a type of polyolefin with the simplest

structure of $(C_2H_4)_x$ and with more than 85 wt.% carbon content, PE is one of the most inexpensive polymers in the world that has well-developed production lines. It not only has linear semi-crystallinity structures that are favorable for producing precursor fibers with good mechanical properties, but it also can be synthesized easily via coordination polymerization by using the Ziegler-Natta catalyst and the metallocene/MAO catalyst. Since Karl Ziegler and Giulio Natta invented the Ziegler-Natta catalyst in the 1950s, polymerization involving the utility of transition metal coordination chemistry started a new chapter for industrial manufacturing of polyolefins such as PE, PP, and so on. Conventional Ziegler-Natta catalysts are heterogeneous with multiple active sites, which are composed of titanium or magnesium compounds with an internal electron donor, and aluminum-alkyls are typically used as a co-catalyst during the polymerization. Later in the 1980s, the discovery of the metallocene/MAO homogeneous catalyst system by Walter Kaminsky promoted the synthesis of polyolefins to a higher level in polymer science. By tailoring the homogeneous catalyst with a well-defined organic ligand and single active site, polymer structure and properties including tacticity, molecular weight, and molecular weight distribution, crystallinity, and melting temperature can be controlled more efficiently and accurately.¹²³ The invention of these novel catalyst systems brings new possibilities for producing functionalized PE with desired properties, by introducing comonomers containing heteroatoms and unsaturated side groups in the polymer backbone, via the transition metal coordination process.¹²⁴

The potential of PE as a CF precursor has drawn significant interest among researchers due to its low cost and ease of processing. The pyrolysis of plain PE does not produce any carbon without stabilization by introducing covalent cross-linkages into the polymer structure. PE can be cross-linked by many different methods, including radiation, peroxide, silane coupling agents, and sulfonation.¹²⁵ Among all these methods, sulfonation can reach the highest cross-linking density and therefore becomes the most promising method for converting PE to a CF precursor.¹²⁶ In 1978, the first research work following this direction led to a patent filing by Horikiri et al.¹²⁷

at Sumitomo Chemical Company of Japan. In their study, high-density polyethylene (HDPE) fibers were first sulfonated and stabilized with either chlorosulfonic acid, sulfuric acid, fuming sulfuric acid, or a mixture of any two of them. After carbonization, the resultant fibers were reported to have excellent graphitizability, based on the large size crystal (002) parallel to the fiber axis. In the 40 years since then, the method for preparing CF precursors by PE sulfonation has been extensively investigated and several major improvements have resulted. Postema et al.¹²⁸ observed that low linear density polyethylene (LLDPE) can be stabilized by chlorosulfonic acid at a lower temperature than HDPE. They successfully converted sulfonated LLDPE fibers to CFs with a maximum tensile strength of 1.2 GPa. Younker et al.¹²⁹ investigated the thermal pyrolysis pathway of sulfonated PE by studying the reaction mechanism of heptane-4-sulfonic acid at high temperatures (Figure 1.21). They discovered that a radical chain mechanism is dominated to yield a trans-alkene structure at a temperature below 550°K, while an internal elimination reaction mechanism is dominated to yield cis-alkene structure at higher temperatures. They also studied the effect of the degree of sulfonation on the carbon yield, showing that the fully sulfonated PE fiber gave a maximum charred residue of 40% with an optimized heating rate.

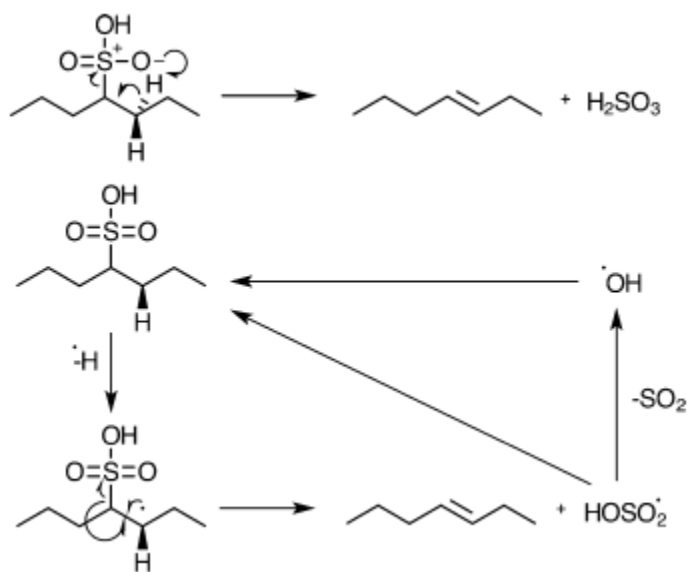


Figure 1.21 Scheme showing E1cB elimination reaction (top) and the radical chain reaction (bottom).¹²⁹

Barton et al.¹³⁰ further investigated the overall mechanism by which PE transforms to carbon from sulfonated C₁₉-C₂₂ and polyolefins by using evolved gas analysis (EGA), elementary analysis, and liquid chromatography-mass spectrometry (LC-MS). They also found that as the PE fibers are treated with sulfonation agents such as sulfuric acid, their chemical structure transforms to a highly conjugated alkene-like system containing functional groups such as carboxylic acids, sulfonic acids, and ketones (Figure 1.22). With a heat treatment at the temperature range 120-220°C, desulfonation reaction occurs within the resultant fibers, accompanied by the formation of an extensively conjugated structure in the form of a cross-linked network. At 600-800°C, dehydrogenation occurs, releasing H₂ molecules from the material and gradually turning it into a more graphite-like structure.

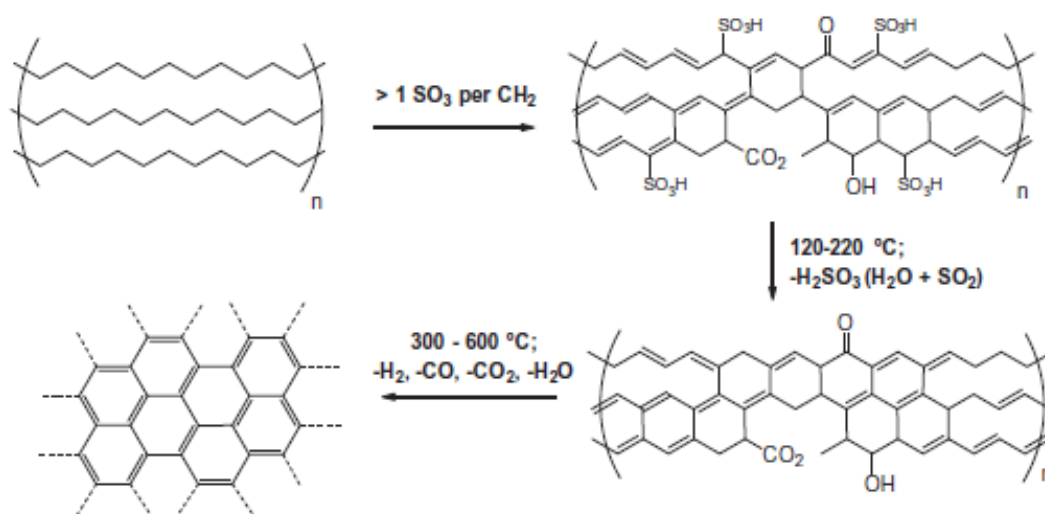


Figure 1.22 A simplified mechanistic transformation of sulfonated PE to carbon.¹³⁰

From the studies described above, we know that sulfonation would increase the carbon yield of PE as a CF precursor. Although the transformation from alkane to a more stable alkene structure with electron delocalization was determined to be a valid stabilization route for PE, the carbon yield of sulfonated PE is still lower than 40%, and thus does not meet the requirement for efficient mass production of CFs. Additionally, sulfonation also requires a large quantity of strong acid that is difficult to recover, causing severe environmental concerns. Therefore, it could

be useful to design an alternate functionalized PE that can follow a similar stabilization route of formation of alkene-like backbones, but be prepared by a more economic and efficient method.

1.6.2 Polymer-Pitch Blend

As mentioned previously, pitch-based CFs have the advantage of high carbon yield and melt-spinnability. However, producing them on a large scale would require overcoming several challenges, including the extremely low strength of pitch precursor fibers, their large energy consumption for coalescence and stabilization, and the low tensile strength of resultant CFs. But what if we can connect the pitch molecules to a polymer such as PE copolymer with the reactive functional groups? PE is a semi-crystalline polymer with a degradation point up to 450°C. When the pitch molecules are connected on linear PE polymer chains, the difficulties in handling could be overcome by the chain entanglements and semi-crystalline structure of PE if side group content is well-controlled, while their melt-processability as pitch derivative could still be maintained. Meanwhile, the resultant polymer could be easily stabilized by cross-linking reactions via polycondensation that create a network structure to infusibilize the precursor fibers more rapidly and efficiently compared to individual and small pitch molecules. Additionally, for a linear polymer with pitch-like side groups, the presence of polymer chains in the material matrix may generate a more turbostratic carbon structure after carbonization that has been proven to enhance the tensile strength of produced CFs, while the pre-existing polycyclic aromatic pitch molecule can form a more graphitic structure to keep the high modulus.

The mechanism of interaction between pitch molecules and polymer during blending at high temperatures has been investigated in several studies. Mochida et al.¹³¹ investigated how the blending of the pitch with PVC changes the oxidation behavior of the pitch. They found that the rate of oxidative stabilization of modified coal-tar pitch by PVC was improved, while the mechanical properties of pitch fibers remained unchanged. The authors did not convert the PVC-

modified coal tar pitch into CFs. The amount of heat released by a faster oxidation reaction would present a drawback by affecting the quality of the CF. They also did not blend PVC with petroleum pitch, because of the low compatibility of the two. This creates a limitation on practical applications because of the much greater presence of insoluble particles in coal-tar pitch compared to petroleum-derived pitch. Hlatshwayo et al.¹³² studied and discussed the rheology and thermal results of pitch/PVC blends with more experimental results. They showed that blends with more polymer content exhibit greater shear-thinning behavior and also showed the improvement of carbon yield after heat-treating the blend in air/O₂ atmosphere at 400°C. However, considering applying it as a precursor material for CF production, the material would be softened and become fusible before reaching the oxidative stabilization temperature that helps improve the carbon yield. Several studies have demonstrated that the formation of liquid crystals in mesophase can be accelerated by adding some polymers in the isophase pitch during heating. Machnikowski et al.¹³³ studied the effect on the formation of mesophase pitch by adding various polymers, including PVC, PS, PET, and PEG, to the coal-tar pitch. They found that both types of polymer above can accelerate the growth of the mesophase unit in the early stage of transformation. They also concluded that this phenomenon is due to the dehydrogenative activity (Figure 1.23) of low molecular weight compounds as a result of polymer thermal degradation. Liu et al.¹³⁴ reported similar findings when they modified and carbonized pitch with PS. The mechanism of the acceleration of mesophase formation on pitch by polymer addition was investigated by Cheng et al.⁷⁶ by using a blend of PE and petroleum pitch, then heating it up to a temperature of approximately 450°C. By studying how the modification of conditions such as temperature and polymer content affect the formation rate of mesophase pitch and its carbonization behavior, the authors concluded that the formation of mesophase is accelerated by the polycondensation reaction between the free radicals on pitch molecules and the free radicals generated from the thermal cleavages of PE at high temperature.

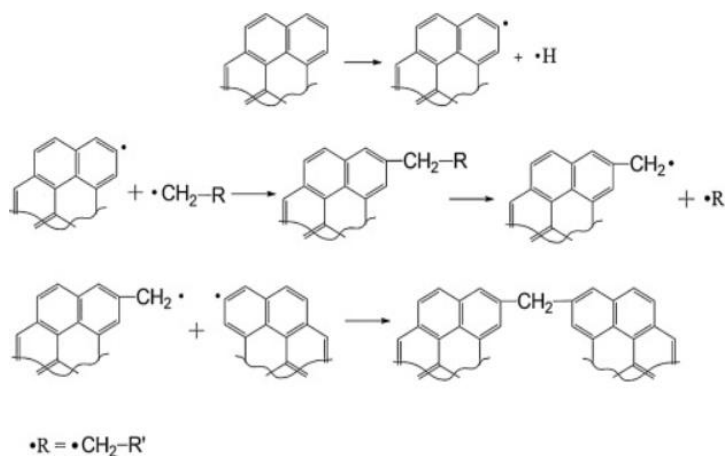


Figure 1.23 Scheme of the condensation reaction of pitch initiated by the formation of free radicals.⁷⁶

However, none of these authors mentioned how the degradation of polymer components affect the polymeric properties of the product after heat treatment. The polymer backbones would break into small fragments at a high temperature, according to these authors, thus resulting in the pitch molecule still interacting with others by weak Van der Waals force instead of covalently connecting to linear polymer chains.

1.6.3 Conclusion

Inspired by these findings, in my thesis study, we focused primarily on designing a new type of PE copolymer with functional groups (-R) that would react with pitch molecules at a lower temperature than the decomposition temperature of this copolymer, to produce a copolymer with a linear PE backbone and pendant groups with polycyclic aromatic structure (Figure 1.24), shortened as 'PE-g-Pitch'.

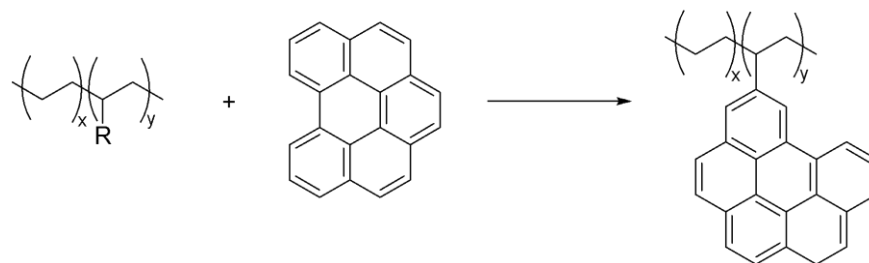


Figure 1.24 The proposed preparation route of PE-g-Pitch.

Several hypotheses were considered to make this copolymer a good candidate for a CF precursor, including:

1. The incorporation of pitch molecules with polyaromatic structure will increase the C/H ratio of the copolymer, therefore increase the carbon yield.
2. The resultant polymer is melt/solution spinnable to produce precursor fibers that can be easily handled.
3. The polycyclic aromatic pendant groups will initiate a stabilization mechanism that converts the saturated alkane structure to an unsaturated alkene structure at a certain temperature.
4. The formed PE copolymer with polycyclic aromatic pendant groups will form a cross-linked network with or without the involvement of an oxidative agent at a temperature lower than its softening point at a rapid rate.

Chapter 2

A New Precursor System Based on Poly(phenylacetylene) Derivatives

2.1 Introduction

In the early stage of our investigation, we first focused on how to design a synthetic hydrocarbon polymer as carbon fiber (CF) precursor that is soluble in common organic solvents for wet-spinning and graphitizable to form carbon material with a high carbon yield. For synthetic polymers, especially polypropylene and polyethylene, despite carbon is the dominant element in their compositions, they are completely decomposed to volatile fragments at the temperature higher than their degradation point even in an inert atmosphere, therefore leaving no carbonaceous residue. To become a successful CF precursor, a synthetic polymer should meet several structural criteria^{135,136} that firstly either have, or can form, polycyclic aromatic hydrocarbon (PAH) moieties during the stabilization step to achieve the carbon conversion. The first example is synthetic pitch that already contains PAH moieties. These PAH moieties can undergo a thermally induced polycondensation reaction and form a more π -electrons conjugated structure during the stabilization step. The second example is polyacrylonitrile (PAN) with the reactive side groups that can effectively *in situ* form PAH moieties under a low temperature condition. PAN does not have any pre-existing PAH group; however, the nitrile side groups can undergo cyclization and dehydrogenation reactions to generate the PAH structure during the stabilization. In the subsequent carbonization of these two CF precursors at a higher temperature, ring fusion gradually takes place to remove heteroatoms and forms the graphitic structures.^{137,138} In addition to the ability to form the graphitized carbon, a proper CF precursor must be solution- or melt- processible for fiber spinning in forming the corresponding precursor fibers, before any thermal conversion reactions.

In this chapter, I will discuss a new CF precursor design strategy by the systematic study of two poly(phenylacetylene) derivatives, including poly(PA-A) with 4-ethynyl side group, and poly(PA-PA) with 4-phenylethynyl side group, as illustrated in Figure 2.1. For their polymer backbones, the presence of π -electrons conjugation increases the bond energy in the C-C bonds along the polymer chain, which increases polymer thermal stability and prevent premature polymer chain decomposition during the stabilization step. In addition, the combination of highly reactive ethynyl side groups and π -electrons conjugation throughout the entire polymer structure (both polymer backbone and aromatic side groups) also offers the favorable cycloaddition reaction that can *in situ* generate PAH moieties at low temperature. During this study, the parent poly(phenylacetylene), shortened as poly(PA), with an π -electrons conjugated structure and more stable phenyl side groups, was investigated as a reference to understand the effects of reactive side groups during the stabilization mechanism and the subsequent carbonization.

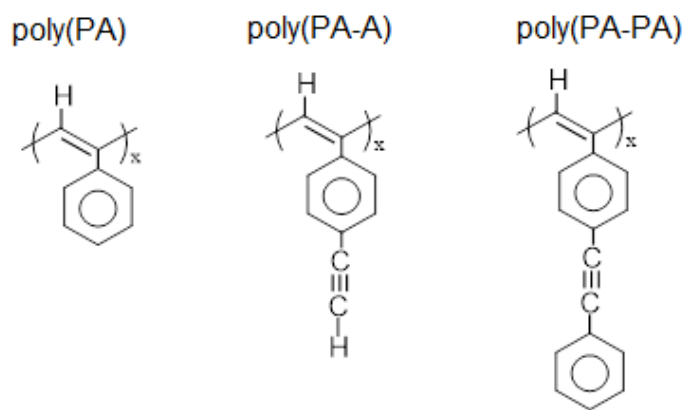


Figure 2.1 Schematic structures of poly(PA) and two derivatives poly(PA-A) and poly(PA-PA) polymers.

2.2 Experimental Section

2.2.1 Materials & Instrumentation

Inert reaction conditions were carried out inside an argon-filled atmosphere dry box or under N₂ flow conditions through a vacuum line. The following chemical reagents, including tungsten (VI) chloride (WCl₆), tetraphenyl tin (Ph₄Sn), 4-bromophenylethynyl, (triisopropylsilyl)acetylene, trimethylsilyl acetylene, tetrahydrofuran, tetrabutylammonium fluoride trihydrate (TBAF) in THF (1M), triethylamine, and calcium hydride were purchased from Sigma Aldrich and used as received. Toluene (WileyOrganics) was distilled over sodium benzophenone under argon. All the ¹H NMR spectra were recorded on a Bruker AM-300 spectrometer, in which the samples were dissolved in 1,1,2,2- tetrachloroethane-d or dichloromethane-d. The ¹³C NMR spectra were acquired using a Bruker AV-III-HD 500 system operating at RT, in which ~1024 scans were obtained, and ~ 10-15 mg samples were dissolved in 1 mL of *d*-1,1,2,2-tetrachloroethane. The FTIR spectra of the powdered samples (128 scans) were obtained using a Bruker Vertex 70 FTIR spectrometer equipped with deuterated triglyceride sulphate (DTGS) detector. The GPC experiments were performed on an EcoSEC HLC-8320GPC (Tosoh Bioscience) equipped with a DAWN multiangle light scattering detector (Wyatt Technology). The thermal transition data were obtained with a TA Instruments Q2000 differential scanning calorimeter (DSC) at a heating rate of 10 °C/min. Thermogravimetric analysis- mass spectrometry (TGA-MS) was performed from a range of 100-1000 °C at a heating rate of 10 °C/min, gas flow rate of 50 mL/min, using a TGA Q5500 instrument coupled with discovery MS under N₂ atmosphere. FEI Nova NanoSEM 630 field emission scanning electron microscopy (FESEM), with a resolution of 1.7 nm, was used to study the morphology of the fibers. The GC-MS measurements were conducted in a spectrometer using a Trace 1310 gas chromatograph coupled to a triple quadrupole mass spectrometer (TSQ; Thermo Scientific). After dissolving 100

ng/ μ l of a sample in hexane, 1 ml of the dissolved sample was injected through the GC inlet that was operated in splitless mode and held at 300°C. Separation was achieved on a TG-5 column (30 m; Thermo Scientific) with initial hold at 40°C (4 min) followed by a ramp of 12.5°C/min to 320°C and a final hold of 7 min. The TSQ was operated in electron ionization mode, with full scan of m/z 30-550. Transfer line and source temperatures were 320°C and 300°C, respectively, were coated with 5 nm iridium before studying their morphologies via SEM. XRD measurements were conducted on a Panalytical XPert Pro MPD theta-theta Diffractometer from Malvern at 40 kV and 40 mA with Cu K(α) radiation $\lambda = 0.15418$ nm. Diffraction patterns were recorded on a 0.8 collimator, with an oscillation of the samples between 10 and 80° and an imaging plate detector. The scan rate was 0.2°/min with an interval of 0.045°. The interlayer distance d002 was calculated using the position of the 002-reflection and Bragg's equation. The crystallite thickness Lc was determined with the (002) reflection and Scherrer's equation while the lateral size La was determined using the (10) reflection and Scherrer's equation. Raman spectra were collected from Horiba LabRam HR Evolution. All of the calculations on XRD and Raman were finished by using Origin software. The SEM images were collected from the Apreo 2 (Thermo Fisher).

2.2.2 Synthesis of Monomers and Polymers

Synthesis of [4-(phenylacetylene)-1-[(trimethylsilyl)ethynyl]benzene

In a 250 mL round bottom flask, 8.04 g (31.8 mmol) of 4-bromo(trimethylsilyl)acetylene was combined with 150 mg (1.7 mmol) of Pd(PPh₃)₂Cl₂, and 129 mg (0.9 mmol) of CuI. The flask was placed under N₂ atmosphere before the addition of triethylamine/THF (150 mL) via a syringe. The solution was stirred for 5 min to allow the reagents to dissolve and 5.12 mL (54 mmol) of phenylacetylene was added to the reaction flask. The solution turned dark brown upon the addition of phenylacetylene. The solution was stirred at room temperature for 4 days. After 4

days, the volatiles were removed in vacuo, and the crude product was purified by column chromatography on a silica gel, with a hexane/dichloromethane mixed solvent used as the eluant, to produce 7.4 g (85% yield) of [4-(phenylacetylene)-1-[(trimethylsilyl)ethynyl]benzene product as a yellow liquid. Data: $^1\text{H NMR}$ δ 0.25 (s, 9 H), 1.12 (s, 21 H), and 7.39 (s, 4 H).

Synthesis of the (4-phenylethynyl) phenylacetylene monomer

In a 100 mL flask, 4.80 g (17.49 mmol) of [4-(phenylacetylene)-1-[(trimethylsilyl)ethynyl]benzene was dissolved in 45 mL of tetrahydrofuran (THF). Then, 1.6 mL of a 1M TBAF/THF solution was slowly added to the solution. The reaction mixture was stirred for 3 h at RT. The reaction was quenched with 30 mL of water and extracted with 3 \times 25 mL portions of diether ether. The combined organic fractions were dried over anhydrous Na_2SO_4 , and the solvents were removed in vacuo. The crude product was purified by column chromatography on a silica gel, with dichloromethane used as the eluant. After drying overnight in air, 2.48 g (70% yield) of (4-phenylethynyl)phenylacetylene monomer was obtained as a yellow powder. Data: $^1\text{H NMR}$ δ 3.15 (s, 1 H), and 7.45 (dod, 9 H). $^{13}\text{C NMR}$ (100 MHz, 1,1,2,2-tetrachloroethane): δ 132.5, 132.1, 131.9, 129.1, 128.9, 124.0, 123.1, 122.1, 91.8, 89.8, 83.7, and 81.8. GC-MS (parent peak, $m/z = 202$)

Synthesis of Poly(4-triisopropylsilylethynyl-phenylacetylene)/poly(PA-ASi)

In a 50 mL round bottom flask, a WCl_6 catalyst (95 mg, 20 mM) and Ph_4Sn cocatalyst (102.5 mg, 20 mM) were dissolved in 6 mL of toluene under inert conditions (N_2). The solution was mixed for 10-15 minutes at 0°C . At the same time, 4-triisopropylsilylethynyl-phenylacetylene monomer (3.39 g, 12 mmol) was dissolved in 6 mL of toluene in a separate flask under N_2 conditions. A syringe was used to slowly transfer the monomer solution into the mixed

catalyst solution. Upon addition, the viscosity of the solution increased, and the stirring rate had to be increased to enable continuous stirring. The solution color gradually changed from dark to red. After stirring the solution for 24 h at 0°C, the solution was extremely viscous and stopped stirring. The reaction was quenched by the addition of MeOH to the solution. The product was isolated and purified with a MeOH/HCl solution. The reaction yielded 3.226 g (95%) of poly(4-triisopropylsilylethynyl-phenylacetylene) after drying under vacuum at 80°C. The resulting poly(PA-ASi) polymer is a fine dark red polymer with polymer molecular weight ($M_n = 274$ kg/mol and dispersity = 1.90), based on GPC measurement with a light scattering detector. Data: IR (KBr) ν (cm⁻¹): 2870-2964 (s, C-H), 2153 (s, C \equiv C-Si), 1469-1505 (s, C=C-H)). ¹H NMR (400 MHz, 1,1,2,2-tetrachloroethane-d): δ 1.10 (s, 21H), 6-7.5 (C₆H₄) and (H-C=C) (broad, 5H).

Synthesis of poly(4-ethynyl-phenylacetylene)/poly(PA-A)

In a 100 mL round bottom flask under an N₂ atmosphere, 24 mL of tetrahydrofuran (THF) was added to poly(4-triisopropylsilylethynyl-phenylacetylene)(0.980 g, 3.47 mmol) powder. The solution was stirred for 30 min to ensure the formation of a homogeneous dark red solution. Tetrabutylammonium fluoride trihydrate (TBAF) in THF (0.861 mL, 0.861 mmol) was then added dropwise to the solution. The solution color turned dark black after the addition of a few drops of TBAF solution. Upon completion of the addition of TBAF, solid particles started to form at the bottom and on the walls of the flask. The mixture was stirred at room temperature for 1 h. The reaction mixture was precipitated by the addition of 9 mL of methanol to the solution. A huge black lump of polymer was isolated, which was purified with THF several times. The compound was dried under vacuum at 80°C overnight to yield 0.283 g (65%) of the poly(PA-A) polymer. Data: FTIR (KBr) ν (cm⁻¹): 2105 (s, C \equiv C-H) and overtone 3289 (s, C \equiv C-H), 1505 (s, C=C-H).

Synthesis of Poly(4-phenylethynyl-phenylacetylene)/poly(PA-PA)

In a 50 mL round bottom flask, a WCl_6 catalyst (23.7 mg, 10 mM) and Ph_4Sn cocatalyst (25.6 mg, 10mM) were dissolved in 3 mL of toluene under N_2 atmosphere. The solution was aged for 10-15 minutes at 0°C . In another flask, 1.2 g (5.9 mmol) of (4-phenylethynyl) phenylacetylene monomer was dissolved in 3 mL of toluene under N_2 . A syringe was used to add the mixture slowly to the aged catalyst. Upon adding the monomer, the viscosity of the solution increased, and the color of the aged solution gradually changed from dark to dark-red. The solution was left to stir for 24 h at 0°C . After 24 h, the solution was extremely viscous and could not be stirred. The reaction was quenched by the addition of MeOH to the solution. The product was isolated and purified with an MeOH/HCl solution. After drying under vacuum at 80°C , the reaction yielded 0.98 g (82%) of poly(PA-PA) as a dark red polymer solid with molecular weight ($M_n=141$ kg/mol and dispersity= 1.25), based on GPC measurement with a light scattering detector. Data: ^1H NMR (400 MHz, 1,1,2,2-tetrachloroethane): δ 6-7.5 (C_6H_4), (C_6H_5), and ($\text{H-C}\equiv\text{C}$) (broad, 10H), ^{13}C NMR (400 MHz, 1,1,2,2-tetrachloroethane): δ 89.8, 123.1, 128.4, 131.6.

2.3 Results & discussion

As illustrated in Figure 2.2, the preparation of poly(4-ethynyl-phenylacetylene), i.e., the poly(PA-A) polymer precursor, involves the Ziegler-Natta catalyst ($\text{WCl}_6/\text{Ph}_4\text{Sn}$)-mediated polymerization of a silane-protected 4-triisopropylsilylethynyl-phenylacetylene (PA-ASi) monomer and the subsequent de-protection reaction of the resulting poly(PA-ASi) polymer, i.e., poly(4-triisopropylsilylethynyl-phenylacetylene).

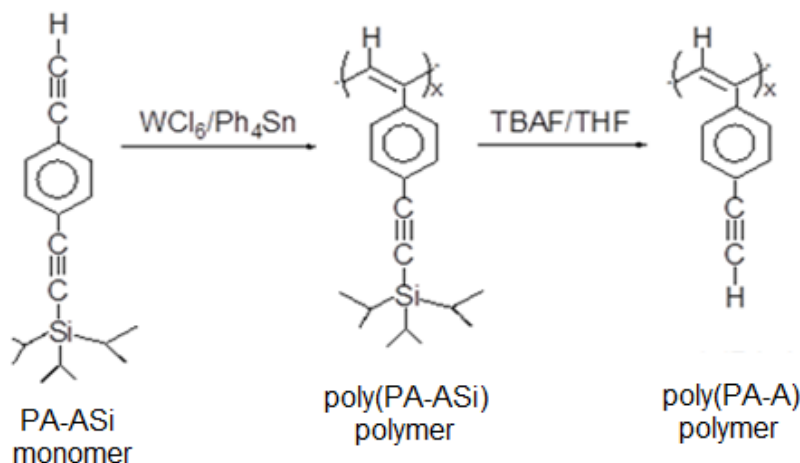


Figure 2.2 The reaction route to prepare poly(PA-ASi) and poly(PA-A) homopolymers from 4-triisopropylsilylethynyl-phenylacetylene (PA-ASi) monomer.

The polymerization of the silane-protected monomer was carried out by using the WCl_6/Ph_4Sn Ziegler-Natta catalyst in toluene at $0^\circ C$ for 24 hours. This coordination-insertion mechanism was highly effective in the polymerization of phenylacetylene derivatives, as shown in previous papers.^{139–141} The resulting poly(PA-ASi) polymer was isolated with a 90% yield as a dark red solid that is soluble in common aromatic solvents, such as toluene. Figure 2.3 compares the 1H NMR spectra of the PA-ASi monomer and the resulting poly(PA-ASi) polymer. The sharp chemical shift at 3.23 ppm, corresponding to the acetylene proton in the monomer, completely disappears in the poly(PA-ASi) polymer spectrum, but the same two proton peaks at 1.12 and 1.65 ppm, corresponding to the methyl and tertiary protons in the triisopropylsilyl protecting group, respectively, are present in both spectra. As expected, this Ziegler-Natta polymerization reaction only involves a terminal acetylene group (not the internal silane-protected acetylene). Note the new and very broad aromatic/olefinic peak at approximately 7 ppm, indicating that a fully π -electron conjugated sp_2 carbon structures are presented along the poly(PA-ASi) polymer chain. Overall, the reaction scheme offers an effective and efficient reaction process for preparing the poly(PA-ASi) polymer.

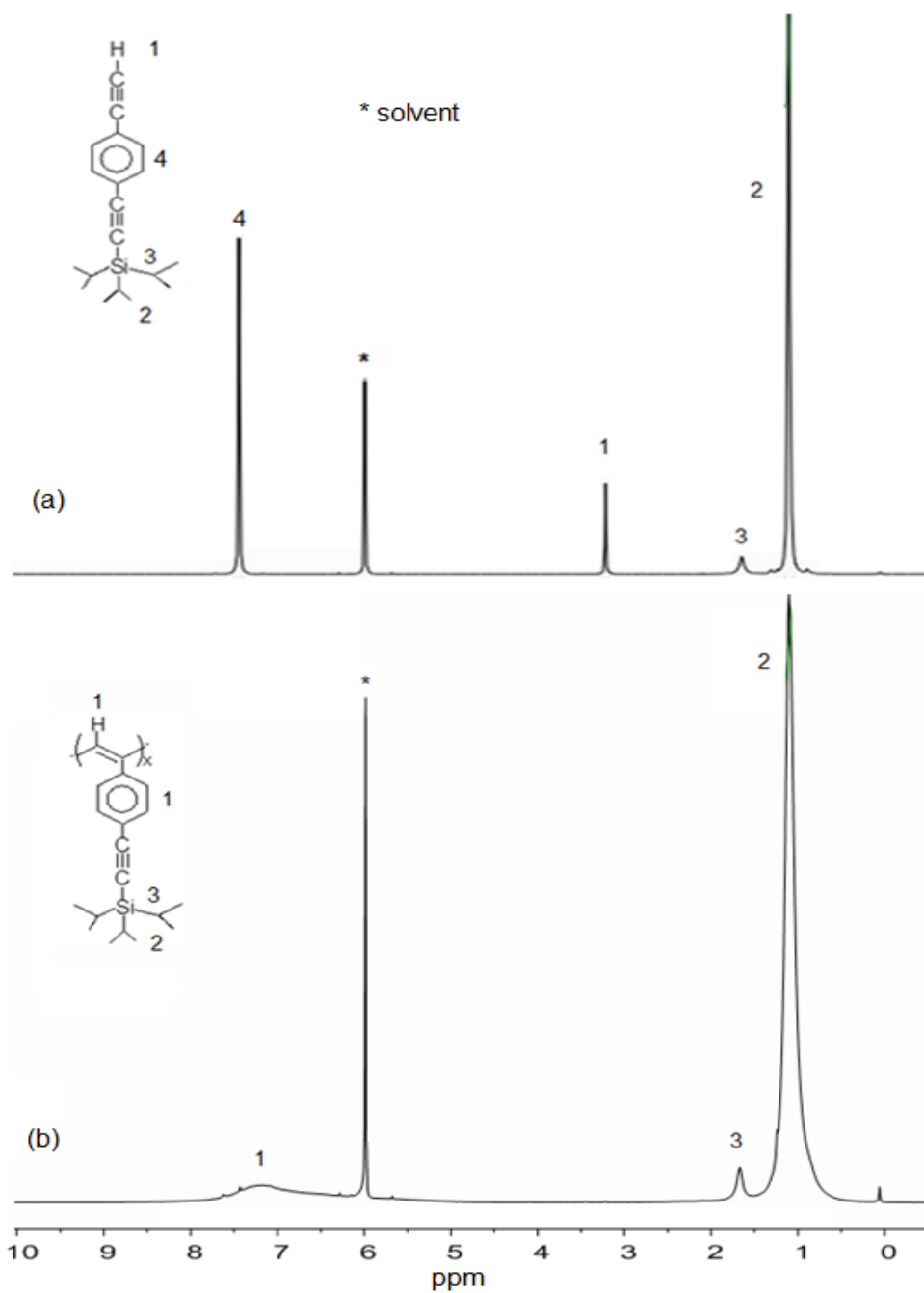


Figure 2.3 ^1H NMR spectra of (a) 4-triisopropylsilylethynyl-phenylacetylene (PA-ASi) monomer and (b) the corresponding poly(PA-ASi) polymer.

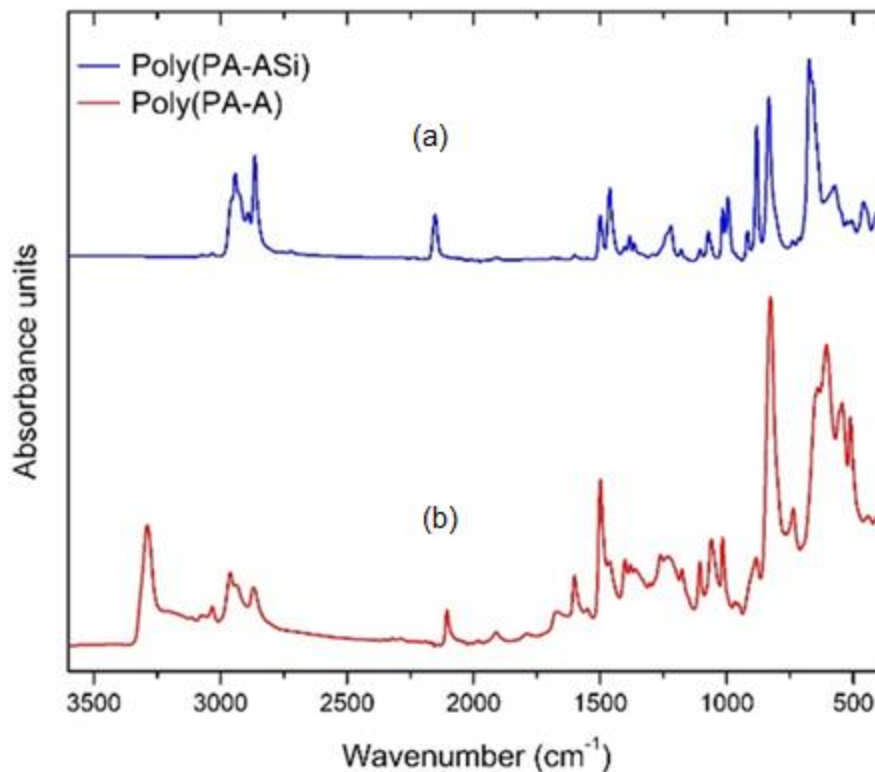


Figure 2.4 FTIR spectra of (a) poly(PA-ASi) and (b) poly(PA-A) polymers.

As illustrated in Figure 2.2, the resulting poly(PA-ASi) polymer was further converted to the poly(4-ethynyl-phenylacetylene) (poly(PA-A)) polymer precursor by removing the triisopropylsilane protecting group. This de-protection reaction involves the strong base tetrabutylammonium fluoride trihydrate (TBAF) in THF at room temperature. The resulting poly(PA-A) polymer is a dark orange solid, with limited solubility in organic solvents, such as aromatic hydrocarbons, THF, and CHCl_3 . The combination of reactive terminal acetylene side groups (without a protecting group) and a relatively rigid polymer backbone (with a fully p-electron conjugated structure) may result in some cross-linked units (by light or heat) or/and crystalline domains that reduce the overall polymer solubility at ambient temperature conditions. Figure 2.4 compares the FTIR spectra of poly(PA-ASi) and poly(PA-A) polymers, before and after the silane de-protection reaction. The presence of the $\nu(\equiv\text{C-H})$ band at 3293 cm^{-1} , corresponding to the terminal acetylene group, and the absence of the $\nu(\text{C}\equiv\text{CSi})$ band at 2153 cm^{-1}

¹ are evidence of the effective desilylation of the protected acetylene group in the side chains. The result is further supported by the large reduction in the absorption band intensity in the region from 2800 to 3000 cm^{-1} , which is mostly associated with the $\nu(\text{C-H})$ vibrational bands of isopropyl groups.

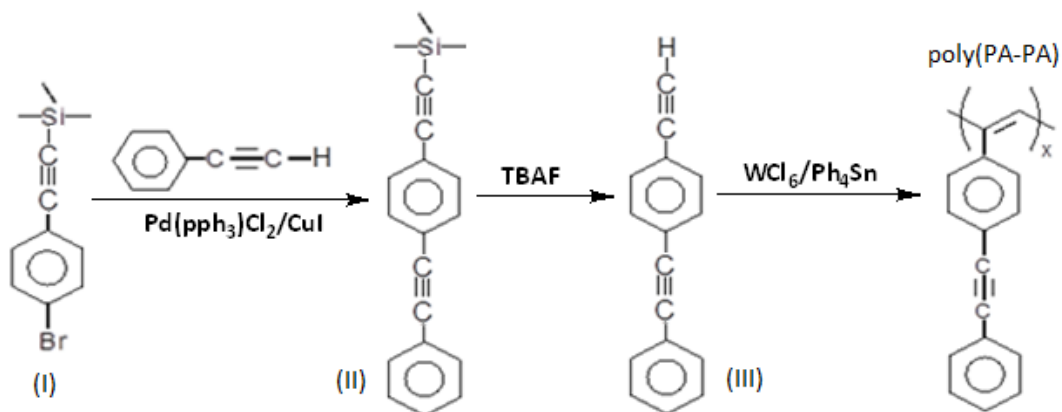


Figure 2.5 Reaction route to prepare 4-phenylethynyl-phenylacetylene monomer (III) and the corresponding poly(PA-PA) polymer.

The combination of multiple reaction steps and the limited solubility of the poly(PA-A) polymer prompts us to search further for a poly(phenylacetylene) derivative that is soluble and does not require silane protection during polymerization. Ideally, the new acetylene-protecting group can also be incorporated into the graphitic structure during thermal conversion. Thus, we decided to investigate a poly(PA-PA) polymer that has a phenylacetylenyl side group in each monomer unit along the poly(phenylacetylene) chain. The internal alkyne groups are more stable during and after polymerization, and the bulkier side groups create more free volume to improve the polymer's solubility in common organic solvents. As illustrated in Figure 2.5, the preparation of the 4-phenylethynyl-phenylacetylene monomer (III) involved two reaction steps. The first step was a similar palladium-catalyzed Sonogashira cross-coupling reaction between 4-bromophenylethynyl-trimethylsilane (I) and phenylacetylene to form the intermediate of 1-(trimethylsilyl)ethynyl-4-phenylethynyl benzene (II). This aryl-acetyl coupling reaction was highly selective and also resulted in a quantitative yield.

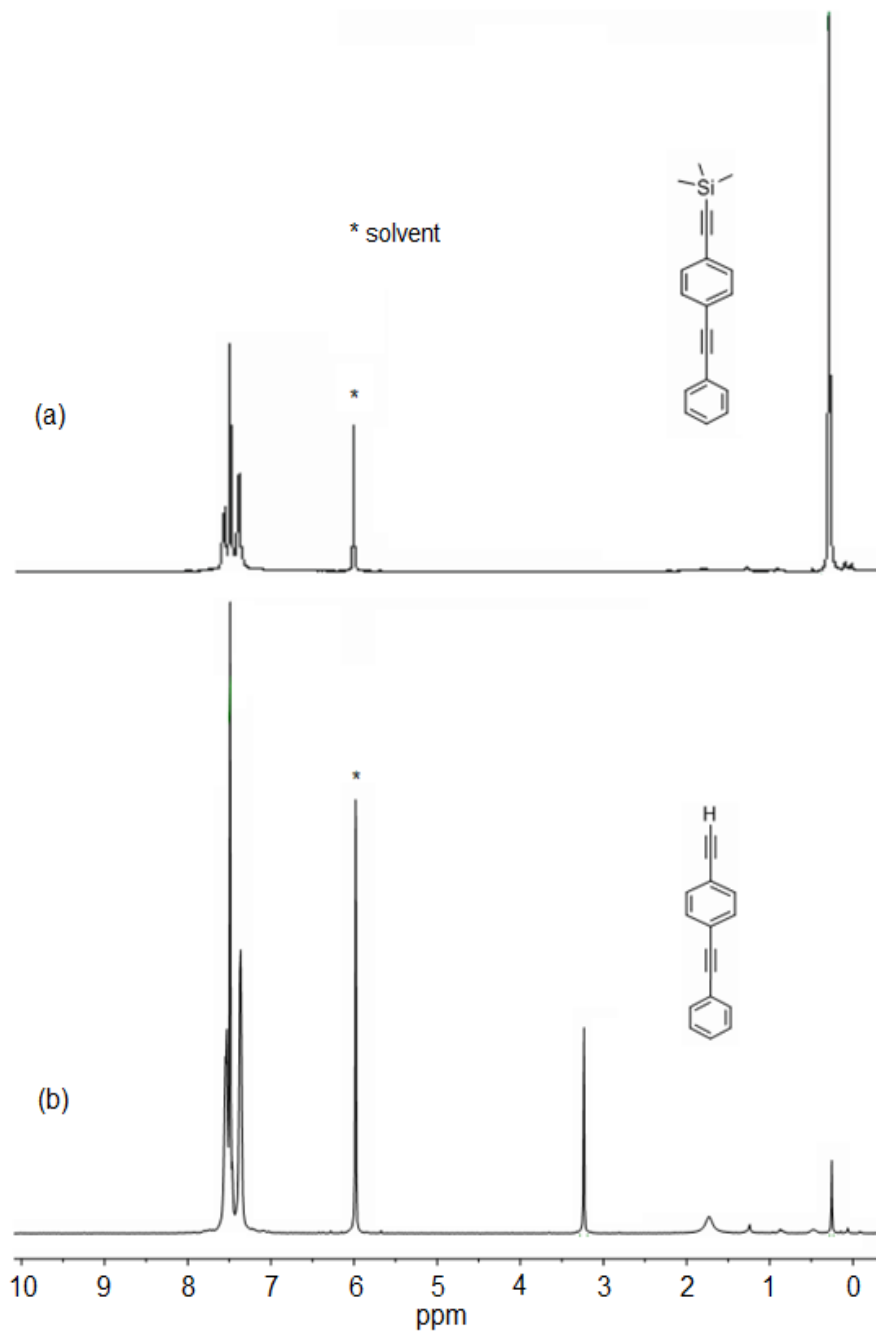


Figure 2.6 ^1H NMR spectra of (a) 1-trimethylsilylethynyl-4-phenylethynyl benzene intermediate (II) and (b) the corresponding 4-phenylethynyl-phenylacetylene monomer (III).

Figure 2.6(a) shows the ^1H NMR spectrum of the resulting 1-trimethylsilylethynyl-4-phenylethynyl benzene (II) compound, exhibiting the chemical shifts expected for aromatic protons and methyl protons in the silane group and a near 1:1 peak intensity ratio. The second reaction step was a de-protection reaction that removed the trimethyl silane group by TBAF

(tetrabutylammonium fluoride trihydrate) in THF at room temperature. Figure 2.6(b) shows the ^1H NMR spectrum of the resulting 4-phenylethynyl-phenylacetylene monomer (III), including both the expected peaks for aromatic protons at 7.3-7.7 ppm and acetyl protons at 3.23 ppm and a minor silane peak at 0.25 ppm (indicating some incomplete de-protection reactions). Since the minor silane-protected reagent does not interfere with polymerization, we decided to apply the same $\text{WCl}_6/\text{Ph}_4\text{Sn}$ -mediated Ziegler-Natta polymerization of 4-phenylethynyl-phenylacetylene monomer in toluene at 0°C for 24 hours to form the corresponding poly(PA-PA) polymer precursor (red solid) with a high yield ($>75\%$). This poly(PA-PA) polymer showed a very good solubility in common organic solvents, including THF, toluene, and xylene, at ambient temperature. Figure 2.7 shows the solution ^1H and ^{13}C NMR spectra of the resulting poly(PA-PA) polymer. In the ^1H NMR spectrum, there is only a major (broad) proton band in the range of 6.5-7.8 ppm, corresponding to all of the aromatic protons in the side groups and alkenyl protons in the polymer backbone with a fully π -electron conjugated structure. The carbon peaks in the ^{13}C NMR spectrum provide more detailed information; they show that the chemical shift at 90 ppm corresponds to the acetylene carbons and the chemical shifts between 120 and 140 ppm correspond to the aromatic and alkenyl carbons. The shifts between 120 and 130 ppm can be attributed to the carbons along the backbone, while the carbons on the benzene rings correspond to the peaks between 130 and 140 ppm. There are no peaks appearing below 90 ppm, indicating the absence of alkyl carbons.

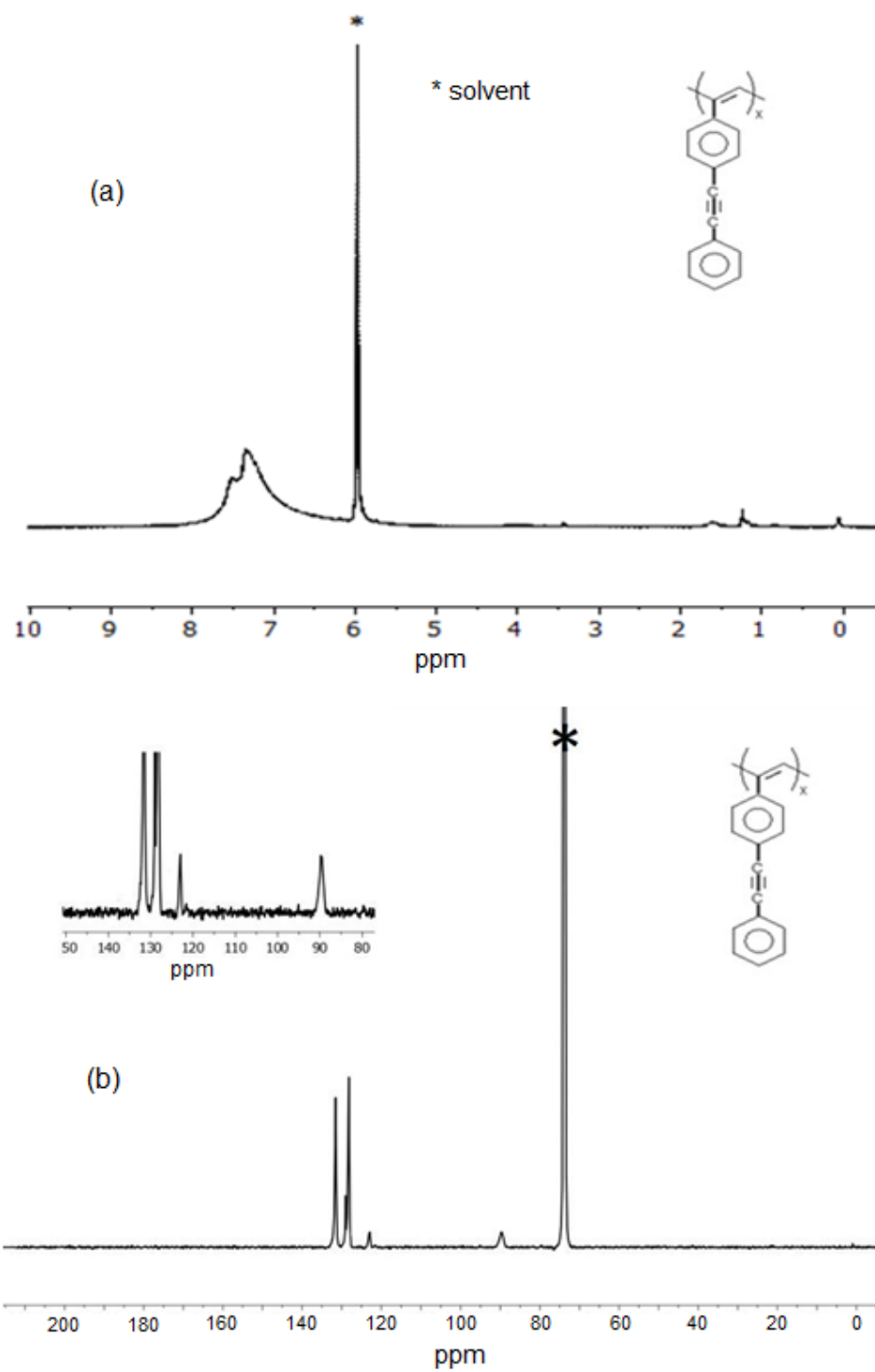


Figure 2.7 (a) ^1H NMR and (b) ^{13}C NMR spectra of poly(PA-PA) polymer.

The combination of TGA-MS and DSC was used to compare and understand the thermal conversion process and carbonization efficiency of the various poly(phenylacetylene) derivatives. The derivatives were heated in a one-step process under N₂ atmosphere from ambient temperature to high temperatures (1000°C) with a heating rate of 10°C/min. Figure 2.8 shows the TGA-MS spectra of the poly(PA), which is the control sample. This polymer started its thermal decomposition at ~300°C, producing benzene (78 AMU) and toluene (92 AMU) as the major evolved gases, and lost most of its weight in a range between 300° and 500°C. The evolved H₂ gas was observed only at ~500°C, implying some ring fusion activities, after losing 87% of its weight. This poly(PA) polymer has only phenyl side groups that are not sufficiently reactive to engage in any meaningful low-temperature stabilization reactions.

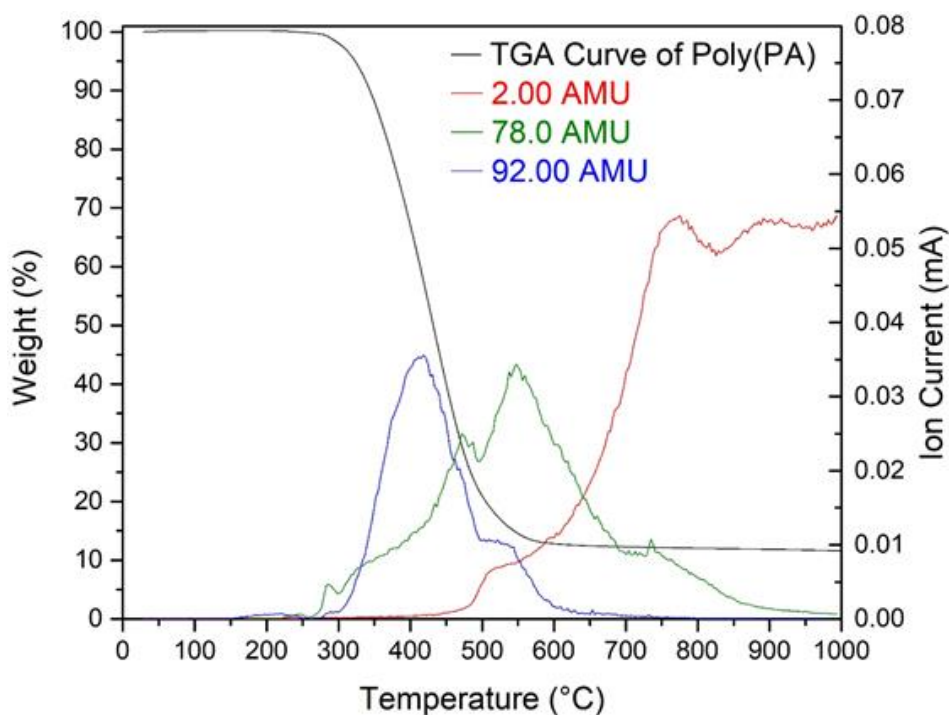


Figure 2.8 TGA-MS spectrum of poly(phenylacetylene) polymer, with a heating rate of 10°C/min under N₂ atmosphere.

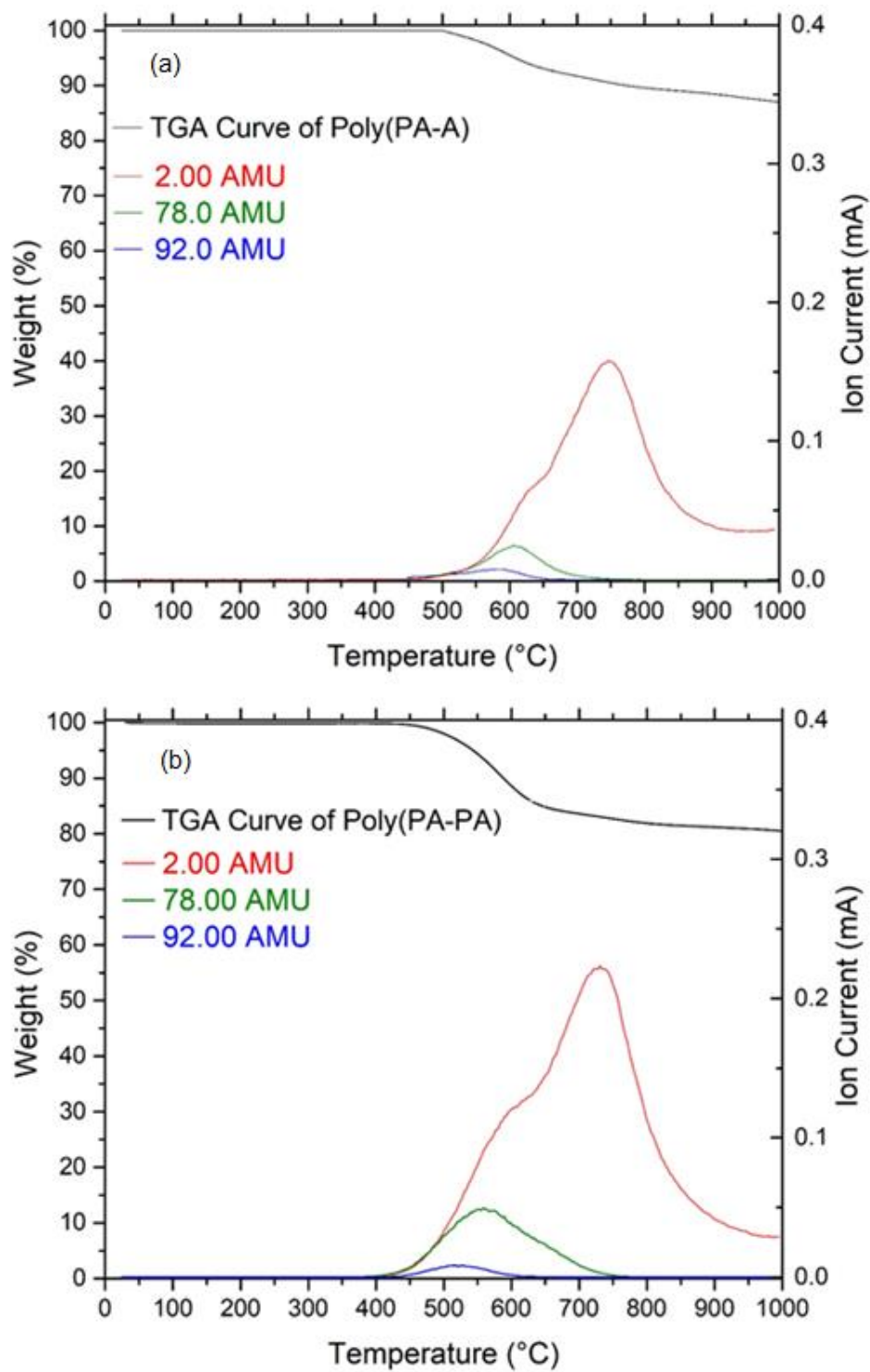


Figure 2.9 TGA-MS spectrum of (a) poly(PA-A) and (b) poly(PA-PA) polymers, with a heating rate of 10°C/min under N₂ atmosphere.

Figure 2.9 shows the TGA-MS spectra of the two poly(PA-A) and poly(PA-PA) derivatives under the same heating rate, 10°C/min, in an N₂ atmosphere. Both the poly(PA) derivatives with reactive π -electrons conjugated side groups (acetylenyl or phenylacetylenyl substitutes) show very high carbon yields, much higher than the 10% carbon yield obtained for the parent poly(PA) polymer. In the poly(PA-A) case, the carbon yield reaches ~90% with only a trace amount of benzene and toluene evolved gases observed at ~450°C. At the same temperature, the H₂ (2AMU) gas is also evolved and becomes a dominant evolved gas, which indicates active ring fusion reactions to transform the linear polymer chain to a carbon material with 2D hexagonal graphene sheets (as discussed later). Furthermore, there is nearly no weight loss at <450°C in the poly(PA-A) polymer, and this temperature is much higher than the poly(PA) chain degradation temperature, which started at 300°C. Most of the 10% weight loss (namely dehydrogenation) in poly(PA-A) occurs in the range of 500-800°C.

Poly(PA-PA) also exhibits a similar TGA-MS spectroscopy pattern with a slightly reduced carbon yield. The weight loss also occurs after 450°C, resulting in a weight loss of approximately 15% between 500-700°C and a carbon yield of ~75% at 1000°C. Both TGA-MS profiles of poly(PA-A) and poly(PA-PA) seem to indicate that a similar smooth stabilization process (namely, [4+2] cycloaddition and cross-linking) also occurs in the poly(PA-PA) precursor to form inter- and intra-chain polyaromatic moieties in the precursor structure without weight loss. Evidently, the additional π -electrons conjugated acetylene or phenylacetylene moiety along the poly(PA) chain dramatically increased the stabilization activities in the low temperature range (<450°C), which must involve inter- and intra-chain [4+2] cycloaddition reactions occurring between the triple bond and aromatic moieties without weight loss. These cycloaddition reactions increase the poly-aromaticity of the polymer and form a cross-linking structure, which is essential to the subsequent carbon conversion process. Without the presence of oxygen and nitrogen heteroatoms in the precursor, the carbonization process involves only ring fusion and the

elimination of hydrogen atoms, which is much more efficient in forming 2D graphene structures than with the presence of oxygen and nitrogen heteroatoms. The higher carbonization temperature (>800°C) further promotes ring fusion and chain diffusion to form larger graphene sheets in the resulting carbon material (discussed later).

It is useful to understand the stabilization details, especially the temperature in which the reactions start to occur and the kinetics of the reactions. The [4+2] cycloaddition reaction can happen without weight loss at quite low temperatures <200°C.¹⁴² The reaction temperatures were revealed by DSC measurements that were conducted under similar heating conditions at 10°C/min under an N₂ atmosphere. Figure 2.10 shows DSC curves with two consecutive heating/cooling cycles for poly(PA-A) and poly(PA-PA). For the poly(PA-A) in Figure 2.10(a), a sharp exothermic peak is present in the first heating cycle, starting at <150°C and completing at <300°C. There was no peak observed in the subsequent cooling cycle and second heating-cooling cycle, indicating no further reaction happened in these cycles. Because the TGA curve of the poly(PA-A) sample in Figure 2.9(a) exhibits no weight loss in this temperature range, these DSC results clearly imply that a facile [4+2] inter- and intra-chain cycloaddition reaction happened and was completed within 15 minutes during the heating between 150° and 300°C under a steady-state condition (without any agitation). In Figure 2.10(b), similar exothermic results were also observed in the poly(PA-PA) sample during the first heating cycle, with a broad exothermal band that implies that several stabilization reactions happened at different temperatures. The stabilization reaction starts at 200°C, which is approximately 50°C higher than that of poly(PA-A), and continues up to 400°C and beyond. The somewhat subdued stabilization process in poly(PA-PA) may also be associated with its bulky side groups, which hinder the regio-selective cycloaddition reaction and ring fusion; this is consistent with the corresponding TGA observation shown in Figure 2.9(b). However, the early stabilization reaction is sufficient to prevent any polymer chain degradation (<450°C) and allow the completion of the stabilization reactions.

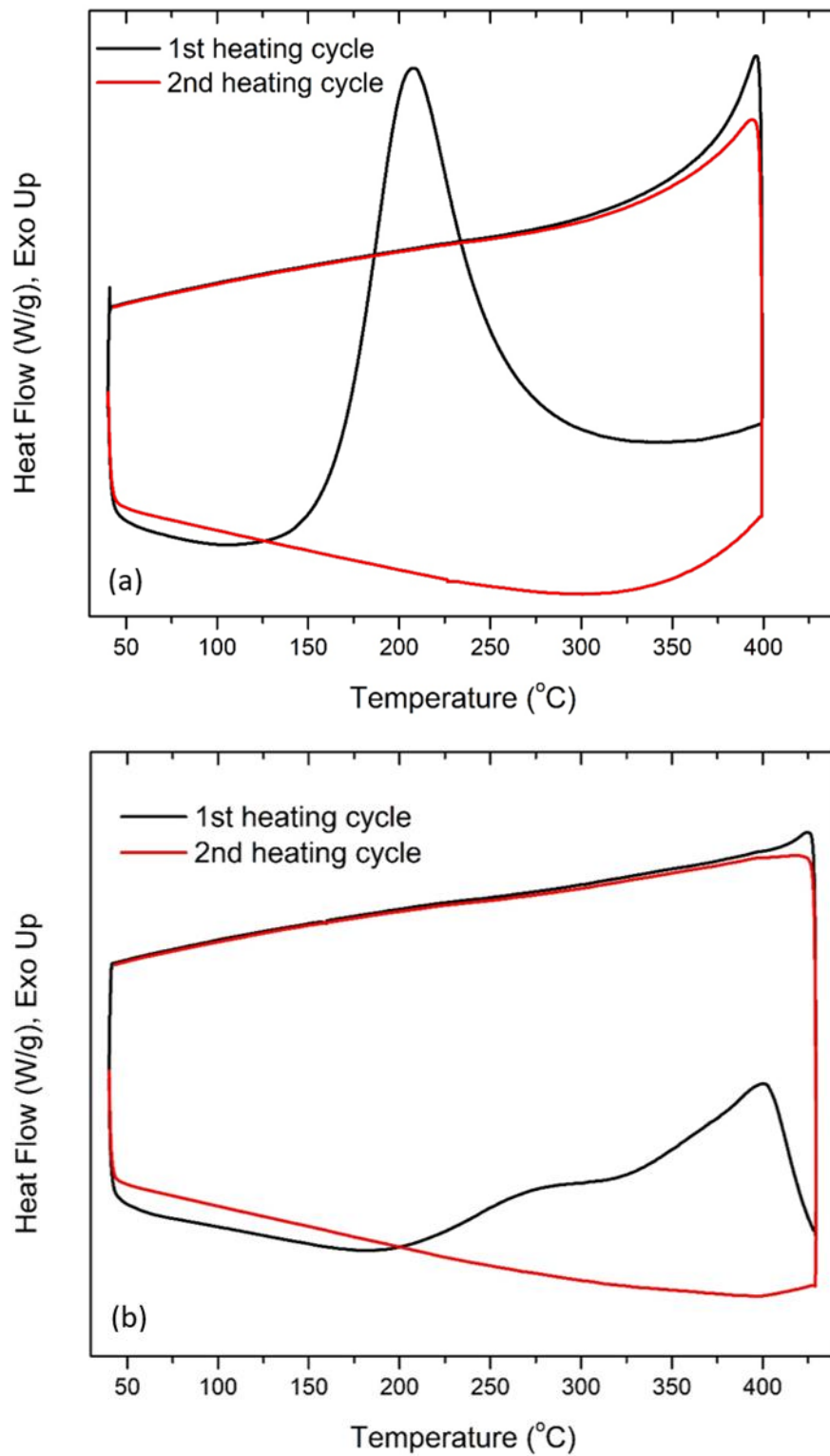


Figure 2.10 DSC curves of (a) poly(PA-A) and (b) poly(PA-PA) hydrocarbon polymer precursors.

One major requirement of a CF precursor is its processability, i.e., its ability to form the corresponding precursor fibers, using either melt- or wet-spinning processes. Due to the small-scale experimental samples, an electrospinning technique was applied to produce microfibers from a polymer solution. Although this electrospinning technique is different from commercial wet-spinning processes, this relatively accessible experimental setup offers valuable information due to its fiber-forming ability.^{143,144} As discussed, the poly(PA-A) polymer exhibits limited solubility in common organic solvents, due to the combination of reactive acetylene side groups and some crystallinity. Thus, the electrospinning study was carried out using several poly(PA-PA) solutions in THF (or toluene), and in various concentrations and spinning conditions. All of the spinning conditions produce a fine jet from the Taylor cone, which travels through the electric field (elongated and solidified) to a collector. Figure 2.11 shows SEM images of the as-spun poly(PA-PA) fiber with an approximately 5 μm diameter, which was prepared from a 30 wt.% poly(PA-PA)/THF solution. The relatively uniform fibers (with a few larger fiber diameters) imply a high molecular weight polymer with good solubility in common organic solvents.

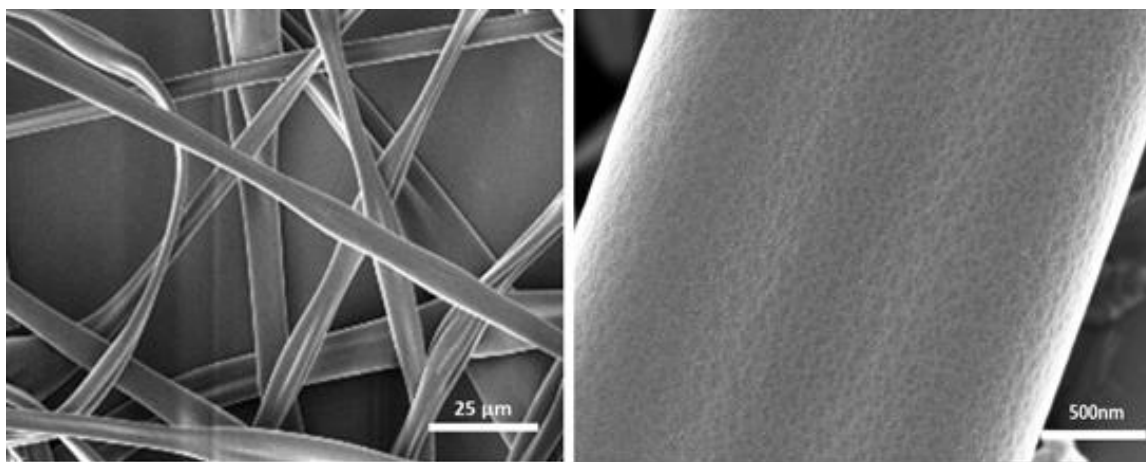


Figure 2.11 SEM image of the electro-spun poly(PA-PA) fibers from a 30 wt.% polymer/THF solution, with voltage of 15 kV, flow rate of 7.5 mL/hr., and distance of 20 cm.

The resulting poly(PA-PA) precursor fibers were carbonized by heating the samples up to 2100°C under N₂ atmosphere, without applying any external tension. The resulting CFs were then characterized by Raman spectroscopy and XRD to determine their graphitic structure. Raman spectroscopy is the easiest and most common method to probe the inelastic scattering of light from a sample surface under ambient conditions. Figure 2.12(a) shows the Raman spectra for several resulting CFs, obtained using a laser excitation wavelength at 514.5 nm. These CFs were prepared by thermal treatment of the same poly(PA-PA) precursor fiber at 1000°, 1200°, 1500°, 1900°, and 2100°C for one hour under an N₂ atmosphere. Both an order G band at 1582 cm⁻¹ and a disorder-induced D band at 1350 cm⁻¹ of carbon structures are clearly observed, indicating a polymorphous morphology. Figure 2.12(b) shows the integrated intensity ratio $I_{(D)}/I_{(G)}$ of the D and G bands to determine the order/disorder ratios, which are inversely proportional to the carbonization temperature and reach 1.33 for the CFs after heating to a temperature of 2100°C. Overall, the trend of this $I_{(D)}/I_{(G)}$ intensity ratio is similar to that of typical PAN-based CFs, in which the $I_{(D)}/I_{(G)}$ ratio continuously reduces, and the crystalline domains increase with increasing heat. This polymorphous structure contains some relatively ordered graphene layer structures that are embedded in a more disordered region. The order of the domain structure is slightly less than that of some PAN-based CFs, which may be associated with the lack of mechanical stretching that can facilitate chain motion and orientation.

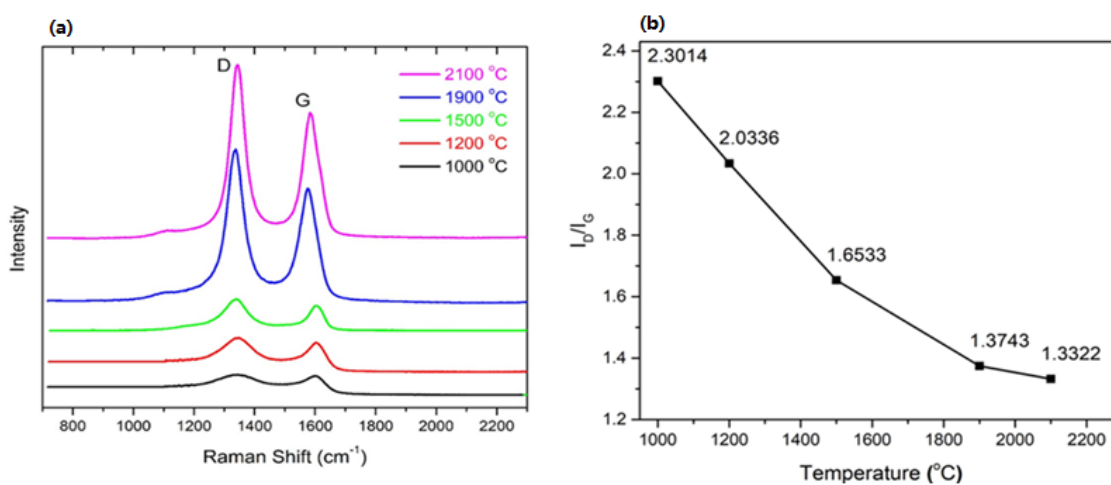


Figure 2.12 (a) Raman spectra of carbon fibers after carbonization at various heating temperatures and (b) the peak intensity ratio between D and G bands vs. carbonization temperature.

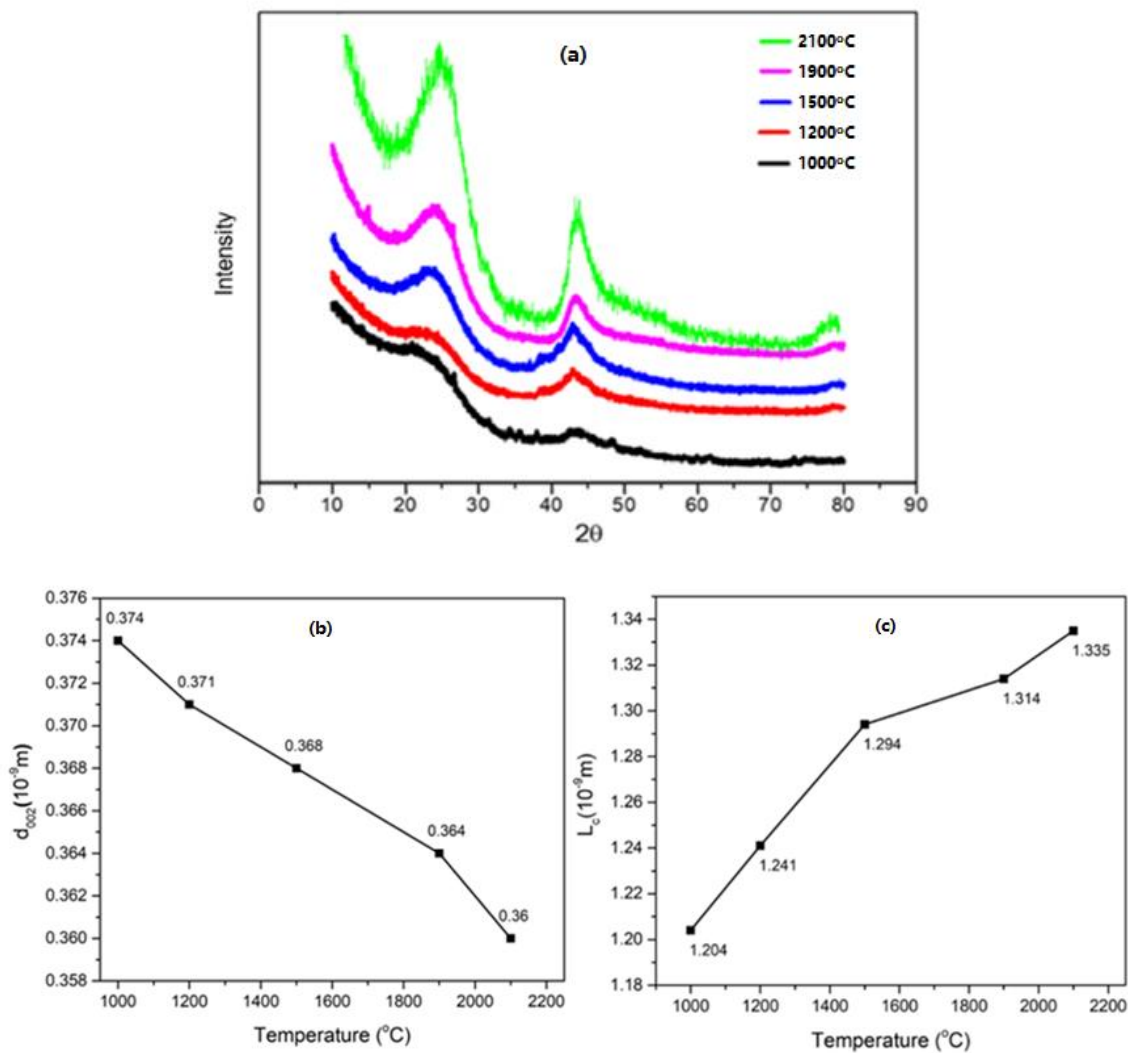


Figure 2.13 (a) XRD patterns of several carbon fibers and their (b) interlayer d-spacing and (c) stacking height (L_c). They are prepared by sequential heat treatment of the same poly(PA-PA) fiber at various temperatures (with 1 hour at each temperature) under an N_2 atmosphere.

The observation of crystalline domains was further analyzed by XRD patterns. Since the wide-angle diffraction patterns have coherence zones with minimum lengths between 1 and 2 nm, the XRD pattern reflects only the sizes and layer distances of the best-ordered domains. Figure 2.13 (a) shows XRD patterns of the same set of CFs prepared by the one-step thermal treatment of the poly(PA-PA) precursor fiber at 1000°, 1200°, 1500°, 1900°, and 2100°C under an N₂ atmosphere. Figure 2.13 (b) and (c) compare the interlayer d-spacing (d_{002}) and the stacking height (L_c) in crystalline domains of CFs. The two distinctive X-ray peaks at 2 θ ~24° and ~43°, corresponding to (002) and (100) planes, are typical of carbon crystallites that start to appear at ~1000°C and grow with an increase in temperature. The peak parameters were used to calculate the crystallite size. The CFs treated at 2100°C exhibits d_{002} = 0.360 nm and L_c = 1.335 nm, which are very close to those (d_{002} = 0.364 nm and L_c = 1.3 nm) of high strength PAN-based CFs.¹⁴⁵

2.4 Conclusion

The primary goal of this research is to investigate a new CF precursor based on a high molecular weight hydrocarbon polymer with a specific molecular structure that can offer good solubility in common organic solvent, high carbon yield, and a simple one-step thermal conversion process under an inert atmosphere, without any external reagent. Two poly(phenylacetylene) derivatives, poly(PA-A) containing para-substituted acetylenyl groups and poly(PA-PA) with phenylacetylenyl groups, were synthesized and evaluated under a continuous heating process in an N₂ atmosphere. The poly(PA-A) polymer shows 90% carbon yields, nearly reaching the theoretical value with only the removal of hydrogen atoms in its structure during the whole conversion process. Unfortunately, this polymer has a limited solubility for wet-spinning processes. On the other hand, poly(PA-PA) offers not only a good carbon yield (~75%) but also good solubility in common organic solvents. The additional phenylacetylene moiety in each phenylacetylene monomer unit creates bulky side groups to increase its solubility while

maintaining a high reactivity. The facile thermal-induced cycloaddition and cross-linking reactions (stabilization mechanism) start at 200°C without oxygen. During carbonization, the combination of the pure hydrocarbon precursor structure (without nitrogen and oxygen heteroatoms) and thermal conversion under an inert atmosphere dramatically reduces the ejection of volatile gases, which are essential for achieving high carbon yield and reducing structural defects. The combination of the Raman and XRD results of the resulting poly(PA-PA)-based CFs clearly indicates the formation of a polymorphous carbon structure and carbon crystallites similar to those in high-strength PAN-based CFs. Evidently, this new poly(PA-PA) polymer is a potential new CF precursor that is worthy of further investigation. However, the preparation of poly(PA-PA) is a three-step synthesis route with expensive monomers and palladium catalyst as reagents, which will further increase the cost of CF compared to current technology. Additionally, the precursor fibers prepared from poly(PA-PA) were found to be very brittle and weak. Their poor mechanical properties would pose difficulties in mass production.

Although this study of poly(phenylacetylene) derivatives does not directly relate to the low-cost PE-g-Pitch precursor that is the main focus of my thesis work, it showed us the importance of side groups in the polymer precursor, which should be able to produce PAH moieties for the cross-linking (cycloaddition) reaction in order to form a network structure during the stabilization step. The side groups also greatly influence processability. Furthermore, the polymer with an π -electrons conjugated system is more likely to achieve a high carbon yield. The overall information is very helpful to us in designing new, low-cost, PE-based precursors discussed in the next chapters.

Chapter 3

Preparation and Evaluation of Polyethylene-graft-Pitch Precursors by Cycloaddition Reaction between Diphenylacetylenyl Side Groups-Contained PE copolymer and Pitch

3.1 Introduction

In Chapter 1, I have explained our motivations for designing a new type of polyethylene-based precursor. In Chapter 2, our research activities focused on the understanding of structural design principles in the hydrocarbon polymer that can be thermally converted to graphitized carbon structure with high carbon yield. In addition, the polymer must not be cross-linked before the fiber-spinning. The experimental results show that poly(PA-PA) polymer, with a π -electrons conjugated polymer backbone and diphenylacetylenyl (DPA) side groups, can meet both key requirements. This polymer is soluble in toluene and THF for forming precursor fibers and offers a high carbon yield of more than 75%. Also, we learned that the incorporated DPA moieties engage in a facile cycloaddition reaction at low temperature under N_2 atmosphere to form the polycyclic aromatic hydrocarbon (PAH) moieties with a network (cross-linked) structure during the stabilization step, which assures a high carbon conversion during high-temperature thermal transformation. Unfortunately, this π -electrons conjugated polymer precursor requires expensive monomers and multiple-step synthesis routes, making it too expensive for practical applications.

In this chapter, our basic research idea was to apply the same reactive DPA side group to the polyethylene (PE) polymer chain, in other words, to prepare PE-DPA copolymer containing DPA side groups. As illustrated in Figure 3.1, we further extended the chemistry to develop the objective PE-g-Pitch precursor that contains the highly graphitizable PAH side groups for the thermal conversion to a carbon structure by a grafting reaction. Based on the experimental results as shown in Chapter 2, combining with some previous studies about the estimated activation

energy between various PAH molecules and acetylene moiety that will be discussed in the next section, the DPA side groups of PE-DPA copolymer should be reactive with PAH molecules in the pitch via a Diels-Alder cycloaddition reaction under a mild reaction condition in N_2 atmosphere to accomplish the grafting. If successful, the combination of large availability and low cost of PE copolymer and Pitch material would offer PE-g-Pitch graft copolymer as a low-cost CF precursor.

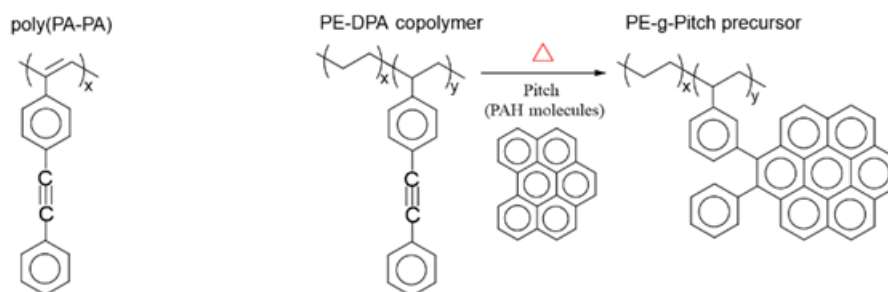


Figure 3.1 Molecular structures of poly(PA-PA) with DPA side groups, PE-DPA copolymer, and the corresponding PE-g-Pitch precursor.

There are many questions for this preparation route of PE-g-Pitch precursor. How many DPA side groups in the PE chain are required to prepare this precursor with an effective thermal transformation to carbon material with a high carbon yield? Will the reactive DPA side groups have cycloaddition reactions with themselves as well as the PAH molecules? If so, what is the most suitable preparation condition to minimize these self-reactions? Is it possible to conduct the melt-spinning instead of the solution-spinning process on the PE-g-Pitch precursor to form the low-cost precursor fibers? How does the saturated PE backbone engage in the stabilization and carbonization reactions? In this chapter and the next, I will explain our research activities and key experimental observations toward answering these questions.

3.2 Cycloaddition Reaction Between PAH Molecules and Acetylene Derivatives

Diels-Alder type cycloaddition is a well-known chemical reaction. It is the interaction between a conjugated diene and a dienophile, which can either be alkene or alkyne, to form a cyclic alkene structure. To be more specific, because it is activated by thermal energy and involves 4 π -electrons from a diene and 2 π -electrons from a dienophile, this reaction is commonly classified as a thermally allowed [4+2] cycloaddition reaction. Based on molecular orbital (MO) theory, the interaction can be considered as the overlap between the electron-rich diene's highest occupied molecular orbital (HOMO) and the electron-deficient dienophile's lowest unoccupied molecular orbital (LUMO).

Numerous studies have shown that the acetylene 'HC \equiv CH' can act as a dienophile active site, hence initiating a Diels-Alder type thermal cycloaddition reaction with PAH molecule that contains dienes systems.¹⁴⁶⁻¹⁴⁸ The reaction follows Clar's sextet rule that the Kekule resonance structure with the largest number of disjoint aromatic π -sextets is the most important for the characterization of properties of PAHs,¹⁴⁹ namely that a PAH's structure with a larger number of aromatic π -sextets is more stable than its isomers with fewer π -sextets. Additionally, in this PAH structure, the rings with π -sextets behave more as aromatic centers, and thus are less reactive than the other rings. The Clar's sextet rule can be used to predict that the π bonds in the rings of a PAH without π -sextets are more favorable for serving as dienes in a [4+2] Diels-Alder cycloaddition.¹⁵⁰ As illustrated in Figure 3.2a, Fort et al.¹⁴⁷ synthesized 7,14-dimesitylbisanthene and heated it with diethyl acetylenedicarboxylate in toluene for 24 hours at 120°C. In this case, the bay regions located at the side of the center rings are more reactive, as a result of the lower aromaticity. The researchers discovered that adding two acetylene species transforms the bay regions at the rim into two new benzene rings via a dehydrogenation reaction. They conducted a similar experiment on diethyl acetylenedicarboxylate and perylene (Figure 3.2b) with fewer inner benzene rings at the same concentration and also found the same cycloaddition reaction via

dehydrogenation. However, only 50% conversion was achieved, despite a higher temperature of 150°C and longer reaction time of 72 hours. Furthermore, this reaction was regio-selective, taking place in only one of the bay regions. The reactivity difference between these two reactions is a result of their different activation energy for the Diel-Alder cycloaddition reaction that happens between acetylene moieties and bay regions. Because both the acetylene and bay region of PAH are feeble dienophile and dienes,^{151,152} very high energy is usually required to initiate this reaction. However, as shown in Figure 3.3, the PAH with a higher number of inner benzene rings has a smaller HOMO-LUMO gap¹⁵³, which reduces the amount of activation energy needed for cycloaddition. As a result, 7,14-dimesitylbisanthene can react with diethyl acetylenedicarboxylate at a lower temperature but with higher conversion.

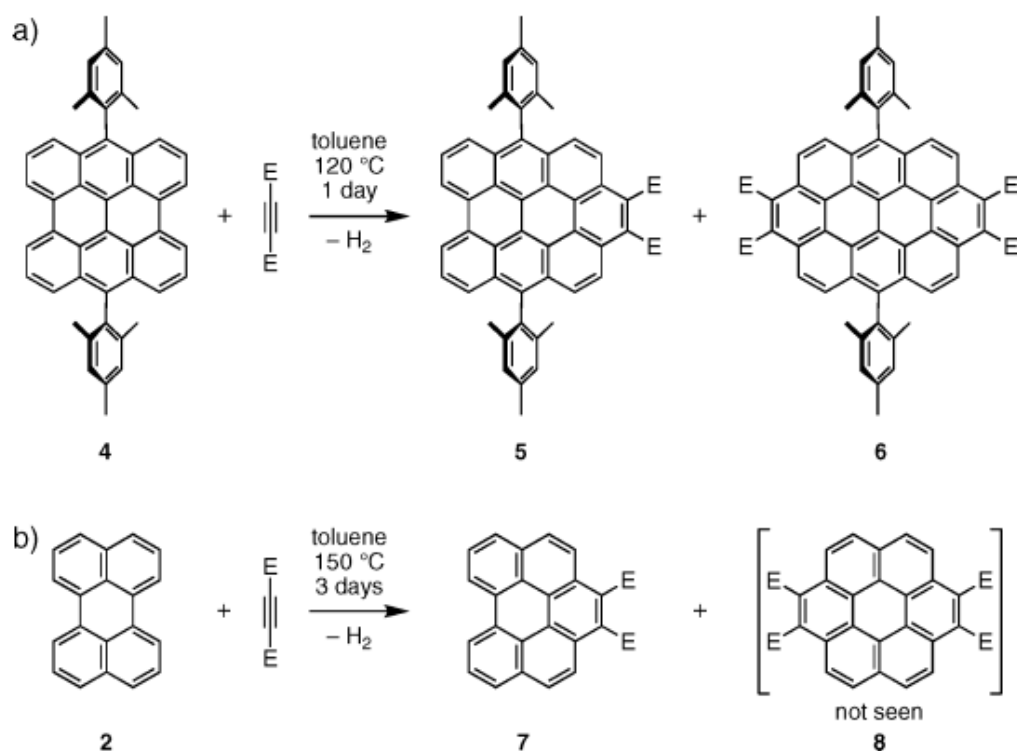


Figure 3.2 Diels-Alder cycloadditions of diethyl acetylenedicarboxylate to (a) 4,11-dimesitylbisanthene and (b) perylene.¹⁴⁷

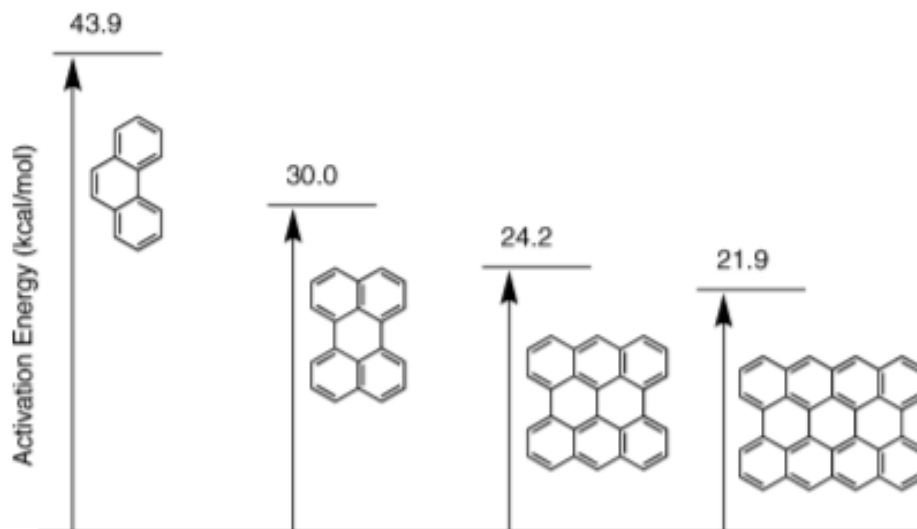


Figure 3.3 Activation energies calculated for Diels-Alder cycloadditions of acetylene to aromatic hydrocarbon bay regions.¹⁴⁷

Based on the same principle, the acetylene species on the side groups of PE copolymer would be an ideal feedstock for the preparation of PE-g-Pitch precursor, by incorporating pitch molecules (mostly a mixture of PAHs with different molecular weights also containing bay regions).^{154,155} However, from our previous study of poly(PA-A) polymer with terminal C≡C-H moieties, we have known that this polymer was cross-linked easily in light due to the inter-reactions between the highly reactive triple bonds at the terminal position, which causes material handling/processing difficulties. Therefore, we applied a protection strategy of steric hindrance by adding a phenyl group at the terminal position of the phenylacetylenyl side group to form the less reactive DPA side group. Although this protection strategy works well based on our observation on poly(PA-PA)'s good solubility, we still have some concerns about the DPA side groups on PE polymer chains that may still react to each other via cycloaddition at elevated temperatures, especially during the cycloaddition reaction with PAH molecules. Even a small degree of self-cycloaddition would cross-link the polymer chains, thus generating a premature network structure that largely affects the processability of the PE-g-Pitch precursor. Therefore, the content of reactive side groups in the PE-DPA copolymer must be well-controlled. As will be

discussed, we have adopted a melt-blending procedure between the PE-DPA copolymer and pitch molecules. It is known that pitch material starts to liquefy when the temperature rises beyond its softening point. Therefore, during the melt-blending between the PE-DPA copolymer and an excess quantity of pitch molecules, the liquified pitch can act as a solvent to dissolve the polymer, meanwhile maintaining the homogeneity of the binary system throughout the entire mixing process. With the increasing temperature, the cycloaddition reactions between DPA and PAH molecules are more likely to occur, thus converting DPA side groups into the grafted PAH side groups and minimizing the DPA self-reactions. To achieve this, the most important aspect of this study is to understand how the content of DPA side groups in the PE-DPA copolymer and the reaction conditions of cycloaddition affect the thermal stability of the resulting PE-g-Pitch precursor, and maximize its carbon yield.

3.3 Experimental Section

3.3.1 Materials

4-bromostyrene (TCI) was vacuum distilled after drying overnight by CaH_2 . MMAO-12 7% toluene solution (Sigma Aldrich) was dried by vacuum at 50°C to become white powders. AIBN (Sigma-Aldrich), CuI (Sigma-Aldrich), Bis(triphenylphosphine) palladium(II) dichloride (Sigma-Aldrich) phenylacetylene (TCI), diisopropylamine (Sigma-Aldrich), and $[(\text{C}_5\text{Me}_4)\text{SiMe}_2\text{N}(\text{t-Bu})]\text{TiCl}_2$ (Boulder Scientific) were used as received. THF and toluene (Wiley Organics) were purified via the Grubbs type solvent purification system. Petroleum pitch ZL 250M with a softening temperature of 250°C were kindly provided by Rutgers Basic Aromatics GmbH.

3.3.2 Characterization

Liquid state ^1H NMR and ^{13}C NMR spectra were obtained by using Bruker AV 300 with a measurement temperature of 90°C . For a typical ^1H NMR measurement, 10mg of sample was completely dissolved by 1ml of *d*-1,1,2,2-tetrachloroethane at 90°C in a thin wall NMR sample tube, while in the ^{13}C NMR measurement, 30mg of sample was dissolved in 1 ml of the same type of deuterated solvent. A Ubbelohde viscometer (Cannon 9721) was used to measure the viscosity average molecular weight (M_v) of the polymer products with 1,2,4 trichlorobenzene (TCB) as the solvent and 135°C as measurement temperature. Mark-Houwink equation, $[\eta_i] = kM_v^{-a}$, was applied to convert intrinsic viscosity to M_v with parameters a and K of 0.706 and 0.000517 dl/g that based on PE solution at the same condition.¹⁵⁶ TGA measurements were conducted on an Sdt-600 (TA Instruments). Around 10 mg of sample was loaded into the sample pan and heated at a rate of $10^\circ\text{C}/\text{min}$. DSC was performed on a DSC Q2000 (TA Instruments) by using hermetic aluminum pans. Around 5 mg of sample was loaded into a pan and then sealed by a sample press. The heating rate was $10^\circ\text{C}/\text{min}$ and N_2 was selected as the measurement atmosphere for both TGA and DSC. Evolved gas analysis mass spectrometry (EGA-MS) measurements were conducted on a TA TGA5500 with a mass spectrometer in argon with a flow rate of 25ml/min and a heating rate of $10^\circ\text{C}/\text{min}$. The weight of the sample was fixed to be 15mg in every measurement. Rheology measurement was conducted on ARES-G2 (TA instruments) in the N_2 atmosphere with a heating rate of $10^\circ\text{C}/\text{min}$. The angular frequency was 1 rad/s and strain was 10%. All samples were pre-molded with a diameter of 8mm and thickness of $\sim 1.5\text{mm}$ by using a vacuum hot press. XRD measurements were conducted on a Panalytical XPert Pro MPD theta-theta Diffractometer from Malvern at 40 kV and 40 mA with Cu $\text{K}(\alpha)$ radiation $\lambda = 0.15418$ nm. Diffraction patterns were recorded on a 0.8 collimator, with an oscillation of the samples between 10 and 80° and an imaging plate detector. The scan rate was $0.2^\circ/\text{min}$ with an interval of 0.045° . The interlayer distance d_{002} was calculated using the position of the 002-reflection and

Bragg's equation. The crystallite thickness L_c and the lateral size L_a were determined using the (002) and (10) reflection, respectively, and Scherrer's equation. Raman spectra were collected from Horiba LabRam HR Evolution with 532nm laser excitation. All of samples were grounded into form of fine powders for XRD and Raman measurements. All of the calculations on XRD and Raman were finished by using fitting curve function of Origin software. The SEM images were collected from the Apreo 2 (Thermo Fisher).

3.3.3 Synthesis of Poly(4-bromostyrene)

The synthesis of poly(4-bromostyrene) was conducted in a 50ml glass round bottom flask via bulk free radical polymerization with AIBN as initiator. Firstly, 0.05g AIBN was loaded into the flask with a stir bar, and the air was removed by vacuum and argon refill for three times. Then 4.2g (3ml) of distilled 4-bromo styrene was injected into the flask by a 5ml needle syringe. The mixture was heated to 80°C and allowed to be stirred for 30 min. After that, the viscous liquid was poured into 300ml of chill methanol then washed with 50 ml of methanol three times. In the end, the white product was dried in a vacuum oven at 80°C overnight and then weighted to be 3.8g.

3.3.4 Synthesis of Poly (4-phenylacetylenyl styrene)

Poly(4-bromostyrene) (1.73g) was firstly dissolved in 15ml THF with 0.265g bis(triphenylphosphine) palladium (II) chloride and 0.1g copper(I) iodide in a two-neck air-free 50ml round bottom flask equipped with a condenser. Then 4.2 ml diisopropylamine and 3.3ml phenylacetylene were loaded in the drop column and added drop-wisely to the polymer solution. The reaction was heated at 60°C for 96 hours. After cooling, the dark solution was poured into 100ml of distilled H₂O saturated with ammonium chloride in a separatory funnel and applied with

vigorous shaking. Then the water solution was extracted by dichloromethane (100ml×3). The dark organic portion was rotovaped and concentrated to 10ml and poured in 300ml chill methanol to get the polymer product coagulated. The product was dissolved in 10ml toluene and precipitated in 50 ml methanol 3 times. After filtered by a funnel, the product in a form of brown powders was vacuum dried at room temperature and weighted to be 1.35g.

3.3.5 Copolymerization of Ethylene and 4-Bromostyrene

The copolymerization reaction was conducted in a Parr 500ml stainless autoclave equipped with a mechanical stirrer as shown in Figure 3.4. The reactor was firstly charged with 220ml of toluene, a certain amount of 4-bromostyrene (*run 1*: 2ml, *run 2*: 3ml, *run 3*: 6.5ml) and 10ml of 20wt.% of methylaluminoxane (MAO) solution in toluene, with argon protection and stirring. Then the solution was saturated with 50 psi ethylene at 40°C. To the mixture, 1.1 ml of [(C₅Me₄)SiMe₂N(t-Bu)] TiCl₂ (constrained geometry catalyst/CGC) solution in toluene (20umol/ml) was injected into the reactor to initiate the reaction. After 1 hour, ethylene was replaced by argon and the reaction was terminated by adding 30ml of isopropanol. The solution mixture was then poured into 600ml of diluted HCl solution of methanol. The resulting PE-BrSt copolymer was isolated by filtration and was washed with 200ml×3 of methanol before drying in a vacuum oven overnight at 60°C.

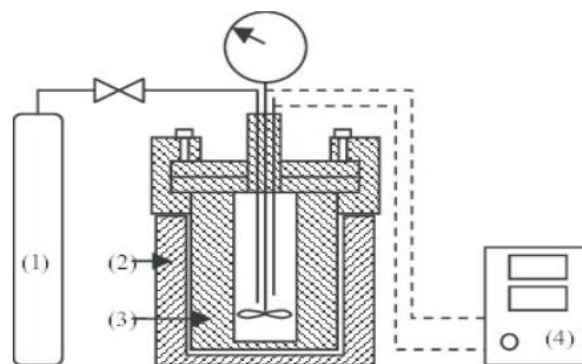


Figure 3.4 Schematic diagram of high-pressure reactor with (1) gas cylinder, (2) heating mantle, (3) reaction vessel and (4) temperature/pressure monitor.

3.3.6 Synthesis of Poly(ethylene-co-4-phenylacetylenyl Styrene)

In a typical reaction, 5 g of PE-BrSt copolymer was initially dissolved in 230ml of toluene in a 500ml three-neck round bottom flask with a condenser under 90°C in a N₂ atmosphere. Then 0.1g of CuI, 0.2g of Bis(triphenylphosphine) palladium (II) dichloride, and phenylacetylene (3 × mol% of BrSt) were added into the flask. The reaction was initiated by adding 25ml of diisopropylamine drop-wisely by using a dropping funnel. After 96 hours, the solution mixture was poured into 600ml of saturated ammonium chloride/methanol solution with vigorous stirring. The product PE-DPA copolymer was dissolved in toluene and precipitated in methanol until the liquid portion became colorless, then was dried at 30°C in a vacuum oven overnight. All products were in light brown while the color became darker with higher comonomer%.

3.3.7 Preparation of Melt-Spinnable PE-g-Pitch/Pitch Blend Precursors

PE-DPA copolymer and petroleum pitch were first dissolved in toluene with 5 wt.% concentration at 90°C in a round bottom flask. Then, at the same temperature, the prepared homogeneous solution was dried with vigorous stirring under an airflow until it became a slime-

like product with 90% toluene removed. The mechanical blending of the slime-like product was conducted in a twin-screw blender with nitrogen flowing through the system all the time with a flow rate of 100ml/min. This system has three thermocouples located at the outer cover, sample chamber, and inner wall to have a close monitor on temperature control. The heating rate was set to 10°C/min for all experiments. Argon was purged in the blending chamber through a rubber tube to create an air-free environment during mixing. When finished heating, the sample chamber was cooled down with a cooling rate of 10°C/min. After blending, all collected samples were grounded into a form of powders by a mortar.

3.3.8 Gel Content Measurement

At room temperature, 0.5g of sample and 10ml of THF were loaded into a vial. Then, the vial was kept idle for 24 hours. Then, the insoluble portion was separated and dried in a vacuum oven at 60°C overnight. The gel content is determined by dividing the insoluble fraction over the original weight of precursor fibers.

3.4 Results and Discussion

As illustrated in Figure 3.5, there are several experimental steps in this study to convert the designed PE-DPA copolymer containing DPA side groups into the stabilized PE-g-Pitch fibers. The experimental results in each step will be discussed in detail.

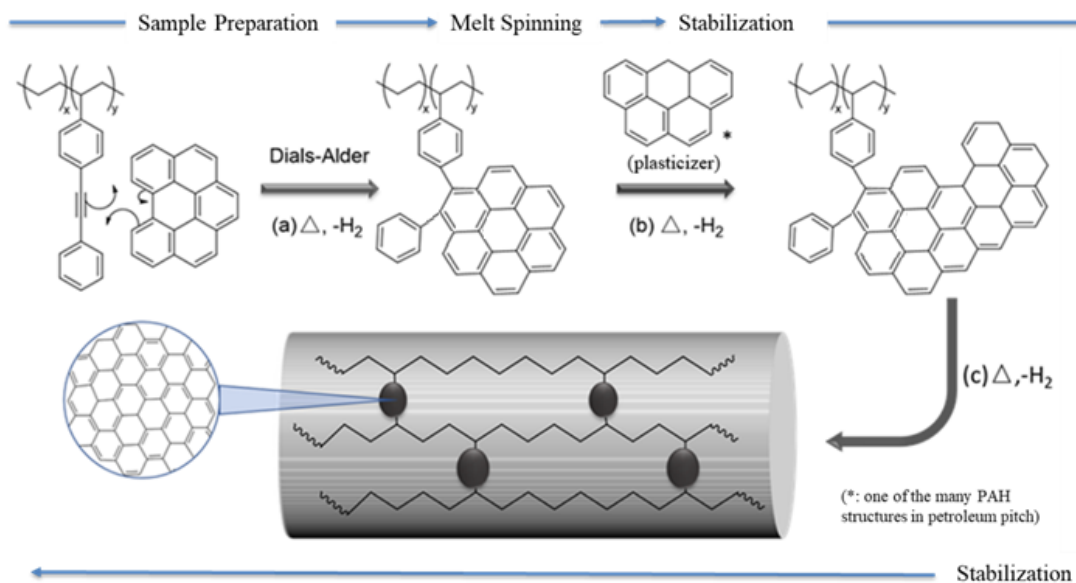


Figure 3.5 Illustration of structural transformation from PE-DPA copolymer to PE-g-Pitch precursor, to precursor fiber, and to stabilized fiber. (*one of the many PAH structures in petroleum pitch)

3.4.1 Preparation of Diphenylacetylenyl Side Group-Contained Polymers and Reactivity of Diphenylacetylenyl Side Group

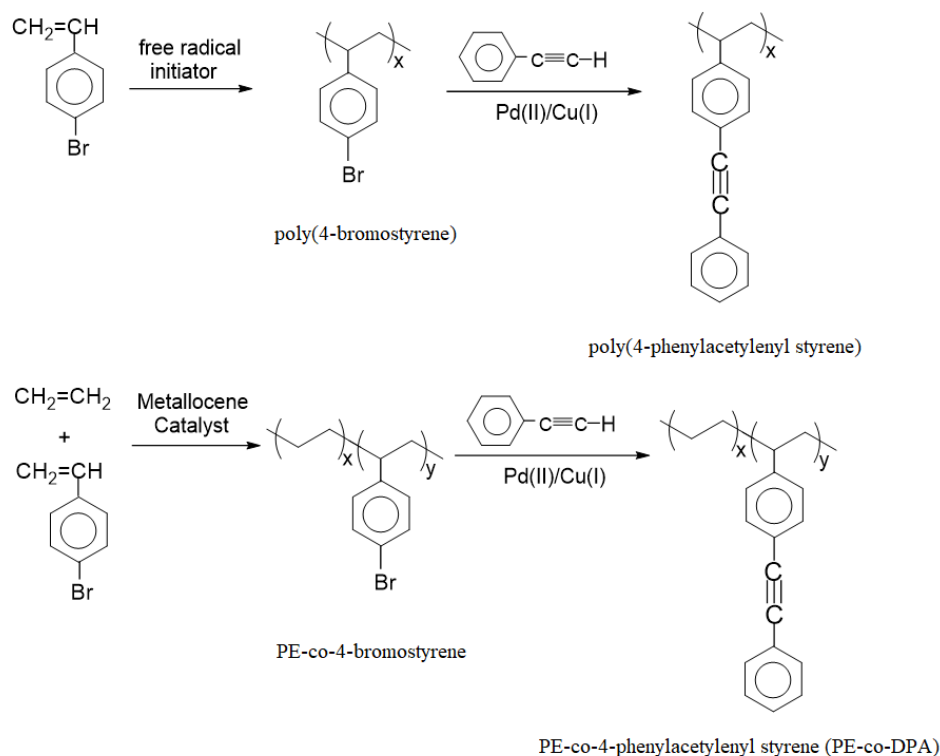


Figure 3.6 Synthesis equations of (top) poly(4-phenylacetylenyl styrene) and (bottom) PE-DPA copolymer.

First, we needed to develop an effective chemical route to prepare PE-DPA copolymers with good control of DPA concentration, then examine their chemical reactivities under elevated temperatures, especially the thermal-induced Diels-Alder cycloaddition between the DPA side group and PAH molecules in pitch. As discussed, it was essential to avoid any DPA side groups' self-cycloaddition reaction in forming the cross-linked polymer structure. To understand this reaction, we also prepared a poly(4-phenylacetylenyl styrene) homopolymer (control experiment), which has a DPA side group in every monomer unit. Figure 3.6 shows the chemical routes for preparing poly(4-phenylacetylenyl styrene) homopolymer and PE-DPA copolymer, respectively. In both cases, the DPA side groups were quantitatively derived from 4-bromostyrene comonomer units in the corresponding intermediate polymers, i.e., poly(4-

bromostyrene) and PE-BrSt copolymer. They were prepared by two different polymerization mechanisms. Poly(4-bromostyrene) homopolymer was synthesized by free radical-mediated polymerization, and PE-BrSt copolymer was initiated by CGC metallocene mediated coordination polymerization (Table 3.1).

Table 3.1 Summary of PE-BrSt copolymers synthesized by CGC metallocene catalyst.

Run	[BrSt] ^a (mol%)	Activity ^b (kg/mol*hr)	M _v ^c (10 ³ g/mol)	T _m (°C) ^d	T _c (°C) ^d
1	7.2	310	310.7	121.89	108.2
2	3.2	280	191.5	125.04	110.7
3	2.1	256	180.3	127.29	107.56

^a [BrSt] indicates the 4-bromostyrene content (mol%) in copolymers determined by ¹H NMR. ^b Activity is defined as kilograms of polymer by 1mol of CGC catalyst per hour. ^c M_v was estimated by intrinsic viscosity of polymer/TCB diluted solution at 135°C with a of 0.706 and K of 0.000517 dl/g. ^d T_m and T_c were determined by DSC in N₂ at 10°C/min, with thermal history removed.

Figure 3.7 shows ¹H NMR and ¹³C NMR spectra of poly (4-phenylacetylenyl styrene) homopolymer, both of which match the spectra reported in the literature.¹⁵⁷ Figure 3.8 compares ¹H NMR spectra between a typical PE-BrSt copolymer (with 7.2 mol% of BrSt comonomer content) and the corresponding PE-DPA copolymer. For PE-BrSt in Figure 3.8 (a), two peaks were found with chemical shifts centered at 7.39 and 6.95 ppm, corresponding to four aromatic protons. Due to the existence of bromo group with high electronegativity, the two protons with positions closer to the bromide shifted to a lower field, resulting in the split into two peaks with identical intensity. There was a main peak at 1.35 ppm, corresponding to CH₂ in the PE backbone, while its small shoulder at 1.55 ppm and the minor peak at 2.41 ppm correspond to the CH₂ and CH in the comonomer units. After the conversion, as shown in Figure 3.8 (b), the two aromatic peaks merged to a multi-let peak centered at 7.30ppm due to the removal of electron-withdrawing -Br groups and replaced by the less polar phenylacetylenyl groups. Theoretically, after the reaction, the number of aromatic protons should have increased from 4 to 9, while the number of aliphatic protons remained constant. By integrating the intensity of the aromatic region and aliphatic region, it was found that I_{ali}/I_{aro} decreased from 13.97 to 6.16 after the coupling

reaction, which matches the intensity change due to the increase in aromatic protons. This result indicates the complete conversion from 4-bromophenyl groups to DPA groups after the coupling reaction. This can be further supported by the ^{13}C NMR spectrum of PE-DPA copolymer at where exhibit signal intensity at $\sim 89\text{ppm}$, which is corresponding to the acetylene carbons ' $\text{C}\equiv\text{C}$ ' based on the results on poly (4-phenylacetylenyl styrene) homopolymer.

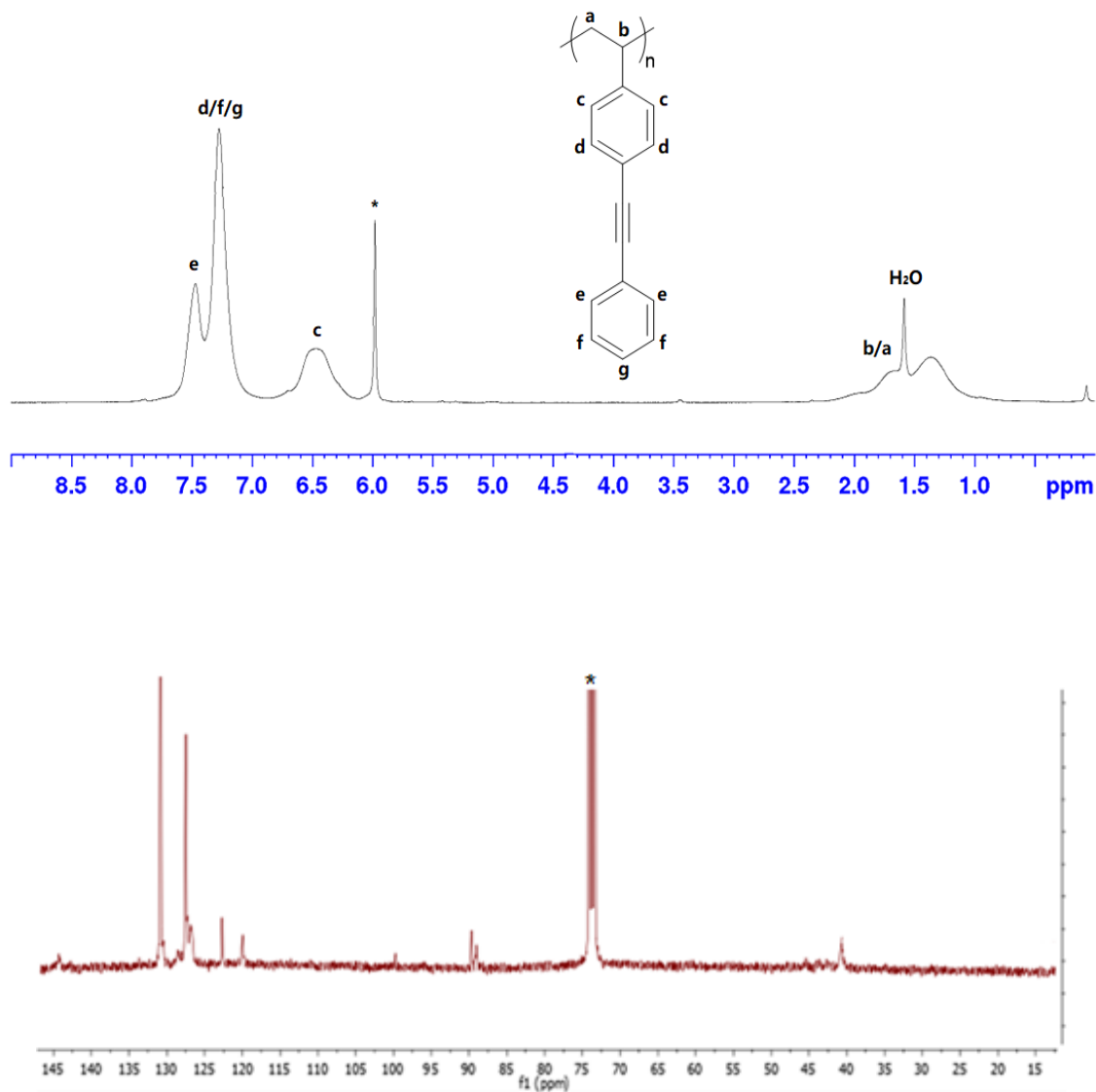


Figure 3.7 (top) ^1H NMR and (bottom) ^{13}C NMR spectra of poly(4-phenylacetylenyl styrene).

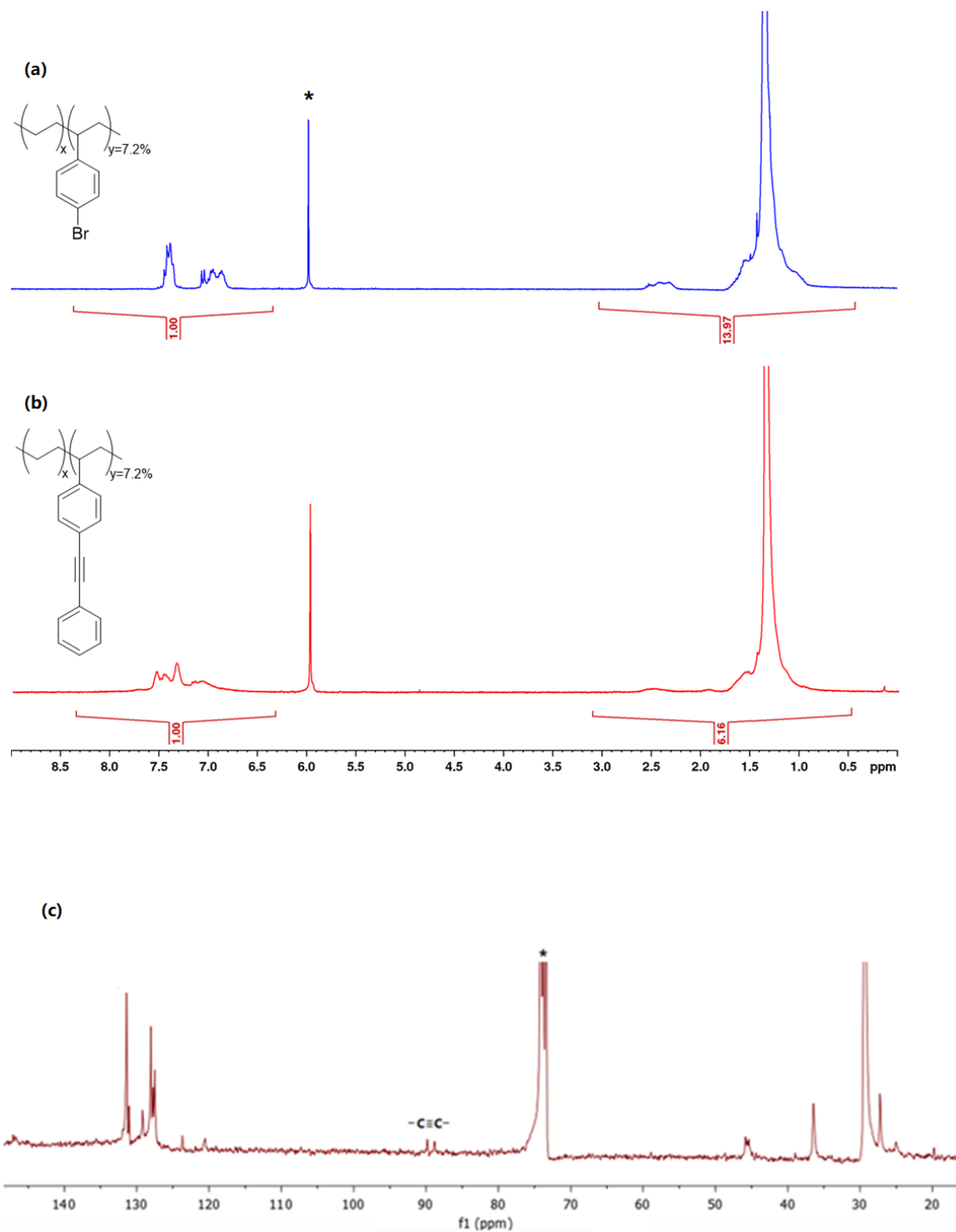
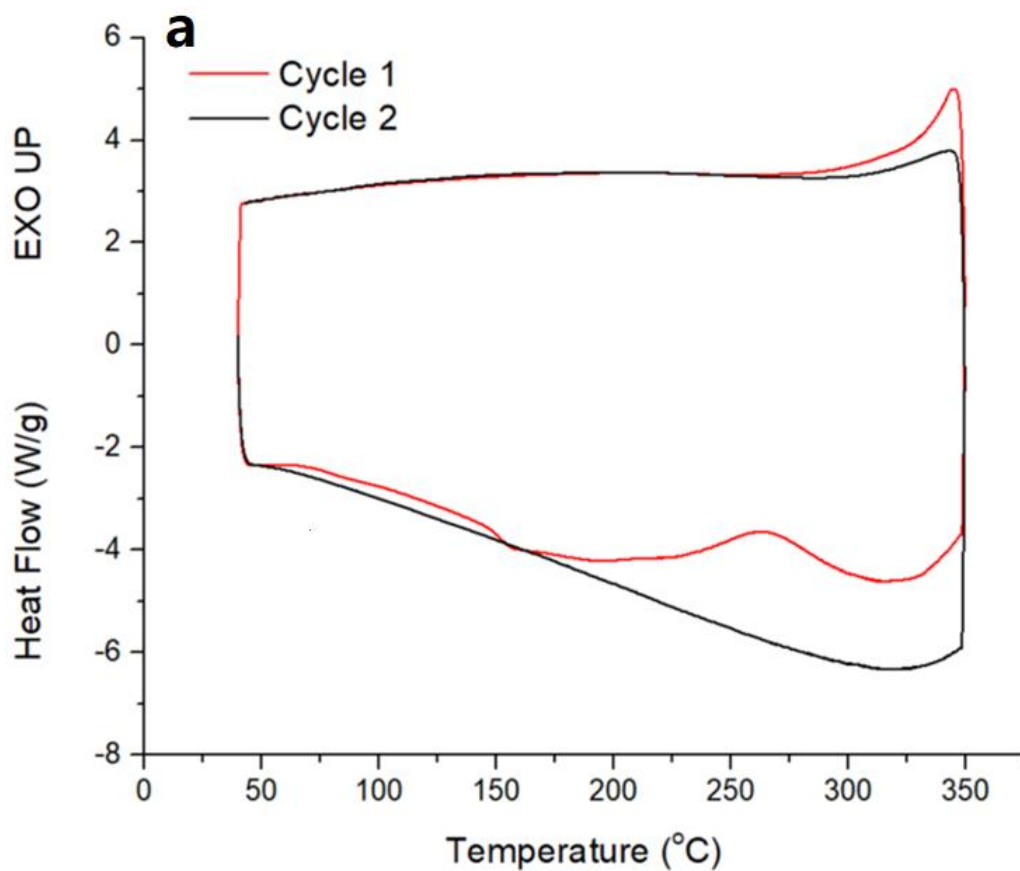


Figure 3.8 ^1H NMR spectra of (a) PE-BrSt copolymer and (b) the corresponding PE-DPA copolymer with 7.2% functional group content and (c) ^{13}C NMR spectrum of PE-DPA copolymer with 7.2% functional group content.

Because of the high DPA concentration in poly(4-phenylacetylenylstyrene) homopolymer, this polymer was selected to examine the DPA self-cycloaddition reaction. Due to the exothermic nature of a cycloaddition reaction toward a more negative free energy, a calorimetric investigation was performed on poly(4-phenylacetylenyl styrene) polymer. Figure 3.9(a) shows DSC curves in two consecutive heating and cooling cycles in N₂ atmosphere. The first cycle shows a glass transition at ~152°C, followed by a broad exothermic peak ranging from 170°C to 320°C arising from the cycloaddition reaction between DPA side groups. As the temperature further increased to 325°C, another exothermic reaction was observed, attributable to the decomposition of the polymer backbone. In the thermogram of the second cycle, neither the glass transition behavior nor the exothermic reaction below 325°C can be observed, indicating that the polymer has become fully cross-linked by the thorough reaction in the first heating cycle. To validate the exothermic peak determined by DSC results is due to the cycloaddition reaction, a gel content test was also conducted, comparing the dissolution behaviors of a pristine poly(4-phenylacetylenyl styrene) sample before and after heat-treatment at 220°C in N₂ for 1 hour, using THF as the solvent. As shown in Figure 3.9(b), the poly(4-phenylacetylenyl styrene) with 0% gel content became completely insoluble with 100% gel content as a result of this heat treatment. Additionally, no swelling was found for the heat-treated sample after soaking in THF for 24 hours, indicating the formation of a thoroughly cross-linked network at 220°C.



b



poly(4-phenylacetylenyl styrene)
not heat-treated



poly(4-phenylacetylenyl styrene)
heat-treated @220°C

Figure 3.9 (a) DSC curve of poly(4-phenylacetylenyl styrene) in N_2 with two heating/cooling cycles and (b) images illustrating solubility of poly(4-phenylacetylenyl styrene) without (left) and with (right) heat treatment at 220°C in N_2 for 1 hour.

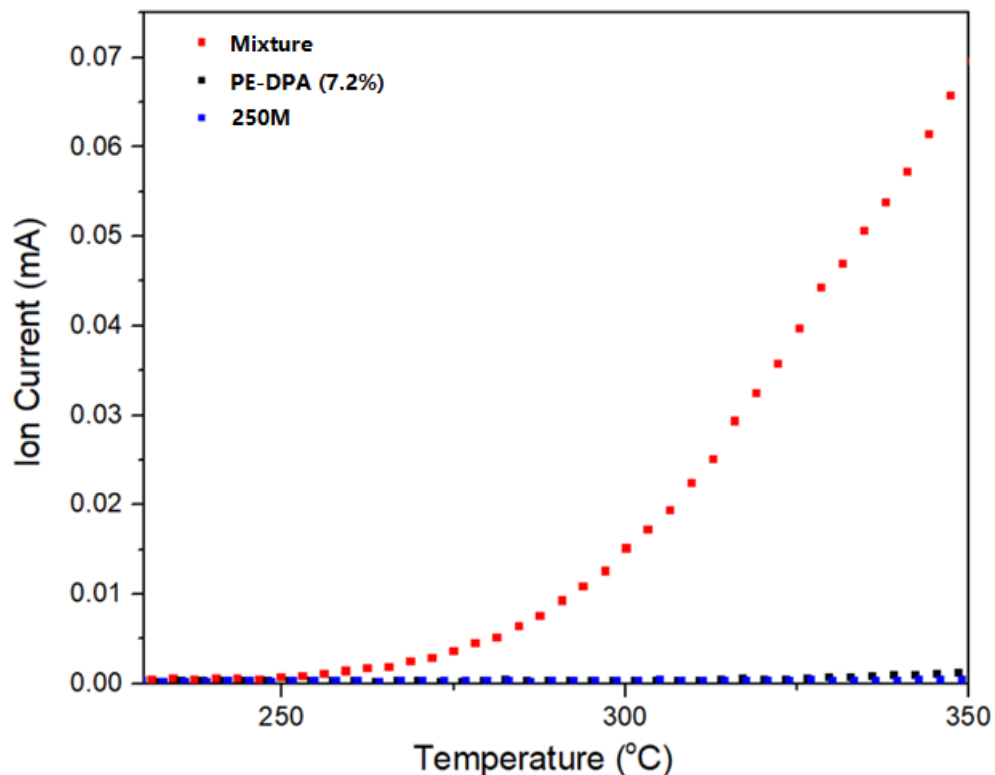


Figure 3.10 H₂ gas evolution in EGA-MS Spectra of PE-DPA (7.2%) copolymer, pitch (250M), and their mixture with 1 to 3 weight ratio.

The next experiment was to understand the cycloaddition reaction between DPA moieties in the polymer and PAH molecules in pitch. From previous studies as discussed in Section 3.2, we have known that the Diels-Alder cycloaddition reaction between the acetylene and bay-region of PAH molecule would be followed by the release hydrogen. This consecutive dehydrogenation reaction converts the newly formed cyclic ring into a more conjugated aromatic structure. Therefore, the released hydrogen is a promising indicator, showing at what temperature the reaction between diphenylacetylene moieties and pitch molecules starts to happen. Figure 3.10 compares three EGA-MS curves, detecting H₂ release, between PE-DPA copolymer with 7.2 mol% comonomer percentage, pitch (250M), and the mixture of these two components with 1:3 weight ratio. The mixture was prepared by simply dissolved the two substances in toluene at 90°C and then dried at 60°C in vacuum oven. There was no obvious evolved H₂ gas observed from two raw materials in the temperature range of measurement. For the mixture, the H₂ release started at

about 250°C and increased exponentially as the temperature rose. Since the dehydrogenation happened after the cycloaddition reaction to form aromatic rings, the EGA-MS results imply that the starting temperature of the cycloaddition reaction between PE-DPA and pitch (250M) is below 250°C. Overall, the experimental results indicate that the DPA moieties located along the polymer chain are quite reactive under elevated temperature conditions of more than 200°C. They can simultaneously engage in Diels-Alder cycloaddition reactions with themselves and with PAH molecules in pitch.

3.4.2 Preparation and Thermal Conversion of PE-g-Pitch/Pitch Blend Precursors

As discussed, it is essential to prepare CF precursors with good processibility, without any premature cross-linking structure. Thus, during the preparation of PE-g-Pitch precursor by the thermal-induced cycloaddition reaction between PE-DPA copolymer and PAH molecules, we needed to be very diligent in finding the suitable reaction conditions to avoid the potential self-cycloaddition reaction between DPA side groups in the PE-DPA copolymer. Table 3.2 summarizes the preparation conditions of a series of samples, to identify the optimal reaction conditions, including the DPA content in the copolymer in mol% and the PE-DPA/pitch weight ratios for blending, as well as the specific blending temperature.

Table 3.2 A summary of cycloaddition reaction between PE-DPA copolymers and Pitch(250M) under various experimental conditions.

Run	Sample	DPA content in PE copolymer (mol %)	Polymer:Pitch Weight Ratio	Mixing Temp/Time (°C/hr)
control	PE-1/5	0	1:5	310/1
1	PE-DPA(2.1%)-1/5	2.1	1:5	310/1
2	PE-DPA (3.2%)-1/5	3.2	1:5	310/1
3	PE-DPA (7.2%)-1/3	7.2	1:3	310/1
5	PE-DPA (7.2%)-1/5	7.2	1:5	310/1
6	PE-DPA (7.2%)-1/10	7.2	1:10	310/1
7	PE-DPA (7.2%)-1/10-2	7.2	1:10	280/1
8	PE-DPA (7.2%)-1/10-3	7.2	1:10	250/1

Based on previous experimental results, showing that Diel-Alders cycloaddition between DPA moieties and PAH molecules occur at temperatures above 200°C, and the polycondensation reaction between pitch molecules at temperatures above 350°C as discussed in Chapter 1, the cycloaddition (grafting) reaction was conducted at 310°C between the PE-DPA copolymer and pitch (250M) by heating the mixture in a Brabender with blending for one hour under an N₂ atmosphere with a flow rate of 100 ml/min. To minimize the potential cross-linking reaction within the PE-DPA copolymer, the DPA concentration was limited to a small percentage (i.e., 2.1, 3.2, and 7.2%), and largely excess pitch (PAH) molecules were used in the mixture, as shown in Table 3.2. This grafting reaction produces PE-g-Pitch graft copolymer, having a semi-crystalline PE backbone and some PAH side groups, as well as some excess (ungrafted) pitch molecules. It is highly beneficial to have some free ungrafted pitch molecules presented with the PE-g-Pitch; they serve as the plasticizer to reduce the overall melt viscosity of PE-g-Pitch/pitch blend during the melt-spinning process to form the corresponding fiber. Additionally, pitch is a low-cost precursor that is melt-spinnable after reaching its softening temperature. The presence of ungrafted pitch in the blend can reduce the precursor cost. As will be discussed later, it is quite unexpected to observe this PE-g-Pitch/pitch blend exhibiting higher carbon yield (>70%) than the

corresponding starting materials PE-DPA copolymer and pitch, which were also heat-treated at 310°C for one hour under N₂ atmosphere. Figure 3.11 shows several comparative TGA results between PE-g-Pitch/pitch blends and their corresponding PE-DPA copolymer and pitch (250M). The experiment was focused on the understanding of the most suitable blending condition between PE-DPA copolymer and pitch (250M), which can offer the resulting PE-g-Pitch/pitch blend with a high carbon yield at 1000°C.

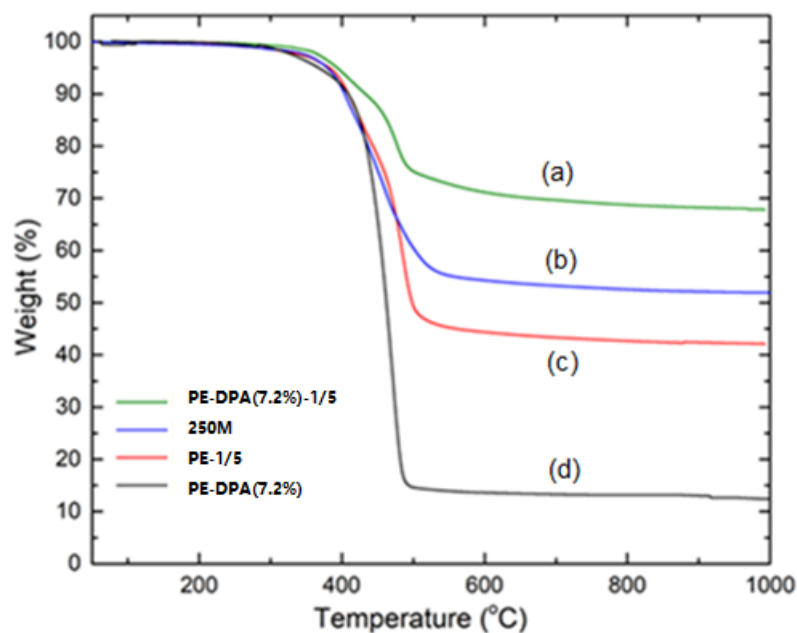


Figure 3.11 TGA curve comparisons of (a) PE-DPA (7.2 mol% DPA content)/pitch (250M) blend with 1/5 weight ratio, (b) pitch (250M), (c) PE/pitch blend with 1/5 weight ratio, and (d) PE-DPA copolymer (7.2 mol% DPA content).

Figure 3.11 compares TGA curves of the PE-DPA (7.2 mol% DPA content)/pitch (250M) blend with 1/5 weight ratio and its two starting materials, as well as a blend between PE homopolymer and pitch (250M) with the same 1/5 weight ratio. All samples were thermally treated under the N₂ atmosphere at 310°C for one hour before TGA measurements. Both the PE-DPA copolymer and pitch showed a one-step weight loss curve in the range from ~350° to ~500°C. In contrast, the weight loss of both blend samples exhibited a two-step pattern, with the first step at ~350-430°C and the second step at ~430-500°C. This suggests two distinctive weight

loss mechanisms that are attributable to the evaporation of pitch molecules with a low molecular weight at the lower temperature range and PE backbone decomposition at the higher temperature range, respectively. It was a pleasant surprise to observe the significantly higher carbon yield of 68% for this PE-DPA copolymer/pitch blend than the carbon yield of 42% for a similar PE/pitch blend (with the same 1/5 weight ratio but without the reactive DPA moieties located along the polymer chain). The carbon yield of the PE-DPA copolymer/pitch blend was also significantly higher than those of individual starting materials, pitch (250M) with 52% and PE-DPA copolymer with only 12%. Since the PE homopolymer was completely decomposed during the pyrolysis at $>500^{\circ}\text{C}$, the carbon yield of a simple PE/pitch blend was mostly dominant with the pitch content in the blend. In other words, two components in this PE/pitch blend independently responded to the thermal treatment, without any reaction between them. On the other hand, the cycloaddition reactions happened between the PE-DPA copolymer and pitch molecules at $<310^{\circ}\text{C}$ (from the result in section 3.4.1) to form a PE-g-Pitch graft copolymer with PAH side groups, prior to the first weight loss in the heating range of $350\text{-}430^{\circ}\text{C}$. Evidently, the grafting reaction did happen to reduce the amount of free (ungrafted) small pitch molecules and reduce the weight loss to only ~ 13 wt.% in this heating range. After the temperature reached 430°C , the polymer backbone started to engage the thermal transformation accompanied by the further evaporation of some ungrafted pitch molecules. The TGA curve shows only about $\sim 10\%$ weight loss in the second thermal step ($\sim 430\text{-}500^{\circ}\text{C}$). As will be discussed in the next chapter, when we examine the detailed reaction mechanism, the resulting PE-g-Pitch graft copolymer engaged in a dehydrogenation reaction along the polymer chain to form a more thermally stable polymer structure with extensive π -electrons conjugation. In this temperature range, the isotropic pitch molecules also engaged in a polycondensation reaction to form a mesophase pitch structure.¹³ Overall, the comparative TGA results indicate the importance of reactive DPA moieties in the PE-DPA copolymer, which react with PAH molecules in pitch to transform the copolymer to the desirable PE-g-Pitch graft copolymer.

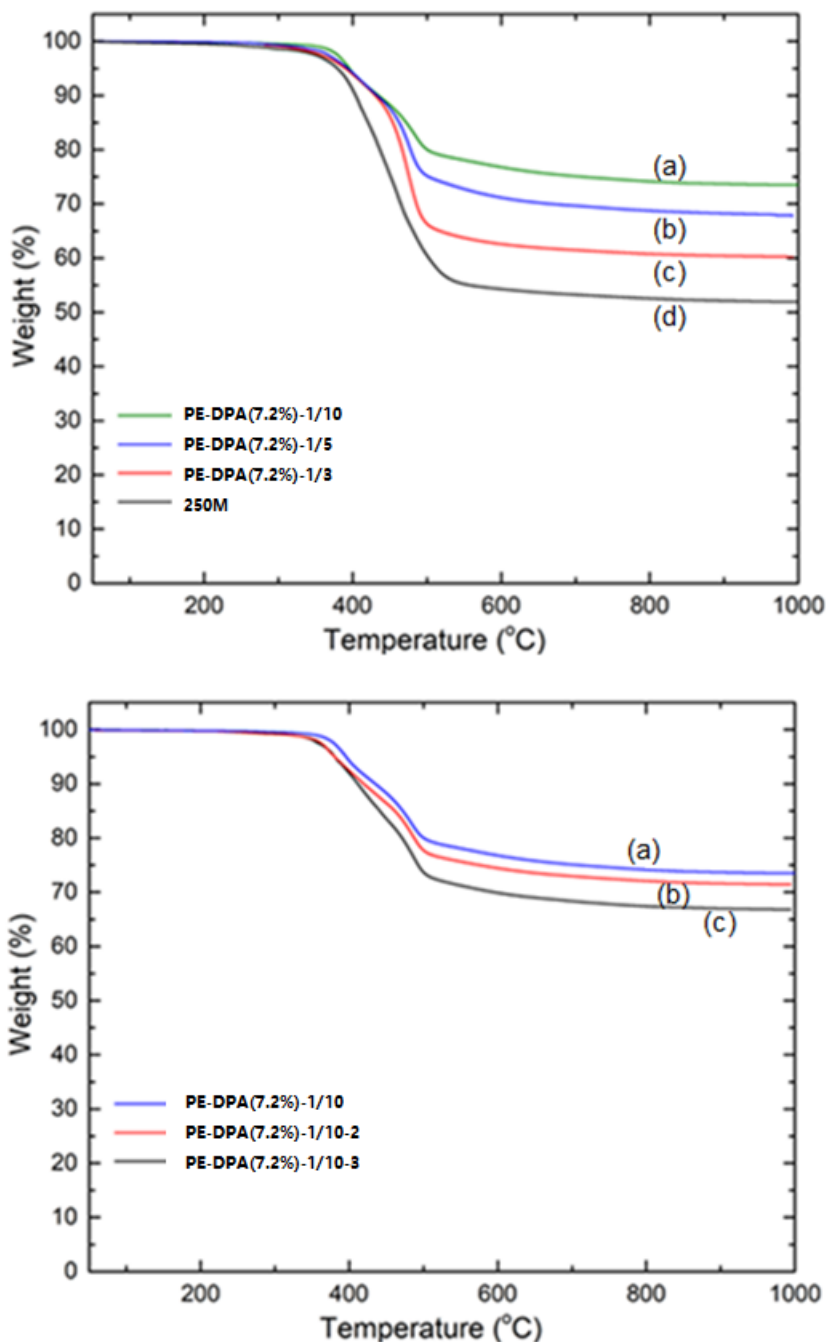


Figure 3.12 TGA curve comparisons (top) between three PE-DPA (7.2 mol% DPA content)/pitch (250M) blends with (a) 1/10, (b) 1/5, and (c) 1/3 weight ratios and (d) pitch (250M), (bottom) PE-DPA (7.2 mol% DPA content)/pitch (250M) with 1/10 weight ratio blend prepared at different temperature (a) 310°C, (b) 280°C, and (c) 250°C for 1 hour before the TGA measurement.

The next question is how the blending ratios between the PE-DPA copolymer and pitch affect the carbon yield of the blend? As expected, the higher percentage of the low-cost and melt-

processable pitch in the blend will be the preferred composition. Figure 3.12 (top) compares the TGA curves of three PE-DPA (7.2 mol%) copolymer/pitch (250M) blends with 1/10, 1/5, and 1/3 weight ratios, as well as pitch (250M) reference. All samples were thermally treated with blending under an N₂ atmosphere at 310°C for one hour to form the PE-g-Pitch structure before TGA measurements. In the first weight loss thermal range of 350-430°C, all three blends showed very similar weight loss ~13 wt.%, which was significantly lower than that of pitch (250M) reference. In the second weight loss thermal range of 430-500°C, the blend with the lowest polymer content exhibited the highest weight remaining. Based on the previous result showing the PE-DPA copolymer with only 13% carbon yield, it may be logical to think that the higher carbon yield of PE-DPA(7%)-1/10 may be due to the lower polymer content. However, considering both of the blend samples showed higher carbon yields than pitch 250M, it is clear that the stabilization reaction that happened in this temperature range effectively prevented the PE backbones from being decomposed.

Figure 3.12 (bottom) compares the TGA curves of three PE-DPA (7.2 mol%)/pitch (250M) blends with 1/10 weight ratio, with blending temperatures of 250°, 280°, and 310°C, respectively. It is notable that increasing blending treatment temperature (before the TGA measurement) also improved the carbon yield. The results indicate that the reaction temperature between DPA side groups and PAH molecules in pitch is more favorable at 310°C in forming the desirable PE-g-Pitch graft copolymer structure that is essential to this new precursor technology.

Figure 3.13 shows the TGA comparison of four PE-DPA/pitch (1/5 weight ratio) blends with DPA group content of 0, 2.1, 3.2, and 7.2 mol%. The carbon yield keeps increasing with functional group content from 0 to 3.2%. However, the difference between 3.2% and 7.2% is very small, even with the content of DPA increased to more than double, which may indicate there is an upper limit of PAH side groups that are effective in the stabilization/carbonization process of PE-g-Pitch.

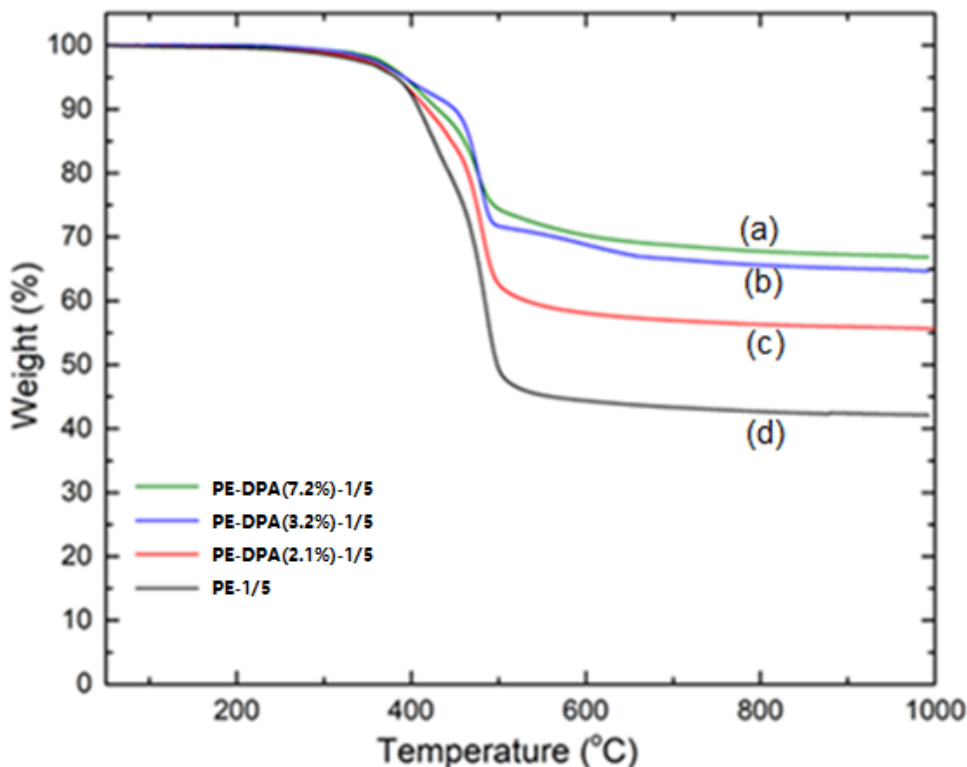


Figure 3.13 TGA comparisons of three PE-DPA/pitch (250M) blends with (a) 7.2 mol%, (b) 3.2 mol%, and (c) 2.1 mol% of DPA content in the copolymer and (d) PE/pitch (1/5) blend as the reference.

It is interesting to note an important benefit of this PE-g-Pitch precursor technology: It does not require the O_2 atmosphere for stabilization. The whole stabilization and carbonization thermal treatment procedure (Figure.3.5) can be carried out in a one-step continuous manner under an inert atmosphere to form the carbon structure. As discussed in Chapter 1, both PAN and pitch precursor fibers must be carefully heated at the stabilization temperature $<300^\circ\text{C}$ in an air (oxygen) environment for facilitating the formation of a network (infusible) structure, before high-temperature thermal conversion to the carbon material. In addition to the long stabilization time, there are several serious concerns with this O_2 -treatment procedure. Due to the rapid and highly exothermal oxidation reactions, the large amount of heat generated creates difficulty in controlling the heating uniformly, and the localized high temperature accelerates more reactions and releases more heat. The other major problem is the inhomogeneity of oxygen diffusion from

the surface to the inner core of the fibers. Even for a PAN fiber with a small diameter of $\sim 5\mu\text{m}$, the outer part of the fiber engages more oxidative stabilization reactions. As a result, hollow CF structures can easily form, and only the outer skin has an ultimate mechanical strength. Therefore, this new PE-g-Pitch precursor may ease concerns about excess heat generation and oxygen diffusion, and a homogeneous CF morphology may be achieved by simply one-step heating under an inert atmosphere.

3.4.3 Melt Rheology of PE-g-Pitch//Pitch Blend Precursors

As discussed in Chapter 1, processibility is an essential consideration in designing a CF precursor. It is highly preferred to have a precursor polymer that is melt-spinnable into precursor fiber. The melt-processability and the suitable processing condition can be determined by rheological measurement, with loss modulus (G''), storage modulus (G'), and complex viscosity (η^*). The comparison of the values G' and G'' is one way to characterize the solidification behavior of the precursor. The complex viscosity reflects the ability of the precursor to be extruded and drawn into fibers. As shown in Figure 3.14, both temperature- and time-sweep rheology measurements were conducted to understand the most suitable precursor and conditions during the fiber spinning process.

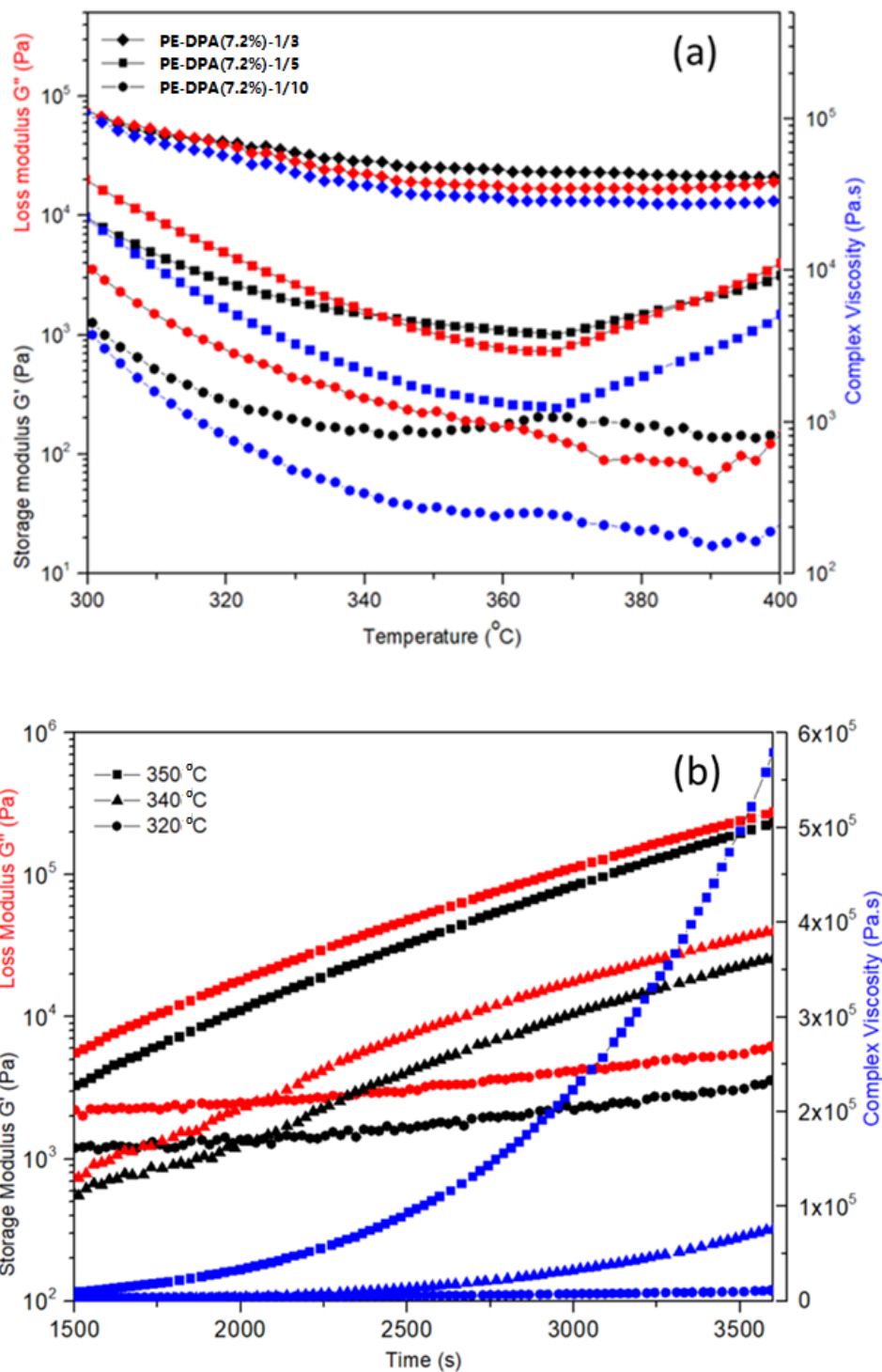


Figure 3.14 (a) oscillatory rheology by temperature-sweep measurement of three PE-g-Pitch/pitch blends prepared from PE-DPA(7.2mol%)/pitch (250M) blends with 1/10, 1/5, and 1/3 weight ratios, (b) time-sweep rheology measurement of the precursor from the PE-DPA(7.2%)/pitch (1/10) sample at different temperatures of 320, 340 and 350 $^{\circ}\text{C}$.

Figure 3.14 (a) shows the temperature-sweep rheology behaviors for three PE-g-Pitch/pitch blends. They were prepared by heating PE-DPA (7.2 mol%)/pitch (250M) blends with 1/10, 1/5, and 1/3 weight ratios, respectively, at 310°C for one hour under the N₂ atmosphere. The melt viscosity of the blend is highly sensitive to the pitch content. At 400°C, the viscosity of the PE-DPA(7.2%)-1/10 blend was 222.8 Pa.s while the viscosity values of PE-DPA(7.2%)-1/5 and PE-DPA(7.2%)-1/3 were 6262.8 Pa.s and 29425.8 Pa.s, respectively. Interestingly, the merging of G' and G'' happened at a low temperature for PE-DPA (7.2%)-1/3 sample with the highest PE-DPA copolymer content. From the previous DSC result on poly (4-phenylacetylenyl styrene), it is known that the cycloaddition between DPA groups begins at ~170°C. The result here suggests that due to the limited dilution by pitch (250M) during the reactive blending process at 310°C, some of the DPA groups on polymer chains have experienced self-cycloaddition reaction and formed some cross-linked structures in the contest with the grafting reaction between DPA and pitch. Though the majority part of the material was still pitch that can be liquefied, the formation of the polymer network caused the material to show solid-like behavior, differing from the sample with DPA functional groups diluted by a larger quantity of petroleum pitch. For PE-DPA(7.2%)-1/10 blend, the sample reached its gel point at about 360°C, which is very close to the temperature of thermal polycondensation among PAH molecules in pitch. This experimental result indicates that PAH side groups in the polymer chain reacted to each other, and generating a cross-linking network structure. More details about the cross-linking reaction will be discussed in the following time-sweep measurements of this sample. The comparison on the rheological behaviors of the blend samples prepared with different weight ratios of starting materials shows the importance of mixing PE-DPA copolymer with an adequate amount of pitch (250M) to effectively prevent the premature network formation in the produced PE-g-pitch/pitch precursor. Meanwhile, the free ungrafted pitch can be used as a plasticizer to control the viscosity of the blended mixture during fiber melt-spinning.

To further investigate the thermal stability of the PE-g-Pitch/pitch blend, we conducted time-sweep experiments for the PE-DPA (7.2%)-1/10 sample at three different measurement temperatures: 320°C, 340°C, and 350°C as illustrated in Figure 3.14(b). All experiments were allowed a waiting time of 1500 seconds before the measurement started to reach homogeneous thermal distribution within the whole sample. When it was measured at 320°C, the PE-DPA (7.2%)-1/10 sample showed a complex viscosity increment from ~4004 to 7624 Pa.s within 30 minutes. This increment may be due to the loss of volatile pitch molecules with small molecular weight by nitrogen flow at this temperature. But the rheology behavior was different when the measurement temperature was changed to 340°C, only 20°C higher than the previous experiment. In this case, the complex viscosity showed a larger increment, from 1473 to 32473 Pa.s in 30 minutes. We also found that a higher temperature could further promote the viscosity increment when we repeated the same procedure at 350°C, at which the complex viscosity increased from 10421 to 223439 Pa.s. This suggests that a heat treatment higher than 340°C encourages more pitch molecules to react with the polymer side groups, therefore increasing the average molecular weight of the polymer portion and reducing the amount of plasticizer within the material, both of which can increase the viscosity. As discussed earlier, the cycloaddition between unsaturated functional groups and aromatic clusters in pitch has a hindrance restriction that prevents the clusters with high molecular weight from becoming reactive, due to their low mobility at 310°C. However, when the temperature is increased beyond 340°C, those large free clusters become more mobilized and reactive. It also explains why the degree of complex viscosity increment starts to increase exponentially as a function of time. Additionally, on the rheology curve of heating at 350°C, a clear merging between G' and G'' can be found, indicating that the pitch molecules bonded to the polymer backbones start to react to each other and form a cross-linking network. Overall, the rheology results suggest that the suitable melt-spinning temperature for a PE-g-Pitch/pitch precursor prepared from the PE-DPA (7.2%)-1/10 blend sample is in the 320-

340°C range. The as-spun precursor fiber can be heated at >350°C to form the infusible fiber structure (stabilization step) under N₂ atmosphere, without the involvement of oxygen.

3.4.4 Melt-spinning of PE-g-Pitch//Pitch Blend Precursor Fibers

The PE-DPA (7.2%)-1/10 blend sample, prepared by mixing PE-DPA copolymer with 7.2 mol% comonomer percentage and pitch (250M) with a 1/10 weight ratio and pre-treated at 310°C for one hour in N₂ atmosphere, was subjected to a melt-spinning process at Oak Ridge National Laboratory using a piston fiber extruder through a die with a diameter of 100 μm. This blend precursor was continuously spun at 320°C. As seen in Figure 3.15 (a), this precursor can be wound up by a spin winder at a constant speed. The SEM images in Figure 3.15 (b) show the morphology of the as-spun precursor fiber made from PE-DPA (7.2%)-1/10. After spinning, the precursor fiber was slightly stretched to a reduced diameter of around 60 μm. The as-spun fibers revealed an uneven striated surface with longitudinal ridges oriented along the filament axis, indicating some cross-linking reactions might happen during the melt-spinning although the network structure had not been formed yet. Additionally, due to a large quantity of pitch in the precursor material, the formed precursor fibers are very brittle, and thus could be continuously spun for only a short period of 5 minutes on average.

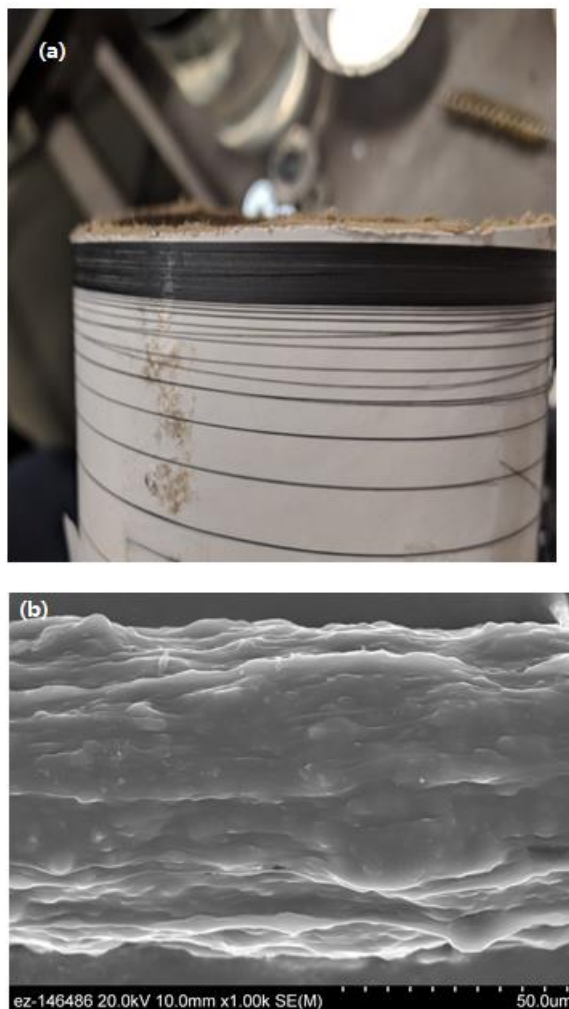


Figure 3.15 (a) optical picture and (b) SEM micrograph of as-spun precursor fibers by melt-spinning of PE-DPA (7.2%)-1/10 blend.

The as-spun precursor fibers were preliminarily carbonized to 1000°C in an inert atmosphere without any mechanical stretching after stabilized at 360°C for 2 hours. Figure 3.16 shows the SEM micrograph of the resulting carbon fiber. Without mechanical tension, the fiber diameter almost remained the same before and after carbonization, and the pores created by the involuting gases could not be healed. Many pores are obviously present on and beneath the fiber surface.

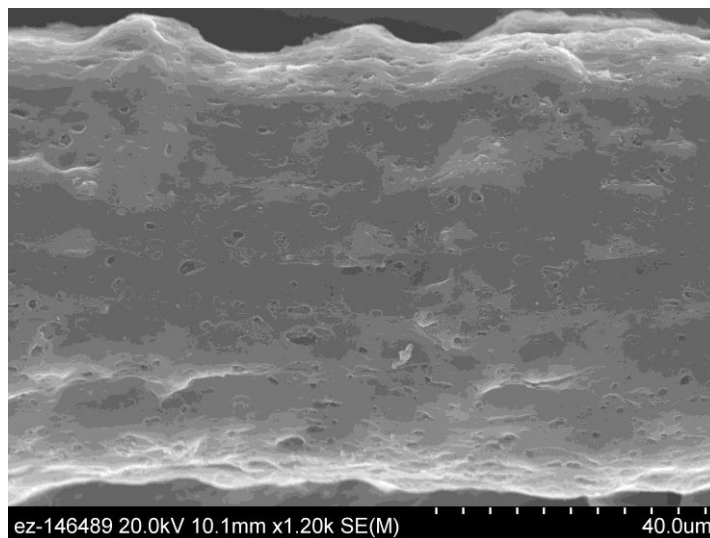


Figure 3.16 SEM micrograph of carbon fiber by melt-spinning of PE-DPA (7.2%)-1/10 blend.

3.4.5 Carbon Structures Resulted from PE-g-Pitch//Pitch Precursors

The resulting CFs were characterized by XRD and Raman spectroscopy to determine their graphitic structure. Figure 3.17 (top) compares XRD patterns for several carbon materials obtained from PE-DPA (7.2%)-1/10 by conducting carbonization at five different temperatures, including 800°C, 1100°C, 1400°C, 1700°C, and 1900°C, respectively, under N₂ atmosphere. Figure 3.17(bottom) shows Raman spectra of the same set of carbon materials, using visible light with a wavelength of 532 nm. Figure 3.18 summarizes the values of carbon interlayer d-spacing (002), the stacking height (L_a), and lateral size (L_c) of the crystallite, calculated according to Bragg's Law and the Scherrer formula, and the Raman peak intensity ratio between D and G bands versus carbonization temperature.

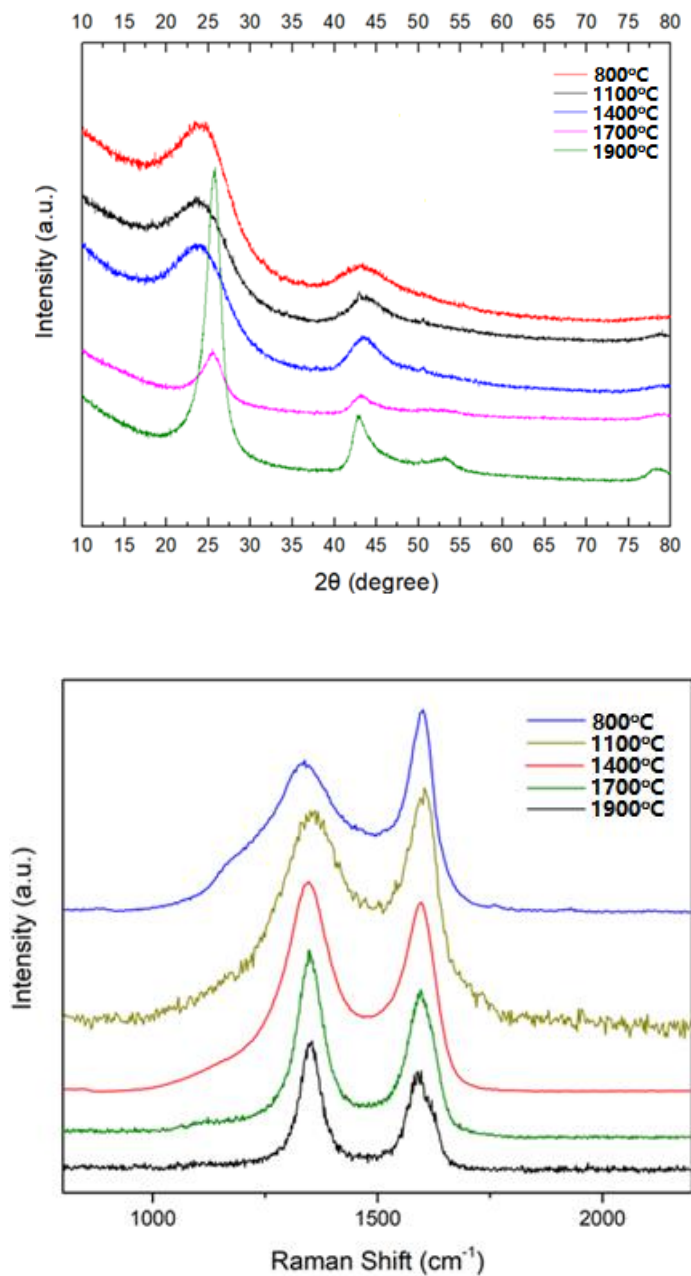


Figure 3.17 (top) XRD and (bottom) Raman spectra of carbon products prepared from PE-DPA (7.2%)/pitch (250M) 1/10 blend at carbonization temperature of 800°C, 1100°C, 1400°C, 1700°C, and 1900°C, respectively.

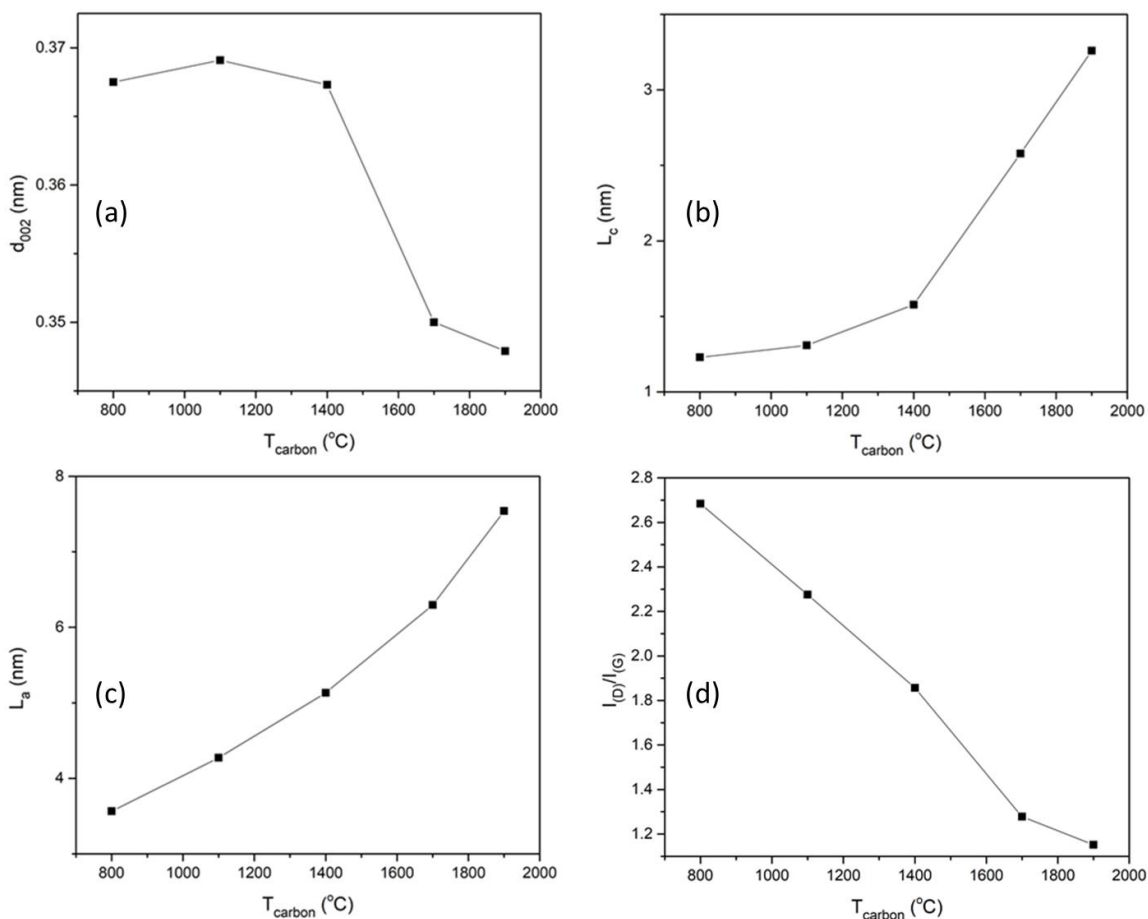


Figure 3.18 Plots of (a) d-spacing (002), (b) lateral size (L_c), (c) stacking height (L_a) of the crystallite, and (d) the peak intensity ratio between D and G bands in Raman spectra vs carbonization temperature.

The PE-DPA (7.2%)-1/10 blend was subjected to heat treatment under temperatures reaching 1900 °C. As shown in Figure 3.16, when the carbonization temperature was increased from 800 °C to 1400 °C, the d (002) value first increased slightly from 0.3675 nm to a larger spacing of 0.3691 nm, then decreased back to 0.3673 nm. The d-spacing increment between 800 °C and 1100 °C is due to the release of hydrogen still occurring at this temperature range, therefore interrupting the stacking of graphite layers. As the temperature increased to 1700 °C and 1900 °C, the d spacing reduced dramatically to 0.35 nm and 0.3479 nm, respectively, indicating that the carbon layers transformed from a disordered turbostratic structure to a more ordered graphite-like structure. Both the lateral size L_a and stacking height L_c of PE-DPA (7.2%)-1/10 showed

exponential growth between 800°C and 1900°C. The sample carbonized at 1100°C showed L_c of 1.3080 nm, which is similar to the stacking height of a carbonized PAN precursor fiber of 1.3 nm at this temperature, while its L_a of 4.2717 nm is higher than the 2.3 nm in PAN.^{158,159} This could be a result of the high content of aromatic structure in PE-g-Pitch/pitch blend promoting the growth of carbon layers in the layer plane direction, while the small content of polymer chains disturbs the packing of these layers in the normal direction.

All Raman curves had two peaks located at 1356 cm^{-1} as D band and 1600 cm^{-1} as G band, which reveals these carbonized samples have a graphite-like structure. The peak intensity ratio between D and G bands ($I_{(D)}/I_{(G)}$) showed a significant reduction from 800-1900°C. These results indicate that the regularity of carbon layer structure improves and defects within the structure reduce with higher heat treatment in this temperature range.

3.5 Conclusion

The primary objective of this study was to develop a new type of CF precursor to replace the conventional PAN precursor, which forms CFs with a high cost and low carbon yield. We designed a new PE-g-Pitch precursor that was prepared from a mixture of PE-copolymer with some reactive side groups (i.e., PE-DPA copolymer) and petroleum pitch (i.e., pitch 250M). We systematically studied the preparation, processibility, and thermal transformation behaviors of a series of precursor compositions. We identified a PE-g-Pitch/pitch blend precursor, prepared by heating a PE-DPA (7.2 mol% DPA content)/pitch (250M) mixture with 1/10 weight ratio at 310°C for one hour under N_2 atmosphere; this showed the highest carbon yield of ~73% among all of the prepared samples in different mixture ratios. It is ~21% higher than petroleum pitch 250M and ~60% higher than PE-DPA (7.2mol%) copolymer, both of which were the starting materials to prepare this precursor. In oscillatory rheology measurements of several PE-g-

Pitch/pitch blends, we found that the mixing ratio had a considerable effect on the viscosity and solidification temperature. When mixing PE-DPA (7.2%) copolymer with a greater amount of petroleum pitch, the as-prepared PE-g-Pitch/pitch blend precursor showed a higher solidification temperature and lower viscosity, which makes it more favorable for the fiber spinning process. We also observed that the viscosity of this precursor showed a rapid increase with liquid-like behavior maintained before reaching the solidification point. These results indicate that the molecular weight of the polymer portion increases due to the continuous incorporation of free pitch molecules into pitch-like side groups. The PE-DPA (7.2%)-1/10 precursor was carbonized at different temperatures up to 1900°C. From XRD and Raman spectroscopy, we observed that both the carbon crystal layers' size and the amount of stacking increased and the structure had fewer defects with a higher carbonization temperature. Even with pitch as a major component when carbonized at 1100°C, the carbon structure had d_{002} and L_c values close to those of a PAN-based CF treated at the same temperature, but with a much higher L_a . This comparison also indicates that the incorporated pitch molecules in the polymer chain continue the polycondensation reaction during the entire heating process. However, the existence of the PE portion prevents these condensed pitch molecules from stacking regularly like pure PAH. By using a piston extruder, PE-DPA (7.2%)-1/10 was successfully spun to precursor fibers that can be wound up using a spin winder at a constant speed. However, the as-spun fibers revealed an uneven striated surface with longitudinal ridges oriented along the filament axis due to the inevitable premature cross-linking reaction that happened during the sample preparation although the DPA content had been diluted by the ungrafted pitch. Additionally, the large quantity of pitch in the precursor material resulted in the precursor fibers that were very weak and brittle and could be continuously spun for only a short period.

Chapter 4

Mechanistic Study of Thermal Transformation from Polyethylene-graft-Pitch to Carbon Materials

4.1 Introduction

In Chapter 3, I have discussed a new class of PE-g-Pitch/pitch blend precursors that not only offer high carbon yield (>70%) in a one-step heating process under N₂ atmosphere but also are melt-processable to form the precursor fibers. The combination provides a potential new approach for preparing low-cost carbon fibers (CFs). Evidently, the graft copolymer PE-g-Pitch plays a key role in the whole carbon conversion mechanism. We have postulated several likely thermally induced chemical reactions during the transformation process. However, the reaction mechanism details for the stabilization are still not clear, and we especially need to better understand the main functions of PE-g-Pitch graft copolymer with the structural characteristics that are essential in designing polymer blend precursors. In this chapter, I will focus on the thermal transformation reactions in the pure PE-g-Pitch graft copolymer with all the un-grafted pitch molecules removed from the corresponding polymer blend. The experiments will involve the preparation of a series of pure PE-g-Pitch graft copolymers and an analysis of their thermal conversion reactions, especially the reactions during the stabilization step.

To investigate the stabilization mechanism, we used numerous scientific approaches, including TGA, DSC, XRD, solid-state cross-polarization magic angle spinning Carbon-13 nuclear magnetic resonance (CP-MAS ¹³C NMR), and EGA-MS—to characterize and analyze the thermal degradation behavior and transformation of the chemical and bulk structure during heat treatment at different temperatures.

4.2 Experimental Section

4.2.1 Characterization

Liquid state ^1H NMR spectra were obtained by using Bruker AV 300 at 90°C. CP-MAS ^{13}C NMR spectra were obtained by using a Bruker Avance-III-HD ss500 at room temperature with magic angle spinning (MAS). The sample was first grounded into a fine powder using a mortar and then loaded into a ZrO_2 rotor. The spinning frequency applied was 10000 Hz and the number of scanning was 12000. Matrix-assisted Laser Desorption/Ionization Time of Flight Mass Spectrometry (MALDI-TOF-MS), were performed on a Bruker UltrafleXtreme instrument. TGA measurements were conducted on an Sdt-600 (TA Instruments). Around 10 mg of sample was loaded into the sample pan and heated at a rate of 10°C/min in the N_2 atmosphere with a gas flow rate of 50ml/min. EGA-MS measurement was conducted on a TA TGA5500 with a mass spectrometer in argon with a heating rate of 10°C/min and a flow rate of 25ml/min. The weight of the sample was fixed to be 15mg on each measurement. XRD measurements were applied on samples in powder form and conducted on a Panalytical XPert Pro MPD theta-theta Diffractometer from Malvern at 40 kV and 40 mA with Cu $\text{K}(\alpha)$ radiation $\lambda = 0.15418$ nm. Diffraction patterns were recorded on a 0.8 collimator, with an oscillation of the samples between 10 and 80° and an imaging plate detector. The scan rate was 0.2°/min with an interval of 0.045°.

4.2.2 Materials

4-Bromostyrene (TCI) was vacuum distilled after drying overnight by CaH_2 . MMAO-12 7% toluene solution (Sigma Aldrich) was dried by vacuum at 50°C to become white powders. AIBN (Sigma-Aldrich), CuI (Sigma-Aldrich), Bis(triphenylphosphine) palladium (II) dichloride (Sigma-Aldrich) phenylacetylene (TCI), diisopropylamine (Sigma Aldrich), and

$[(C_5Me_4)SiMe_2N(t-Bu)]TiCl_2$ (Boulder Scientific) were used as received. Toluene (Wiley Organics) was purified via the Grubbs type solvent purification system. Petroleum pitch (250M) with a softening temperature of 250°C were kindly provided by Rutgers Basic Aromatics GmbH.

4.2.3 Copolymerization of Ethylene and 4-Bromostyrene

A typical copolymerization reaction was conducted in a Parr 500ml stainless autoclave equipped with a mechanical stirrer. The reactor was firstly charged with 220ml of toluene, a certain amount of 4-bromostyrene (*run 1*: 5.5ml, *run 2*: 3ml, *run 3*: 1ml), and 10ml of 20wt.% of methylaluminumoxane (MAO) solution in toluene, with argon protection and stirring. Then, the solution was saturated with 50 psi ethylene at 40°C. To the mixture, 1.1 ml of $[(C_5Me_4)SiMe_2N(t-Bu)]TiCl_2$ solution in toluene (20 μ mol/ml) was injected into the reactor to initiate the reaction. After 1 hour, ethylene was replaced by argon and the reaction was terminated by adding 30ml of isopropanol. The solution mixture was then poured into 600ml of diluted HCl solution of methanol. The resulting poly(ethylene-co-4-bromostyrene) (PE-BrSt copolymer) was isolated by filtration and was washed with 200ml of methanol 3 times before drying in a vacuum oven overnight at 60°C. The comonomer percentage (BrSt mol%) of product from each run was determined by 1H NMR (*run 1*: 6.2%, *run 2*: 3.2%, *run 3*: 1.4%)

4.2.4 Synthesis Poly(ethylene-co-4-phenylacetylenyl Styrene)

In a typical reaction, 5 g of PE-BrSt copolymer from the previous reaction was initially dissolved in 230ml of toluene in a 500ml three-neck round bottom flask with a condenser under 90°C in a nitrogen atmosphere. Then 0.1g of CuI, 0.2g of Bis(triphenylphosphine) palladium (II) dichloride, and phenylacetylene (3 \times BrSt mol%) were added into the flask. The reaction was initiated by adding 25ml of diisopropylamine drop-wisely by using a dropping funnel. After 96

hours, the solution mixture was poured into 600ml of saturated ammonium chloride/methanol solution with vigorous stirring. The polymer product (PE-DPA copolymer) was dissolved in toluene and precipitated in methanol until the liquid portion became colorless.

4.2.5 Preparation of Toluene-soluble Pitch

A Soxhlet extraction apparatus was applied to extract the toluene-soluble portion from petroleum pitch 250M. It consists of a still pot containing solvent and a stir bar, a distillation path, a Siphon top and exit, a cone-shape filter paper with 8um hole size as sample holder, and a condenser with cool water flowing through. The solvent in the still pot used in this study was toluene and it was heated by an oil bath at 140°C. The temperature of the distilled solvent surrounding the sample holder was measured by a thermocouple and the value was 65°C. The collected solution was firstly dried with air-flow at 100°C and then dried in a vacuum oven at 100°C overnight. The product 250M(S) has an average molecular weight of 567.86 g/mol and a carbon yield of about 44% in N₂ at 900°C, determined by MALDI-TOF-MS and TGA, respectively.

4.2.6 Preparation of PE-g-Pitch//Pitch Blend

PE-DPA copolymer and 250M(S) were first dissolved in toluene with 5 wt.% concentration at 90°C in a 600ml beaker. Then, at the same temperature, the prepared homogeneous solution was dried with vigorous stirring under an airflow until it became a slime-like product that contained 20% toluene. The mechanical blending of the slime-like product was conducted in a twin-screw blender with nitrogen flowing through the system all the time with a flow rate of 100ml/min. This system has three thermocouples located at the outer cover, sample chamber, and inner wall to have a close monitor on temperature control. The heating rate was set

to 10°C/min for all experiments. Argon flows in the system through a rubber tube that is inert to a high temperature to create an air-free environment during mixing. When finished heating, the sample chamber was cooled down at a cooling rate of 10°C/min. After blending, all collected PE-g-Pitch/pitch blend samples were grounded into a form of powders by mortar.

4.2.7 Free Pitch Removal from PE-g-Pitch/Pitch Blend

To remove the unreacted pitch from the PE-g-Pitch/pitch blend mixture, the same Soxhlet extraction set-up was utilized as the one we used to prepare the toluene-soluble pitch 250M(S). The as-prepared product was washed with hot toluene for 24 hours until the liquid in the sample chamber (after washing) became colorless. The remaining product was then washed by stirring in toluene at 65°C and centrifuged to ensure no unreacted pitch remained in the product.

Subsequently, the solid product was washed with hexane and dried at 100°C in a vacuum oven for 12 hours to obtain pure PE-g-Pitch graft copolymer.

4.2.8 Heat Treatment of Pure PE-g-Pitch Graft Copolymer

The heat treatment of PE-g-Pitch was conducted in a Lindberg/Blue M single-zone tube furnace. In the beginning, the sample was loaded on a boat-shaped ceramic crucible before putting into the glass tube in the furnace. Then, one of the tube ends was sealed by a glass stopper, while the other end was connected to a vacuum line. The tube was vacuumed and refilled with argon by three times before applying heating to the target temperature at the rate of 10°C/min.

4.3 Results and Discussion

4.3.1 Proposed Stabilization Mechanism

As discussed in Chapter 1, prior studies have revealed the importance of the stabilization process for a CF precursor; this process directly affects the subsequent carbonization behavior. For PAN precursor fibers, their stabilization under an O₂ atmosphere involves a series of reactions, including cyclization and dehydrogenation, which transform a linear polymeric structure to a π -electron conjugated ‘ladder’ structure. In the sulfonated PE fiber case, the treatment of PE fibers with excess sulfonation agents can generate a partially conjugated alkene structure along the PE backbones. Additionally, the saturated portion on sulfonated PE’s backbones can be continually converted to more alkenes by the sulfonic groups during the heating. From the study in Chapter 2, we also found that the polyacetylene derivatives poly (PA-PA) with a complete π -electron conjugated structure can achieve a high carbon yield of ~75%. All of these studies imply that the formation of a highly conjugated structure during the stabilization step is essential for effectively converting the precursor to carbon materials.

The prior studies also give us an insight into the stabilization mechanism of PE-g-Pitch graft copolymers that are composed of a PE backbone and many pitch-like pendant groups with the structure of a polycyclic aromatic hydrocarbon (PAH). As discussed, the PAH side groups can easily be converted to carbon via a thermodynamically driven polycondensation reaction at high temperature. By contrast, the PE backbone with -CH₂-CH₂- repeat units must transform to a more stable π -electron conjugated structure for a successful carbon conversion. Otherwise, they would be broken into small and volatile fragments via thermal cleavage starting at ~450°C, even in an inert atmosphere.



Figure 4.1 General equation of elimination reaction.

The transformation mechanism from alkanes to alkenes is well known. The most common alkene-forming chemistry is the elimination reaction (Figure 4.1) with the bond breakages of C-A and C-B and the formation of a double bond between the two carbons. In most cases, either A or B is a hydrogen atom, and the other is a leaving group. In the case of the elimination of haloalkane, for example, the electron pairs break between halogen (X) and carbon and form X^- as a result. The X^- can combine with the proton with a positive charge released from the adjacent carbon, while the double bond is formed between the two carbons via either the E1 or E2 mechanism. However, for the PE-g-Pitch that is considered to be pure hydrocarbons, there are only hydrogens bonding to the carbons. Therefore, a more likely route for transforming alkane on PE-g-Pitch to alkene structure is via dehydrogenation. This is commonly used in the chemical industry as a value-added method for converting the abundant and inexpensive alkanes to more valuable alkenes. Dehydrogenation of alkanes is a highly endothermic process due to the high positive enthalpy of reaction. The dehydrogenation of isobutane and cyclohexane (Figure 4.2), for example, has a ΔH_r° of 118KJmol^{-1} .¹⁶⁰ Additionally, the dissociation energy of the C-C bond ($\sim 246\text{kJ/mol}$) is lower than C-H ($\sim 363\text{kJ/mol}$); as a result, the dehydrogenation cannot be carried out thermally in most cases without cracking the hydrocarbons.¹⁶¹ Therefore, catalytic dehydrogenation is usually applied on the large-scale conversion by using Pt-based catalysts to activate C-H bonds, coupled with a deactivated effect for the breakage of C-C bonds.^{161–163}

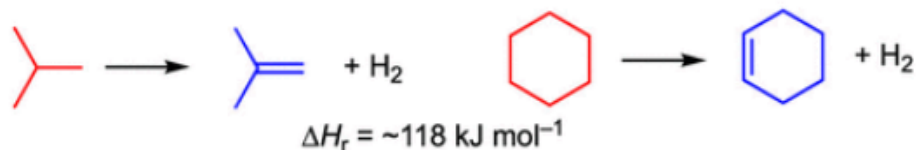


Figure 4.2 Nonoxidative dehydrogenation of (left) isobutane and (right) cyclohexane.¹⁶⁰

Compared to typical alkanes such as isobutane and cyclohexane, PE-g-Pitch has highly π -electron conjugated side groups in the form of PAH connecting to its alkane portion. The energy of C-H bonds on α -carbons connecting to these side groups can be reduced dramatically, causing these C-H bonds to break more easily and generate free radicals at a high temperature. The formed free radicals on α -carbons can be stabilized by the resonance effect from the highly conjugated side groups, as well as by the hyperconjugation effect from the adjacent $-\text{CH}_2-$ repeat units. After the formation of a tertiary free radical on α -carbon, due to the driven force to form a more stable structure thermodynamically, the C-H bonds on β -carbon are affected by the extended conjugation effect on α -carbon, and tend to break as a result, generating a double bond and hydrogen molecules. Because of the nature of the linear polymeric structure of PE-g-Pitch backbones, the conjugation system can be extended to the next carbon once the new double bond is formed, therefore promoting the formation of the other double bonds as a chain effect. This is shown in Figure 4.3.

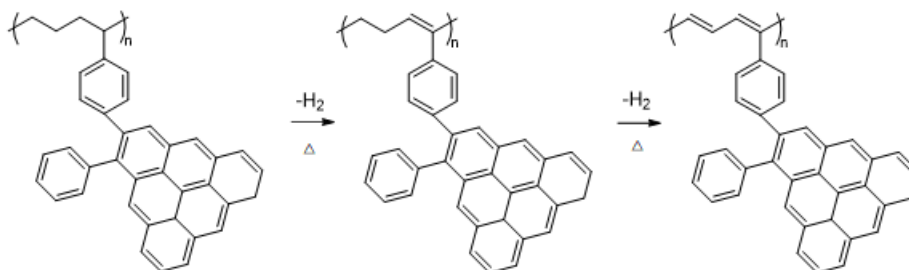


Figure 4.3 Proposed stabilization mechanism of PE-g-Pitch backbone via dehydrogenation.

4.3.2 Synthesis of Pure PE-g-Pitch Graft Copolymer

As discussed in the experimental section, to prepare pure PE-g-Pitch graft copolymer, we first blended functionalized PE-DPA copolymers containing diphenylacetylenyl (DPA) side groups with an excess amount of toluene-soluble pitch 250M(S) in an inert gas environment by heating. After the grafting reaction, the unreacted toluene-soluble pitch was completely removed by Soxhlet extraction. Table 4.1 summarizes the reaction condition for preparing the three pure PE-g-Pitch graft copolymers that were used in this study.

Table 4.1 Blending conditions in the preparation of PE-g-Pitch graft copolymers.

Graft Copolymer	Blending Condition				^b Weight Remain after Extraction (%)
	PE-DPA/250M(S) (wt/wt)	^a DPA mol% in the copolymer	T _{blend} (°C)	t _{blend} (hr)	
PE-g-Pitch-1	1/10	6.2	310	1	21.8±1.7
PE-g-Pitch-2	1/10	3.2	310	1	19.6±1.1
PE-g-Pitch-3	1/10	1.4	310	1	13.2±2.3

^a DPA mol% was determined by ¹HNMR. ^b Weight remain% was calculated by the weight of collected PE-g-Pitch divided by the origin weight of PE-g-Pitch/pitch blend

The yields for all PE-g-Pitch graft copolymers after purification are significantly larger than the starting PE-DPA copolymer (only about 9% in the mixture); this suggests that an effective grafting reaction happened at 310°C. The weight percentages of both the PE-g-Pitch-1 and PE-g-Pitch-2 graft copolymers doubled from their original values, both with nearly 1/1 weight ratio between the PE backbone and grafted PAH pendant groups; even the starting PE copolymers have only 6.2 and 3.2 mol% DPA functional groups, respectively. As mentioned in Chapter 3, the acetylene species within DPA side groups can act as dienophile active sites, initiating a Diels-Alder type thermal cycloaddition reaction with bay-regions of petroleum pitch molecules that contain a large number of dienes systems. It appears that the DPA side groups in the copolymer react with PAH molecules in pitch to form the PE-g-Pitch structure with PAH molecules incorporated into the side groups. Based on Flory theory, the crystallization ability of the polymer chain of a copolymer is controlled by the branch density, instead of the size of the side groups.¹⁶⁴ Thus, the

resulting PE-g-Pitch should maintain the same semi-crystalline morphology, and the PE crystallinity can act as a physical cross-linker during the purification. With the well-controlled temperature, PE-g-Pitch would not be removed by Soxhlet extraction, as pitch 250M(S) would be.

4.3.3 Thermal Conversion of PE-g-Pitch Graft Copolymer

The resulting pure PE-g-Pitch graft copolymers were then examined by a combination of TGA and DSC measurements. Figure 4.5 compares TGA curves between PE-g-Pitch-1 with its two starting materials, including PE-DPA copolymer with 6.2 mol% DPA comonomer content and toluene-soluble pitch 250M(S), under N₂ atmosphere. Both PE-DPA copolymer and pitch 250M(S) show weight loss beginning at about 350°C. On the other hand, the PE-g-Pitch-1 shows higher thermal stability with a single-step weight loss initiated at 420°C, indicating not only that the excess pitch has been completely removed but also that the PAH side groups transform the polymer backbone to a more stable form by increasing the bond energy during the stabilization step. Besides the higher initial weight-loss temperature, PE-g-Pitch-1 also offers a significantly higher carbon yield of 61.8% at 1000°C, which is much higher than pitch 250M(S) and PE-DPA copolymer, which show a carbon yield of 44.4% and 12.5%, respectively.

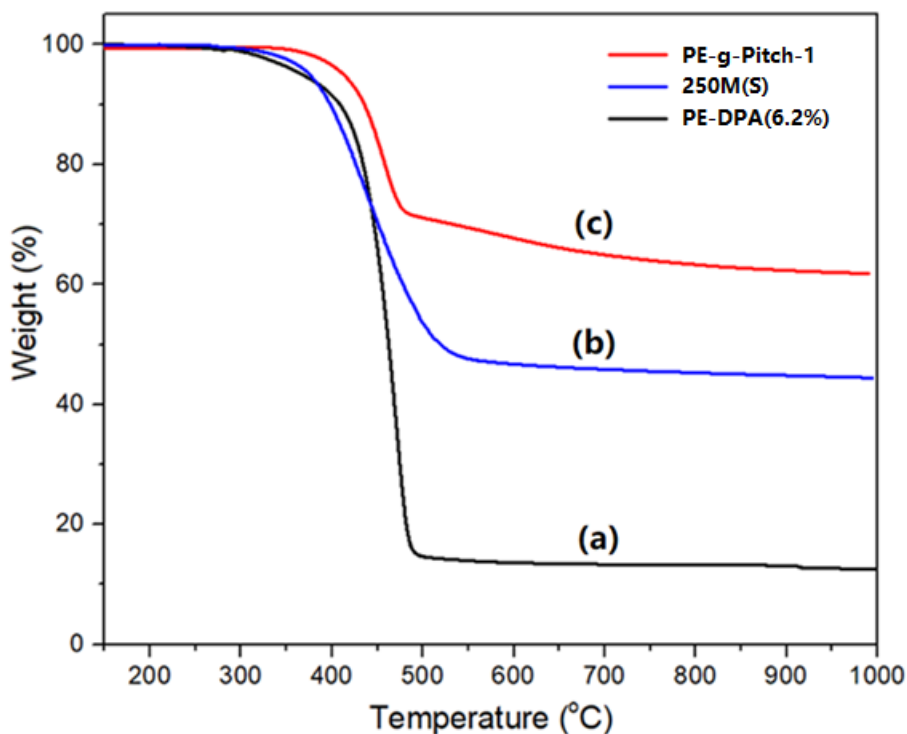


Figure 4.4 TGA curve comparisons of (a) PE-DPA copolymer (6.2 mol% DPA content) (b) pitch 250M(S), and (c) PE-g-Pitch-1 prepared from 250M(S) and PE-DPA copolymer (6.2 mol% DPA content).

As discussed, the pristine PE polymer is completely decomposed with 0% carbon yield at temperatures above 500°C in the noble gas environment.^{165,166} By contrast, the incorporation of PAH side groups to the PE backbone of PE-g-Pitch graft copolymer dramatically increase its carbon yield. This suggests that PE-g-Pitch can engage a specific stabilization reaction (discussed later) that increases the thermal degradation temperature. The stabilized structure allows the polycondensation reaction to occur between the pendant PAH groups, resulting in the enlarged and more stable PAH structure. Another potentially useful finding is that PE-DPA copolymer can also be converted to carbon, although the conversion yield is much lower. This result suggests that these DPA side groups can only partially stabilize this copolymer at high temperatures. But this stabilization effect is limited compared to the one in PE-g-Pitch, a result of the smaller PAH structure in the DPA group that is less π -electron conjugated than the PAH groups.

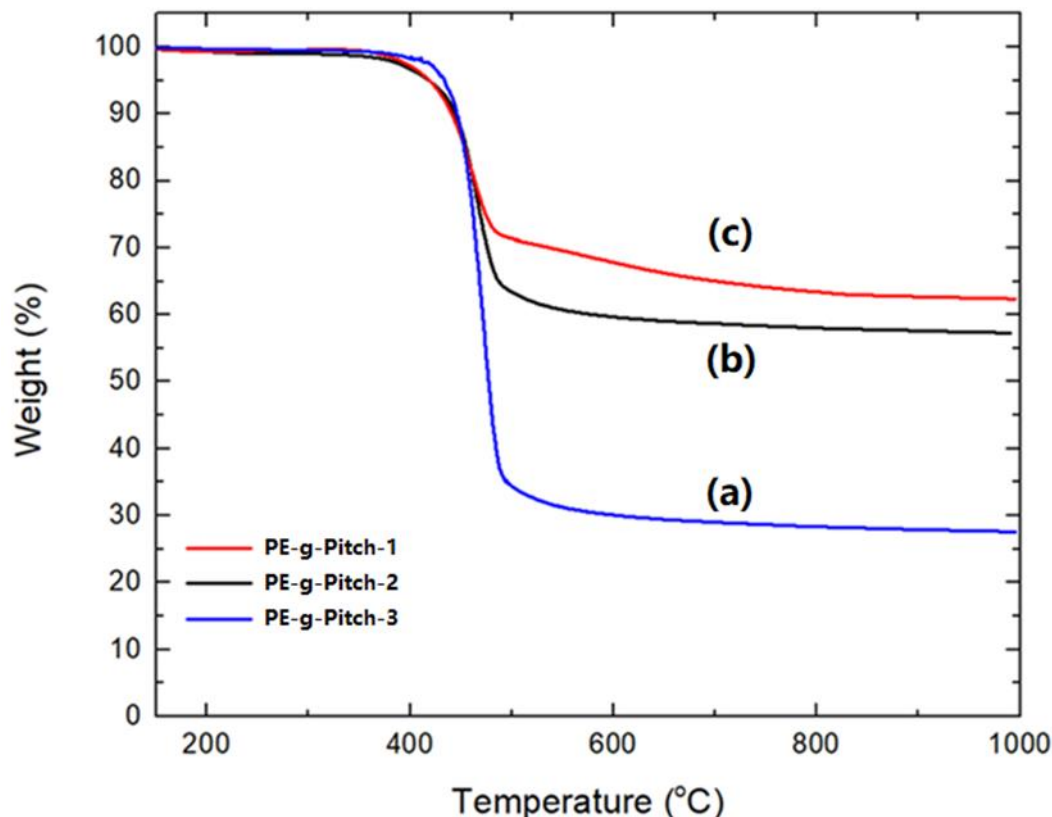


Figure 4.5 TGA curve comparisons of PE-g-Pitch samples prepared from 250M(S) and PE-DPA copolymer with comonomer percentage of (a) 1.4 (b) 3.2 (c) 6.2 mol%.

Another important question is how the content of side groups affect the stabilization.

Figure 4.6 shows the TGA curves for PE-g-Pitch graft copolymer with various content of pitch-like side groups. As the side group content of starting PE-DPA copolymer increases from 1.4% to 3.2%, the carbon yield of the resulting PE-g-Pitch sample increases dramatically from 27% to 57%. However, a further increase in the side group content from 3.2% to 6.2% results in an additional increment in carbon yield of only about 9%, which indicates that the stabilization effect from pitch-like side groups is becoming smaller. Based on the proposed stabilization mechanism, one pitch-like side group can induce dehydrogenation of multiple adjacent $-\text{CH}_2-\text{CH}_2-$ units and form a stable π -electron conjugated sequence. It is reasonable to consider that a maximized stabilization effect can be achieved with a certain value of side group content. Therefore, the effect of stabilization would decrease as the side group content begins to exceed that value.

4.3.4 Stabilization Reaction of PE-g-Pitch Graft Copolymer

The TGA results discussed in the previous section prompt us to further investigate the details of stabilization reactions. A combination of DSC, XRD, CP-MAS ^{13}C NMR, and EGA-MS measurements was used to analyze the thermal degradation behavior and transformation of the chemical structure and bulk structure during heat treatment at different temperatures.

As mentioned in Chapter 2, one of the structural criteria for a precursor to be converted successfully to carbon is the formation of a π -electron conjugated network structure in the form of PAH during the stabilization step. For a semi-crystalline PE-g-Pitch graft copolymer, the formation of a network structure would prevent the polymer chains from effective packing by limiting the chain movement, hence reducing its degree of crystallinity. To investigate this process, DSC was applied on PE-g-Pitch-1 heated to different temperatures—300°C and 400°C—with two measurement cycles, as shown in Figure 4.7. All samples were heated to 150°C with a heating/cooling rate of 10°C in N_2 to remove thermal history before the measurements. For the sample heated to 300°C (Figure 4.7a), the curve slope remained constant and no obvious difference was observed between the first and second cycles, indicating that no chemical reaction occurred during this process. As the temperature was further increased toward 400°C (Figure 4.7b), an exothermic reaction was found starting at approximately 310°C, attributed to the formation of a more stable structure in a lower energy state. The heating also reduced the melting and crystallization enthalpy in the second cycle compare to the first. There are several possible reasons for this phenomenon. The first is the cleavage of the PE backbone; however, this is most unlikely, as the thermal decomposition is very limited at this temperature range from the TGA result. The second possible reason is the cross-linking reaction between pitch-like side groups, which limits the mobility of the PE backbone. Because the polycondensation reaction between pitch molecules starts at about 350°C, it is reasonable to consider this as one of the factors. A third reason could be that the chemical structure of the PE backbone portion was changed during

heating before decomposition could occur, thus resulting in the less flexible polymer chain of the derivative of PE-g-Pitch structure.

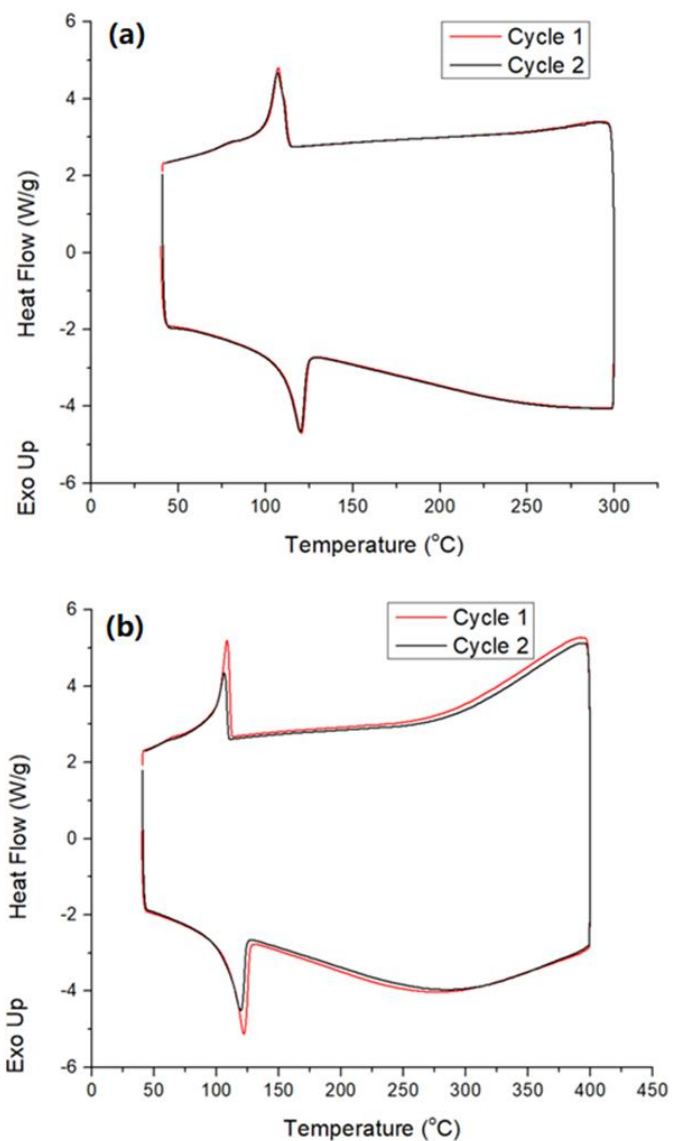


Figure 4.6 DSC curves of PE-g-Pitch-1 heated to (a) 300°C and (b) 400°C with the heating/cooling rate of 10°C/min in N₂ atmosphere.

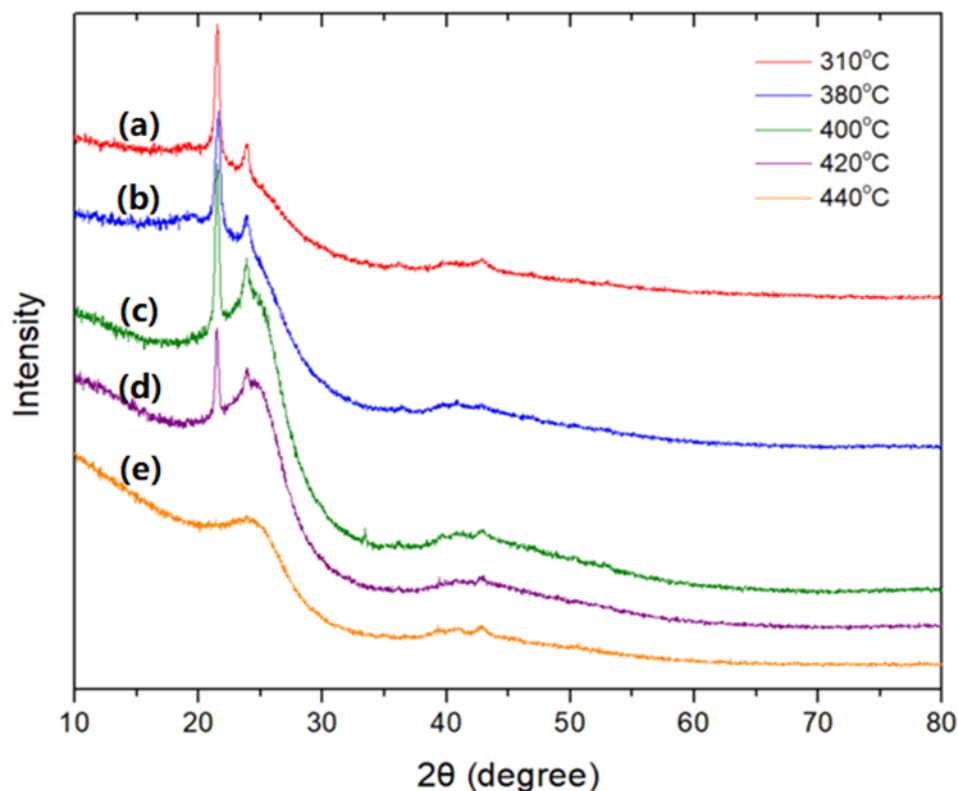


Figure 4.7 XRD comparisons of PE-g-Pitch-1 heat-treated at different temperature of (a) 310°C (b) 380°C (c) 400°C (d) 420°C and (e) 440°C for 1 hour.

The thermal transformation of PE-g-Pitch morphology during the stabilization process was determined by XRD technique. Figure 4.8 compares the XRD reflection patterns of PE-g-Pitch-1 graft copolymer heated at different temperatures for one hour, which reveals how the average bulk structure changes during the thermal stabilization. All samples except the one heated to 440°C show two distinct peaks, one at $2\theta = 21-22^\circ$ and another at $2\theta = 23.5-24^\circ$, corresponding to the (110) and (200) diffractions related to the orthorhombic crystal structure of the PE chain.¹⁶⁷ For the samples treated at 310°C and 380°C, there is no obvious difference in the peak intensity and location, except the appearance of a ramp ranging from 25° to 30°. For the sample treated at 400°C, a broad peak can be found centered at $2\theta = 24-25^\circ$, corresponding to (002) diffraction related to the presence of microcrystalline in a mostly amorphous carbon material. When the temperature was increased to 420°C, (110) and (220) PE peaks were reduced, then completely disappeared at 440°C. The comparison of XRD spectra suggests that there is a chemical

transformation within PE-g-Pitch from 380° to 440°C that diminishes the effective packing of PE chains to generate crystallinity. Besides supporting the result from the DSC measurement, the comparison also provides evidence that the polycondensation reactions start to happen between PAH side groups to generate a planar carbon-like structure at about 400°C, which is reflected as the broad peak centered at $2\theta = 24\text{-}25^\circ$.

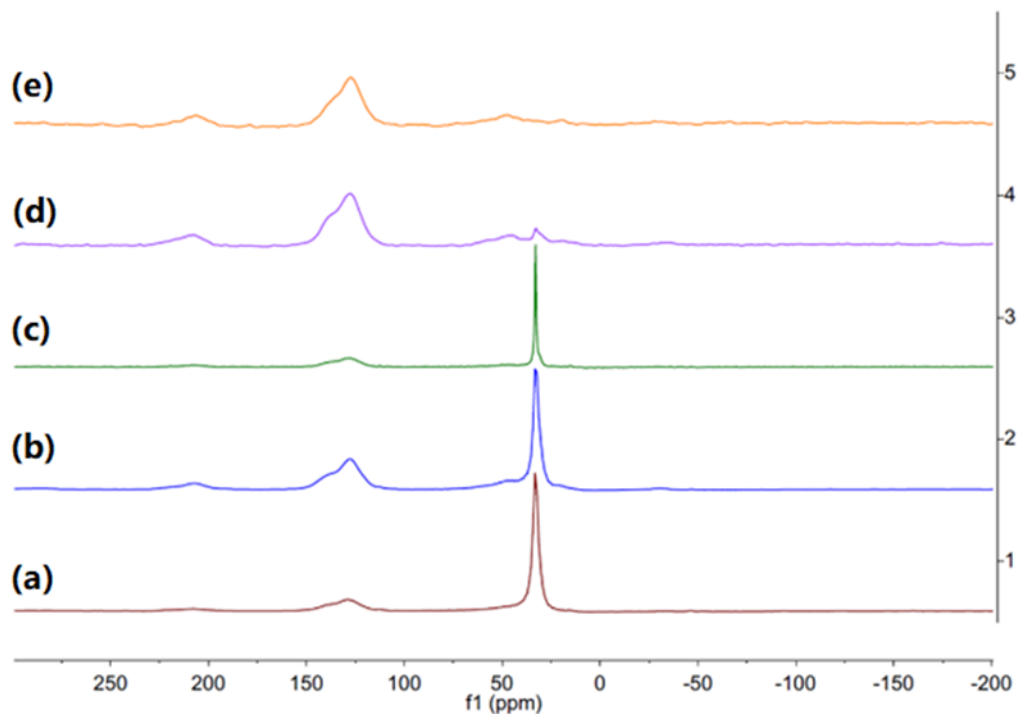


Figure 4.8 Solid State CP-MAS ^{13}C NMR spectra of PE-g-Pitch-1 heat-treated at different temperatures of (a) 310°C (b) 380°C (c) 400 °C (d) 420°C and (e) 440°C for 1 hour.

Although the DSC and XRD show the temperature range of stabilization reactions and the change in the bulk structure of PE-g-Pitch during thermal stabilization, the difference in the chemical structure before and after stabilization is still unclear. To understand the chemical structure transformation during the thermal stabilization process, the same set of PE-g-Pitch-1 graft copolymer samples heated at different temperatures for one hour were also monitored by solid-state CP-MAS ^{13}C NMR. Figure 4.9 compares their ^{13}C NMR spectra. For the samples heated to 310, 380, and 400°C, they all show a sharp peak center at 29 ppm corresponding to the aliphatic region of saturated PE backbones, and a broad peak at 130ppm attributable to the side

groups with polyaromatic structure. As the heat treatment temperature increased to 420°C, there is an obvious reduction in PE peak as the unsaturated hydrocarbons dominate the structure. At 440°C, there is only one major peak on the spectrum, with two sidebands located at 50ppm and 200ppm. This suggests that all PE carbons have been turned to unsaturated hydrocarbons.

Previous studies have shown that for pristine PE, only small char formation and alkene transformation happen at 450°C, while its cyclization and aromatization take place at around 500°C.^{168,169} Therefore, most PE repeat units should remain at 440°C in the form of saturated hydrocarbons. However, there is no such peak found on the NMR spectrum corresponding to the saturated hydrocarbons in PE-g-Pitch heat-treated at 440°C, which suggests that the hydrocarbons were converted to the other structure at this temperature. As the chemical shifts of most of unsaturated carbons locate in the range of 120-140 ppm, this structural transformation could be mostly a result of the linear PE backbone changing to cis- and trans- (CH)_x polyacetylene-like structures that have a chemical shift at 129 and 139ppm respectively.¹⁷⁰

The byproduct analysis can further illuminate the key transformation from alkane to alkene structure in PE-g-Pitch, with hydrogen gas evolution during the proposed stabilization step. Therefore, the chemical species released during the heating were determined by EGA-MS. Figure 4.10 compares the EGA-MS results, targeting the released H₂ (2 AMU), between the PE-g-Pitch-1 copolymer and its starting PE-DPA copolymer with 6.2mol% comonomer percentage and pitch 250M(S). They were heated from 320 to 420°C and kept at 420°C for one hour. From the EGA-MS results, pitch 250M(S) shows a much lower H₂ evolution compared to the PE-g-Pitch sample, indicating the majority of dehydrogenation reactions happened on the PE backbone. The massive amount of H₂ gas released in PE-g-Pitch starts at 380°C, followed by an exponential increase as the temperature goes higher. This suggests an acceptor-less dehydrogenation reaction happened in this temperature range. It also explains how the saturated hydrocarbons in PE-g-Pitch turn to an unsaturated alkene structure before the major weight loss begins. The corresponding PE-DPA

copolymer also shows that H₂ evolved in a similar temperature range but with much less intensity. As mentioned in the TGA results, PE-DPA copolymer can also be converted to a small amount of carbon material with its smaller side groups. The comparison here indicates that the degree of the dehydrogenation reaction along the PE backbone is proportional to the level of π -conjugation on the side groups of the PE copolymers.

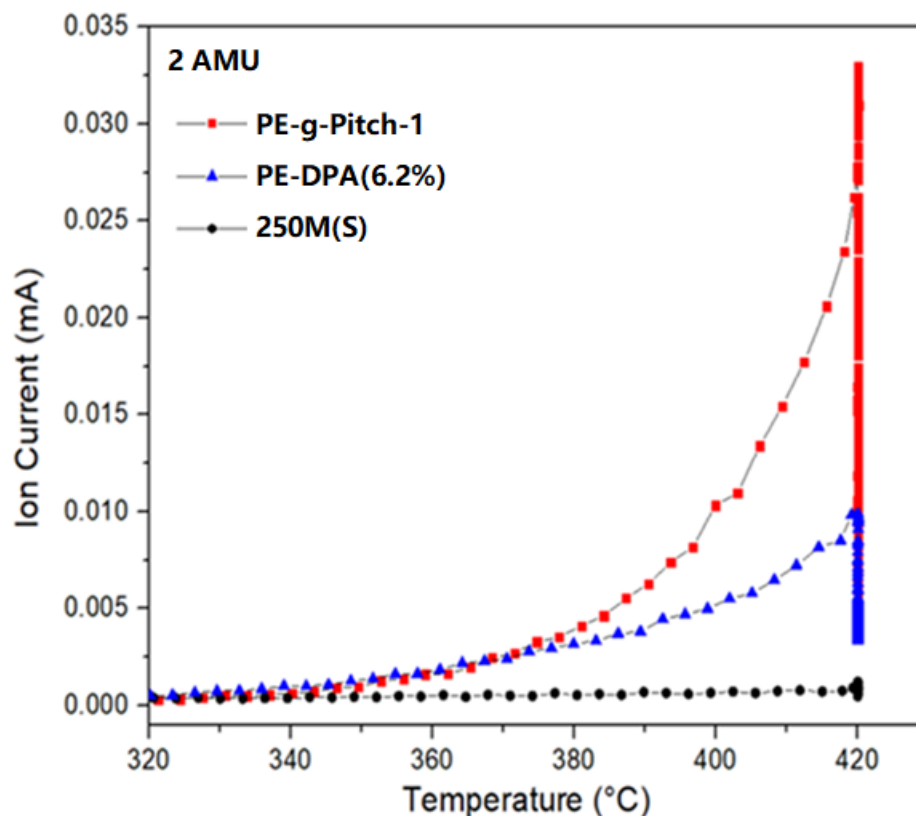


Figure 4.9 EGA-MS spectra on H₂ evolution of PE-g-Pitch-1, PE-DPA copolymer with 6.2mol% comonomer percentage, and Pitch 250M(S) heated from 320-420°C, and stayed at 420°C for 1hour.

4.4 Conclusion

In this study, we start with the preparation of a series of pure PE-g-Pitch graft copolymers, which involves the grafting reaction of PE-DPA copolymer with toluene-soluble pitch molecules at 310°C for one hour under N₂ atmosphere and the subsequent solvent extraction to remove

ungrafted pitch molecules. The experimental results indicate that each DPA side group in the PE-DPA copolymer reacts with PAH molecules in pitch at this temperature to form the PE-g-Pitch graft structure that has multiple incorporated PAH molecules in each side group. The research then focused on understanding the stabilization mechanism during the thermal transformation of the resulting PE-g-Pitch graft copolymer to the carbon material. We conducted a systematic, side-by-side comparison between the PE-g-Pitch graft copolymer and its two starting materials: PE-DPA copolymer and pitch, by using the combination of TGA, DSC, XRD, CP-MAS ^{13}C NMR, and EGA-MS monitoring techniques. Based on this comparison, we concluded that the stabilization mechanisms are centered in two reactions, including a cross-linking reaction between PE-g-Pitch polymer chains and the dehydrogenation of PE polymer to form a π -electrons conjugated chain (similar to polyacetylene), as illustrated in Figure 4.11.

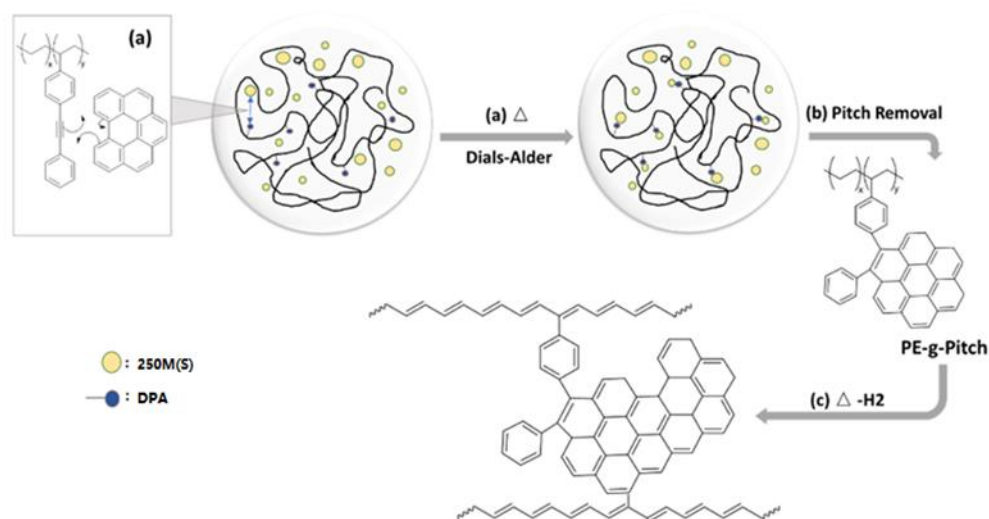


Figure 4.10 Proposed chemical structural transformation of functionalized PE copolymer and petroleum pitch to stabilized PE-g-Pitch.

In summary, we have observed a new stabilization mechanism for a PE-g-Pitch graft copolymer that can offer a carbon yield of 61.8% at 1000°C. We found that the highly π -electron conjugated side groups in the PE-g-Pitch graft copolymer promote the dehydrogenation of saturated hydrocarbons along polymer chains at temperatures greater than 380°C. The initial formation of one double bond adjacent to the side group further extends to the entire polymer

chain, to form the complete π -electrons conjugated polymer chain with higher thermodynamic stabilization. Additionally, a network structure is formed in PE-g-Pitch at the temperature range of 310°-400°C by the condensation reaction between pitch-like side groups. Therefore, the carbon yield of PE-g-Pitch is increased by the collective effect of these two stabilization processes.

Chapter 5

Synthesis and Evaluation of Polyethylene-graft-Pitch Precursors Prepared by Cycloaddition between Pitch and Poly(ethylene-co-4-bromostyrene) Prepared by Direct Polymerization Method

5.1 Introduction

In Chapter 3, I introduced our strategy that uses excess pitch as a solvent to limit the self-cycloaddition (cross-linking) reactions between diphenylacetylenyl (DPA) side groups in the PE-DPA copolymer, hence allowing the cycloaddition reaction to happen between DPA and pitch to generate the uncross-linked and processible PE-g-Pitch graft copolymer. However, the SEM images suggest that the formation of a cross-linked network is still taking place during the blending, due to the low thermal energy required for these self-cycloaddition reactions between DPA side groups in the PE-copolymer. Therefore, the next step of our study is to find a type of PE copolymer with the specific side groups that are reactive to the polycyclic aromatic hydrocarbon (PAH) molecules in petroleum pitch, but without the self-cycloaddition reactions that result in the unfavorable cross-linked network during the preparation step of PE-g-Pitch graft copolymer.

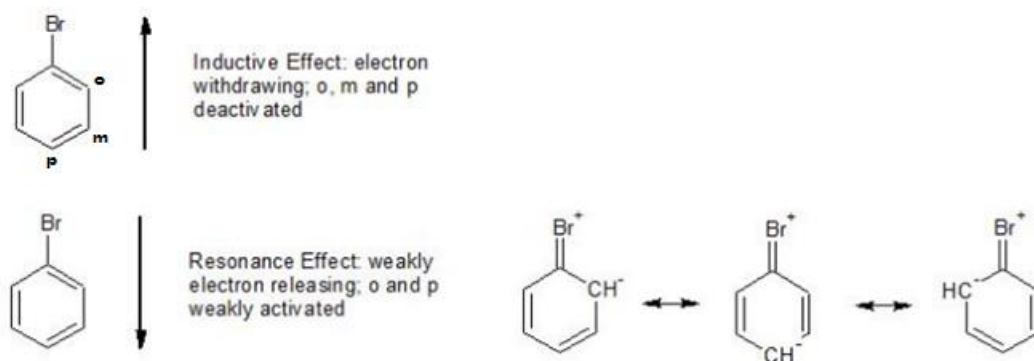


Figure 5.1 The electron density distribution affected by the inductive effect and resonance effect on bromostyrene. (o: ortho, m: meta, p: para)

As mentioned, petroleum pitch is a mixture of PAH molecules with electron-rich diene systems, and hence can undergo a Diels-Alder type cycloaddition with chemical species containing dienophiles. Therefore, we investigated poly(ethylene-co-4-bromostyrene), shortened as PE-BrSt copolymer, in the thermal-induced cycloaddition reaction with petroleum pitch under the same polymer blending technique shown in Chapter 3. The Br moiety in the 4-bromophenyl group has an electron-withdrawing effect on the functional group. Meanwhile, the poor overlap between the large 4p orbital in Br and 2p orbital in C creates a resonance effect that is too weak to offset this strong electron-inductive effect. As shown in Figure 5.1, the contest between the electron-withdrawing inductive effect and electron-donating resonance effect still decreases the overall electron density of the six-member ring in the 4-bromophenyl group, hence allowing it to provide the electron-deficient dienophile to react with the electron-rich diene of PAH molecule, as illustrated in Figure 5.2. After the accomplishment of the cycloaddition reaction, a subsequent dehydrogenation reaction will happen to convert the side group into a more stable π -electron conjugated structure with H_2 released as the byproduct. Because of the good thermal stability of both starting materials, the grafting reaction can be allowed to occur at a large reaction temperature window ($<350^\circ\text{C}$) without any external reagent or catalyst. This selective reaction can result in the desirable PE-g-Pitch with the highly π -electron conjugated PAH side groups.

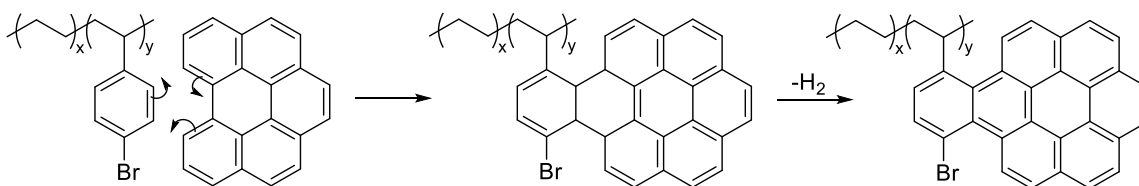


Figure 5.2 Scheme of proposed reaction route of preparation of PE-g-Pitch by PE-BrSt copolymer and pitch via Diels-Alder cycloaddition.

One important reason for considering the PE-BrSt copolymer as the preferred starting material in the preparation of PE-g-Pitch is its simple, cheaper, and faster

preparation process, which can be accomplished by a coordination polymerization between ethylene and 4-bromostyrene using a commercially available constrained geometry catalyst (CGC). Compared to the previous PE-DPA copolymer that contains DPA side groups (discussed in Chapters 3 and 4), the preparation of PE-BrSt copolymer does not require a post-polymerization Sonogashira coupling reaction that involves a long reaction time (more than four days) and an expensive palladium catalyst. Additionally, the PE-BrSt copolymer can also be prepared with a much lower cost by a post-polymerization method, namely the bromination of poly(ethylene-styrene) copolymer, which will be discussed in Chapter 6. Besides the lower cost and shorter preparation time, another advantage is that the PE-BrSt copolymer does not contain any unsaturated moieties that can eagerly undergo a self-cycloaddition reaction to generate an unwanted cross-linked network structure during the preparation of PE-g-Pitch.

In this chapter, I will discuss the preparation and evaluation of two PE-g-Pitch-based CF precursors made from PE-BrSt copolymer and toluene soluble pitch 250M(S). The first is a solution-spinnable precursor that consists of only PE-g-Pitch with the ungrafted pitch completely removed after blending. The second is a melt-spinnable precursor that contains extra pitch as the plasticizer. Both were successfully converted to CFs in our study.

5.2 Experimental Section

5.2.1 Characterization

Liquid state ^1H NMR spectra were obtained by using Bruker AV 300 at 90°C with *d*-1,1,2,2-tetrachloroethane. TGA measurements were conducted on a TA Sdt-600. Around 10 mg of sample was loaded into the sample pan and heated at a rate of 10°C/min in the N_2 atmosphere with a gas flow rate of 50ml/min. DSC measurements were conducted on a TA Q2000 with a

heating/cooling rate of 10°C/min. EGA-MS measurement was conducted on a TA TGA5500 with a mass spectrometer in argon with a heating rate of 10°C/min and a flow rate of 25ml/min. The weight of the sample was fixed to be 15mg in every measurement. Solution oscillatory rheology measurements were conducted on TA Discovery HR30 with a strain of 10%. Melt oscillatory rheology measurement was conducted on TA ARES-G2 in the N₂ atmosphere with a heating rate of 10°C/min. The angular frequency was 1 rad/s and strain was 10%. All samples were pre-molded with a diameter of 8mm and thickness of ~1.5mm by using a vacuum hot press. TMA was conducted on a TA Q400 in the N₂ atmosphere with a heating rate of 10°C/min. The sample was molded into a cylinder shape with a thickness of 1cm before measurement. XRD measurements were conducted on a Panalytical XPert Pro MPD theta-theta Diffractometer from Malvern at 40 kV and 40 mA with Cu K(α) radiation $\lambda = 0.15418$ nm. Diffraction patterns were recorded on a 0.8 collimator, with an oscillation of the samples between 10 and 80° and an imaging plate detector. The scan rate was 0.2°/min with an interval of 0.045°. Raman spectra were collected from Horiba LabRam HR Evolution with laser excitation of 532nm. Both samples measured by XRD and Raman were grounded in the form of fine powders. All of the calculations on XRD and Raman were finished by using Origin software. The SEM images were collected from the Apreo 2 (Thermo Fisher).

5.2.2 Materials

4-bromostyrene (TCI) was vacuum distilled after drying overnight by CaH₂. MMAO-12 7% toluene solution (Sigma Aldrich) was dried by vacuum at 50°C to become white powders. [(C₅Me₄)SiMe₂N(t-Bu)]TiCl₂ (Boulder Scientific), 1,2,4-trichlorobenzene (Sigma Aldrich) and acetone (VWR) were used as received. Toluene (Wiley Organics) was purified via the Grubbs type solvent purification system. Petroleum pitch (250M) with a softening temperature of 250°C were kindly provided by Rutgers Basic Aromatics GmbH.

5.2.3 Copolymerization of Ethylene and 4-Bromostyrene

The copolymerization reaction was conducted in a Parr 500ml stainless autoclave equipped with a mechanical stirrer. The reactor was firstly charged with 220ml of toluene, 9 ml of 4-bromostyrene, and 10ml of 20wt.% of methylaluminoxane (MAO) solution in toluene, with argon protection and stirring. Then the solution was saturated with 50 psi ethylene at 40°C. To the mixture, 1.1 ml of [(C₅Me₄) SiMe₂N(t-Bu)] TiCl₂ (CGC) solution in toluene (20umol/ml) was injected into the reactor to initiate the reaction. After 1 hour, ethylene was replaced by argon and the reaction was terminated by adding 30ml of isopropanol. The solution mixture was then poured into 600ml of diluted HCl solution of methanol. The resulting PE-BrSt copolymer was isolated by filtration and was washed with 200ml×3 of methanol before drying in a vacuum oven overnight at 60°C. The weight of the copolymer was 5.65g. The comonomer percentage was 8.4% determined by ¹H NMR.

5.2.4 Toluene-soluble Pitch 250M(S) Extraction

A Soxhlet extraction apparatus was applied to extract toluene-soluble portion 250M(S) from petroleum pitch 250M. It consists of a still pot containing solvent and a stir bar, a distillation path, a Siphon top and exit, a cone-shape filter paper with 8um hole size as sample holder, and a condenser with cool water flowing through. The solvent in the still pot used in this study was toluene and it was heated by an oil bath at 140°C. The temperature of the distilled solvent surrounding the sample holder was measured by a thermocouple and the value was 65°C.

5.2.5 Preparation of PE-g-Pitch/Pitch Blend

PE-BrSt copolymer and 250M(S) were first dissolved in toluene with 5 wt.% concentration at 90°C in a 600ml beaker. Then, at the same temperature, the prepared homogeneous solution was dried with vigorous stirring under an airflow until it became a slime-like product that contained 20% toluene. The mechanical blending of the slime-like product was conducted in a twin-screw blender with nitrogen flowing through the system all the time with a flow rate of 100ml/min. This system has three thermocouples located at the outer cover, sample chamber, and inner wall to have a close monitor on temperature control. The heating rate was set to 10°C/min for all experiments. Argon flew in the system through a rubber tube that is inert to a high temperature to create an air-free environment during mixing. When finished heating, the sample chamber was cooled down at a cooling rate of 10°C/min. After blending, all collected samples were grounded into a form of powders by mortar.

5.2.6 Free Pitch Removal

To remove the unreacted pitch from the mixture obtained after blending to get PE-g-Pitch, the same Soxhlet extraction set-up was utilized as the one we used to prepare the toluene-soluble pitch 250M(S). For the preparation of solution-spinnable precursor, the as-blended product was washed with hot toluene for 24 hours until the liquid in the sample chamber became colorless. The product was then washed by stirring in toluene at 65°C and centrifuge to ensure no unreacted pitch remained. For the preparation of melt-spinnable precursor, the as-blended product was washed with hot toluene with different Soxhlet cycles to remove different amounts of the excess pitch. In the end, both precursors were washed with hexane and dried at 100°C in a vacuum oven for 12 hours.

5.2.7 Fiber Spinning

Solution spinning of PE-g-Pitch was conducted by using the spinning set-up as shown in Figure 5.3, with 1,2,4-trichlorobenzene (TCB) and acetone applied as solvent and coagulation bath, respectively. The melt-spinning of PE-g-Pitch/pitch blend was conducted by using the set-up as same as the setup discussed in Chapter 3.

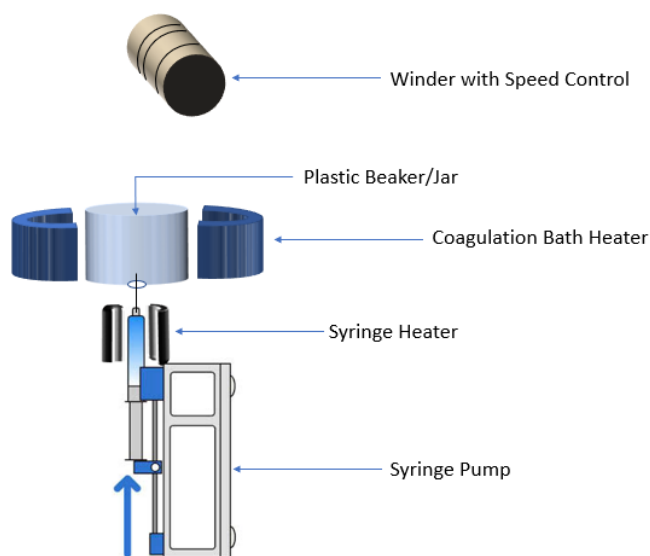


Figure 5.3 A schematic diagram of the solution-spinning setup.

5.2.8 Stabilization and Carbonization of PE-g-Pitch Fibers

The stabilization of PE-g-Pitch was conducted in a tube furnace with an air flowing at a rate of 100ml/min and a heating rate of 10°C/min, and with no tension applied. The carbonization of PE-g-Pitch fibers was conducted in a graphitizing furnace. In the beginning, 2g of sample was loaded on a boat-shaped ceramic crucible before putting into the furnace. Then, the furnace was vacuumed and refilled with argon three times before temperature raising to the target temperature at the rate of 10°C/min.

5.2.8 Gel Content Measurement

At room temperature, 0.5g of stabilized precursor fibers and 10ml of 1,2,4 trichlorobenzene were loaded into a vial. Then, the vial was put in an oven at a temperature of 120°C and kept idle for 24 hours. Then, the insoluble portion was separated and dried in a vacuum oven at 120°C overnight. The gel content is determined by dividing the insoluble fraction over the original weight of precursor fibers.

5.3 Results and Discussion on PE-g-Pitch Precursors

As discussed in Chapter 3, one reason the precursor fibers prepared from a PE-g-Pitch/pitch blend have poor mechanical properties is the major component of the unreacted pitch. Therefore, we removed the unreacted pitch, retaining only the PE-g-Pitch portion; the resulting material is theoretically stronger than the blend, because of its higher molecular weight, semi-crystallinity, and linear polymer structure. This method also prevents the formation of phase separation, which would result in CFs with a porous structure. However, we found that the softening point of PE-g-Pitch is very high (as will be discussed later); thus it cannot be melt-spun without the presence of a plasticizer. Therefore, in this section, we discuss the potential of using PE-g-Pitch as a solution-spinnable CF precursor. First, EGA-MS and ¹H NMR were used to characterize the chemical composition change during the preparation process. The processibility of the PE-g-Pitch was studied by using an oscillatory rheometer, while the stabilization temperature was determined by DSC and TMA. The carbonization behavior of precursor fibers made from PE-g-Pitch was investigated by using TGA, XRD, and Raman spectroscopy. The morphology of the precursor fibers and CFs was studied by SEM.

5.3.1 Preparation of PE-g-Pitch Graft Polymer by Cycloaddition between Poly(ethylene-4-bromostyrene) Copolymer and Pitch

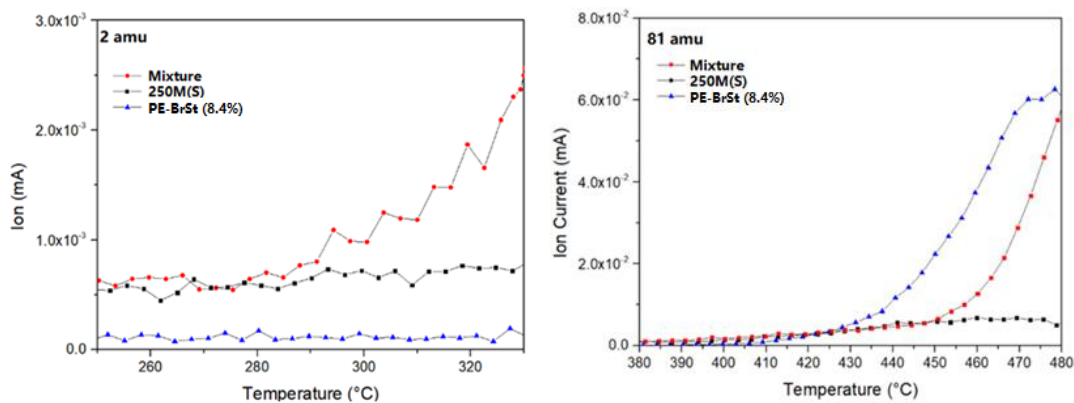


Figure 5.4 EGA-MS of PE-BrSt (8.4%) copolymer, 250M(S), and their mixture (1:3 in weight) targeting on H₂ (left) and Br (right) fragments.

As mentioned in the proposed reaction mechanism in Figure 5.2, the byproducts of the as-proposed reaction are hydrogens, which can be used as an indicator to determine the occurrence of the successful grafting reaction. To verify this reaction and determine the reaction temperature, EGA-MS was performed with approximately 15mg of sample for each of the PE-BrSt (8.4%) copolymer, 250M(S), and their mixture with the weight ratio of 1 to 3. The curves in Figure 5.4 (left) illustrate the release of H₂ from these three samples in the temperature range of 250 to 330°C. Compared to the pure copolymer and pitch samples with constant values of H₂ emission, the EGA-MS curve of the mixture shows an increased formation of H₂ starting from 290°C, indicating the grafting reaction between PE-BrSt copolymer and pitch was happening as discussed.

In addition to the release of H₂, another indicator is the Br moiety in 4-bromophenyl side group, which not only provides an inductive effect to the nearby carbons but also is stabilized by the π -electron delocalization to the aromatic moieties attaching to it. Therefore, the structural change on the resonance contributors can effectively change the bond energy of the C-Br bond. The EGA-MS curves of these three samples targeted at amu=81, which corresponds to the bromine ion fragments, are illustrated in Figure 5.4 (right) in the temperature range of 380° to

480°C. In contrast to H₂, the release of bromine fragments happens at a much higher temperature for both samples. Interestingly, PE-BrSt copolymer has the cleavage on its C-Br bonds starting at 425°C, while for the mixture the starting point is at around 450°C. These results suggest that, although the bromine was not directly involved in the reaction between copolymer and petroleum pitch, the incorporated PAHs from pitch to the copolymer side groups still make an impact by enlarging the π -conjugated system, thus making it a more effective resonance contributor that further increases the stability of C-Br bond.

Based on the EGA-MS results, both the increased release of H₂ and the higher bond energy of C-Br suggest that a successful grafting reaction between PE-BrSt copolymer and pitch has occurred. In this study, we will mainly focus on studying the effect of reaction (blending) time on the chemical composition and properties of the resulting PE-g-Pitch.

Table 5.1 Preparation conditions of PE-g-Pitch samples.

Run	Sample	BrSt content in PE copolymer (mol %)	Polymer:Pitch	Mixing Temp/Time (°C/hr)
			Weight Ratio	
1	PE-g-Pitch(8.4%)-1	8.4	1:10	310/1
2	PE-g-Pitch(8.4%)-2	8.4	1:10	310/2
3	PE-g-Pitch(8.4%)-3	8.4	1:10	310/3

Table 5.1 summarizes the preparation conditions of a series of PE-g-Pitch samples, to identify a suitable reaction time for the reaction between PE-BrSt (8.4%) copolymer and 250M(S) to prepare a CF precursor. Based on the previous EGA-MS result, we found that a dehydrogenation reaction begins at about 280°C on the mixture of these two materials to generate the PAH side groups. We also know that the polycondensation reaction between PAH molecules in pitch starts at 350°C as mentioned in Chapter 1. Therefore, a midpoint of 310°C was selected as the blending temperature to prepare PE-g-Pitch, which ensures that the reaction occurs at a considerable rate while preventing the occurrence of side reactions. The two materials were

blended in a weight ratio of 1:10 between copolymer and pitch, which had proved to be a suitable mixing ratio for PE-DPA copolymer as discussed in Chapter 3.

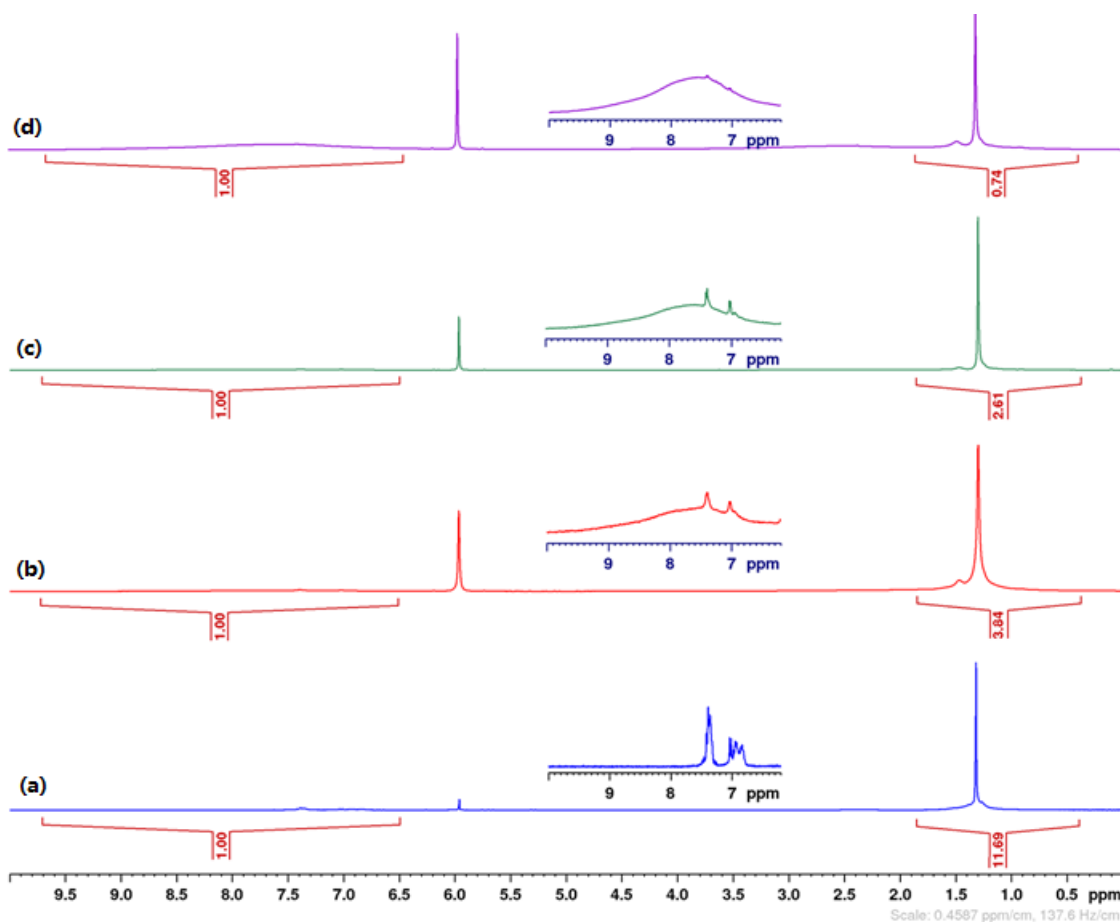


Figure 5.5 ^1H NMR of (a) PE-BrSt (8.4%) copolymer and PE-g-Pitch(8.4%) samples prepared with different reaction time of (b) 1, (c) 2, and (d) 3 hours at 310°C .

^1H NMR was used to elucidate the transformation of the molecular structure of the copolymer after the reaction. Figure 5.5 shows the ^1H NMR spectra of PE-BrSt (8.4%) copolymer and the PE-g-Pitch samples prepared from it at 310°C with blending times of one, two, and three hours. Both spectra exhibit an up-field peak centered at 1.3 ppm associated with aliphatic protons on the PE repeat units. The small shoulder at 1.4 ppm and a minor peak at 2.4 ppm on the spectra of PE-BrSt(8.4%) copolymer are associated with beta protons and alpha protons attaching to the 4-bromophenyl side groups. The main difference between the spectra of PE-BrSt copolymer and PE-g-Pitch is reflected in the aromatic region from 6.5-10 ppm. After the reaction, the two

distinct peaks centered at 6.95 and 7.4 ppm with the identical intensity of PE-BrSt copolymer were combined to a broad peak that spans the whole aromatic region, indicating the incorporation of the PAH molecules into the copolymer. By intergrading the intensity of saturated aliphatic protons (I_{ali}) and the intensity of aromatics protons (I_{aro}) in PE-g-Pitch spectra, we observed that the content of aliphatic protons decreases with the longer blending time. This observation will be discussed in more detail later, joint with a calibration curve that determines the relationship between $I_{\text{ali}}/I_{\text{aro}}$ and the content of PE-BrSt portion in PE-g-Pitch. Interestingly, both PE-g-Pitch spectra still show the two distinct peaks corresponding to the unreacted 4-bromophenyl groups, even for the one with three hours of blending time. This can be explained by the bulkiness of pitch molecules, which makes them more likely to react with pendant side groups with no steric hindrance, namely the 4-bromophenyl groups not located in a consecutive sequence of 4-bromostyrene repeat units in the PE-BrSt copolymer. The finding can be supported by the EGA-MS result as shown in Figure 5.6 for homopolymer poly-4bromostyrene and 250M(S) mixture following the same experimental condition as the previous EGA-MS measurement. There is no observable increase on the H_2 release in the temperature range of the grafting reaction between copolymer and PAH molecules, indicating there was no reaction happening on this completely consecutive sequence of 4-bromostyrene repeat units. More experimental results supporting this point of view will be discussed in Chapter 6.

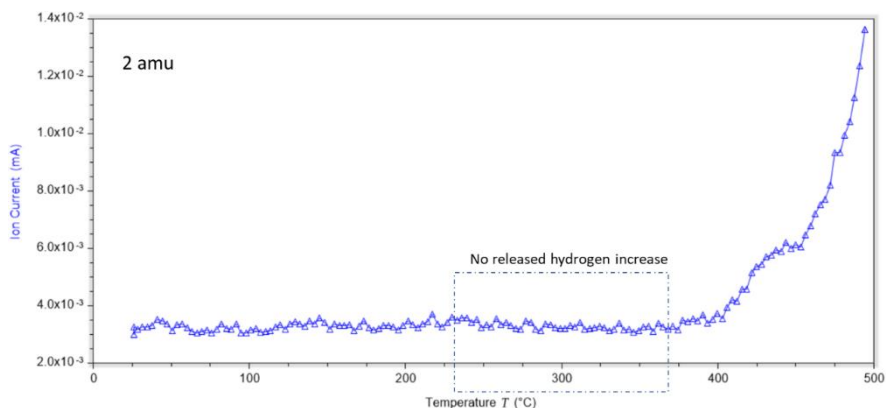


Figure 5.6 EGA-MS targeting on H_2 of the mixture of poly(4-bromostyrene) and 250M(S) (1:3 in weight).

5.3.2 Thermal Conversion and Solution-Spinnability of Pure PE-g-Pitch Graft Copolymers

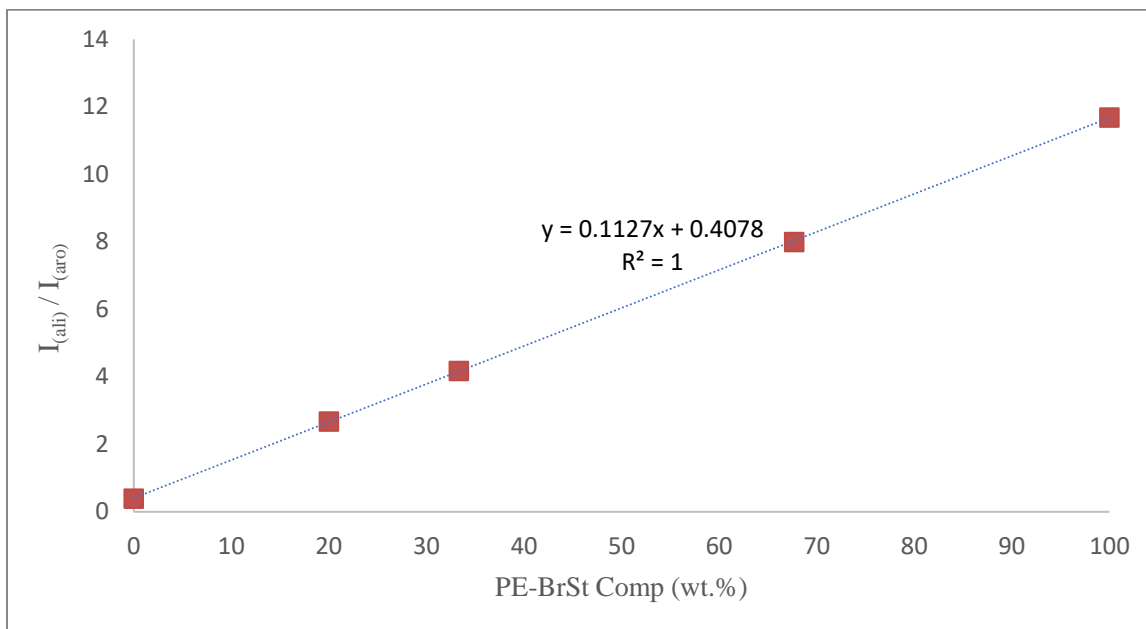


Figure 5.7 Calibration curve of PE composition vs. intensity ratio of the aliphatic and aromatic region from ^1H NMR spectra of the PE-BrSt(8.4%) copolymer/250M(S) mixture.

Table 5.2 Comparisons of solution fiber-spinnability and carbon yield of PE-g-Pitch samples

Sample	^1H NMR $I_{(Ali)}/I_{(Aro)}$	^b PE-BrSt Comp (wt.%)	^c Carbon Yield (%)	Spinnability	
	^a BrSt Deducted			5wt.% ^d	10wt.% ^d
PE-g-Pitch(8.4%)-1	3.84	37.1	37.2	N	Y
	4.59				
PE-g-Pitch(8.4%)-2	2.61	22.5	51.7	N	N
	2.94				
PE-g-Pitch(8.4%)-3	0.74	3.1	78.8	N	N
	0.76				

^a The intensity ratio of $I_{(ali)}$ and $I_{(aro)}$ after deduction of peak intensity of two aromatic protons on BrSt. ^b Weight percentage of PE-BrSt copolymer is determined by the intensity ratio after deduction and calibration curve. ^c Samples were heated to 900°C in N_2 at a rate of 10°C/min. ^d Solution concentration is determined by the weight of solute over the weight of solution.

Table 5.2 summarizes the PE-g-Pitch (8.4%) samples' $I_{(al)}/I_{(aro)}$ between the saturated aliphatic region and unsaturated aromatic region on ^1H NMR spectra, the weight composition percentage of the PE-BrSt portion, the carbon yield at 900°C in N_2 , and the spinnability of PE-g-Pitch/1,2,4 trichlorobenzene (TCB) solutions with two different concentrations of 5 and 10wt.%.

As discussed in the previous NMR section, we were able to obtain the ratios between $I_{(ali)}$ and $I_{(aro)}$ of all PE-g-Pitch samples from their 1H NMR spectra. Then we used these ratios to approximately determine the weight percentage of the PE-BrSt copolymer portion after the grafting of PAH molecules for each sample. Assuming an extreme condition that all of the 4-bromophenyl groups were involved in the grafting reaction, and considering that these side groups also contain aromatic protons, the number of aromatic protons on 4-bromophenyl group will reduce from four to two after the grafting reaction as shown in Figure 5.2. The intensity of the remained aromatic protons was deducted from the total intensity of the aromatic region, to obtain the intensity of the aromatic protons that only correspond to the grafted PAH molecules. After this, the approximate content of the PE-BrSt portion in weight percentage for each sample can be calculated by inputting the ratio values into a calibration curve that was obtained by the 1H NMR spectra of the mixtures of PE-BrSt (8.4%) and pitch 250M(S) in different known weight ratios. By using the calibration curve as a reference, the sample PE-g-Pitch (8.4%)-3 with three hours of blending time has a PE-BrSt portion of only approximately 3.1% in weight, while 96.9% of weight contributes to PAH molecules. Therefore, the experimental weight ratio between the pitch and PE-BrSt portion is 31.25.

Then, let us consider the case that each of the 4-bromophenyl groups was grafted by one PAH molecules from 250M(S). Based on the 1H NMR spectrum of PE-BrSt copolymer and the MALDI-TOF-MS (Chapter 4) result of 250M(S), the starting PE-BrSt copolymer has an 8.4mol% comonomer percentage, and PAH molecules in 250M(S) has an average molecular weight of around 567.86g/mol. The theoretical value of weight ratio between the pitch and PE-BrSt portion after two PAH molecules react with each one of 4-bromophenyl group can be approximated as follows:

$$\frac{W(\text{pitch})}{W(\text{PE} - \text{BrSt})} = \frac{\frac{567.86g}{mol} * 8.4\%}{\frac{28g}{mol} * 91.6\% + \frac{181g}{mol} * 8.4\%} = \frac{1.16}{1}$$

In both cases, we assumed all of the 4-bromophenyl groups in PE-BrSt (8.4%) were grafted by one PAH molecules. Therefore, we can compare the weight ratios we obtained from the experimental results and the theoretical calculation. It's clear that the experimental weight ratio of PE-g-Pitch (8.4%)-3 is much higher than the theoretical weight ratio, indicating the number of grafted PAH molecules is much more than one for this PE-g-Pitch sample. The explanation is that the incorporation of PAH molecules from pitch increases the number of six-membered rings on the copolymer pendant substituents, hence reducing the activation energy of the polycondensation reaction between these side groups and the free PAH molecules that surround them. Therefore, the side groups are continually enlarged at the same temperature with a longer reaction (blending) time. (Figure 5.8)

The calculations above may not be accurate, because in the real case, the experimental results suggest that not all of the 4-bromophenyl groups can get involved in the reaction. Additionally, the minimum molecular weight of PAH molecules that can react with 4-bromophenyl groups at 310°C also has not been determined yet. Because less activation energy is required to undergo cycloaddition reaction for larger PAH molecules as mentioned previously, it is likely the value of this minimum molecular weight of PAH molecules for this reaction is higher than the average molecular weight of 250M(S). Therefore, these calculations are considered to produce approximate values for the weight ratio between the incorporated pitch and the PE-BrSt portion.

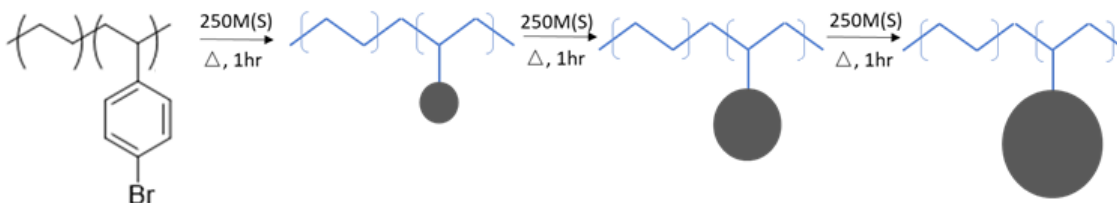


Figure 5.8 The structural transformation of PE-g-Pitch during the blending process. (The black circle represents the PAH side group)

The postulation about the enlarged PAH side groups can also be supported by the carbon yields summarized in the table measured by using TGA. Table 5.2 shows that PE-g-Pitch (8.4%)-3 has a carbon yield of ~78.8% at 900°C. As discussed in Chapter 1, the isotropic pitch (IP) must be heated to a temperature higher than 350°C to undergo the polycondensation reaction, converting IP to mesophase pitch (MP). Without this conversion, IP such as the 250M(S) we used in this study has a carbon yield of only about 44%. MP, by contrast, has a high carbon yield of around 80%, which is similar to the carbon yield of PE-g-Pitch (8.4%)-3. Therefore, this sample must have its side groups enlarged to become more favorable for carbon conversion. As the PE-BrSt composition% decreases with the shorter reaction time, the carbon yield of PE-g-Pitch (8.4%) becomes lower and shows a value of only 37.2% for PE-g-Pitch (8.4%)-1 with a blending time of one hour. But combining its PE-BrSt weight composition of 37.1% in this PE-g-Pitch sample, while considering the 0% and 44% carbon yields of PE-BrSt (8.4%) and 250M(S), respectively, we found that the carbon yield of PE-g-Pitch (8.4%)-1 is higher than the theoretical value of 27.6% without any stabilization. This finding agrees with the stabilization effect by PAH molecules on PE backbones as we mentioned in Chapter 4.



Figure 5.9 Pictures of PE-g-Pitch(8.4%)/TCB solutions showing (a) no spinnability and (b) good spinnability in the coagulation bath.

The spinnability of these samples was tested using a solution spinning setup as shown in the experimental section. All the samples can be dissolved in TCB with concentrations of 5wt.% and 10wt.%. The spinnability results are shown in Table 5.2. All the samples marked as ‘N’ showed no spinnability and could not be drawn into fibers in the coagulation bath. Instead, the materials coagulated into beads as shown in Figure 5.9(a). For PE-g-Pitch (8.4%)-2 & 3, the excessively long blending time converts the 4-bromophenyl group into a large and highly π -electron conjugated structure, which creates strong π - π interaction between polymer chains and forms physical cross-linking that prevents the effective alignment of the polymer chain. For PE-g-Pitch (8.4%)-1 with 5% concentration, the solid content is too low, resulting in solidified fibers with low viscosity in the coagulation bath. Among all these samples, PE-g-Pitch (8.4%)-1/TCB 10wt.% concentration showed good spinnability as shown in Figure 5.9(b). It was successfully converted to precursor fibers by solution spinning.

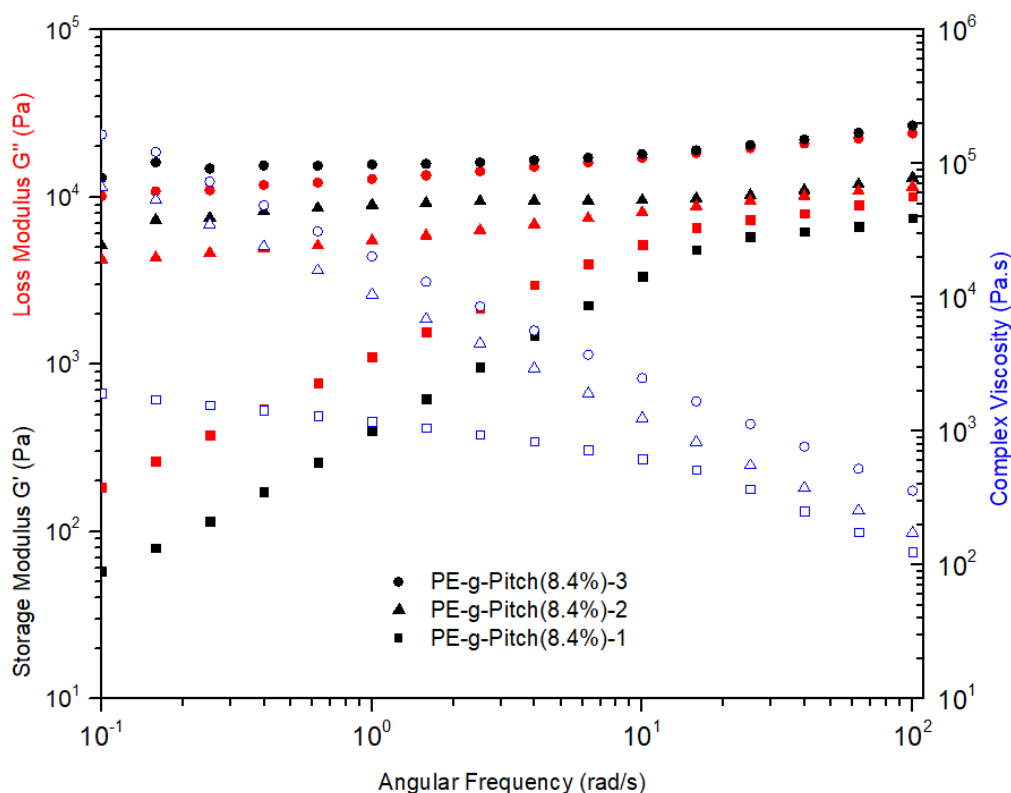


Figure 5.10 Oscillatory rheology (frequency-sweep) comparison of PE-g-Pitch(8.4%)-1, 2 and 3 with blending time of 1, 2 and 3 hours, respectively, in 10wt.% TCB solution at 90°C.

To study the processibility of these PE-g-Pitch samples in more detail, frequency-sweep rheological measurements were conducted on PE-g-Pitch(8.4%)-1, 2, and 3/ TCB (10 wt.%) solution at temperatures of 90°. Based on Figure 5.10, the solution of the PE-g-Pitch (8.4%)-1 with one hour blending time behaved like a liquid in the frequency range of measurements, although the difference between G'' and G' became smaller as the frequency increased, indicating the transition of the polymer solution from the rubbery plateau to the development of glassy behavior. The liquid-like behavior suggests that there is no formation of chemically or physically cross-linked network structure during the preparation of PE-g-Pitch. In contrast, both of PE-g-Pitch (8.4%)-2 and 3 with longer blending time behaved solid-like in the low-frequency range of 0.1-10rad/s. It agrees with the previous explanation on these samples' spinnability that the strong π - π interaction between the enlarged PAH side groups generates the physically cross-linked network structure.

Shear-thinning is defined as the non-Newtonian behavior of fluids, i.e., that its viscosity decreases as the shear rate increases. This behavior originates from the ability of a moving matter to rearrange its microstructure, an effect that is accomplished by reducing its entanglement density and thus decreasing the energy needed for it to flow.¹⁷¹ Based on the curves of complex viscosity, it was found that the values of both PE-g-Pitch solution samples experienced a decrease with the increasing angular frequency. For an oscillatory excitation, the shear rate $\dot{\gamma}$ with the angular frequency ω and shear amplitude γ_0 is given by:¹⁷²

$$\dot{\gamma}(\omega, t) = \gamma_0 \cdot \omega \cdot \cos(\omega t) \quad (5-1)$$

With a constant γ_0 , the shear rate is proportional to the angular frequency. Therefore, the viscosity reduction of both PE-g-Pitch solution samples as described above indicates the occurrence of shear-shinning at the measurement temperatures, which is due to the disentanglement of polymer chains in the PE-g-Pitch structure, regardless of the size of the PAH side groups.

Although no zero-shear viscosity can be obtained from these measurements, the complex viscosity curve of PE-g-Pitch (8.4%)-1 exhibits a trend to be constant in the lower angular frequency region from 10 to 0.1 rad/s. It was also found the complex viscosity of PE-g-Pitch solution with the same concentration increases with longer blending time within the angular frequency range of measurement. This suggests the increase of molecular weight of PE-g-Pitch due to more grafted PAH molecules into the PE backbones. Among all of these samples, the solution of PE-g-Pitch (8.4%)-1 exhibits liquid-like behavior with complex viscosity around 100Pa.s at the angular frequency of 100 rad/s, which is within the range of the fiber spinning of polyacrylonitrile of less than 200Pa.s as discussed in Chapter 1.

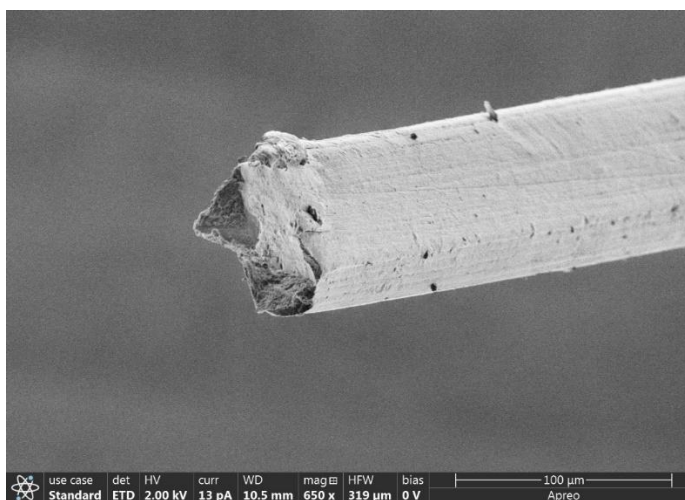
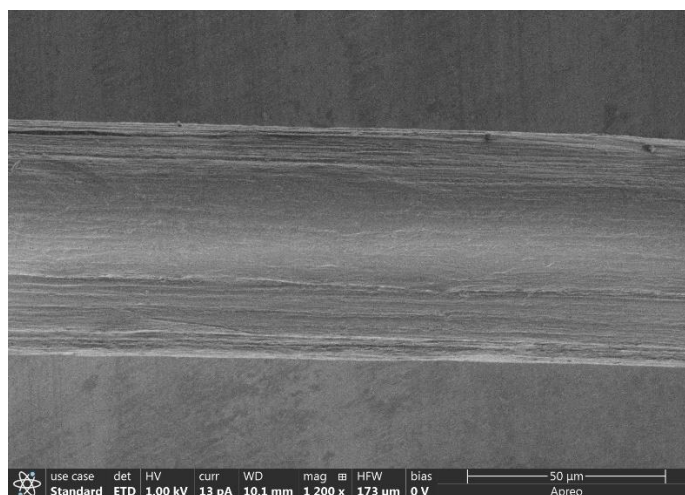


Figure 5.11 The SEM images of PE-g-Pitch(8.4%)-1 (top) fibers surface and (bottom) cross-section with blending time of 1 hour at 310°C.

After studying its rheology behavior, PE-g-Pitch (8.4%)-1/ TCB (10 wt.%) solution was successfully spun to fibers at 100°C with acetone as a coagulation bath. SEM images (Figure 5.11) show the as-spun precursor fiber has a diameter of about 62.5 μm and a smooth surface without porosity, indicating no occurrence of the cross-linking reaction and phase separation during the sample preparation. The strained patterns along the fiber surface were formed as a result of stretching during the fiber spinning process in the coagulation bath.

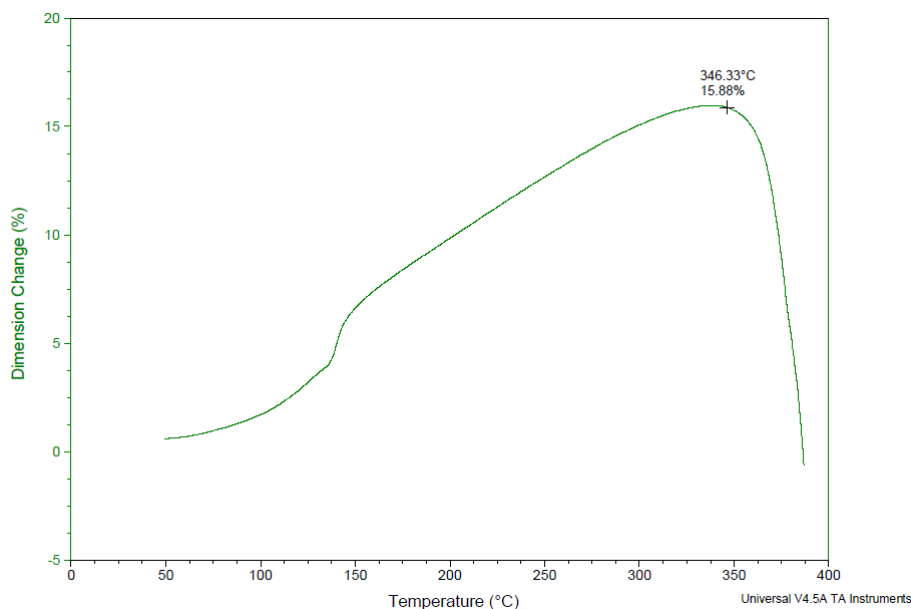


Figure 5.12 TMA of PE-g-Pitch (8.4%)-1 in N_2 with a heating rate of 10°C/min.

Stabilization is usually applied on precursor fibers to form a cross-linked network before transforming them to CFs. The temperature of the stabilization reaction should be lower than the softening point of the precursor, to prevent the fibers from collapsing during carbonization. To determine the softening point of our precursor, TMA was conducted in N_2 with a heating rate of 10°C/min on PE-g-Pitch (8.4%)-1, as illustrated in Figure 5.12. After experiencing thermal expansion at the low temperature, the precursor material started to become soft at around 325°C, then underwent a sharp dimensional reduction starting at around 346°C. The softening point of PE-g-Pitch is much higher than the typical PE copolymers, which are generally liquified at the

temperature above their melting point. This may be a result of the incorporation of PAH side groups that not only have the bulky size to prevent polymer segments from rotating freely but also provide the strong interaction between polymer chains, which requires high thermal energy to overcome. The high softening point is favorable for the as-spun precursor fibers to maintain their form at the temperature of oxidative stabilization; however, it is too low for the oxygen-free stabilization (as discussed in Chapter 3) via the polycondensation of pitch-like side groups.

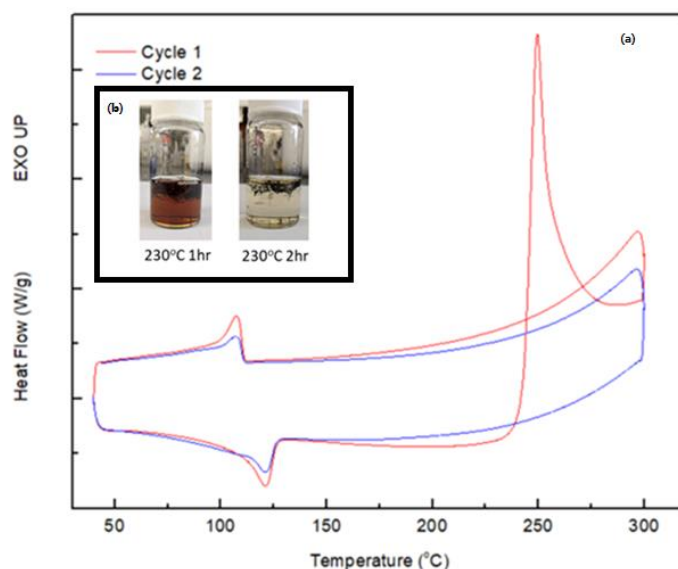


Figure 5.13 (a) DSC measurement of PE-g-Pitch (8.4%)-1 in air with two heating cycles. (b) images illustrating solubility of PE-g-Pitch (8.4%) fibers with heat-treatment in air at 230°C for (left) one and (right) two hours.

As mentioned, PE-g-Pitch is a copolymer with PAH side groups grafted on PE backbones. Both PE and pitch can be oxidatively stabilized in the air at a temperature range of 200–300°C to generate a π -conjugated network structure, according to previous studies.^{75,173,174} To determine the temperature required to oxidatively stabilize the PE-g-Pitch, DSC on PE-g-Pitch (8.4%)-1 was measured in air with a heating rate of 10°C/min as shown in Figure 5.13(a). A pre-run in N₂ from 40° to 200°C had been conducted to remove the thermal history of the sample. To investigate the starting point of oxidative stabilization and its effect on the polymer structure, we subjected the sample to two heating and cooling cycles in the temperature range of 40° to 300°C. For the first cycle, an exothermic ramp was found starting at around 220°C, suggesting the occurrence of the

oxidation reaction. Following this ramp, a huge exothermic peak was found from 235°C to 280°C, indicating that a large amount of heat had been released within a short period. Similar exothermic behavior was also found on linear low-density polyethylene (LLDPE) in a previous study¹⁷³, in which the researchers suggested that it corresponds to the incorporation of oxygen in the forms of ketones and -C-O-C bridges, hence generating a thermally stable structure to survive the harsh carbonization conditions. As discussed, oxidative stabilization is the most significant step in determining the mechanical properties of produced CFs. An extensive heat generation within a short time can cause defects and inhomogeneity in the fiber structure. Therefore, we conducted a gel content test on the precursor fibers heated to the lowest limit of the stabilization reaction of 230°C and heat-treated for a certain time in the air. As shown in Figure 5.13(b), the gel content of the precursor fibers heat-treated at 230°C for two hours was 100%. Additionally, no fiber swelling was found, indicating the generation of a polymer network with high cross-linking density.

5.3.3 Carbon Fibers Prepared from PE-g-Pitch Stabilized Precursor Fibers

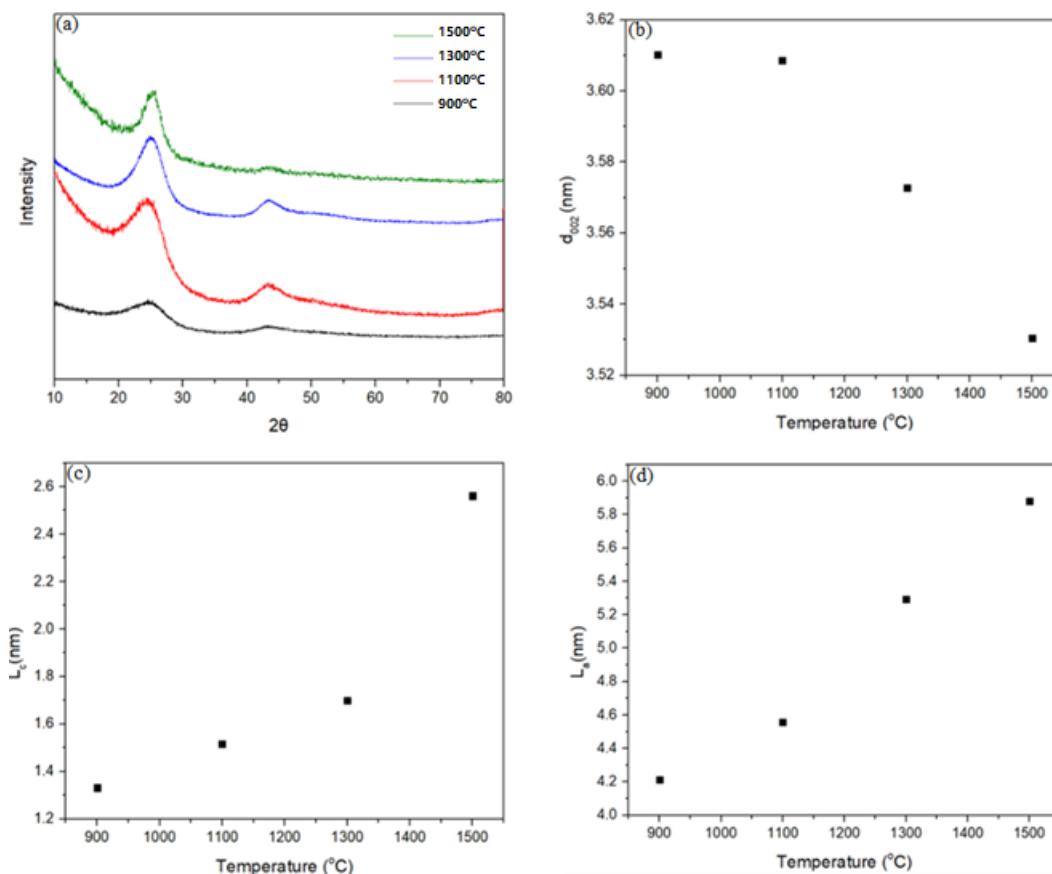


Figure 5.14 Comparisons of (a) XRD spectra and calculated (b) d_{002} , (c) L_c , and (d) L_a of carbonized PE-g-Pitch (8.4%)-1 at temperatures of 900, 1100, 1300 and 1500°C.

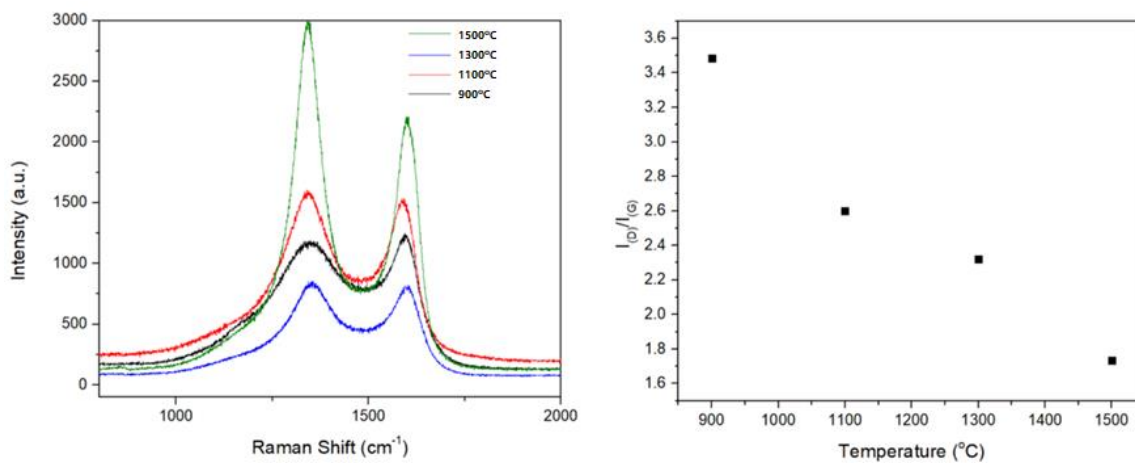


Figure 5.15 Comparisons of (left) Raman spectra and (right) calculated $I(D)/I(G)$ of carbonized PE-g-Pitch (8.4%)-1 fibers at temperatures of 900, 1100, 1300, and 1500°C.

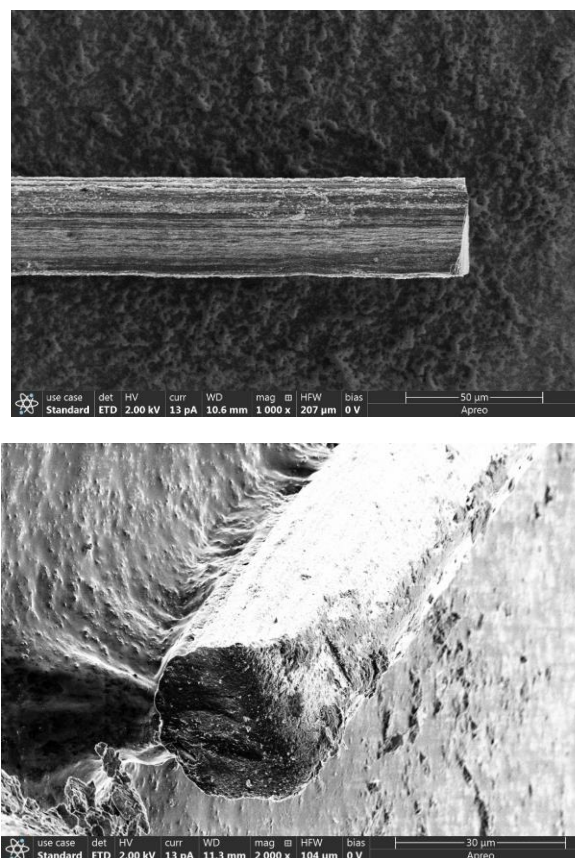


Figure 5.16 SEM image of (top) fiber surface and (bottom) cross-section CF converted from PE-g-Pitch (8.4%)-1 at 900°C.

PE-g-Pitch (8.4%)-1 precursor fibers were stabilized in the air at 230°C for two hours, then subjected to heat treatment under temperatures from 900 to 1500°C. The bulk structure of carbonized fibers was determined by XRD and Raman spectroscopy. Based on the XRD spectra as shown in Figure 5.14, microcrystals were formed in both temperatures. When the carbonization temperature was increased from 900 to 1500°C, the $d(002)$ value slightly decreased from 0.361 nm to smaller spacing of 0.3608 nm at 1100°C, then decreased more rapidly to 0.3573 nm and 0.3526 nm at 1300 and 1500°C, respectively. The small difference of $d(002)$ values between 900 and 1100°C is a result of the disruption from hydrogen emission offsetting the size growth of microcrystals; this agrees with the finding on PE-g-Pitch/pitch blend discussed in Chapter 3. The L_a and L_c increase with the higher temperature indicates the growth of carbon microcrystals within the fibers to generate a more graphite-like structure. Raman results in Figure

5.15 show that I_D/I_G has a significant reduction from 900 to 1500°C. These results suggest that the regularity of the carbon layer structure improves with higher heating temperatures. The Raman shift of G peak firstly decreases from 900 to 1100°C, and then keeps increasing as the temperature rises to 1300 and 1500°C, indicating the transformation of PE-g-Pitch from a mostly amorphous structure that contains sp^3 carbons at 900°C to a microcrystalline carbon structure with only sp^2 carbons at 1500°C.¹⁷⁵ Based on the SEM images in Figure 5.16, no porous structure was found on the surface and cross-section of the CF which carbonized at 900°C, indicating no phase separation and the cross-linking reaction was happening during the sample preparation step. The circular geometry of the CF remained unchanged on its cross-section, indicating the two-hour stabilization at 230°C effectively infusibilized the precursor fiber before the carbonization.

5.3.4 Melt Spinnable Carbon Fiber Precursor by PE-g-Pitch Graft Copolymer with Unreacted Pitch

As mentioned in Chapter 1, the solution spinning of fibers usually utilizes a large amount of expensive and un-eco-friendly organic solvent. Although a solvent recovery system can be designed to achieve the reuse of solvent, it would further increase the expense of the overall process. Therefore, in this section, we discuss using the melt-spinning method to spin the PE-g-Pitch precursor prepared from PE-BrSt with an excess of the unreacted pitch as a plasticizer. The study is like the previous study in Section 2.4 for PEP-g-Pitch, but in this case, we replaced the starting material—PE-DPA (7.2%) copolymer—with PE-BrSt (8.4%) copolymer. Additionally, due to the brittle nature of the pitch, the excess unreacted pitch was partially removed by using a Soxhlet extractor. In the following section, we examine the effect of the amount of the unreacted pitch removed on both the carbon yield and the rheology behavior of the PE-g-Pitch/pitch blend. We also discuss the oxidative stabilization of PE-g-Pitch/pitch blend. In the end, we will exhibit

the successful conversion from the precursor fibers to CFs with mechanical properties suitable for general purposes.

Table 5.3 The preparation conditions for PE-g-Pitch/pitch blends with different amount of free pitch removed.

Sample	BrSt mol%	Weight Ratio	T_{blend} (°C)	t_{blend} (hr)	^b RP%
		Polymer:250M(S)			
PE-BrSt(8.4%)-74% ^a	8.4	1:10	310	1	25.60%
PE-BrSt(8.4%)-56% ^a	8.4	1:10	310	1	43.66%
PE-BrSt(8.4%)-34% ^a	8.4	1:10	310	1	66.00%

^aThe percentage after the dash symbol indicates the weight remained after extraction. ^bRP%=[1-(W_f/W_o)]×100%, where W_o is the original weight of the sample before extraction and W_f is the weight of collected product after extraction

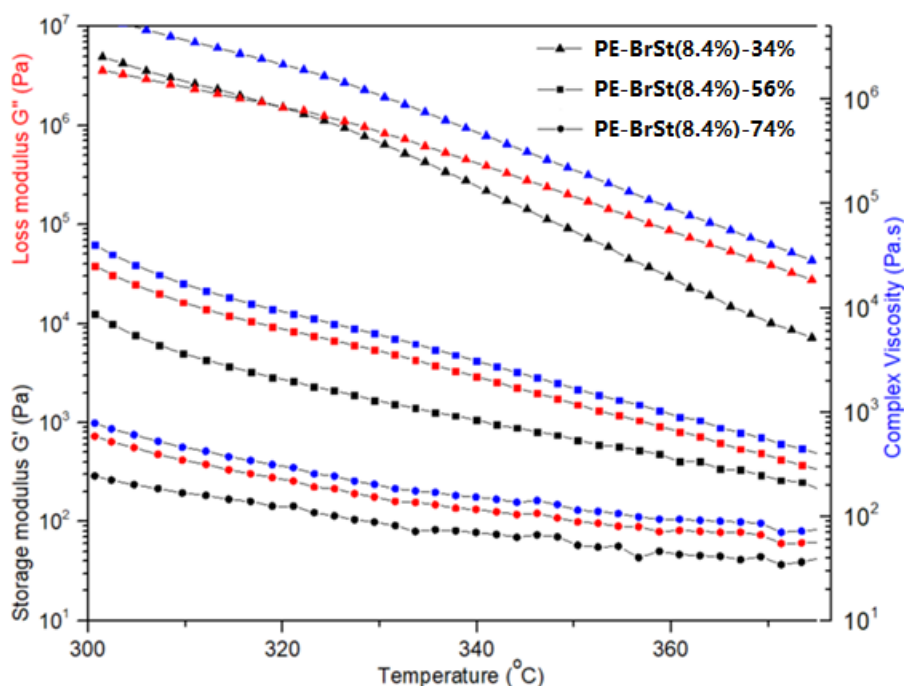


Figure 5.17 Temperature sweep oscillatory melt-rheology results of PE-g-Pitch/pitch blends with 66.00%, 43.66%, 25.60% of free pitch removed.

From the melt-rheology curves from oscillatory measurements, as shown in Figure 5.17, we observed the PE-BrSt(8.4%)-74% and 56% were in the more liquid state in the temperature range of measurement. PE-BrSt(8.4%)-34% behaved more solid-like at the beginning and started to liquefy at ~320°C. For PE-g-Pitch (8.4%)-1 without any unreacted pitch remaining, its melt

viscosity is not lower enough for the melt rheology characterization in the temperature range of measurement; therefore, no result can be obtained. The complex viscosity of the PE-g-Pitch/pitch blend decreases as the amount of remaining pitch increases and can reach less than 1000Pa.s with a certain amount of unreacted pitch as the plasticizer that is favorable for melt-spinning. All of the PE-g-Pitch/pitch blends prepared from PE-BrSt copolymer in these measurements show better thermal stability in the aspect of processability compared to the blends prepared from PE-DPA copolymer in Chapter 3. This may be attributed to the slower reaction between PAH molecules and 4-bromophenyl groups, which forms smaller PAH side groups with a blending time of one hour that require higher energy to undergo the intermolecular cross-linking reaction via polycondensation. Therefore, it is necessary to apply oxidative stabilization on the as-spun precursor fibers, preventing them from melting during the following carbonization process. Compared to the other two samples, PE-BrSt (8.4%)-56% shows a viscosity range that ensures good processability for melt-spinning, while providing enough dimensional stability for the as-spun fibers in the temperature range of oxidative stabilization. Therefore, the study described next focuses on this sample.

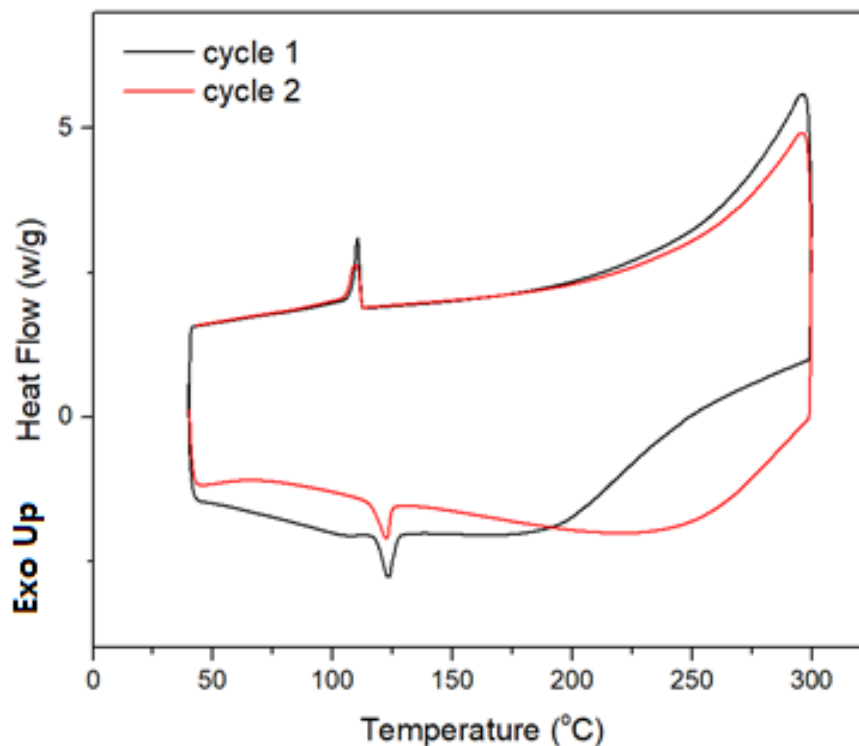


Figure 5.18 DSC results of PE-BrSt(8%)-56% with two heating-cooling cycles in an air atmosphere (10°C/min).

To investigate the oxidation behavior of this type of precursor, we conducted a DSC measurement in the air atmosphere (Figure 5.18) for PE-BrSt(8.4%)-56%, which has the most promising rheology results for fiber spinning among all of the prepared samples in this study. All samples were heated to 150°C and cool to room temperature with a heating/cooling rate of 10°C/min in N₂ to remove their thermal history. The sample was set to have two heating and cooling cycles continually between 50° and 300°C with a heating and cooling rate of 10°C/min. For the first cycle, an exothermic ramp was found starting from ~200°C, indicating that the oxidation reaction on PE-g-Pitch/pitch started at this temperature. Interestingly, this initiative temperature is 20°C lower than the PE-g-Pitch for solution-spinning we discussed in the previous section. It is due to the presence of unreacted pitch in the mixture that starts to react with oxygen at a lower temperature than the PE-g-Pitch. An exothermic pattern similar to that of the first cycle can be observed in the second cycle, but starting from a higher temperature of ~250°C. By comparing the crystallization peaks during cooling located at ~115°C between the first and

second cycles, it showed that the packing of PE polymer chains was suppressed by the previous exothermic reaction. This can be explained by the introduction of oxygen at a high temperature, which can generate covalent cross-linkages between pitch-like side groups, therefore limiting the mobility of PE chains. It also explains why the exothermic reaction started at a higher temperature in the second round. It is because the formation of a cross-linking structure densifies the precursor material; therefore, it requires higher thermal energy to mobilize the structure to let oxygen diffuse into the inner portion. The DSC results suggested that the oxidative stabilization temperature should be higher than 210°C for the PE-g-Pitch/pitch blend to become infusibilized.

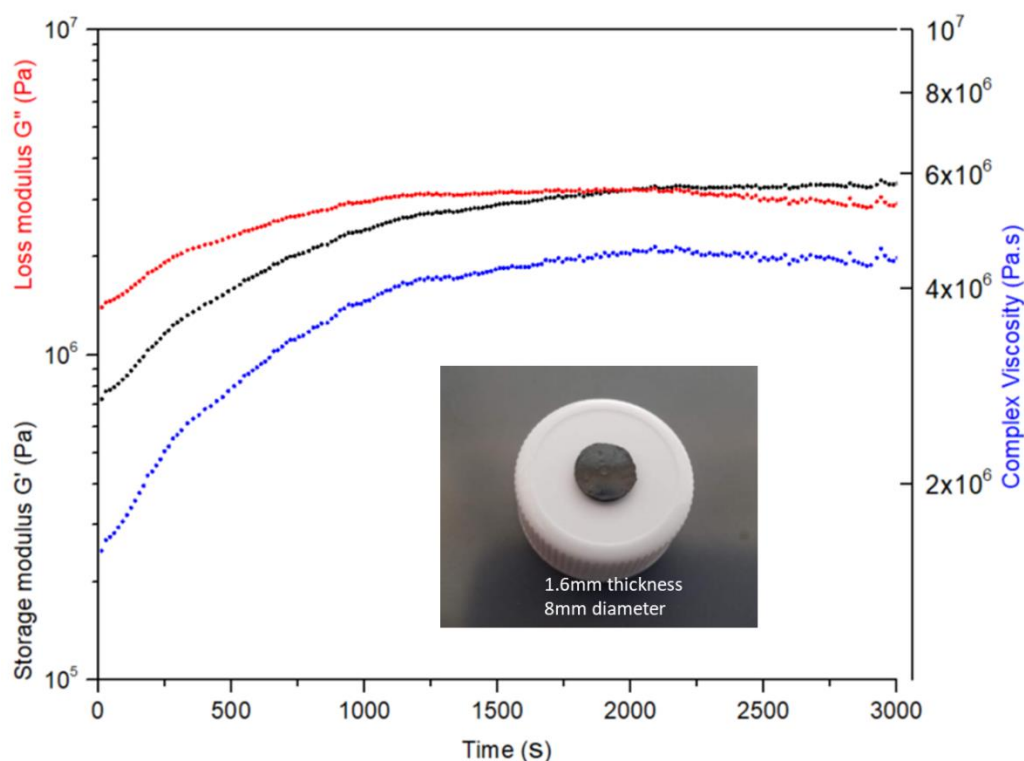


Figure 5.19 Time-sweep oscillatory rheology results of PE-BrSt(8.4%)-56% in the air atmosphere at 210°C.

Time-sweeps oscillatory rheology measurement was conducted to demonstrate the rate of the network formation in PE-g-Pitch/pitch blend by air. PE-BrSt(8.4%)-56% was molded into a disc-like sample with a thickness of 1.6mm and a diameter of 8mm before the measurement. The testing temperature was selected to be 210°C, a temperature higher than the starting point of the

oxidation reaction; this preserves the high viscosity of precursor material and, in turn, maintains the shape of the sample during the oxidation process. As shown in Figure 5.19, the complex viscosity of PE-BrSt(8.4%)-56% increased to double within 1000 seconds, indicating the rapidly increasing molecular weight of PE-g-Pitch/pitch blend due to the oxidation reaction. The sample became solid-like 2100 seconds after the measurement, indicating the formation of a network structure. Because of the much smaller dimensions, we expect that the time required to infuse a precursor fiber would be much less than the disc-like sample for this oxidative stabilization process.

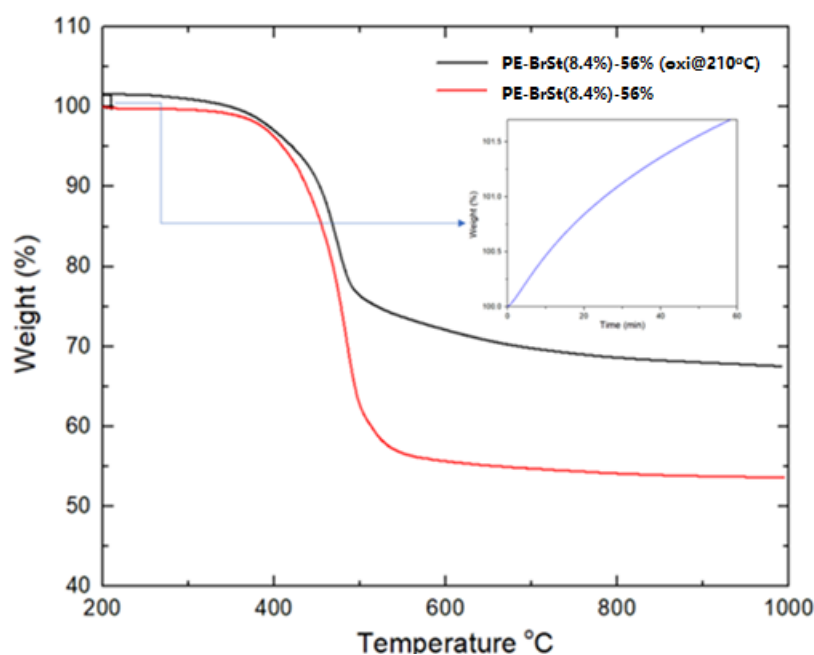


Figure 5.20 TGA comparison of PE-BrSt(8.4%)-56% samples with and without heat treatment in air at 210°C.

We also found that heat treatment in the air would improve the carbon yield of this precursor. Figure 5.20 compares the thermal degradation in N_2 of PE-BrSt(8.4%)-56% samples with and without heat treatment in air at 210°C for one hour. Interestingly, the carbon yield of the blend is higher than the PE-g-Pitch-1 of about 37% and 250M(S) of about 44%. The reason may be that, within a blend, the PE-g-Pitch can continually react with the surrounding free PAH molecules during the process of carbonization. The sample with air heat treatment at 210°C had a

slight weight increment of 1.7% within one hour of heating time, indicating the incorporation of oxygen molecules into the precursor structure. These oxygen molecules not only help to generate cross-linkages, as discussed in the rheology and DSC study, but also promote the dehydrogenation reaction to form a more stable structure. Therefore, the carbon yield of the air-treated sample is ~13% more than the untreated sample.

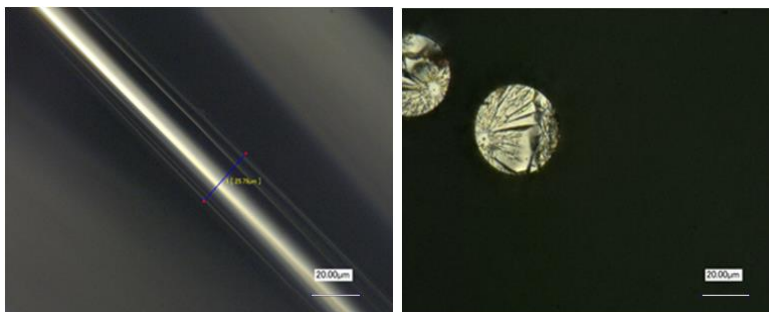


Figure 5.21 Optical microscopy images of (left) surface and (right) cross-section of PE-BrSt(8.4%)-56% melt-spun precursor fiber.

PE-BrSt(8.4%)-56% was successfully spun using a piston fiber extruder through a die with a diameter of 100 μ m. The material was spun by our collaborators at Oak Ridge National Laboratory in a continuous manner for more than 30 minutes of active spinning time without any breakage. The precursor fibers have an average diameter of around 25 μ m and a smooth surface. Additionally, no porosity was found beneath the surface based on the cross-sectional image, indicating that no phase separation occurred during air cooling of precursor fibers. The as-spun precursor fibers were stabilized and carbonized to carbon fibers without applying tensile stress. The ones with the best mechanical properties so far were stabilized at 260°C for two hours and heated to 1200°C. They show tensile strength of 603.6 MPa and modulus of 43.37 GPa, which is suitable for general-purpose applications.

5.4 Conclusion

In the first section of this chapter, we discussed the carbon yield, rheology behaviors, oxidative stabilization reaction, and carbonization behavior of a pure PE-g-Pitch polymer precursor prepared from PE-BrSt copolymer. The carbon yield of PE-g-Pitch increases with larger PAH side groups; however, the oversized side groups cause PE-g-Pitch to be physically cross-linked and unable to be spun into fibers. The sample PE-g-Pitch (8.4%)-1 with one hour of blending time was successfully solution-spun, stabilized, and carbonized to CFs. The XRD and Raman show that the precursor fibers are graphitizable, and their structure becomes more ordered and graphite-like with the higher carbonization temperature.

In the second half of the chapter, we first studied the rheological behaviors of a series of PE-g-Pitch/pitch blends prepared from PE-BrSt(8.4%) copolymer and 250M(S) with different amounts of ungrafted pitch removed. We found that as the more unreacted pitch was removed, the complex viscosity increased proportionally. However, in contrast to the PE-DPA/pitch blend, no rapid solidification behavior took place on these samples in the temperature range of 300° to 400°C. Therefore, we conducted a DSC measurement to determine the temperature range of the stabilization reaction, which starts at about 210°C. We applied oxidative stabilization at 210°C on the blend with the most suitable viscosity and observed the rapid generation of the cross-linked network within 2100 seconds. Additionally, we found that oxidative stabilization effectively increased the carbon yield of the blend to an additional 13%. The PE-g-Pitch/pitch blend was successfully spun into precursor fibers with a smooth surface by melt-spinning at 340°C. After carbonization at 1200°C, the formed CFs showed mechanical properties suitable for general purposes.

Chapter 6

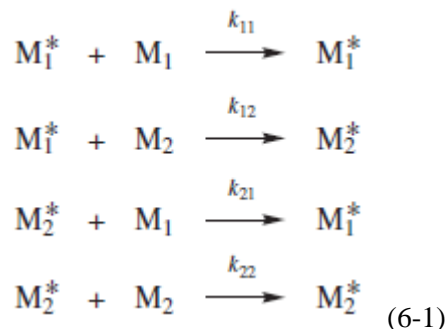
Synthesis and Evaluation of PE-g-Pitch Precursors Prepared from Poly(ethylene-co-4-bromostyrene) by Post Polymerization Process: Bromination of Poly(ethylene-co-styrene)

6.1 Introduction

In the previous study in Chapter 5, we found a new method to prepare the PE-g-Pitch graft copolymer. The chemistry was based on the PE-BrSt copolymer prepared by direct copolymerization of ethylene and 4-bromostyrene using a metallocene catalyst. The PE-BrSt copolymer proved to be reactive with pitch to form a PE-g-Pitch graft copolymer via thermal-induced cycloaddition reaction. However, the resulting PE-g-Pitch graft copolymer with good solution spinnability offered a carbon yield of only 37%, while the ones showing higher carbon yields (prepared with longer blending time) were not drawable in the coagulation bath during the fiber-spinning process. The analysis of their chemical composition indicates that the long blending time allows the continued growth of the polycyclic aromatic hydrocarbons (PAH) side groups, which generate stronger π - π interaction that acts as the physical cross-linker and prevents the alignment of polymer chains. Additionally, the experimental results also indicate that the inhomogeneous PE-BrSt copolymer microstructure is a result of the big difference in comonomer reactivity ratios between ethylene and 4-bromostyrene during the copolymerization reaction. The resulting long sequence of 4-bromostyrene units in the PE-BrSt copolymer chain exhibits reduced chemical reactivity with the PAH molecules in pitch.

The microstructure of a copolymer is controlled by the reactivity of two monomers (M1 and M2) toward the propagating site.¹⁷⁶ The copolymerization reaction involves two types of propagating sites, M_1^* and M_2^* . The asterisk represents the propagating species regardless of the type of polymerization. Therefore, there are four types of possible propagation reactions,

assuming that the reactivity of the propagation site depends only on the monomer type at the end of the chain, including:



Here, k_{11} , k_{12} , k_{21} , and k_{22} are the rate constants for a propagating site ending in M_1 adding to monomer M_1 , a propagating site ending in M_1 adding to M_2 , and so on. The monomer reactivity ratios r_1 and r_2 can be given by:

$$r_1 = \frac{k_{11}}{k_{12}} \quad \text{and} \quad r_2 = \frac{k_{22}}{k_{21}} \quad (6-2)$$

The monomer reactivity ratio is defined as the ratio of the rate constant for a reactive propagating site adding its own type of monomer to the rate constant for adding the other monomer.¹⁷⁶ The parameters r_1 and r_2 are used to determine the microstructure of a copolymer. When $r_1 \times r_2 = 1$, a random copolymer will be formed with a uniform microstructure. On the other hand, an alternating copolymer will be obtained when $r_1 \times r_2 = 0$, and a block copolymer microstructure will be observed when $r_1 \times r_2 \gg 1$. 4-Bromostyrene is a bulky comonomer with an electron-withdrawing halide group; this combination reduces its reactivity during the metallocene-mediated ethylene/4-bromostyrene copolymerization reaction. In other words, the r_1 value for ethylene (M_1) is very high, with the resulting blocky copolymer structure.

Thus, the primary goal of this study is to develop an alternative route for preparing the PE-BrSt copolymer with a more homogeneous microstructure. The resulting homogeneously

distributed 4-bromostyrene units along the PE chain may exhibit high reactivity with PAH molecules, which may produce the desirable spinnable PE-g-Pitch precursor, i.e., one with reduced reaction time and high carbon yield.

6.2 Experimental Section

6.2.1 Characterization

Liquid state ^1H NMR and ^{13}C NMR spectra were obtained by using Bruker AV 300 at 90°C, with *d*-1,1,2,2 tetrachloroethane solvent. TGA measurements were conducted on a TA Sdt-600. Around 10 mg of sample was loaded into the sample pan and heated at a rate of 10°C/min in the N_2 atmosphere with a gas flow rate of 50ml/min. DSC measurements were conducted on a TA Q2000 with a heating/cooling rate of 10°C/min. EGA-MS measurement was conducted on a TA TGA5500 with a mass spectrometer in argon with a heating rate of 10°C/min and a flow rate of 25ml/min. The weight of the sample was fixed to be 15mg in every measurement. XRD measurements were conducted on a Panalytical XPert Pro MPD theta-theta Diffractometer from Malvern at 40 kV and 40 mA with Cu $\text{K}(\alpha)$ radiation $\lambda = 0.15418$ nm. Diffraction patterns were recorded on a 0.8 collimator, with an oscillation of the samples between 10 and 80° and an imaging plate detector. The scan rate was 0.2°/min with an interval of 0.045°.

6.2.2 Materials

4-bromostyrene and styrene (TCI) were vacuum distilled after drying overnight by CaH_2 . MMAO-12 7% toluene solution (Sigma Aldrich) was dried by vacuum at 50°C to become white powders. $[(\text{C}_5\text{Me}_4)\text{SiMe}_2\text{N}(\text{t-Bu})]\text{TiCl}_2$ (Boulder Scientific), 1,2,4-trichlorobenzene (Sigma Aldrich), and acetone (VWR) were used as received. Toluene (Wiley Organics) was purified via

the Grubbs type solvent purification system. Petroleum pitch (250M) with a softening temperature of 250°C were kindly provided by Rutgers Basic Aromatics GmbH.

6.2.3 Preparation of Poly(ethylene-4-bromostyrene) Copolymer via Direct Copolymerization

The copolymerization reaction was conducted in a Parr 500ml stainless autoclave equipped with a mechanical stirrer. The reactor was firstly charged with 220ml of toluene, 9 ml of 4-bromostyrene, and 10ml of 20wt.% of methylaluminoxane (MAO) solution in toluene, with argon protection and stirring. Then the solution was saturated with 50 psi ethylene at 40°C. To the mixture, 1.1 ml of $[(C_5Me_4)SiMe_2N(t-Bu)]TiCl_2$ (CGC) solution in toluene (20 μ mol/ml) was injected into the reactor to initiate the reaction. After 1 hour, ethylene was replaced by argon and the reaction was terminated by adding 30ml of isopropanol. The solution mixture was then poured into 600ml of diluted HCl solution of methanol. The resulting PE-BrSt copolymer was isolated by filtration and was washed with 200ml \times 3 of methanol before drying in a vacuum oven overnight at 60°C. The weight of the copolymer was 5.65g. The comonomer percentage was 8.4% determined by 1H NMR.

6.2.4 Copolymerization of Poly(ethylene-styrene) copolymer

The reaction was conducted in a 500ml stainless autoclave equipped with a mechanical stirrer as a reactor. The reactor was firstly charged with 220ml of toluene, 6.5ml of styrene and 30ml of MMAO-12 (7wt.%) with argon protected and stirring. Then the reactor was filled with ethylene at 50 psi and heated to 40°C. After 10 minutes, 1.1 ml of $[(C_5Me_4)SiMe_2N(t-Bu)]TiCl_2$ (20 μ mol/ml) was injected into the reactor to initiate the reaction. After 1 hour, ethylene was replaced by argon and the reaction was terminated by adding 30ml of isopropanol. The solution

mixture was then poured into 600ml of diluted HCl solution of methanol. The polymer was isolated by filtration and was washed with 200ml×3 of methanol before drying in a vacuum oven overnight at 60°C. The yield of the product was 10.35g. The monomer percentage of the product was 8.5% determined by ¹HNMR.

6.2.5 Synthesis of Brominated Poly(ethylene-styrene) Copolymer

The prepared poly(ethylene-styrene) copolymer with 8.5% comonomer (4g) was firstly dissolved in 200ml of 1,1,2,2 tetrachloroethane at 100°C in an air-free 500ml three-neck round bottom flask, equipped with a condenser, a dropping funnel, a stir bar, and oil bath. The solution was then cooled to 70°C at a rate of ~2°C/min before 0.1 g of iron(iii) chloride was added. A solution made from 10ml 1,1,2,2 tetrachloroethane and 1ml of bromine was added to the dropping funnel. Then, the whole reactor was set to light-free before the bromine solution was added drop-wisely into the flask. After 2 hours, the polymer solution was poured into 400ml of hot methanol with vigorous stirring. The obtained polymer was washed with 300ml methanol×1 and 100ml acetone×2. Then the polymer product was dissolved in 200ml toluene and precipitated in 400ml methanol for another two times before drying in a vacuum oven at 60°C. The weight of the product with off-white color was 4.3g.

6.2.6 Toluene-soluble Pitch 250M(S) Extraction

A Soxhlet extraction apparatus was applied to extract toluene-soluble portion from petroleum pitch 250M. It consists of a still pot containing solvent and a stir bar, a distillation path, Siphon top and exit, a cone-shape filter paper with 8um hole size as sample holder, and a condenser with cool water flowing through. The solvent in the still pot used in this study was toluene and it was heated by an oil bath at 140°C. The temperature of the distilled solvent

surrounding the sample holder was measured by a thermocouple and the value was 65°C. After extraction, the solution was cooled to room temperature and conducted centrifuge. There was no insoluble portion found in this solution. Then the collected solution was dried at 100°C with air-flow and 90°C in a vacuum oven overnight.

6.2.7 Preparation of PE-g-Pitch/Pitch Blend

2g of PE-BrSt copolymer and 20g of 250M(S) were first dissolved in 250ml of toluene at 90°C in a 500ml beaker. At the same temperature, the prepared homogeneous solution was then dried with vigorous stirring under an airflow until it became a slime-like product that contained 20wt.% of toluene. The mechanical blending of all premixed samples was conducted in a twin-screw Brabender. This system has three thermocouples located at the outer cover, sample chamber, and inner wall to have a close monitor on temperature control. The heating rate was set to 10°C/min. Nitrogen flowed in the system through a rubber tube to create an air-free environment during mixing at a flow rate of 100ml/min. Firstly, the premixed sample was loaded into the sample chamber at room temperature and was mixed at a rate of 100rpm before the heating started. After the temperature reached the target temperature, the sample was heat-treated for a certain time at this temperature with an increased mixing rate of 300rpm. After it, the sample was cooled down by an air-cooling system with a cooling rate of 5°C/min. After blending, all collected samples were grounded in the form of powders by a mortar.

6.2.8 Free Pitch Removal

The powders were washed by 200ml toluene at room temperature in a beaker with vigorous stirring. Then the solution with suspension was centrifuged with the liquid portion removed. The

same washing process was repeated until the excess of unreacted 250M(S) was completely removed. The collected product was dried at 90°C in a vacuum oven overnight.

6.2.9 Fiber Spinning

Solution spinning of PE-g-Pitch was conducted by using the spinning set-up as shown in Figure 6.1 with 1,2,4-trichlorobenzene as solvent and acetone as a coagulation bath.

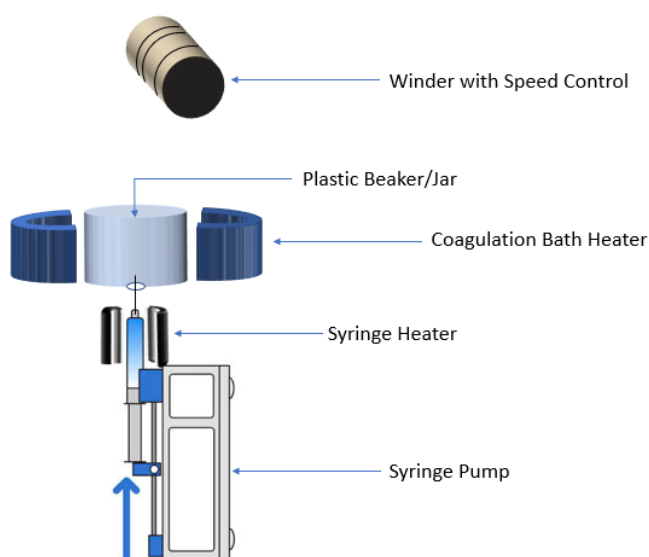


Figure 6.1 A schematic diagram of the solution-spinning setup.

6.2.10 Stabilization and Carbonization of PE-g-Pitch Fibers

The stabilization of PE-g-Pitch was conducted in a tube furnace with an air flowing at a rate of 100ml/min and a heating rate of 10°C/min, and with no tension applied. The carbonization of PE-g-Pitch fibers was conducted in a graphitizing furnace. In the beginning, 2g of sample was loaded on a boat-shaped ceramic crucible before putting into the furnace. Then, the furnace was vacuumed and refilled with argon three times before temperature raising to the target temperature at the rate of 10°C/min.

6.3 Results and Discussion

6.3.1 Synthesis of PE-BrSt Copolymers by Post Polymerization Process

The new chemical route for preparing the PE-BrSt copolymer involves a post-polymerization process in which a commercially available and inexpensive poly(ethylene-styrene) copolymer called PE-St is subjected to a bromination reaction, as illustrated in Figure 6.2. The PE-St copolymer is prepared by a constrained geometry catalyst (CGC) developed by DOW Chemical, $[(C_5Me_4)SiMe_2N(t-Bu)]TiCl_2$ with an alkylamido ligand, which has been proven to be very effective in several ethylene copolymerization reactions, including ethylene-styrene copolymerization.^{177,178} The high catalyst activity in both ethylene and styrene monomers is due to the weaker π -donating effect of the amido ligand and an open active site, i.e., a less sterically hindered reactive center.¹⁷⁷ The PE-St copolymers formed have a homogeneous (random) copolymer microstructure and high polymer molecular weight. With the effective bromination reaction, we expect that it will form the corresponding random PE-BrSt copolymer structure.

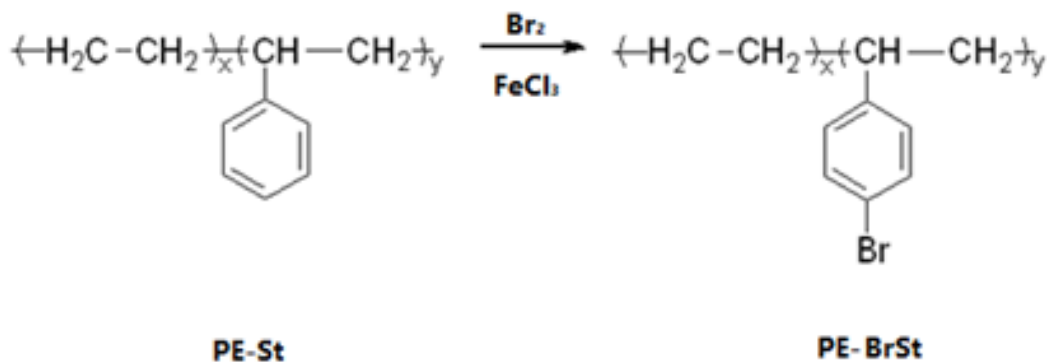


Figure 6.2 Synthetic equation of PE-BrSt copolymer via bromination of PE-St copolymer.

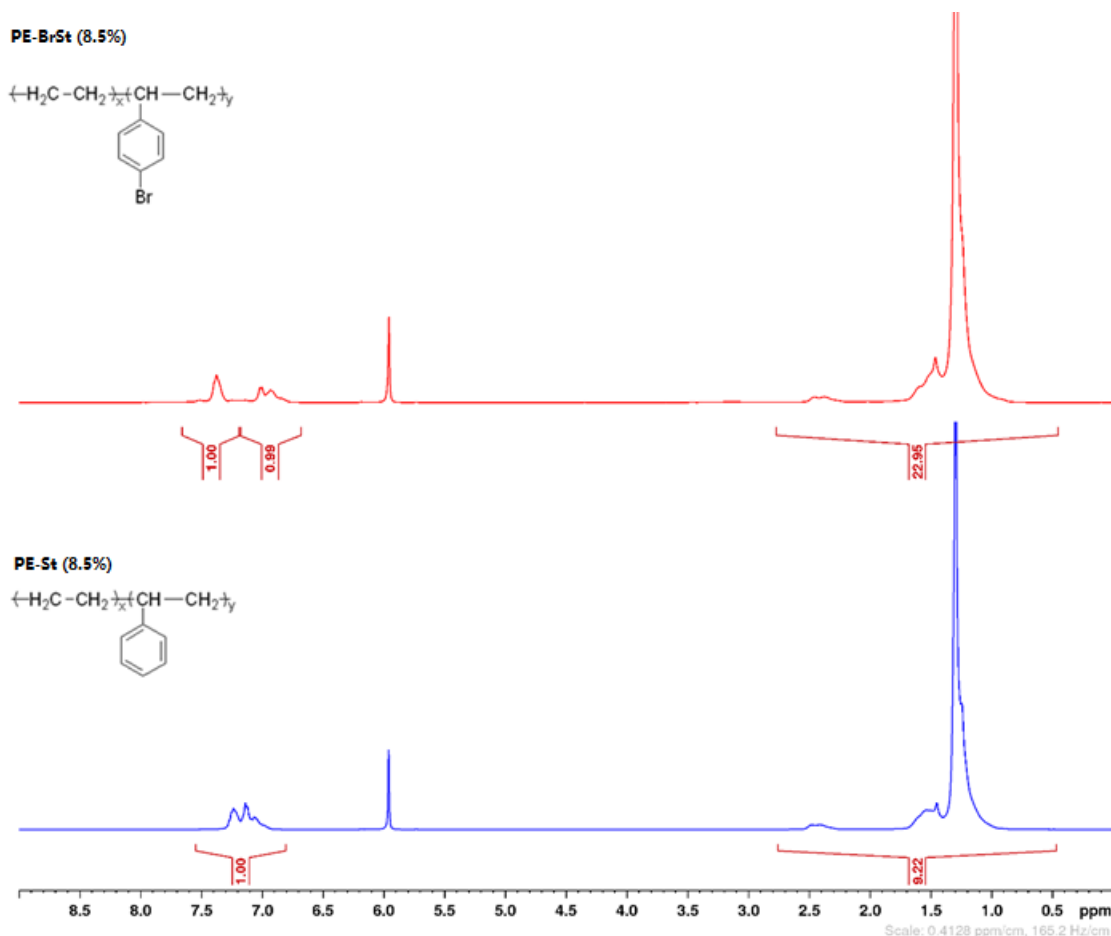


Figure 6.3 ^1H NMR spectrums of (bottom) PE-St copolymer and (top) brominated PE-St with 8.5% comonomer content.

Figure 6.3 compares the ^1H NMR spectra of a starting PE-St copolymer and the resulting PE-BrSt copolymer after bromination. Both samples show a major peak centered at $\sim 1.3\text{ppm}$, corresponding to the aliphatic protons of PE not shielded by the presence of side groups. The small broad peak centered at $\sim 2.4\text{ppm}$ and the shoulder at about 1.5ppm correspond to the methine protons attached to the side groups and the methylene protons near them, respectively. The major difference between these two spectra is the conversion from a broad multi-let peak centered at $\sim 7.2\text{ ppm}$ before bromination into two peaks with identical intensity afterward; this indicates the incorporation of $-\text{Br}$ groups at the para-position of the benzene ring. By calculating the intensity values for these two spectra, we were able to obtain the comonomer percentage of 8.5 mol% on both two copolymers. The identical comonomer percentages indicate the successful

synthesis of PE-BrSt (8.5%) via bromination with a full conversion from styrene groups to 4-bromostyrene groups. The peaks' pattern on the ^1H NMR spectrum of PE-BrSt (8.5%) shows no obvious difference from the one of PE-BrSt (8.4%) prepared by direct copolymerization, which was shown and discussed in Chapter 5.

6.3.2 Comparison of PE-BrSt Copolymers Prepared by Direct and Post Polymerization Processes

Figure 6.4 compares the ^{13}C NMR spectra (aliphatic region) of PE-BrSt copolymers prepared by two different methods with similar 4-bromostyrene comonomer content (8.4mol% for direct copolymerization and 8.5mol% for post-polymerization bromination). A quantitative analysis was performed using inverse-gated decoupling mode and long relaxation delay to minimize the nuclear Overhauser effects and longitudinal relaxation times. Using the reported ^{13}C NMR of PE-St copolymer as a reference to assign the chemical shift to the structure (Figure 6.5),¹⁷⁹ the intense signals in the range of 44.5-45.5ppm correspond to the tertiary and secondary carbons in the 4-bromostyrene sequences (-SSS-), while the ones in the range of 28.8-30.0 ppm are the secondary carbons in the ethylene sequences (-EEE-). The addition peaks centered at 36.4ppm and 27.0ppm result from carbons that are located within a non-consecutive sequence. By comparing the relative intensity ratio between -SSS- and -EEE-, we found that the PE-BrSt (8.4%) copolymer prepared by a direct process has more consecutive 4-bromostyrene units than PE-BrSt (8.5%) copolymer prepared by a post-polymerization process. The direct copolymerization of ethylene and 4-bromostyrene generates a copolymer with a less random microstructure than the ethylene-styrene copolymer prepared by using the DOW CGC catalyst system.

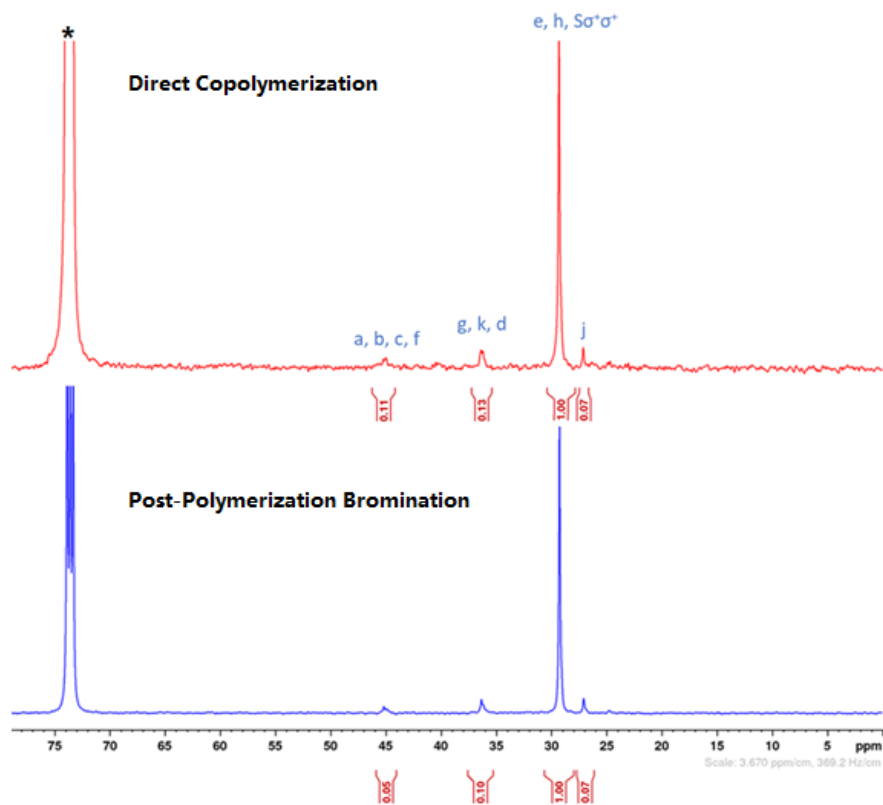


Figure 6.4 Aliphatic region of ^{13}C NMR spectra of PE-BrSt copolymers with (top) 8.4mol% comonomer by direct copolymerization and (bottom) 8.5% comonomer by post-polymerization bromination.

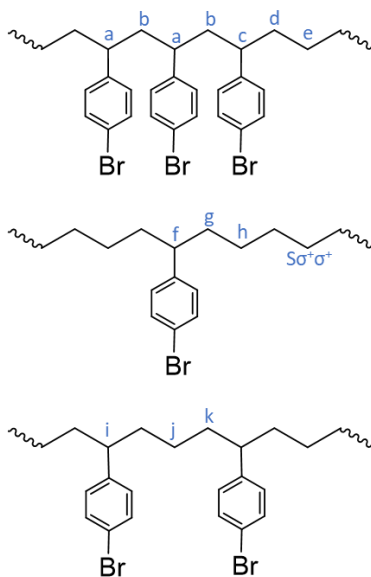


Figure 6.5 Chemical shift assignments of the poly(ethylene-4-bromostyrene) copolymers with different microstructure arrangements.

The melting temperature (T_m) of a PE-copolymer is highly sensitive to its microstructure since the consecutive PE units govern the lamellae thickness.¹⁸⁰ The PE copolymer with a tapered or block structure contains long ethylene sequences; thus the comonomer percentage has a small reduction effect on its T_m . In contrast, the PE copolymer with a random structure where pendant side groups are randomly distributed along the polymer backbones has only short ethylene sequences, so its T_m should be lower than one with the same comonomer percentage but a tapered/block structure. Figure 6.6 compares the DSC curves of the same pair of two PE-BrSt copolymers, prepared by a post-polymerization bromination method and a direct copolymerization method, under a nitrogen atmosphere with a rate of 10°C/min. Both samples were pre-heated to 200°C at the same heating-cooling rate to remove their thermal history. Based on the DSC curves, with almost the same comonomer percentage, PE-BrSt (8.4%) prepared by direct process shows a sharp endothermic melting peak centered at about 118°C, while PE-BrSt (8.5%) prepared by post process has a broader melting peak centered at about 103°C. This suggests that the crystallinity of the PE-BrSt copolymer prepared by the CGC catalyst system is governed by the type of comonomer with which the ethylene copolymerized. The copolymerization of ethylene and styrene generates a more random microstructure with shorter and less consecutive PE units compared to that of ethylene/4-bromostyrene copolymerization, which is consistent with the finding on the ¹³C NMR spectra.

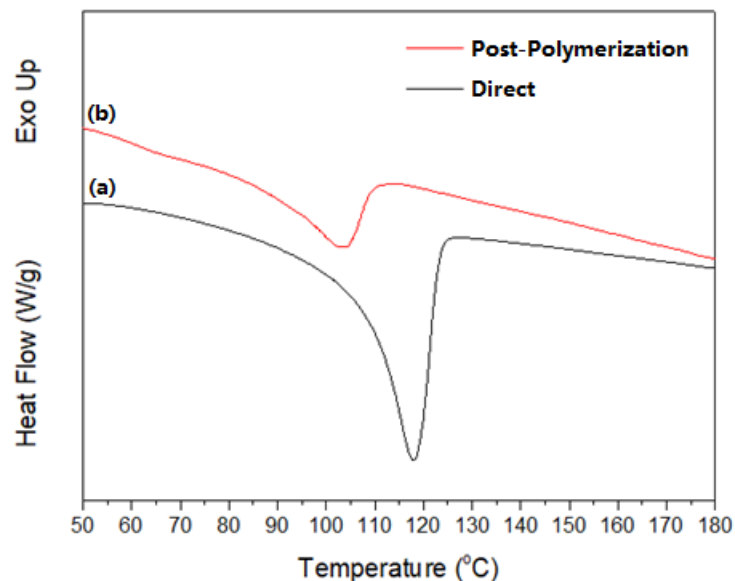


Figure 6.6 DSC comparison of (a) PE-BrSt (8.4%) copolymer by direct-copolymerization and (b) PE-BrSt (8.5%) copolymer by post-polymerization bromination in N₂ atmosphere with a heating rate of 10°C/min.

6.3.3 Preparation of PE-g-Pitch Precursor from the PE-BrSt Copolymers Prepared by Post Polymerization Process

Next, following the thermal-induced cycloaddition reaction described in Chapter 5, the resulting random PE-BrSt copolymer was used to prepare PE-g-Pitch precursor by reactive blending with pitch 250M(S) under elevated temperature (Table 6.1), and then removing all of the unreacted pitch molecules.

Table 6.1 Preparation conditions of PE-g-Pitch samples.

Run	Sample	BrSt content in PE copolymer (mol %) ^a	Polymer/Pitch Weight Ratio	Mixing Temp/Time (°C/hr)
1	PE-g-Pitch(8.5%)-1	8.5	1/10	310/1
2	PE-g-Pitch(8.5%)-2	8.5	1/10	250/1
3	PE-g-Pitch(8.5%)-3	8.5	1/10	250/0.5

^a The content of 4-bromophenyl side groups was determined by ¹H NMR.

As observed in Chapter 5, the PAH molecules in pitch are more likely to react with 4-bromophenyl side groups not in a consecutive sequence of repeat units. Therefore, we expect that the PE-g-Pitch precursor prepared from the random PE-BrSt copolymer would have more incorporated pitch content than the PE-BrSt copolymer prepared by the direct copolymerization process. To test this, we studied PE-g-Pitch samples prepared by blending random PE-BrSt (8.5%) copolymer and pitch 250M(S) at different temperatures and times, and examined the effect of the more random microstructure of the PE-BrSt copolymer on the carbon yield, spinnability, and graphitizability of the resulting PE-g-Pitch precursors.

Figure 6.7 shows ^1H NMR spectra of two resulting PE-g-Pitch precursor samples prepared by using two different blending conditions (Runs 1 and 3 in Table 6.1). The peak patterns on these spectra include the aromatic region from 6.5-10 ppm and the aliphatic region from 1.2-1.7ppm, corresponding to the protons in the PAH side groups and PE backbone, respectively. Additionally, two distinct small peaks were found in the aromatic region, indicating the presence of some unreacted 4-bromostyrene. These patterns are very similar to the ones on ^1H NMR spectra, as shown in the previous chapter.

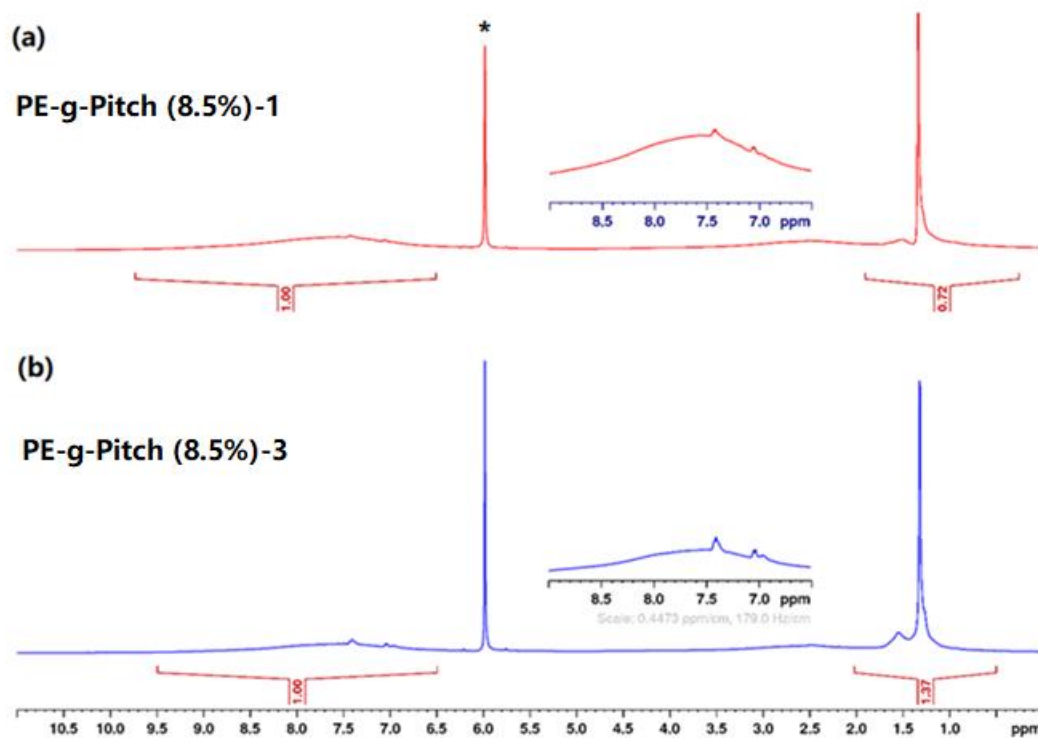


Figure 6.7 ^1H NMR of PE-g-Pitch samples prepared with different reaction temperatures and time of (a) 310°C, 1hr and (b) 250°C, 30min.

Table 6.2 The comparisons of experimental results of PE-g-Pitch samples preparation with different reaction temperatures and times.

Sample	¹ H NMR $I_{(Ali)}/I_{(Aro)}$	^b PE-BrSt Comp (wt.%)	^c Carbon Yield (%)	Spinnability
	^a BrSt Deducted			^d 10wt.%
PE-g-Pitch(8.5%)-1	0.72	2.9	70.1	N
	0.74			
PE-g-Pitch(8.5%)-2	0.83	4.0	68.2	N
	0.86			
PE-g-Pitch(8.5%)-3	1.37	9.3	58.6	Y
	1.46			

^aThe intensity ratio of $I_{(ali)}$ and $I_{(aro)}$ after deduction of peak intensity of two aromatic protons on BrSt. ^bWeight percentage of PE-BrSt copolymer is determined by the intensity ratio after deduction and the calibration curve.

^cSamples were heated to 900°C in N₂ at a rate of 10°C/min. ^dSolution concentration is determined by the weight of solute over the weight of solution.

Table 6.2 summarizes the experimental results for three PE-g-Pitch samples, including the peak intensity ratio between the saturated aliphatic region and unsaturated aromatic region $I_{(al)}/I_{(aro)}$ on ¹H NMR spectra, the weight composition of the PE-BrSt portion, the carbon yield at 900°C in N₂, and the spinnability of PE-g-Pitch/TCB solutions with 10wt.% polymer solution. One observation is that the content of aromatic protons increases with the blending time; this is consistent with the finding on PE-g-Pitch prepared from PE-BrSt copolymer by direct copolymerization in Chapter 5. As described in that chapter, we previously found that the carbon yield of PE-g-Pitch (8.4%) prepared from less random PE-BrSt (8.4%) at 310°C for one hour is only 37.2%. Surprisingly, the PE-g-Pitch made from random PE-BrSt (8.5%) copolymer under the same blending condition exhibits a carbon yield of 70.1%, with a large weight composition of pitch of 97.1%, calculated from the combination of its ¹H NMR spectrum and the calibration curve as shown in Chapter 5. This finding suggests that the PE-BrSt copolymer with a more random microstructure can react with PAH molecules in the pitch at a faster rate; this is attributable to the lower steric hindrance on the non-consecutive 4-bromostyrene repeat units in the copolymer. PE-g-Pitch (8.5%)-3 prepared under 250°C for 30 minutes shows a carbon yield of 58.6%, which is still higher than the conventional PAN precursor.

6.3.4 Solution Spinning of PE-g-Pitch Precursor Fibers

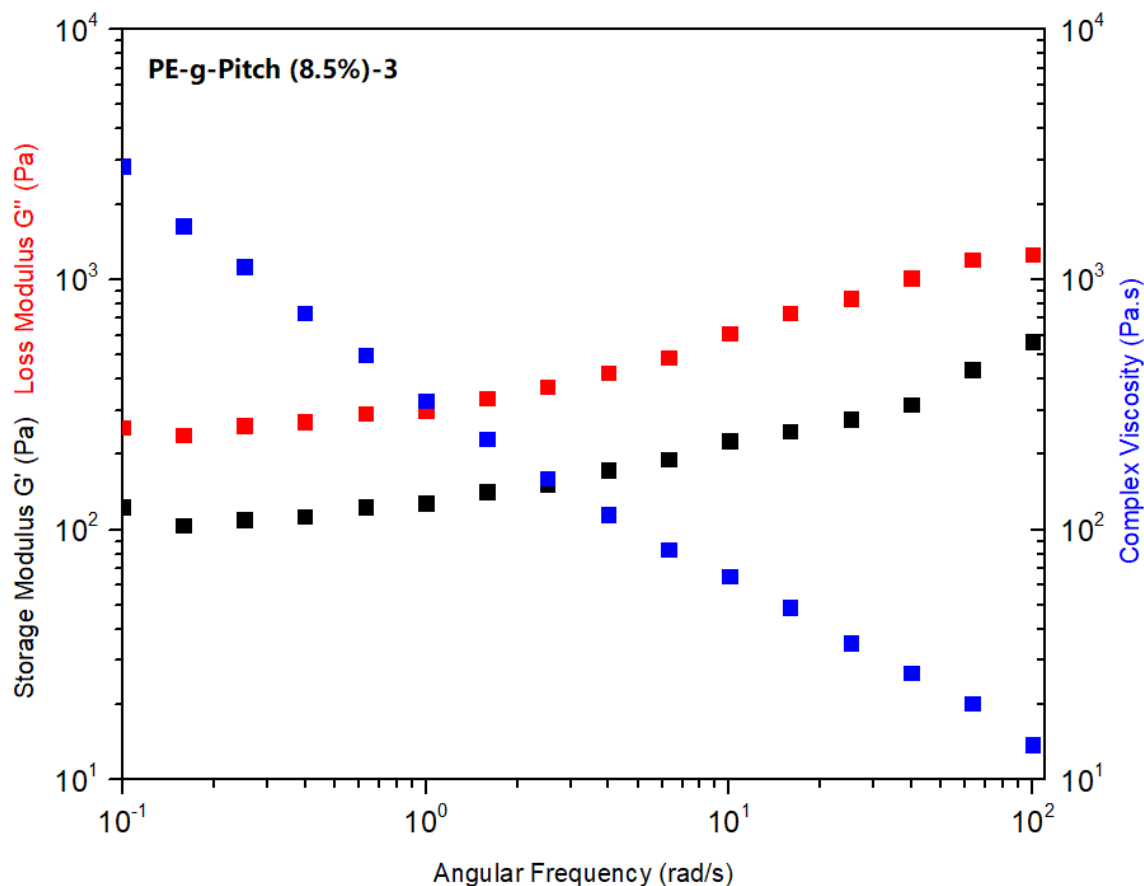


Figure 6.8 Oscillatory rheology (frequency-sweep) of PE-g-Pitch (8.5%)-3 with blending time of 30min at 250°C, in 10wt.% TCB solution at 90°C.

The PE-g-Pitch (8.5%)-1 and 2 were not able to be solution-spun due to the large PAH side groups on the polymer chains, which provide a strong π - π interaction as physical cross-linking. By contrast, PE-g-Pitch (8.5%)-3 shows solution spinnability in TCB with 10wt.% concentration, even though it contains only 9.3wt.% of the PE-BrSt portion. Interestingly, based on the frequency-sweep oscillatory rheology measurement at 90°C as illustrated in Figure 6.8, the solution exhibited liquid-like behavior in the angular frequency range of measurement, indicating no formation of a physical cross-linked network structure. Based on the ^1H NMR result, PE-g-Pitch (8.5%)-3 is mostly comprised of PAH side groups. However, with only a blending time of

30 minutes and a low blending temperature of 250°C, these PAH side groups did not grow to a size that is large enough to generate strong π - π interaction. Therefore, the interaction between the polymer chains can be overcome by the thermal energy at 90°C in the solution. PE-g-Pitch-3 was successfully converted into the fiber with a diameter of about 60 μ m as shown in Figure.6.9 by spinning a 10wt.% TCB solution at 90°C. No sign of porous structure and phase separation was found on either the fiber surface or the cross-section. However, because of the smaller degree of crystallinity and much higher PAH weight percentage, the precursor fibers derived from PE-g-Pitch-(8.5%)-3 had much weaker mechanical strength than the solution-spinnable PE-g-Pitch sample in Chapter 5, and thus could not be stretched in the coagulation bath. Therefore, the fibers had a non-circular cross-section.

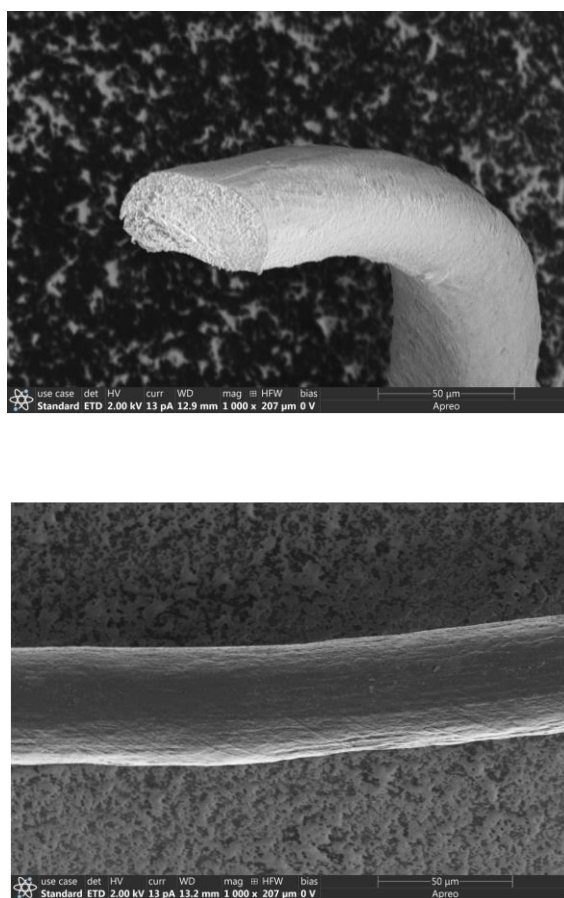


Figure 6.9 SEM images of as-spun fiber of PE-g-Pitch (8.5%)-3 on (top) cross-section and (bottom) fiber surface.

6.3.5 Carbon Fibers Prepared from PE-g-Pitch Precursors

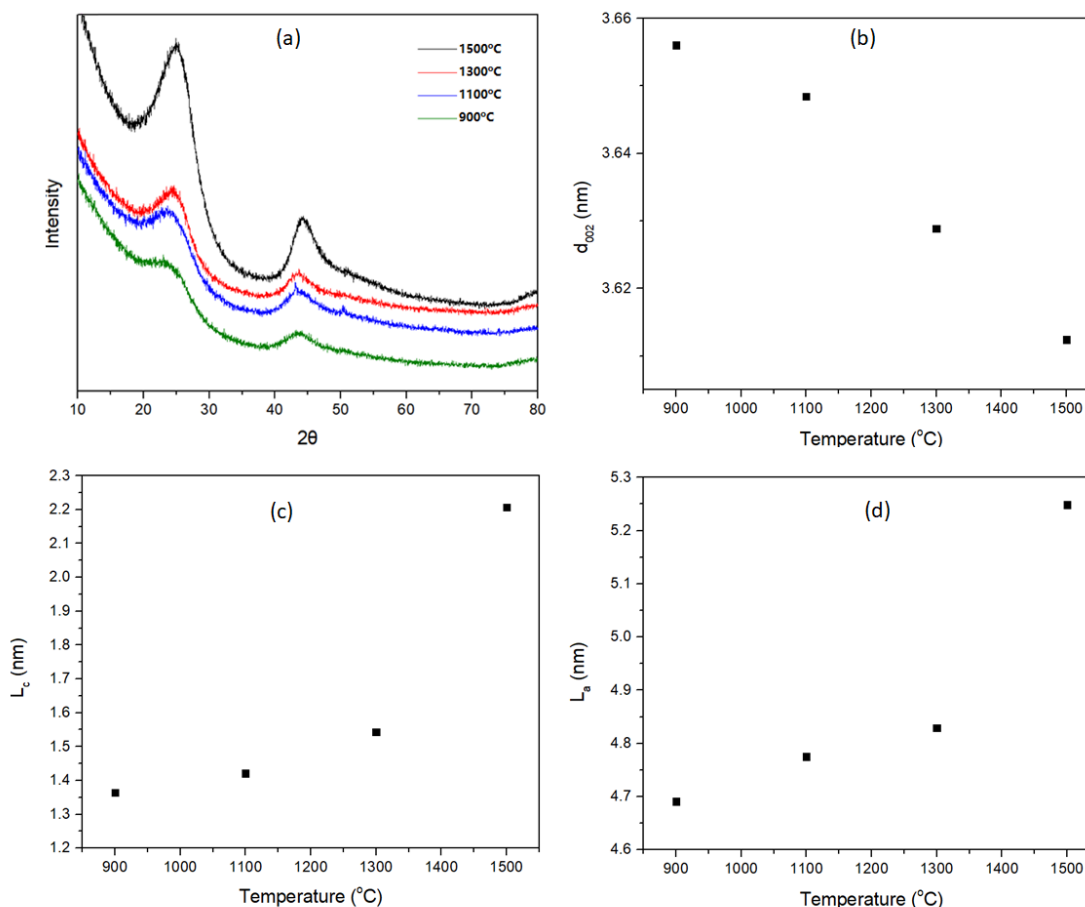


Figure 6.10 Comparisons of (a) XRD spectra and calculated (b) d_{002} , (c) L_c , and (d) L_a of carbonized PE-g-Pitch (8.5%)-3 at temperatures of 900°C, 1100°C, 1300°C and 1500°C.

PE-g-Pitch (8.5%)-3 precursor fibers were stabilized in air at 230°C for two hours, then subjected to heat treatment under temperatures from 900° to 1500°C. The bulk structure of carbonized fibers was determined by XRD as shown in Figure 6.10. Based on the XRD spectra as shown in Figure, microcrystals were formed in both temperatures. When the carbonization temperature was increased from 900° to 1500°C, the $d(002)$ value first decreased from 0.3656nm to smaller spacing of 0.3648nm at 1100°C, then decreased to 0.3629nm and 0.3613nm at 1300° and 1500°C, respectively. The L_a and L_c increases with the higher temperature, indicating the growth of carbon microcrystals within the fibers to generate a more graphitic structure.

6.4 Conclusion

The major objective of research in this chapter is using PE-BrSt copolymer and petroleum pitch to prepare a PE-g-Pitch precursor that can simultaneously offer good fiber spinnability and high carbon yield in forming CFs. To achieve this goal, we applied an alternative method for synthesizing PE-BrSt copolymer, by first copolymerizing ethylene and styrene, then conducting a post-polymerization bromination on the resulting copolymer. We found that this copolymer has a more random microstructure than the one synthesized by the direct ethylene/4-bromostyrene copolymerization. The more random structure allowed the copolymer to react with petroleum pitch at a higher rate. The solution-spinnable PE-g-Pitch made from this copolymer exhibited a high carbon yield of about 59% with a blending temperature of 250°C and blending time of 30 minutes, and was successfully converted to precursor fibers via solution-spinning. XRD results indicate the formation of a polymorphous carbon structure and carbon crystallites within the stabilized precursor fibers at a temperature higher than 900°C, and the crystal size continually grows with the higher carbonization temperature.

Chapter 7

Summary and Future Research Directions

7.1 Summary and Conclusions

It is both scientifically challenging and technologically important to develop a new method for preparing low-cost and high-strength carbon fibers. Current PAN-based carbon fibers are too expensive for general applications, because of a combination of high precursor cost, an expensive fiber-spinning process, long and complicate thermal conversion reactions, and low carbon yield.

The research in this thesis has demonstrated strategies to prepare a novel carbon-fiber (CF) precursor, called 'PE-g-Pitch', with linear polyethylene (PE) backbones and polycyclic aromatic hydrocarbons (PAH) side groups. This PE-g-Pitch precursor can be prepared via the grafting reactions between petroleum pitch and two types of PE copolymers: one is poly(ethylene-co-4-phenylacetylenyl styrene) (PE-DPA copolymer) with diphenylacetylenyl (DPA) side groups, and the other is poly(ethylene-co-4-bromostyrene) (PE-BrSt copolymer) with 4-bromophenyl side groups. Based on our experimental results, grafting the PAH onto the PE backbone can effectively increase the carbon yield of the resulting material by promoting the dehydrogenation reaction before reaching the decomposition temperature, hence generating a highly π -electron conjugated structure during the stabilization step. Additionally, the PAH side groups in PE-g-Pitch can undergo a polycondensation reaction at a temperature higher than 350°C. This allows the unreacted PAH molecules (if there are any) to continually graft into the polymer side groups, generating a larger PAH structure that is favorable for carbon conversion. This also interconnects the polymer chains and forms a cross-linked network without the involvement of oxygen, thus allowing the precursor fibers to retain their fiber structure during carbonization. We also developed two methods for spinning PE-g-Pitch into precursor fibers: one by melt-spinning the

blend of PE-g-Pitch with the excessive pitch that can act as a plasticizer to control the melt viscosity, the other by solution-spinning using 1,2,4-trichlorobenzene as a solvent. The precursor fibers formed by these two spinning methods were both graphitizable with structural order improved at a temperature higher than 900°C in a noble gas environment. Overall, the discovery of a PE-g-Pitch graft copolymer provides a comprehensive strategy for preparing CFs from functionalized polyethylene and petroleum pitch with lower cost and less energy consumption.

7.2 A New Precursor System Based on Poly(phenylacetylene) Derivatives

At an early stage of this research, a series of poly(phenylacetylene) derivatives were synthesized and studied, to investigate the relationship between the polymer's structure and its ability to convert to the carbon material. We compared the carbon yields of two types of polymers, both containing conjugated polymer backbones—12% for poly(PA) with phenyl side groups and 75% for poly(PA-PA) with DPA side groups. We found that the presence of side groups in the polymer precursor is important for reaching high carbon conversion; these side groups must be able to produce PAH moieties via the cycloaddition and dehydrogenation reactions in order to form a network structure with highly π -electron conjugation during the stabilization step. We also found that poly(PA-PA) is solution-spinnable by dissolving in a common organic solvent such as THF, and is also graphitizable at temperatures higher than 1000°C. Although the synthesis of poly(PA-PA) requires expensive monomers and a long preparation route, thus limiting its mass production, the finding inspired us to design and investigate the PE-g-Pitch precursor in subsequent studies.

7.3 PE-g-Pitch Precursors Prepared by Cycloaddition between Petroleum Pitch and Diphenylacetylenyl Side Group-Contained PE Copolymer

In this study, we successfully prepared PE-g-Pitch precursors via a thermally induced Diels-Alder cycloaddition reaction by blending PE-DPA copolymers with petroleum pitch at a high temperature. We also systematically studied the relationship between preparation conditions and the processibility and thermal-transformation behaviors of a series of PE-g-Pitch/pitch blend samples with different comonomer percentages, blending ratios, and blending temperatures. The presence of the PE-g-Pitch graft copolymer prevents the evaporation of the volatile portion of pitch and stabilizes fully decomposable PE polymer chains. In the oscillatory rheology measurement of several PE-g-Pitch/pitch blends, we found that the mixing ratio had a significant effect on the viscosity and solidification temperature. When mixing PE-DPA copolymer with a greater amount of petroleum pitch, the as-prepared PE-g-Pitch/pitch blend precursor showed higher solidification temperature and lower viscosity, both of which make it more favorable for the melt-spinning process. We also observed that the viscosity of this precursor showed a rapid increase with liquid-like behavior maintained before reaching the solidification point at the temperature of polycondensation between the PAH molecules in petroleum pitch. These results indicate that the molecular weight of the polymer portion increases as a result of the continuous incorporation of ungrafted PAH molecules in pitch into the PAH side groups of the PE-g-Pitch graft copolymer, followed by the formation of a cross-linked network structure from the polycondensation between PAH side groups. By using a piston extruder, we successfully melt-spun the PE-g-Pitch/pitch precursor to fibers that can be wound up using a spin winder at a constant speed. However, the as-spun fibers revealed an uneven striated surface with longitudinal ridges oriented along the filament axis, indicating the occurrence of a cross-linking reaction during the melt-spinning, although the network structure was not formed. Additionally, due to a large quantity of pitch in the precursor material, the formed precursor fibers were very brittle, and thus could be continuously spun for only a short period. The PE-g-Pitch/pitch precursor fibers

proved to be graphitizable at temperatures higher than 900°C. They had a carbon structure with d_{002} and L_c values close to those of PAN-based CFs treated at the same temperature, but with a much higher L_a .

To study the stabilization mechanism of PE-g-Pitch, we obtained the PE-g-Pitch portion from the blend by using toluene-soluble pitch as starting material, which can be completely removed by a Soxhlet extractor after blending. By investigating the change in chemical structure and bulk structure of PE-g-Pitch at different temperatures, we found that the highly π -electron conjugated PAH side groups in PE-g-Pitch promote the formation of double bonds from saturated hydrocarbons along polymer chains via dehydrogenation at temperatures greater than 380°C. The formation of one double bond extends the conjugated system, therefore initiating a dehydrogenation reaction at near positions to achieve thermodynamic-driven stabilization along the polymer chain in the form of alkenes. Additionally, a network structure is formed in PE-g-Pitch at the temperature range of 310-400°C by the condensation reaction between PAH side groups. The collective effect of these two stabilization processes increases the carbon yield of PE-g-Pitch.

7.4 PE-g-Pitch Precursors Prepared by Cycloaddition Reaction between Petroleum Pitch and 4-bromophenyl Side Groups-Contained PE Copolymer

Because the self-reactions between DPA side groups easily generate a premature cross-linked network structure within the precursor, we successfully developed a new preparation route for PE-g-Pitch, by blending petroleum pitch and a PE-BtSt copolymer that is synthesized by direct copolymerization between ethylene and 4-bromostyrene. The grafting of PAH molecules onto the PE backbone was also accomplished by a thermally induced cycloaddition reaction based on our study. The formed PE-g-Pitch can be melt-spun into precursor fibers by blending with excess pitch acting as a plasticizer. Because there is no self-reaction (cross-linking) between

the 4-bromophenyl side groups in the temperature range of precursor preparation, the morphology study showed the as-spun fibers had a porous-free and smooth surface, without any sign of the network formation and phase separation. By partially removing the content of the brittle pitch component, the PE-g-Pitch/pitch blend was able to be melt-spun for more than 30 minutes without a breakage. However, the oscillatory rheology study suggests that the PE-g-Pitch in the blend did not exhibit a rapid cross-linking behavior via the polycondensation between pendant PAH side groups. Therefore, an oxidative stabilization was applied to infusibilize the as-spun fibers. This stabilization process also increased the carbon yield of the blend. The stabilized precursor fibers were carbonized and successfully converted to CFs with mechanical properties suitable for general purposes.

We also extracted the PE-g-Pitch by completely removing the excess unreacted pitch from the blend. It was found the grafting reaction between copolymer and PAH molecules is more likely to happen on the 4-bromophenyl groups not located at a consecutive sequence of repeat units. It was also found the PAH side groups continually grew with longer blending time during the precursor preparation. The enlarged side groups increased the carbon yield of the PE-g-Pitch precursor but meanwhile generated a strong π - π interaction that increases the softening point of this precursor to a value close to the temperature of the polycondensation reaction between PAH side groups. Therefore, without any free pitch as a plasticizer, PE-g-Pitch can be converted into fibers only by solution spinning. The interaction also affects the spinnability of PE-g-Pitch; hence only the precursor with short blending time could be solution-spun into fibers, with a carbon yield of about 37%. The spun fibers exhibited good graphitizability and formed microcrystals starting at 900°C.

To increase the carbon yield of PE-g-Pitch and maintain its spinnability, we applied an alternative method to synthesize PE-BrSt copolymer, by first copolymerizing ethylene and styrene, then conducting a post-polymerized bromination on the resulting copolymer. We found

that the resulting PE-BrSt copolymer has a more random microstructure than the one synthesized by direct copolymerization; this more random microstructure allowed the copolymer to react with petroleum pitch at a higher rate, even at a lower temperature. The solution-spinnable PE-g-Pitch made from this copolymer exhibited a high carbon yield of about 59% and was successfully converted to precursor fibers that are also graphitizable at temperatures above 900°C.

7.5 Future Work

The study provides two preparation routes for PE-g-Pitch precursors by blending petroleum pitch with two different PE-copolymers, with the one with 4-bromophenyl side groups showing more promise based on our experimental results. However, the reaction mechanism between 4-bromophenyl side groups and petroleum pitch was not well-studied. It is possible that by replacing 4-bromophenyl groups with the other type of styrenic functional groups containing stronger electron-withdrawing moieties, the preparation of PE-g-Pitch would be more effective. Additionally, the study shows that the grafting reaction of PAH molecules is less likely to happen on the 4-bromophenyl side groups in a consecutive sequence of repeat units. Although we changed the microstructure of the PE-BrSt copolymer to more random by applying the post-polymerization bromination method, the ^1H NMR spectra of the resulting PE-g-Pitch still show unreacted 4-bromophenyl side groups. These unreacted groups not only reduce the crystallinity of PE-g-Pitch and weaken the mechanical properties of the as-spun fibers, but also incorporate more heteroatoms into the system, reducing the carbon yield of the precursor. Thus, a promising way to improve the precursor is by finding a synthesis route to prepare the PE-BrSt copolymer with a more random microstructure, but with less comonomer percentage, for the preparation of strong PE-g-Pitch precursor fibers with high carbon yield.

In addition to optimizing the chemical composition and microstructure of the starting copolymer, it may also be useful to improve the conditions for fiber-spinning of PE-g-Pitch. For the solution spinning of pure PE-g-Pitch graft copolymer, we have not conducted a systematic study on the effect of the choice of solvent and coagulation bath on the morphology and mechanical properties of the as-spun fibers. Additionally, the temperatures of the solution for spinning and coagulation bath are also very crucial for producing precursor fibers and CFs with good performance. When melt-spinning PE-g-Pitch with some unreacted pitch acting as a plasticizer, the existence of PE backbones within PE-g-Pitch/pitch blend will result in as-spun fibers that are more stretchable than pure pitch material when the heat is applied. Therefore, applying tension on the precursor fibers during stabilization may improve the mechanical performance of the resulting precursor fibers and CFs.

Reference

- (1) Das, T. K.; Ghosh, P.; Das, N. C. Preparation, Development, Outcomes, and Application Versatility of Carbon Fiber-Based Polymer Composites: A Review. *Adv. Compos. Hybrid Mater.* **2019**, *2* (2), 214–233.
- (2) Hu, H.; Liu, Y. High Modulus, High Tenacity Yarns. In *Technical Textile Yarns*; **2010**; pp 329–386.
- (3) Fang, W.; Yang, S.; Wang, X.-L.; Yuan, T.-Q.; Sun, R.-C. Manufacture and Application of Lignin-Based Carbon Fibers (LCFs) and Lignin-Based Carbon Nanofibers (LCNFs). *Green Chem.* **2017**, *19* (8), 1794–1827.
- (4) Chand, S. Carbon Fibers for Composites. *J. Mater. Sci.* **2000**, *35* (6), 1303–1313.
- (5) Minus, M. L.; Kumar, S. The Processing, Properties, and Structure of Carbon Fibers. *Jom.* **2005**, pp 52–58.
- (6) Pompe, W. W. Watt. B. V. Perov (Hrsg.). Strong Fibres Handbook of Composites. Vol. 1. North-Holland Publishing Company, 1985, 752 Seiten, US \$ 115.00/Dfl. 375.00, ISBN 0-444-87505-0. *Cryst. Res. Technol.* **1986**, *21* (10), 1326–1326.
- (7) De-Yi Wang. *Novel Fire Retardant Polymers and Composite Materials*; Woodhead Publishing, **2017**.
- (8) Anwar, M.; Sukmaji, I. C.; Wijang, W. R.; Diharjo, K. Application of Carbon Fiber-Based Composite for Electric Vehicle. In *Advanced Materials Research*; **2014**; Vol. 896, pp 574–577.
- (9) Frank, E.; Hermanutz, F.; Buchmeiser, M. R. Carbon Fibers: Precursors, Manufacturing, and Properties. *Macromolecular Materials and Engineering.* **2012**, *297* (6), pp 493–501.

- (10) Das, S.; Warren, J.; West, D.; Schexnayder, S. M. Global Carbon Fiber Composites Supply Chain Competitiveness Analysis. *Oak Ridge Natl. Lab.* **2016**, No. May, 102.
- (11) Huang, X. Fabrication and Properties of Carbon Fibers. *Materials*. **2009**, 2 (4), pp 2369–2403.
- (12) Chabot, V.; Higgins, D.; Yu, A.; Xiao, X.; Chen, Z.; Zhang, J. A Review of Graphene and Graphene Oxide Sponge: Material Synthesis and Applications to Energy and the Environment. *Energy and Environmental Science*. **2014**, 5, pp 1564–1596.
- (13) Shearer, C. J.; Slattery, A. D.; Stapleton, A. J.; Shapter, J. G.; Gibson, C. T. Accurate Thickness Measurement of Graphene. *Nanotechnology* **2016**, 27 (12).
- (14) Cao, J.; Zhao, W.; Gao, S. Properties and Structure of in Situ Transformed PAN-Based Carbon Fibers. *Materials (Basel)*. **2018**, 11 (6).
- (15) Fox, B. Making Stronger Carbon-Fiber Precursors. *Science*. **2019**, 366 (6471) pp 1314–1315.
- (16) Gupta, A.; Dhakate, S. R.; Pal, P.; Dey, A.; Iyer, P. K.; Singh, D. K. Effect of Graphitization Temperature on Structure and Electrical Conductivity of Poly-Acrylonitrile Based Carbon Fibers. *Diam. Relat. Mater.* **2017**, 78, 31–38.
- (17) Fitzer, E. Pan-Based Carbon Fibers-Present State and Trend of the Technology from the Viewpoint of Possibilities and Limits to Influence and to Control the Fiber Properties by the Process Parameters. *Carbon*. **1989**, 27 (5), 621–645.
- (18) Reynolds, W. N.; Sharp, J. V. Crystal Shear Limit to Carbon Fibre Strength. *Carbon*. **1974**, 12 (2), 103–110.
- (19) Northolt, M. G.; Veldhuizen, L. H.; Jansen, H. Tensile Deformation of Carbon Fibers and the Relationship with the Modulus for Shear between the Basal Planes. *Carbon*. **1991**, 29

- (8), 1267–1279.
- (20) Kelly, A.; Mortensen, A. Composite Materials: Overview. In *Encyclopedia of Materials: Science and Technology*; **2001**; pp 1361–1371.
- (21) Matsumoto, T. Mesophase Pitch and Its Carbon Fibers. *Pure Appl. Chem.* **1985**, *57* (11), 1553–1562.
- (22) Singer, L. S. Carbon Fibres from Mesophase Pitch. *Fuel* **1981**, *60* (9), 839–847.
- (23) Milbrandt, A.; Booth, S. Carbon Fiber from Biomass. *Clean Energy Manuf. Anal. Cent.* **2016**, No. September, 1–27.
- (24) Nunna, S.; Blanchard, P.; Buckmaster, D.; Davis, S.; Naebe, M. Development of a Cost Model for the Production of Carbon Fibres. *Heliyon* **2019**, *5* (10).
- (25) Ellringmann, T.; Wilms, C.; Warnecke, M.; Seide, G.; Gries, T. Carbon Fiber Production Costing: A Modular Approach. *Text. Res. J.* **2016**, *86* (2), 178–190.
- (26) Nunna, S.; Maghe, M.; Fakhrhoseini, S. M.; Polisetti, B.; Naebe, M. A Pathway to Reduce Energy Consumption in the Thermal Stabilization Process of Carbon Fiber Production. *Energies* **2018**, *11* (5).
- (27) Yang, G. Z.; Li, H. P.; Yang, J. H.; Wan, J.; Yu, D. G. Influence of Working Temperature on The Formation of Electrospun Polymer Nanofibers. *Nanoscale Res. Lett.* **2017**, *12* (1).
- (28) Bawn, C. S. H. *Encyclopedia of Polymer Science and Engineering*, 2nd ed.; John Wiley and Sons, **1987**; Vol. 28.
- (29) Callahan, J. L.; Grasselli, R. K.; Milberger, E. C.; Strecker, H. A. Oxidation and Ammoxidation of Propylene over Bismuth Molybdate Catalyst. *Ind. Eng. Chem. Prod. Res. Dev.* **1970**, *9* (2), 134–142.

- (30) Bhat, G. *Structure and Properties of High-Performance Fibers*; Woodhead Publishing, **2016**.
- (31) Zhao, Y. qi; Wang, C. guo; Bai, Y. jun; Chen, G. wen; Jing, M.; Zhu, B. Property Changes of Powdery Polyacrylonitrile Synthesized by Aqueous Suspension Polymerization during Heat-Treatment Process under Air Atmosphere. *J. Colloid Interface Sci.* **2009**, 329 (1), 48–53.
- (32) Masson, J. C. *Acrylic Fiber Technology and Applications*; CRC, Boca Raton, **1995**.
- (33) Frank, E.; Ingildeev, D.; Buchmeiser, M. R. High-Performance PAN-Based Carbon Fibers and Their Performance Requirements. In *Structure and Properties of High-Performance Fibers*; 2017; pp 7–30.
- (34) Frank, E.; Steudle, L. M.; Ingildeev, D.; Spörl, J. M.; Buchmeiser, M. R. Carbon Fibers: Precursor Systems, Processing, Structure, and Properties. *Angewandte Chemie - International Edition.* 2014, 53, pp 5262–5298.
- (35) Bajaj, P.; Sreekumar, T. V.; Sen, K. Thermal Behaviour of Acrylonitrile Copolymers Having Methacrylic and Itaconic Acid Comonomers. *Polymer (Guildf).* **2001**, 42 (4), 1707–1718.
- (36) Ju, A.; Guang, S.; Xu, H. Effect of Comonomer Structure on the Stabilization and Spinnability of Polyacrylonitrile Copolymers. *Carbon.* **2013**, 54, 323–335.
- (37) Masahiri, T.; Takeji, O.; Takashi, F. Preparation of Acrylonitrile Precursor for Carbon Fiber. U.S. Patent, 59204914, **1984**.
- (38) Knudsen, J. P. The Influence of Coagulation Variables on the Structure and Physical Properties of an Acrylic Fiber. *Text. Res. J.* **1963**, 33 (1), 13–20.
- (39) Moreton, R.; Watt, W. The Spinning of Polyacrylonitrile Fibres in Clean Room

- Conditions for the Production of Carbon Fibres. *Carbon*. **1974**, *12* (5), 543–554.
- (40) Liu, S.; Tan, L.; Pan, D.; Chen, Y. Gel Spinning of Polyacrylonitrile Fibers with Medium Molecular Weight. *Polym. Int.* **2011**, *60* (3), 453–457.
- (41) Newcomb, B. A. Processing, Structure, and Properties of Carbon Fibers. *Compos. Part A Appl. Sci. Manuf.* **2016**, *91*, 262–282.
- (42) Chae, H. G.; Newcomb, B. A.; Gulgunje, P. V.; Liu, Y.; Gupta, K. K.; Kamath, M. G.; Lyons, K. M.; Ghoshal, S.; Pramanik, C.; Giannuzzi, L.; Şahin, K.; Chasiotis, I.; Kumar, S. High Strength and High Modulus Carbon Fibers. *Carbon*. **2015**, *93*, 81–87.
- (43) Tan, L.; Chen, H.; Pan, D.; Pan, N. Investigating the Spinnability in the Dry-Jet Wet Spinning of PAN Precursor Fiber. *J. Appl. Polym. Sci.* **2008**, *110* (4), 1997–2000.
- (44) Chang, H.; Chien, A. T.; Liu, H. C.; Wang, P. H.; Newcomb, B. A.; Kumar, S. Gel Spinning of Polyacrylonitrile/Cellulose Nanocrystal Composite Fibers. *ACS Biomater. Sci. Eng.* **2015**, *1* (7), 610–616.
- (45) Watt, W.; Johnson, W. Mechanism of Oxidisation of Polyacrylonitrile Fibres. *Nature* **1975**, *257* (5523), 210–212.
- (46) Park, O. K.; Lee, S.; Joh, H. I.; Kim, J. K.; Kang, P. H.; Lee, J. H.; Ku, B. C. Effect of Functional Groups of Carbon Nanotubes on the Cyclization Mechanism of Polyacrylonitrile (PAN). *Polymer (Guildf)*. **2012**, *53* (11), 2168–2174.
- (47) Kim, J.; Kim, Y. C.; Ahn, W.; Kim, C. Y. Reaction Mechanisms of Polyacrylonitrile on Thermal Treatment. *Polym. Eng. Sci.* **1993**, *33* (22), 1452–1457.
- (48) Bashir, Z. A Critical Review of the Stabilisation of Polyacrylonitrile. *Carbon*. **1991**, *29* (8), 1081–1090.

- (49) Suresh, K. I.; Thomas, K. S.; Rao, B. S.; Reghunadhan Nair, C. P. Viscoelastic Properties of Polyacrylonitrile Terpolymers during Thermo-Oxidative Stabilization (Cyclization). *Polym. Adv. Technol.* **2008**, *19* (7), 831–837.
- (50) Bajaj, P.; Sreekumar, T. V.; Sen, K. Structure Development during Dry-Jet-Wet Spinning of Acrylonitrile/Vinyl Acids and Acrylonitrile/Methyl Acrylate Copolymers. *J. Appl. Polym. Sci.* **2002**, *86* (3), 773–787.
- (51) Bahrami, S. H.; Bajaj, P.; Sen, K. Effect of Coagulation Conditions on Properties of Poly(Acrylonitrile-Carboxylic Acid) Fibers. *J. Appl. Polym. Sci.* **2003**, *89* (7), 1825–1837.
- (52) Rahaman, M. S. A.; Ismail, A. F.; Mustafa, A. A Review of Heat Treatment on Polyacrylonitrile Fiber. *Polymer Degradation and Stability.* **2007**, pp 1421–1432.
- (53) Seydibeyoğlu, M. Ö.; Mohanty, A. K.; Misra, M. *Fiber Technology for Fiber-Reinforced Composites*; Woodhead Publishing, **2017**.
- (54) Wang, H.; Wang, Y.; Li, T.; Wu, S.; Xu, L. Gradient Distribution of Radial Structure of PAN-Based Carbon Fiber Treated by High Temperature. *Prog. Nat. Sci. Mater. Int.* **2014**, *24* (1), 31–34.
- (55) Gupta, A.; Harrison, I. R. New Aspects in the Oxidative Stabilization of Pan-Based Carbon Fibers: II. *Carbon.* **1997**, *35* (6), 809–818.
- (56) Wu, G.; Lu, C.; Ling, L.; Hao, A.; He, F. Influence of Tension on the Oxidative Stabilization Process of Polyacrylonitrile Fibers. *J. Appl. Polym. Sci.* **2005**, *96* (4), 1029–1034.
- (57) Chen, J. C.; Harrison, I. R. Modification of Polyacrylonitrile (PAN) Carbon Fiber Precursor via Post-Spinning Plasticization and Stretching in Dimethyl Formamide (DMF). *Carbon.* **2002**, *40* (1), 25–45.

- (58) de Lamotte, E.; Perry, A. J. Diameter and Strain-Rate Dependence of the Ultimate Tensile Strength and Young's Modulus of Carbon Fibres. *Fibre Sci. Technol.* **1970**, 3 (2), 157–166.
- (59) Tsai, J. S. Effect of Nitrogen Atmosphere on the Structure and Properties of a PAN-Based Carbon Fiber. *Text. Res. J.* **1994**, 64 (12), 772–774.
- (60) Wangxi, Z.; Jie, L.; Gang, W. Evolution of Structure and Properties of PAN Precursors during Their Conversion to Carbon Fibers. In *Carbon*; **2003**; Vol. 41, pp 2805–2812.
- (61) O'neil, D. J. Precursors for Carbon and Graphite Fibers. *Int. J. Polym. Mater. Polym. Biomater.* **1979**, 7 (3–4), 203–218.
- (62) Liu, Y.; Kumar, S. Recent Progress in Fabrication, Structure, and Properties of Carbon Fibers. *Polymer Reviews.* **2012**, pp 234–258.
- (63) Zander, M.; Collin, G. A Review of the Significance of Polycyclic Aromatic Chemistry for Pitch Science. *Fuel.* **1993**, pp 1281–1285.
- (64) Ziabicki, A. *Fundamentals of Fibre Formation: The Science of Fibre Spinning and Drawing*; Wiley, **1976**.
- (65) IARC Working Group on the Evaluation of Carcinogenic Risks to Humans. Chemical Agents and Related Occupations. *IARC monographs on the evaluation of carcinogenic risks to humans / World Health Organization, International Agency for Research on Cancer.* **2012**, pp 9–562.
- (66) Petrovykha, A. P.; Abaturov, A. L.; Moskalev, I. V.; Kiselkov, D. M.; Astaf'eva, S. A.; Vinokurov, A. I. High-Temperature Synthesis of Pitch. *Coke Chem.* **2017**, 60 (2), 75–79.
- (67) Kim, B. J.; Kotegawa, T.; Eom, Y.; An, J.; Hong, I. P.; Kato, O.; Nakabayashi, K.; Miyawaki, J.; Kim, B. C.; Mochida, I.; Yoon, S. H. Enhancing the Tensile Strength of

- Isotropic Pitch-Based Carbon Fibers by Improving the Stabilization and Carbonization Properties of Precursor Pitch. *Carbon*. **2016**, *99*, 649–657.
- (68) Marsh, H.; Rodríguez-Reinoso, F. Characterization of Activated Carbon. In *Activated Carbon*; **2006**; pp 143–242.
- (69) Mochida, I.; Shimizu, K.; Korai, Y.; Sakai, Y.; Fujiyama, S.; Toshima, H.; Hono, T. Mesophase Pitch Catalytically Prepared from Anthracene with HF/BF₃. *Carbon*. **1992**, *30* (1), 55–61.
- (70) Edie, D. D.; Dunham, M. G. Melt Spinning Pitch-Based Carbon Fibers. *Carbon*. **1989**, *27* (5), 647–655.
- (71) Otani, S.; Oya, A. Progress of Pitch-Based Carbon Fiber in Japan. In *ACS Symposium Series*; **1986**; pp 323–334.
- (72) Chung, D. D. L. Introduction to Carbon Composites. In *Carbon Composites*; **2017**; pp 88–160.
- (73) Mochida, I.; Yoon, S. H.; Takano, N.; Fortin, F.; Korai, Y.; Yokogawa, K. Microstructure of Mesophase Pitch-Based Carbon Fiber and Its Control. *Carbon*. **1996**, *34* (8), 941–956.
- (74) Buckley, J. D.; Edie, D. D. *Carbon-Carbon Materials and Composites*; William Andrew, **1993**.
- (75) Yuan, G.; Li, X.; Xiong, X.; Dong, Z.; Westwood, A.; Li, B.; Ye, C.; Ma, G.; Cui, Z.; Cong, Y.; Zhang, J.; Li, Y. A Comprehensive Study on the Oxidative Stabilization of Mesophase Pitch-Based Tape-Shaped Thick Fibers with Oxygen. *Carbon*. **2017**, *115*, 59–76.
- (76) Cheng, Y.; Fang, C.; Su, J.; Yu, R.; Li, T. Carbonization Behavior and Mesophase Conversion Kinetics of Coal Tar Pitch Using a Low Temperature Molten Salt Method. *J.*

Anal. Appl. Pyrolysis **2014**, *109*, 90–97.

- (77) Lim, T. H.; Yeo, S. Y. Investigation of the Degradation of Pitch-Based Carbon Fibers Properties upon Insufficient or Excess Thermal Treatment. *Sci. Rep.* **2017**, *7* (1).
- (78) Sun, S.; Sun, S.; Cao, X.; Sun, R. The Role of Pretreatment in Improving the Enzymatic Hydrolysis of Lignocellulosic Materials. *Bioresource Technology*. **2016**, pp 49–58.
- (79) C.E. Ford, C. V. M. Fibrous Graphite. U.S. Patent, 3107152, **1963**.
- (80) J.Chen. *Textiles and Fashion*; Woodhead Publishing, **2016**, pp 79-95.
- (81) Bengtsson, A.; Bengtsson, J.; Sedin, M.; Sjöholm, E. Carbon Fibers from Lignin-Cellulose Precursors: Effect of Stabilization Conditions. *ACS Sustain. Chem. Eng.* **2019**, *7* (9), 8440–8448.
- (82) Tang, M. M.; Bacon, R. Carbonization of Cellulose Fibers-I. Low Temperature Pyrolysis. *Carbon*. **1964**, *2* (3), 211–214.
- (83) Rangarajan, P.; Yang, J.; Bhanu, V.; Godshall, D.; McGrath, J.; Wilkes, G.; Baird, D. Effect of Comonomers on Melt Processability of Polyacrylonitrile. *J. Appl. Polym. Sci.* **2002**, *85* (1), 69–83.
- (84) Naskar, A. K.; Walker, R. A.; Proulx, S.; Edie, D. D.; Ogale, A. A. UV Assisted Stabilization Routes for Carbon Fiber Precursors Produced from Melt-Processible Polyacrylonitrile Terpolymer. *Carbon*. **2005**, *43* (5), 1065–1072.
- (85) Mukundan, T.; Bhanu, V. A.; Wiles, K. B.; Johnson, H.; Bortner, M.; Baird, D. G.; Naskar, A. K.; Ogale, A. A.; Edie, D. D.; McGrath, J. E. A Photocrosslinkable Melt Processible Acrylonitrile Terpolymer as Carbon Fiber Precursor. *Polymer (Guildf)*. **2006**, *47* (11), 4163–4171.

- (86) Deng, W.; Lobovsky, A.; Iacono, S. T.; Wu, T.; Tomar, N.; Budy, S. M.; Long, T.; Hoffman, W. P.; Smith, D. W. Poly (Acrylonitrile-Co-1-Vinylimidazole): A New Melt Processable Carbon Fiber Precursor. *Polymer (Guildf)*. **2011**, *52* (3), 622–628.
- (87) Mahmood, S. F.; Batchelor, B. L.; Jung, M.; Park, K.; Voit, W. E.; Novak, B. M.; Yang, D. Study of a Melt Processable Polymer Precursor for Carbon Fiber. *Carbon Lett*. **2019**, *29* (6), 605–612.
- (88) Kim, S.; Park, J.; Lee, J.; Roh, H. gyoo; Jeong, D.; Choi, S.; Oh, S. Potential of a Bio-Disintegrable Polymer Blend Using Alkyl-Chain-Modified Lignin. *Fibers Polym*. **2015**, *16* (4), 744–751.
- (89) Gordobil, O.; Egüés, I.; Llano-Ponte, R.; Labidi, J. Physicochemical Properties of PLA Lignin Blends. *Polym. Degrad. Stab*. **2014**, *108*, 330–338.
- (90) Thunga, M.; Chen, K.; Grewell, D.; Kessler, M. R. Bio-Renewable Precursor Fibers from Lignin/Poly lactide Blends for Conversion to Carbon Fibers. *Carbon*. **2014**, *68*, 159–166.
- (91) Kadla, J. F.; Kubo, S.; Venditti, R. A.; Gilbert, R. D.; Compere, A. L.; Griffith, W. Lignin-Based Carbon Fibers for Composite Fiber Applications. *Carbon*. **2002**, *40* (15), 2913–2920.
- (92) Kubo, S.; Kadla, J. F. Lignin-Based Carbon Fibers: Effect of Synthetic Polymer Blending on Fiber Properties. *J. Polym. Environ*. **2005**, *13* (2), 97–105.
- (93) Chaudhari, A.; Ekhe, J. D.; Deo, S. Non-Isothermal Crystallization Behavior of Lignin-Filled Polyethylene Terephthalate (PET). *Int. J. Polym. Anal. Charact*. **2006**, *11* (3), 197–207.
- (94) Ding, R.; Wu, H.; Thunga, M.; Bowler, N.; Kessler, M. R. Processing and Characterization of Low-Cost Electrospun Carbon Fibers from Organosolv

- Lignin/Polyacrylonitrile Blends. *Carbon*. **2016**, *100* (October 2017), 126–136.
- (95) Liu, H. C.; Chien, A. T.; Newcomb, B. A.; Bakhtiary Davijani, A. A.; Kumar, S. Stabilization Kinetics of Gel Spun Polyacrylonitrile/Lignin Blend Fiber. *Carbon*. **2016**, *101*, 382–389.
- (96) Culebras, M.; Beaucamp, A.; Wang, Y.; Clauss, M. M.; Frank, E.; Collins, M. N. Biobased Structurally Compatible Polymer Blends Based on Lignin and Thermoplastic Elastomer Polyurethane as Carbon Fiber Precursors. *ACS Sustain. Chem. Eng.* **2018**, *6* (7), 8816–8825.
- (97) Xia, K.; Ouyang, Q.; Chen, Y.; Wang, X.; Qian, X.; Wang, L. Preparation and Characterization of Lignosulfonate-Acrylonitrile Copolymer as a Novel Carbon Fiber Precursor. *ACS Sustain. Chem. Eng.* **2016**, *4* (1), 159–168.
- (98) Grumezescu, A. M. *Surface Chemistry of Nanobiomaterials: Applications of Nanobiomaterials Volume 3*; William Andrew, **2016**.
- (99) Arash, B.; Wang, Q. Detection of Gas Atoms with Carbon Nanotubes. *Sci. Rep.* **2013**, *3*.
- (100) Wang, Q. Atomic Transportation via Carbon Nanotubes. *Nano Lett.* **2009**, *9* (1), 245–249.
- (101) Lau, K. tak; Gu, C.; Hui, D. A Critical Review on Nanotube and Nanotube/Nanoclay Related Polymer Composite Materials. *Compos. Part B Eng.* **2006**, *37* (6), 425–436.
- (102) Minus, M. L.; Chae, H. G.; Kumar, S. Polyethylene Crystallization Nucleated by Carbon Nanotubes under Shear. *ACS Appl. Mater. Interfaces* **2012**, *4* (1), 326–330.
- (103) Bhattacharyya, A. R.; Sreekumar, T. V.; Liu, T.; Kumar, S.; Ericson, L. M.; Hauge, R. H.; Smalley, R. E. Crystallization and Orientation Studies in Polypropylene/Single Wall Carbon Nanotube Composite. *Polymer (Guildf)*. **2003**, *44* (8), 2373–2377.

- (104) Li, C. Y.; Li, L.; Cai, W.; Kodjie, S. L.; Tenneti, K. K. Nanohybrid Shish-Kebabs: Periodically Functionalized Carbon Nanotubes. *Adv. Mater.* **2005**, *17* (9), 1198–1202.
- (105) Anoop Anand, K.; Agarwal, U. S.; Joseph, R. Carbon Nanotubes Induced Crystallization of Poly(Ethylene Terephthalate). *Polymer (Guildf)*. **2006**, *47* (11), 3976–3980.
- (106) Minus, M. L.; Chae, H. G.; Kumar, S. Single Wall Carbon Nanotube Templated Oriented Crystallization of Poly(Vinyl Alcohol). *Polymer (Guildf)*. **2006**, *47* (11), 3705–3710.
- (107) Liu, P. Modifications of Carbon Nanotubes with Polymers. *Eur. Polym. J.* **2005**, *41* (11), 2693–2703.
- (108) Grady, B. P.; Pompeo, F.; Shambaugh, R. L.; Resasco, D. E. Nucleation of Polypropylene Crystallization by Single-Walled Carbon Nanotubes. *J. Phys. Chem. B* **2002**, *106* (23), 5852–5858.
- (109) Yang, Z.; Peng, H.; Wang, W.; Liu, T. Crystallization Behavior of Poly(ϵ -Caprolactone)/Layered Double Hydroxide Nanocomposites. *J. Appl. Polym. Sci.* **2010**, *116* (5), 2658–2667.
- (110) Tang, Z.; Huang, Q.; Liu, Y.; Chen, Y.; Guo, B.; Zhang, L. Uniaxial Stretching-Induced Alignment of Carbon Nanotubes in Cross-Linked Elastomer Enabled by Dynamic Cross-Link Reshuffling. *ACS Macro Lett.* **2019**, *8* (12), 1575–1581.
- (111) Chae, H. G.; Minus, M. L.; Rasheed, A.; Kumar, S. Stabilization and Carbonization of Gel Spun Polyacrylonitrile/Single Wall Carbon Nanotube Composite Fibers. *Polymer (Guildf)*. **2007**, *48* (13), 3781–3789.
- (112) Gao, Z.; Zhu, J.; Rajabpour, S.; Joshi, K.; Kowalik, M.; Croom, B.; Schwab, Y.; Zhang, L.; Bumgardner, C.; Brown, K. R.; Burden, D.; Klett, J. W.; van Duin, A. C. T.; Zhigilei, L. V.; Li, X. Graphene Reinforced Carbon Fibers. *Sci. Adv.* **2020**, *6* (17).

- (113) Salim, N. V.; Jin, X.; Razal, J. M. Polyacrylonitrile/Liquid Crystalline Graphene Oxide Composite Fibers – Towards High Performance Carbon Fiber Precursors. *Compos. Sci. Technol.* **2019**, *182*.
- (114) Kim, H.; Jalili, R.; Spinks, G. M.; Wallace, G. G.; Kim, S. J. High-Strength Graphene and Polyacrylonitrile Composite Fiber Enhanced by Surface Coating with Polydopamine. *Compos. Sci. Technol.* **2017**, *149*, 280–285.
- (115) Newell, J. A.; Edie, D. D. Factors Limiting the Tensile Strength of PBO-Based Carbon Fibers. *Carbon.* **1996**, *34* (5), 551–560.
- (116) Matsuda, T. *Future Directions in Biocatalysis*; Elsevier, **2007**.
- (117) Qiao, W. M.; Yoon, S. H.; Mochida, I.; Yang, J. H. Waste Polyvinylchloride Derived Pitch as a Precursor to Develop Carbon Fibers and Activated Carbon Fibers. *Waste Manag.* **2007**, *27* (12), 1884–1890.
- (118) Li, W.; Chen, Z.; Li, J.; Chen, X.; Xuan, H.; Wang, X. Preparation of PAN/Phenolic-Based Carbon/Carbon Composites with Flexible Towpreg Carbon Fiber. *Mater. Sci. Eng. A* **2008**, *485* (1–2), 481–486.
- (119) Fatema, U. K.; Uddin, A. J.; Uemura, K.; Gotoh, Y. Fabrication of Carbon Fibers from Electrospun Poly(Vinyl Alcohol) Nanofibers. *Text. Res. J.* **2011**, *81* (7), 659–672.
- (120) Petkiewa, D. V.; Golubev, E. K.; Kurkin, T. S.; Keчек'yan, A. S.; Rudakova, T. A.; Beshenko, M. A.; Ozerin, A. N. Carbonized Fibers Based on Polyvinyl Alcohol. *Dokl. Chem.* **2017**, *477* (2), 274–277.
- (121) Karacan, I.; Meşeli, H. Characterization of Amorphous Carbon Fibers Produced from Thermally Stabilized Polyamide 6 Fibers. *J. Ind. Text.* **2018**, *47* (6), 1185–1211.
- (122) Karacan, I.; Baysal, G. Investigation of the Effect of Cupric Chloride on Thermal

- Stabilization of Polyamide 6 as Carbon Fiber Precursor. *Fibers Polym.* **2012**, *13* (7), 864–873.
- (123) Shamiri, A.; Chakrabarti, M. H.; Jahan, S.; Hussain, M. A.; Kaminsky, W.; Aravind, P. V.; Yehye, W. A. The Influence of Ziegler-Natta and Metallocene Catalysts on Polyolefin Structure, Properties, and Processing Ability. *Materials.* **2014**, pp 5069–5108.
- (124) Chung, T. C. M. *Functionalization of Polyolefins*; Academic Press, **2002**.
- (125) Kim, K. W.; Lee, H. M.; An, J. H.; Kim, B. S.; Min, B. G.; Kang, S. J.; An, K. H.; Kim, Y. J. Effects of Cross-Linking Methods for Polyethylene-Based Carbon Fibers: Review. *Carbon Letters.* **2015**, pp 147–170.
- (126) Kim, K. W.; Lee, H. M.; Kim, B. S.; Hwang, S. H.; Kwac, L. K.; An, K. H.; Kim, B. J. Preparation and Thermal Properties of Polyethylene-Based Carbonized Fibers. *Carbon Lett.* **2015**, *16* (1), 62–66.
- (127) Horikiri, S.; Amagasaki, J.; Masao Minobe. Process for Production of Carbon Fiber. U.S. Patent, 438704, **1978**.
- (128) Postema, A. R.; De Groot, H.; Pennings, A. J. Amorphous Carbon Fibres from Linear Low Density Polyethylene. *J. Mater. Sci.* **1990**, *25* (10), 4216–4222.
- (129) Younker, J. M.; Saito, T.; Hunt, M. A.; Naskar, A. K.; Beste, A. Pyrolysis Pathways of Sulfonated Polyethylene, an Alternative Carbon Fiber Precursor. *J. Am. Chem. Soc.* **2013**, *135* (16), 6130–6141.
- (130) Barton, B. E.; Patton, J.; Hukkanen, E.; Behr, M.; Lin, J. C.; Beyer, S.; Zhang, Y.; Brehm, L.; Haskins, B.; Bell, B.; Gerhart, B.; Leugers, A.; Bernius, M. The Chemical Transformation of Hydrocarbons to Carbon Using SO₃ Sources. *Carbon.* **2015**, *94*, 465–471.

- (131) Mochida, I.; Toshima, H.; Korai, Y.; Matsumoto, T. Blending Mesophase Pitch to Improve Its Properties as a Precursor for Carbon Fibre Part 1 Blending of PVC Pitch into Coal Tar and Petroleum-Derived Mesophase Pitches. *J. Mater. Sci.* **1988**, *23* (2), 670–677.
- (132) Hlatshwayo, S. R.; Focke, W. W.; Ramjee, S.; Rand, B.; Manyala, N. Rheological Behavior and Thermal Properties of Pitch/Poly(Vinyl Chloride) Blends. *Carbon.* **2013**, *51* (1), 64–71.
- (133) Machnikowski, J.; Machnikowska, H.; Brzozowska, T.; Zieliński, J. Mesophase Development in Coal-Tar Pitch Modified with Various Polymers. *J. Anal. Appl. Pyrolysis* **2002**, *65* (2), 147–160.
- (134) Liu, D.; Li, M.; Qu, F.; Yu, R.; Lou, B.; Wu, C.; Niu, J.; Chang, G. Investigation on Preparation of Mesophase Pitch by the Cocarbonization of Naphthenic Pitch and Polystyrene. *Energy and Fuels* **2016**, *30* (3), 2066–2075.
- (135) Madison, J. J.; Roberts, R. M. Pyrolysis of Aromatics and Related Heterocyclics. *ACS Div. Pet. Chem. Inc. Prepr.* **1956**, *1* (3), 56–79.
- (136) Sazanov, Y. N.; Gribanov, A. V. Criteria of Polymer Carbonization. *Russ. J. Appl. Chem.* **2009**, *82* (3), 473–482.
- (137) Kipling, J. J.; Sherwood, J. N.; Shooter, P. V.; Thompson, N. R. Factors Influencing the Graphitization of Polymer Carbons. *Carbon.* **1964**, *1* (3).
- (138) Burket, C. L.; Rajagopalan, R.; Foley, H. C. Overcoming the Barrier to Graphitization in a Polymer-Derived Nanoporous Carbon. *Carbon.* **2008**, *46* (3), 501–510.
- (139) Masuda, T.; Thieu, K. Q.; Sasaki, N.; Higashimura, T. Polymerization of Phenylacetylenes. 4. Effects of Tetraphenyltin and Initiation Mechanism in the WCl₆-Catalyzed Polymerization. *Macromolecules* **1976**, *9* (4), 661–664.

- (140) Wang, Y.; Fan, X.; Wang, J.; Cheng, G.; Lü, X.; Zhang, M. Synthesis and Characterization of Poly- γ - Glycidoxypolytrimethoxysilane. In *Acta Polymerica Sinica*; **2009**; Vol. 55, pp 962–966.
- (141) Abe, Y.; Masuda, T.; Higashimura, T. Polymerization of (O-methylphenyl)Acetylene and Polymer Characterization. *J. Polym. Sci. Part A Polym. Chem.* **1989**, 27 (13), 4267–4279.
- (142) Lin, W.; Shao, Z.; Dong, J. Y.; Chung, T. C. M. Cross-Linked Polypropylene Prepared by PP Copolymers Containing Flexible Styrene Groups. *Macromolecules* **2009**, 42 (11), 3750–3754.
- (143) Richard-Lacroix, M.; Pellerin, C. Molecular Orientation in Electrospun Fibers: From Mats to Single Fibers. *Macromolecules*. **2013**, pp 9473–9493.
- (144) Deitzel, J. M.; Kleinmeyer, J.; Harris, D.; Beck Tan, N. C. The Effect of Processing Variables on the Morphology of Electrospun Nanofibers and Textiles. *Polymer (Guildf)*. **2001**, 42 (1), 261–272.
- (145) Takaku, A.; Shioya, M. X-Ray Measurements and the Structure of Polyacrylonitrile- and Pitch-Based Carbon Fibres. *J. Mater. Sci.* **1990**, 25 (11), 4873–4879.
- (146) Kislov, V. V.; Sadovnikov, A. I.; Mebel, A. M. Formation Mechanism of Polycyclic Aromatic Hydrocarbons beyond the Second Aromatic Ring. *J. Phys. Chem. A* **2013**, 117 (23), 4794–4816.
- (147) Fort, E. H.; Jeffreys, M. S.; Scott, L. T. Diels-Alder Cycloaddition of Acetylene Gas to a Polycyclic Aromatic Hydrocarbon Bay Region. *Chem. Commun.* **2012**, 48 (65), 8102–8104.
- (148) García-Rodeja, Y.; Solà, M.; Fernández, I. Understanding the Reactivity of Planar Polycyclic Aromatic Hydrocarbons: Towards the Graphene Limit. *Chem. - A Eur. J.* **2016**,

22 (30), 10572–10580.

- (149) Solà, M. Forty Years of Clar's Aromatic π -Sextet Rule. *Frontiers in Chemistry*. **2013**.
- (150) Dabestani, R.; Ivanov, I. N. A Compilation of Physical, Spectroscopic and Photophysical Properties of Polycyclic Aromatic Hydrocarbons. *Photochemistry and Photobiology*. **1999**, pp 10–34.
- (151) Walsh, R.; Wells, J. M. The Kinetics of the Diels–Alder Addition of Cyclopentadiene to Acetylene and the Decomposition of Norbornadiene. *Int. J. Chem. Kinet.* **1975**, 7 (3), 319–329.
- (152) Clar, E.; Zander, M. Syntheses of Coronene and 1:2-7:8-Dibenzocoronene. *J. Chem. Soc.* **1957**, 4616–4619.
- (153) Jiang, D. en; Dai, S. Circumacenes versus Periacenes: HOMO-LUMO Gap and Transition from Nonmagnetic to Magnetic Ground State with Size. *Chem. Phys. Lett.* **2008**, 466 (1–3), 72–75.
- (154) Kershaw, J. R.; Black, K. J. T. Structural Characterization of Coal-Tar and Petroleum Pitches. *Energy and Fuels* **1993**, 7 (3), 420–425.
- (155) Apicella, B.; Tregrossi, A.; Stanzione, F.; Ciajolo, A.; Russo, C. Analysis of Petroleum and Coal Tar Pitches as Large PAH. *Chem. Eng. Trans.* **2017**, 57, 775–780.
- (156) Yao, Z.; Liu, S. J.; Lv, F.; Cao, K. Determination of Mark-Houwink Parameters of Ethylene-Norbornene Copolymers and Molecular Characteristics Estimation. *J. Appl. Polym. Sci.* **2008**, 109 (6), 4010–4014.
- (157) Sessions, L. B.; Cohen, B. R.; Grubbs, R. B. Alkyne-Functional Polymers through Sonogashira Coupling to Poly(4-Bromostyrene). *Macromolecules* **2007**, 40 (6), 1926–1933.

- (158) Liu, H. C.; Chien, A. T.; Newcomb, B. A.; Liu, Y.; Kumar, S. Processing, Structure, and Properties of Lignin- and CNT-Incorporated Polyacrylonitrile-Based Carbon Fibers. *ACS Sustain. Chem. Eng.* **2015**, *3* (9), 1943–1954.
- (159) Samoilov, V. M.; Verbets, D. B.; Bubnenkov, I. A.; Stepanyova, N. N.; Nikolaeva, A. V.; Danilov, E. A.; Ponomareva, D. V.; Timoshchuk, E. I. Influence of Graphitization Conditions at 3000°C on Structural and Mechanical Properties of High-Modulus Polyacrylonitrile-Based Carbon Fibers. *Inorg. Mater. Appl. Res.* **2018**, *9* (5), 890–899.
- (160) McKay, A. I.; Bukvic, A. J.; Tegner, B. E.; Burnage, A. L.; Martínez-Martínez, A. J.; Rees, N. H.; Macgregor, S. A.; Weller, A. S. Room Temperature Acceptorless Alkane Dehydrogenation from Molecular σ -Alkane Complexes. *J. Am. Chem. Soc.* **2019**, *141* (29), 11700–11712.
- (161) Resasco, D. E. Dehydrogenation by Heterogeneous Catalysts. *Encycl. Catal.* **2002**, 1–52.
- (162) Sattler, A.; Paccagnini, M.; Lanci, M. P.; Miseo, S.; Kliewer, C. E. Platinum Catalyzed C-h Activation and the Effect of Metal-Support Interactions. *ACS Catal.* **2020**, *10* (1), 710–720.
- (163) Yu, C.; Ge, Q.; Xu, H.; Li, W. Propane Dehydrogenation to Propylene over Pt-Based Catalysts. *Catal. Letters* **2006**, *112* (3–4), 197–201.
- (164) Flory, P. J. Theory of Crystallization in Copolymers. *Trans. Faraday Soc.* **1955**, *51*, 848–857.
- (165) Dubdub, I.; Al-Yaari, M. Pyrolysis of Low Density Polyethylene: Kinetic Study Using TGA Data and ANN Prediction. *Polymers (Basel)*. **2020**, *12* (4), 891.
- (166) Awad, A. H.; El-Gamasy, R.; Abd El-Wahab, A. A.; Abdellatif, M. H. Assessment of Mechanical Properties of HDPE Composite with Addition of Marble and Granite Dust.

Ain Shams Eng. J. **2020**, *11* (4), 1211–1217.

- (167) Furukawa, T.; Sato, H.; Kita, Y.; Matsukawa, K.; Yamaguchi, H.; Ochiai, S.; Siesler, H. W.; Ozaki, Y. Molecular Structure, Crystallinity and Morphology of Polyethylene/Polypropylene Blends Studied by Raman Mapping, Scanning Electron Microscopy, Wide Angle X-Ray Diffraction, and Differential Scanning Calorimetry. *Polym. J.* **2006**, *38* (11), 1127–1136.
- (168) Tiikma, L.; Tamvelius, H.; Luik, L. Coprocessing of Heavy Shale Oil with Polyethylene Waste. *J. Anal. Appl. Pyrolysis* **2007**, *79* (1-2 SPEC. ISS.), 191–195.
- (169) Onwudili, J. A.; Insura, N.; Williams, P. T. Composition of Products from the Pyrolysis of Polyethylene and Polystyrene in a Closed Batch Reactor: Effects of Temperature and Residence Time. *J. Anal. Appl. Pyrolysis* **2009**, *86* (2), 293–303.
- (170) Maricq, M. M.; Waugh, J. S.; MacDiarmid, A. G.; Shirakawa, H.; Heegerlc, A. J. Carbon-13 Nuclear Magnetic Resonance of Cis- and Trans-Polyacetylenes. *Journal of the American Chemical Society.* **1978**, *100*(24), pp 7729–7730.
- (171) Tsenoglou, C. Non-Newtonian Rheology of Entangled Polymer Solutions and Melts. *Macromolecules.* **2001**, *34*(7), pp 2148–2155.
- (172) Meeuw, H.; Wisniewski, V. K.; Fiedler, B. Frequency or Amplitude?-Rheo-Electrical Characterization of Carbon Nanoparticle Filled Epoxy Systems. *Polymers (Basel).* **2018**, *10* (9), 999.
- (173) Choi, D.; Jang, D.; Joh, H. I.; Reichmanis, E.; Lee, S. High Performance Graphitic Carbon from Waste Polyethylene: Thermal Oxidation as a Stabilization Pathway Revisited. *Chem. Mater.* **2017**, *29* (21), 9518–9527.
- (174) Kil, H. S.; Jang, S. Y.; Ko, S.; Jeon, Y. P.; Kim, H. C.; Joh, H. I.; Lee, S. Effects of

Stabilization Variables on Mechanical Properties of Isotropic Pitch Based Carbon Fibers.

J. Ind. Eng. Chem. **2018**, *58*, 349–356.

- (175) Ferrari, A. C.; Robertson, J. Raman Spectroscopy of Amorphous, Nanostructured, Diamond-like Carbon, and Nanodiamond. *Philosophical Transactions of the Royal Society A: Mathematical, Physical and Engineering Sciences.* **2004**, pp 2477–2512.
- (176) Odian, G. *Principles of Polymerization*; John Wiley & Sons, **2004**.
- (177) Lobón-Poo, M.; Barcina, J. O.; Martínez, A. G.; Expósito, M. T.; Vega, J. F.; Martínez-Salazar, J.; Reyes, M. L. Meso-[Norbornane-7,7-Bis(Indenyl)]Titanium Dichloride: A Highly Active Catalyst for Ethylene Styrene Copolymerization. *Macromolecules* **2006**, *39* (22), 7479–7482.
- (178) Nowlin, T. E. *Business and Technology of the Global Polyethylene Industry: An In-Depth Look at the History, Technology, Catalysts, and Modern Commercial Manufacture of Polyethylene and Its Products*; Wiley, **2014**.
- (179) Caporaso, L.; Izzo, L.; Sisti, I.; Oliva, L. Stereospecific Ethylene - Styrene Block Copolymerization with Ansa-Zirconocene-Based Catalyst. *Macromolecules* **2002**, *35* (13), 4866–4870.
- (180) Zhang, G.; Li, H.; Antensteiner, M.; Chung, T. C. M. Synthesis of Functional Polypropylene Containing Hindered Phenol Stabilizers and Applications in Metallized Polymer Film Capacitors. *Macromolecules* **2015**, *48* (9), 2925–2934.

VITA

Houxiang Li

Houxiang Li was born in Guangxi and raised in Guangdong and Chongqing, China, and received his high school degree in Chongqing No.11 Middle School in 2009. Houxiang started his study at the Pennsylvania State University in 2010 and received his Bachelor of Science degree in Materials Science and Engineering in 2014. After graduation, he worked as a post-undergraduate researcher at the Pennsylvania State University and then started his Ph.D. study in 2016 with Dr. T.C. Mike Chung as his supervisor. His Ph.D. study was mainly focusing on developing a new family of polyethylene-based precursors for carbon fiber production supported by the Department of Energy.